AD-A217 181

Old Dominion University Research Foundation

ARO 24001.6-PH

BEST AVAILABLE COPY

DEPARTMENT OF ELECTRICAL AND COMPUTER ENGINEERING
COLLEGE OF ENGINEERING AND TECHNOLOGY
OLD DOMINION UNIVERSITY
NORFOLK, VIRGINIA 23529

AN ELECTRON-BEAM CONTROLLED SEMICONDUCTOR SWITCH

By

Karl H. Schoenbach, Principal Investigator

Vishnu K. Lakdawala, Co-Principal Investigator

Final Report
For the period ended September 30, 1989

Prepared for
U. S. Army Research Office
Physics Division
P.O. Box 12211
Research Triangle, N.C. 27709

Under
Research Contract DAAL03-86-K-0078
Dr. Bobby D. Guenther
Scientific Program Officer

November 1989

Old Dominion University Research Foundation is a not-for-profit corporation closely affiliated with Old Dominion University and serves as the University's fiscal and administrative agent for sponsored programs.

Any questions or comments concerning the material contained in this report should be addressed to:

Executive Director
Old Dominion University Research Foundation
P. O. Box 6369
Norfolk, Virginia 23508-0369

Telephone: (804) 683-4293
Fax Number: (804) 683-5290

UNCLASSIFIED
SECURITY CLASSIFICATION OF THIS PAGE

MASTER COPY - FOR REPRODUCTION PURPOSES

REPORT DOCUMENTATION PAGE

1a. REPORT SECURITY CLASSIFICATION
Unclassified

1b. RESTRICTIVE MARKINGS

2a. SECURITY CLASSIFICATION AUTHORITY

2b. DECLASSIFICATION / DOWNGRADING SCHEDULE

3. DISTRIBUTION / AVAILABILITY OF REPORT
Approved for public release; distribution unlimited.

4. PERFORMING ORGANIZATION REPORT NUMBER(S)

5. MONITORING ORGANIZATION REPORT NUMBER(S)
ARO 24001.6-PH

6a. NAME OF PERFORMING ORGANIZATION
Old Dominion University

6b. OFFICE SYMBOL *(If applicable)*

7a. NAME OF MONITORING ORGANIZATION
U. S. Army Research Office

6c. ADDRESS *(City, State, and ZIP Code)*
Norfolk, VA 23529

7b. ADDRESS *(City, State, and ZIP Code)*
P. O. Box 12211
Research Triangle Park, NC 27709-2211

8a. NAME OF FUNDING / SPONSORING ORGANIZATION
U. S. Army Research Office

8b. OFFICE SYMBOL *(If applicable)*

9. PROCUREMENT INSTRUMENT IDENTIFICATION NUMBER
DAAL03-86-K-0078

8c. ADDRESS *(City, State, and ZIP Code)*
P. O. Box 12211
Research Triangle Park, NC 27709-2211

10. SOURCE OF FUNDING NUMBERS

PROGRAM ELEMENT NO.	PROJECT NO.	TASK NO.	WORK UNIT ACCESSION NO.

11. TITLE *(Include Security Classification)*
An Electron-Beam Controlled Semiconductor Switch

12. PERSONAL AUTHOR(S)
Karl H. Schoenbach and Vishnu K. Lakdawala

13a. TYPE OF REPORT
Final

13b. TIME COVERED
FROM 6/15/86 TO 9/30/89

14. DATE OF REPORT *(Year, Month, Day)*
November 1989

15. PAGE COUNT

16. SUPPLEMENTARY NOTATION
The view, opinions and/or findings contained in this report are those of the author(s) and should not be construed as an official Department of the Army position, policy, or decision, unless so designated by other documentation.

17. COSATI CODES

FIELD	GROUP	SUB-GROUP

18. SUBJECT TERMS *(Continue on reverse if necessary and identify by block number)*
Semiconductors, Closing Switches, Opening Switches, Switches, Gallium Arsenide Switches, Electron Beams

19. ABSTRACT *(Continue on reverse if necessary and identify by block number)*

The objective of this work was to study the feasibility of using electron-beam controlled semiconductors as closing and opening switches. An Electron-beam with electron energies in the range from 20keV to 150keV was used to generate an electron-hole plasma in the

(OVER)

20. DISTRIBUTION / AVAILABILITY OF ABSTRACT
☐ UNCLASSIFIED/UNLIMITED ☐ SAME AS RPT. ☐ DTIC USERS

21. ABSTRACT SECURITY CLASSIFICATION
Unclassified

22a. NAME OF RESPONSIBLE INDIVIDUAL

22b. TELEPHONE *(Include Area Code)*

22c. OFFICE SYMBOL

cathode region of a GaAs switch. The band-edge radiation provided by the radiatively recombining electron-hole pairs in this region serves as the source function for electron-hole generation in the bulk of the switch. This "self-pumping" effect allows to overcome the space charge limitation of the current flow through the switch and therefore makes it suitable for high power applications. Switch current gains of more than 2000 have been obtained experimentally in semi-insulating GaAs. It was also demonstrated experimentally that doping of the cathodeluminescence region of the switch with high concentrations of a shallow acceptor improves the radiative efficiency of the cathodoluminescence. Modeling results show that improvements by one order of magnitude over the previously reached current gain can be obtained by proper doping of the cathode region of the GaAs switch. The dark current in these devices can be kept in the range of 10 $\mu A/cm^2$ by using a p-i-n structure. The linear dependance of the switch current on the controlling electron-beam current suggest the utilization of these type of switches to replace hard tubes in high power modulators.

DEPARTMENT OF ELECTRICAL AND COMPUTER ENGINEERING
COLLEGE OF ENGINEERING AND TECHNOLOGY
OLD DOMINION UNIVERSITY
NORFOLK, VIRGINIA 23529

AN ELECTRON-BEAM CONTROLLED SEMICONDUCTOR SWITCH

By

Karl H. Schoenbach, Principal Investigator

Vishnu K. Lakdawala, Co-Principal Investigator

Final Report
For the period ended September 30, 1989

Prepared for
U. S. Army Research Office
Physics Division
P.O. Box 12211
Research Triangle, N.C. 27709

Under
Research Contract DAAL03-86-K-0078
Dr. Bobby D. Guenther
Scientific Program Officer

Submitted by the
Old Dominion University Research Foundation
P.O. Box 6369
Norfolk, Virginia 23508-0369

November 1989

TABLE OF CONTENTS

AN ELECTRON-BEAM CONTROLLED SEMICONDUCTOR SWITCH

ABSTRACT

The objective of this work is to study the feasibility of using electron-beam controlled semiconductors as closing and opening switches. An electron-beam with electron energies in the range from 20 keV to 150 keV is used to generate an electron-hole plasma in the cathode region of a GaAs switch. The band-edge radiation provided by the radiatively recombining electron-hole pairs in this region serves as the source function for electron-hole generation in the bulk of the switch. This "self-pumping" effect allows to overcome the space charge limitation of the current flow through the switch and therefore makes it suitable for high power applications. Switch current gains of more than 2000 have been obtained experimentally in semi-insulating GaAs. It was also demonstrated experimentally that doping of the cathodeluminescence region of the switch with high concentrations of a shallow acceptor improves the radiative efficiency of the cathodoluminescence. Modeling results show that improvements by one order of magnitude over the previously reached current gain can be obtained by proper doping of the cathode region of the GaAs switch. The dark current in these devices can be kept in the range of 10 $\mu A/cm^2$ by using a p-i-n structure. The linear dependance of the switch current on the controlling electron-beam current suggest the utilization of these type of switches to replace hard tubes in high power modulators.

INTRODUCTION

While many years have gone into the development of high power gas switches, it is only recently that significant progress has been made in the development of high power semiconductor switches. Because of the size and weight considerations involved with all space applications, solid state switches pose an attractive alternative to the high power gas switches. There are many different types of semiconductor switches which can operate using single or multiple junctions or simply operate by using the bulk characteristics of the material. These devices can be controlled either optically, photoelectrically or electronically.

Currently promising, fast opening, repetitive, high power, solid state switches utilize the bulk characteristics of the material to obtain the desired switch performance. With the exception of one type of bulk semiconductor switch, where lasers with different wavelengths are used to turn the switch conductance on and off [2], the switch conductivity must be sustained by external ionization sources: lasers or electron-beams. In order to obtain short opening times, which for semiconductors means a high electron-hole recombination rate, the sustainment of the conductivity requires a high intensity ionization source operating for the entire duration of the current flow through the switch.

The inability to attain both long conduction times and fast opening with reasonable laser power limits the use of photoconductive switches to the microsecond range. The use of an electron-beam to ionize the semiconductor bulk allows the control of the switch conductivity in the microsecond and even millisecond range. These long electron-beam pulses with current densities of tens of milliamperes can easily be obtained by an electron-beam diode with a heated thoriated-tungsten cathode. Secondly, the limitation in hold-off voltage, which for photo-conductive switches is limited by surface flashover, can be rectified by using a parallel plate configuration where the electron-beam is injected through the contact. For such a configuration, as discussed in the following section, the hold-off voltage is determined by the dielectric strength of the bulk material rather than by the surface properties.

Thirdly, wide bandgap materials with a very high dark resistance, such as diamond or silicon carbide, can be activated. For laser activation, these materials would require multi-photon processes, that means high laser intensities. Fourth, by using photoelectrons it is possible to combine the advantages of photoconductive switching-remote control and picosecond timing-with those of electron-beam controlled switching. The current rise in

photoelectronic switches can be almost as fast as in directly laser-controlled switches. Current rise times of 100 ps were obtained in a photoelectronically controlled switch. Finally, since the ionization source, an electron-beam, can easily be modulated by using triode or tetrode configurations, the e-beam controlled semiconductor can be used as a high power modulator. Such a system would be superior to any of the presently used modulators (See enclosed patents).

CONCEPT OF THE SWITCH

The concept of electron-beam controlled semiconductor switches is based on irradiating a body of well-compensated direct semiconductor material with a high energy electron-beam just below the radiation damage threshold. Both direct and indirect ionization processes are utilized to create a high density of free charge carriers. A schematic sketch of the geometry of the proposed device is given in the figure below.

The configuration consists of a semi-insulating (compensated) gallium arsenide body of a thickness L up to 1 cm (zone II), provided with a highly ($N_a \approx 10^{19}$) p-doped surface layer of $d \approx 25\,\mu$m extension (zone I) at the cathode and a similiar but n-doped layer at the anode (zone III). Appropriate doping materials are for instance zinc and silicon, respectively. The exact density profile depends on the details of the manufacturing process, for our simulation we have utilized the results of a theoretical calculation given by Weisberg and Blanc [1].

In the open state, the bulk material of the switch is highly resistive and can hold off a voltage of up to 400 kV/cm depending on the break-down field strength of the material [2]. The highly doped surface layers reduce drastically the electrical field at the contacts and the concentration of minority carriers (i.e., of electrons at the cathode and holes at the anode), this prevents any current injection in the bulk zone and insures therefore a low dark current (determined by the intrinsic conductivity).

To turn the switch in the conducting state, an electron-beam with energy up to 250 keV (the radiation damage threshold of GaAs [3]) is injected into the cathode side of the sample. Due to the very small penetration depth of the electrons (e.g., about 25 μm for a 100 keV beam) [4], the beam is entirely stopped within the surface zone I where it creates a high concentration of electron-hole pairs by direct ionization. Subsequently, these charge carriers recombine under emission of band-edge radiation which then can penetrate deeper into the material to ionize the bulk zone II of the switch. Also, the abrupt stopping of the energetic electrons generates a beam of bremsstrahlung emitted in forward direction which creates secondary free charge carriers as well. By these means the bulk zone becomes conductive and the space charge limitation of conventional EBS (electron bombarded semiconductor) devices is overcome.

The strong p-type doping of the stopping zone I has two beneficial effects. First, it enhances considerably the efficiency of converting the direct beam energy into secondary band-edge radiation by increasing the relative fraction of direct over indirect (non-radiative) recombinations, and secondly, it changes the spectral characteristic of the emitted radiation towards lower energies [5]. As the absorption coefficient κ near the fundamental edge is a rapidly varying function of the photon energy [2], this allows a deeper penetration of light into the bulk zone II.

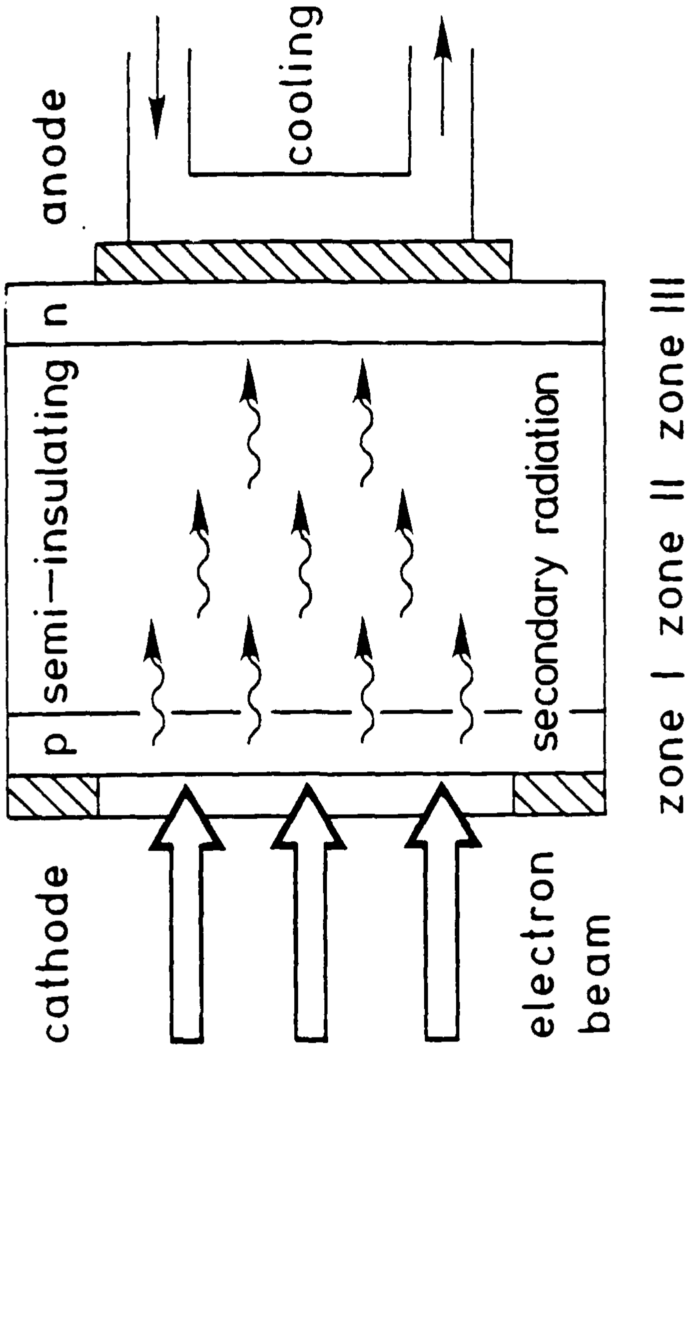
cathode
anode
cooling
p
semi-insulating
n
electron
beam
secondary radiation
zone I
zone II
zone III

REFERENCES

[1] Weisberg and Blanc, Phys. Rev. 131, 1548 (1963).

[2] S.M. Sze, Physics of Semiconductor Devices, (Wiley, New York, 1981).

[3] A.G. Chynoweth, W.L. Feldman, and R.A. Logan, Phys. Rev. 121, 684 (1961).

[4] L.V. Spencer, Energy Dissipation by Fast Electrons, NBS Monograph 1, (NBS, Washington, 1959).

[5] D.A. Cusano, Solid State Communications 2, 353 (1964).

ACHIEVEMENTS IN THE CONTRACT PERIOD FROM JUNE 16, 1986 TO SEPTEMBER 30, 1989

1. A 200 kV electron-beam system, obtained from Kirtland AFB, has been modified for its use as a electron-beam source for semiconductor switching with Electron-beam current densities of up to 500 mA/cm^2. Paper No.[3] *
2. Diagnostic techniques have been developed to study the electron-beam characteristics. A Faraday cup is used to measure the electron-beam with high temporal resolution, a scintillator set-up is used to measure the spatial distribution of the electron-beam current density, and a magnetic spectrometer has been constructed to obtain the energy distribution of the electron beam. [Appendix]
3. A vacuum system has been constructed which allows to deposit ohmic and Schottky contacts on semi-insulating GaAs. [Appendix]
4. A diffusion system has been built which allows the doping of semi-insulating GaAs with Zn, in order to create a highly cathodoluminescent layer at the cathode side of the switch. A new, improved version of such a diffusion system is under construction. [Appendix]
5. In order to study the effect of doping on the recombination radiation, optical measurements were conducted. The samples were irradiated with electron-beam and the band edge radiation emitted from the edges of the samples was monitored using S1 photomultipler tubes. The results demonstrate that doping enhances the radiation efficiency drastically. Spatially resolved radiation measurements allow the determination of absorption lengths. Absorption depths of $\approx$ 0.5 mm in Si-doped GaAs have been measured. [Appendix]

---

* The references in parenthesis indicate where more detailed information can be found on the subject. See list of publications and the appendix which contains material that has not been published yet.

6. Measurements of the current-voltage characteristics of semi-insulating GaAs were performed with the purpose of obtaining information on the dark resistivity and the hold-off voltage of electron-beam controlled GaAs switches. The dark current was found to be a function of voltage and time with response times being in the μs to ms range. The dielectric strength exceeds 140 kV/cm for 3.5 μs FWHM voltage pulses. Paper No.[9]
7. Measurements of the current-voltage characteristics with the temperature as variable parameter allowed us to get information on the deep level structure of semi-insulating GaAs. [Appendix]
8. Chaotic oscillations in the low frequency range were observed in semi-insulating GaAs when dc-biased. A deep level model which allows us to interpret the observed chaotic oscillation, was developed. It is expected that this model will lead to a diagnostic method for the determination of field dependent rate coefficients of deep centers. Paper No.[8]
9. Switch experiments have been performed with differently prepared semi-insulating GaAs. The current-gain was found to be inversely proportional to the resistivity of the switch material. Highest current gains (2200) were obtained in samples with a resistivity of 6×10^6 Ωcm. The change in resistance during switching was more than four orders of magnitude. Paper No.[9]
10. Switch experiments with Zn-doped GaAs show a increase of the current gain of a factor of two over semi-insulating GaAs. Although the doping was not optimized, this experimental result demonstrates the importance of doping for increased switch efficiency. Paper No.[12]
11. Switch experiments with circuits containing a load resistance of 50 Ohm showed that the switch conductance can be varied linearly with the electron beam current. Highest switch conductances of 0.033 Ω^{-1} were obtained with electron-beam currents of 26 mA. Paper No.[9]
12. A laser driven photo-electron diode was built. Space charge limited photo-electron beam current of just under 1 A with 10 ns duration has been achieved with modest laser power. The photo-electron beam diode will be used to study the fast temporal response of the semiconductor switches at high currents. Paper No.[11]
13. An analytical and a numerical model of the switch has been developed. According to the analytical model current densities of several kA/cm^2 at forward voltages of tens of volts can be controlled with an electron beam of 100 keV and 1 A/cm^2. Vacuum

tetrodes with this electron current characteristic are commercially available. The dark current can be reduced to 10 $\mu A/cm^2$ by doping the switch with shallow donors and acceptors, respectively, on cathode and anode face to obtain a p-i-n structure. Paper No.[10]

14. A workshop in "Electron-Beam and Optically Controlled Semiconductor Switches" was held in Norfolk, Virginia in May 1987. This workshop and a special issue of the same topic in IEEE Transactions on Electron Devices edited by one of the P.I.'s (Karl H. Schoenbach), helped to improve the information exchange in this rapidly emerging field of research.
15. The applicability of the electron-beam controlled semiconductor switches was demonstrated by the fact that two patents were granted for this invention.

AN ELECTRON-BEAM CONTROLLED SEMICONDUCTOR SWITCH

RESEARCH PROJECT No. DAAL03-86-K-0078

LIST OF PUBLICATIONS

[1] Karl H. Schoenbach, R. Germer, V.K. Lakdawala, K. Schmitt, and S. Albin, "CONCEPTS FOR ELECTRON-BEAM AND OPTICAL CONTROL OF BULK SEMICONDUCTOR SWITCHES", Proc. SPIE, Los Angeles, CA, 1987, Vol. 735, p. 85.

[2] R. Germer and K. H. Schoenbach, "SIMILARITIES BETWEEN CAVITATION EXPERIMENTS AND ELECTRICAL BREAKDOWN", Nuclear Physics B2, 569, 1987

[3] K.B.J. Schmitt, Karl H. Schoenbach, Thomas J. Powers, and Rudolf Germer, "ELECTRON-BEAM CONTROLLED SEMICONDUCTOR OPENING/CLOSING SWITCHES", Proc. 6th IEEE Pulsed Power Conference, Arlington, 1987, p. 271.

[4] Karl H. Schoenbach, V.K. Lakdawala, K.B.J. Schmitt, T.J. Powers, "ELECTRON-BEAM CONTROLLED SEMICONDUCTOR SWITCHES", Proc. SPIE, Los Angeles, CA, January, 1988, Vol. 871, p.133.

[5] Karl H. Schoenbach, V. Lakdawala, David Stoudt and Tyler Smith, "E-BEAM CONTROLLED SEMICONDUCTOR SWITCH", Proc. Workshop on Optically and Electron-Beam Controlled Semiconductor Switches, Norfolk, VA. May 1988, paper D2.

[6] Glenn Gerdin, K.H. Schoenbach, V.K. Lakdawala and A.N. Dharamsi, "SUBNANOSECOND PHOTOELECTRON BEAM CLOSING SWITCHES", Proc. Workshop on Optically and Electron-Beam Controlled Semiconductor Switches", Norfolk, VA, May 1988, paper D3.

[7] Karl H. Schoenbach, V.K. Lakdawala, Sung T. Ko, M.S. Mazzola, David Stoudt and Tyler Smith, "OPTICAL AND ELECTRON-BEAM CONTROL OF SEMICONDUCTOR SWITCHES", IEEE Conference, Record of the 10th Power Modulator Symposium, Hilton Head, SC, 1988, p. 318.

[8] David Stoudt, Ralf P. Brinkmann, L. Vahala, K.H. Schoenbach, and V.K. Lakdawala, "INVESTIGATIONS INTO CHAOTIC OSCILLATIONS IN GaAs SUBSTRATE", Bulletin of the American Physical Society, Meeting in Baltimore, MD, May 1989

[9] David C. Stoudt, K.H. Schoenbach and V.K. Lakdawala, "THE ELECTRICAL CHARACTERISTICS OF SEMI-INSULATING GaAs FOR HIGH POWER SWITCHES", Proc. 7th IEEE Pulsed Power Conference, Monterey, CA, June 1989

[10] Ralf P. Brinkmann, "ANALYTICAL AND NUMBERICAL MODELING OF ELECTRON-BEAM CONTROLLED SEMICONDUCTOR SWITCHES", Proc. 7th IEEE Pulsed Power Conference, Monterey, CA, June 1989.

[11] Steven G.E. Pronko and Glenn A. Gerdin, "A SHORT-PULSE, LASER-DRIVEN PHOTOELECTRON DIODE", Proc. 7th IEEE Pulsed Power Conference, Monterey, CA, June 1989

[12] Glenn A. Gerdin, K.H. Schoenbach, V.K. Lakdawala, T.F. Smith and R.P. Brinkmann, "A BAND EDGE RADIATION GENERATOR FOR PULSED POWER", Proc. 7th IEEE Pulsed Power Conference, Los Angeles, June 1989

[13] Karl H. Schoenbach, V.K. Lakdawala, David C. Stoudt, Tyler Smith, Ralf P. Brinkmann, "ELECTRON-BEAM CONTROLLED HIGH-POWER SEMICONDUCTOR SWITCHES", IEEE Transactions on Electron Devices, 36, 1733, (1989)

[14] Ralf P. Brinkmann, "MODELING OF ELECTRON-BEAM CONTROLLED SEMICONDUCTOR SWITCHES", submitted to Journal of Applied Physics, Sept 1989

PATENTS

Invention:	**Electron Beam Controlled Bulk Semiconductor Switch with Cathodoluminescent Electron Activation**
Patent No.	4,831,248
Patent Date:	May 16, 1989
Inventors:	Karl H. Schoenbach, Vishnukumar K. Lakdawala, Rudolf K.F. Germer, Klemens B. Schmitt

Invention:	**Electron Beam Controlled Bulk Semiconductor Switch with Cathodoluminescent Electron Activation**
Continuation In-Part:	Continuation of U.S. Patent Application 07/184,680, issued as U.S. Patent No. 4,231,248 on May 16, 1989 which is a continuation-in-part of U.S. Patent No. 4,825,061 on April 25, 1989

Patent Pending: Application:	Attorney Docket No. 576.1009-CIP Filed May 15, 1989 Serial No. 351,218

PARTICIPATING SCIENTIFIC PERSONNEL

DR. KARL H. SCHOENBACH	PRINCIPAL INVESTIGATOR
DR. V.K. LAKDAWALA	CO-PRINCIPAL INVESTIGATOR
DR. RUDOLF K. GERMER	VISITING ASSOCIATE PROFESSOR
DR. RALF PETER BRINKMANN	ASSISTANT RESEARCH PROFESSOR
DR. KLEMENS SCHMIDT	ASSISTANT RESEARCH PROFESSOR
DAVID STOUDT	GRADUATE STUDENT (M.S., FALL 89) "The Electrical Characteristics of Semi-Insulating GaAs for Electron-Beam Controlled High Power Switches"
TYLER SMITH	GRADUATE STUDENT (M.S., FALL 89) "Spatially Resolved Pulsed Cathodoluminescense from GaAs"
T.J. POWERS	GRADUATE STUDENT
W.K. TYMCHYSHIN	GRADUATE STUDENT

APPENDIX

SEMICONDUCTOR MATERIAL

The material used in this investigation is semi-insulating (SI) GaAs. The material parameters for GaAs as well as four other possible switch materials are listed in Table 1, Where E_G and E_M are the bandgap energy and breakdown field of the material, respectively. Also listed for each material is the dielectric constant ϵ_r, the low field drift mobility of electrons μ_n, and the thermal conductivity of the material λ. Some of the advantages of using GaAs are the relatively high breakdown strength and bandgap energy compared to Si and Ge. This allows the switch to be operated at higher fields and reduces the off-state leakage current. Also, the electron mobility for GaAs is much greater than that for the other materials. One problem with GaAs is that the thermal conductivity is much lower than all of the other materials in Table 1. This may lead to problems with heat sinking and may limit the use of GaAs as a high-temperature high-power switch.

The values shown in Table 1 are for intrinsic GaAs. Intrinsic purity is not presently obtainable by GaAs bulk-growth techniques. It is therefore necessary to resort to using SI GaAs to obtain the desired high-resistivity material. In SI GaAs, residual shallow (ie. Si) or deep (ie. EL2) donor impurities are intentionally compensated by shallow (C) or deep (Cr) acceptor impurities to reduce the free-carrier concentration.

One of the most important reasons for choosing SI GaAs for the switch is that it is a direct bandgap material. In this case an electronic transition from the bottom of the conduction band to the top of the valence band can result in the emission of a photon at roughly the bandgap energy. The rate of direct transition in SI GaAs is generally small compared to non-optical transitions through deep centers. A possibility to enhance the direct recombination rate in SI GaAs is to dope it heavily with shallow donors or acceptors. This method and possible gains in efficiency are discussed in Paper No.[12].

The GaAs used in this investigation was grown by the liquid encapsulated Czochralski (LEC) technique. A deep level impurity designated EL2 was found to be dominant in as-grown LEC material with concentrations of up to $2 \times 10^{16} \text{cm}^{-3}$ [12]. The EL2 level is thought to be the result of the arsenic As_{Ga} antisite. EL2 is thought to be a deep donor which acts to compensate residual acceptors, normally carbon. Undoped SI GaAs of this type is characterized by resistivities ranging from 5×10^6 to 1×10^9 Ωcm. Under these conditions the concentration of EL2 is normally higher than that of the acceptors which results in the material being n- type with the Fermi level located above the middle of the bandgap.

SAMPLE PREPARATION

The method of contact formation used in this study was thermal deposition followed by contact annealing. For this method the wafer is cleaved to the desired size and cleaned by a prescribed procedure to remove any surface contamination and oxide layer which may be present. Next the contact area is delineated by a foil mask. The sample is then placed in a vacuum ($p < 10^{-5}$ torr) and a Au(88%)-Ge(12%) alloy is thermally deposited onto the exposed surface to a thickness of 100 nm.

After deposition, the mask is removed and the sample is heated to 450 C° in N_2 at atmospheric pressure for a period of 15 minutes. While the sample is being heated a liquid eutectic mixture of the alloy and the GaAs is formed. During this process the Ga out-diffuses into the eutectic forming a mixture of Au-Ga and Au-Ge on the surface. When the melt is cooled Ge atoms settle into vacant Ga sites, thus forming a heavily doped n^+-layer [2]. This layer then serves to reduce the barrier width and allows field emission to be the dominant mode of current transport. This causes the contacts to behave in an ohmic manner.

SEMICONDUCTOR CHARACTERIZATION

Experimental methods which have been used to characterize the semiconductor material are Hall effect measurements, DLTS techniques, and space charge limited (SCL) current injection. Because of the high resistivity of semi-insulating GaAs, Hall-effect and DLTS techniques are not applicable. We are presently developing a PICTS (Photo Induced Current Transient Spectroscopy) system which will be used to get information on the deep level structure in SI GaAs. Before its completion we rely on SCL-injection techniques, to get information on deep centers in SI GaAs.

The theory of SCL currents in solids was first addressed in 1940 by N.F. Mott and R.W. Gurney [12] and we refer to this book what the theory of SCL concerns. The material used in this SCL investigation was grown by the LEC method. In particular, three different types of Si GaAs were used. The first type (sample 3) was intentionally compensated by the manufacturer with a carbon concentration of about 3×10^{15} cm^{-3} yielding a resistivity of about 3×10^{8} Ωcm. The second type (sample 2) was compensated with chromium at a concentration of 10^{15} to 10^{16} cm^{-3} yielding a resistivity of about 6×10^{8} Ωcm. The third type of material used (sample 1) was as-grown (or EL2-compensated) SI GaAs with a resistivity of about 6×10^{6} Ωcm. All of the relevant data which was given by the manufacturer, or derived from that data, are shown in Table 2.

Current Voltage Measurements

All of the steady-state current-voltage and resistivity-temperature data were measured with a Keithley 617 electrometer which measured the current and supplied the voltage up to 100 V. Potentials above 100 V were supplied with a 3 kV power supply. All measurements were conducted with the sample in the dark and in a vacuum of about 5 mtorr. The vacuum served to provide thermal isolation from the environment when the temperature of the sample was varied. It also prevented condensation from forming on the sample surface when it was cooled. The results are discussed for sample 1. Results for sample 2 and sample 3 are presented in Table 3.

The I-V characteristics of sample 1 are shown in Fig. 1 where the curves were generated at a constant temperature. The dashed lines in Figs. 1, 2, and 3 are all the result of a nonlinear least- squares curve fit to the resistivity-temperature data. The most noticeable feature of the curves is the existence of a linear "ohmic" region which shifts uniformly with temperature. The linear part of the curve follows Ohm's law and the temperature

dependence is the result of the temperature dependence of the concentration of free carriers n_0. Slight deviations from linearity are probably the result of small temperature variations during the measurement. It was found that when the polarity of the voltage was reversed, the resulting I-V curve was symmetrical indicating that the contacts were both ohmic and similar in their electrical characteristics. After the ohmic region, the current rapidly increases as was shown in Fig. 3a for the case of an electron trap initially located below the Fermi level. The voltage at which this transition occurs is called the trap-filled-limit-voltage (V_{TFL}) and was found to be 100 V for a temperature of 297 K. It can be used to calculate the value of p_{t0}, the concentration of empty trap sites at thermal equilibrium. For a sample thickness of 0.065 cm, $p_{t0} = 3.4 \times 10^{11}$ cm^{-3}. The ohmic portion of the curve also yields information on the electron density and the location of the Fermi level. At 297 K the value of $n = 5.8 \times 10^7$ cm^{-3} and $E_c - E_F = 0.58$ eV. Information on the position of the electron trap cannot be obtained from Fig. 7 explicitly. However, if we assume that the dominant trap in semi-insulating GaAs is EL2, we can assume an energy of $E_c - E_t = 0.825$ eV. Once the Fermi and trap energies are known we can calculate N_t. Doing this yields a density of $N_t(\mathrm{EL2}) = 9.6 \times 10^{15}$ cm^{-3}. This is within a factor of two of the value normally quoted for semi-insulating GaAs [12]. The experimental results for all the samples, including sample 2 and 3, are shown in Table 2.

Resistivity-Temperature Measurements

The resistivity-temperature $\rho - T$ data were obtained with the same experimental apparatus used for the I-V measurements. The only difference is that now the applied voltage was held constant and the temperature was varied. The electric fields in the GaAs were in a range of constant mobility. The measured $\rho - T$ results for sample A are shown in Fig. 4.

The circles are the measured values while the solid lines are the result of a nonlinear least-squares fit to the data. The equations used to obtain these curves are derived and discussed by Zucca [3]. The results of these measurements are listed in Table 3 for all three samples.

When we compare the values of $E_c - E_F$ and n in Table 2 with those in Table 3, we find very good agreement between them. This is not unexpected because in Table 2 these values are obtained from the ohmic region of each curve which was already shown to agree with the calculated parameters.

The results demonstrate the strength of this relatively simple diagnostic technique. This allows it to characterize the semi-insulating semiconductors and to predict their performance in a e-beam controlled switch system.

Studies of the Luminiscence of Electron-Beam Irradiated GaAs

The proposed high power semiconductor switch consists of regions I and II (see figure in section "Concept of the Switch"). The length of region I is determined by the mean range of electrons in the GaAs sample. The length of region II is dictated by the desired hold-off voltage of the switch. The conductivity in region II and thus the conductance of the e-beam controlled switch, is determined by photoionization of electron-hole pairs in this region using photons which are generated in region I (cathodoluminescense). The efficiency of the cathodoluminescence can be increased by doping region I.

The integrated and spatially resolved cathodoluminescence is studied as a function of electron energy and current. The material being studied at this point is GaAs doped with Si ($N_d = 10^{18}$ cm^{-3}). At a later date samples of SI GaAs with a zinc-doped layer the length of region I will be used as there are favorable energy shifts in the bandgap. In order to study the cathodoluminescence a diagnostic system was used as shown in figure 5. The electron beam is capable of supplying a maximum current of 500 mA and energies up to 170 keV. The lens magnifies 10 times and focuses the image of the GaAs sample edge on the photo multiplier tube (PMT) by way of a mirror. When the system is being lined up, an image converter tube with S-1 characteristics is used to accurately find the image plane with the edge of the sample illuminated by a GaAs LED.

The purpose of the mirror is to reflect the infrared radiation (of about 0.9 μm wavelength) while not affecting the direction of X-radiation. This allows the PMT to be effectively shielded from X-radiation. The optical signal from the PMT is amplified by an operational amplifier configured as a transconductance amplifier. The calibration of the PMT was carried out using a GaAs LED ($\lambda = 0.94$ μm) and neutral density filters.

Results of the fully spatially integrated intensity emitted from the wafer edge are shown in figure 6, as a function of electron current with the electron energy held constant. As expected, the intensity varies linearly with current. The electron energy does not have a large impact at low currents but seems to approach a linear dependance at high currents. In order to get spatial resolution of the cathodoluminescense a shutter in the image plane was used which can be moved across the image of the wafer edge (see figure 5). Data

accumulated in this fashion yielded the spatially integrated intensity as a function of distance. In order to extract the intensity as a function of distance, a derivative of the integrated intensity was taken. Results of the integrated intensity versus voltage for a constant current of 75 mA/cm^2 are shown in figure 7 on a semi-logarithmic graph. The intensity seems to follow a exponential function.

The integrated intensity as a function of distance is given by equation 1 and is listed on each plot:

$$\int_x^L I(x)\,dx = n_0 \exp(-x/d_p) \tag{1}$$

where n_0 is the intensity at the edge of the sample, $d_p = 1/\kappa$ represents the distance in which the signal decays by 1/e and L is the sample thickness. As shown on the plots, the value of d_p increased with decreasing energy in all but one case. Taking a derivative of (1) gives the intensity as a function of distance,

$$I(x) = I(0)\exp(-x/d_p) = \frac{n_0}{d_p}\exp(-x/d_p) \tag{2}$$

A plot of n_0 versus electron energy while the current is held at 75 mA/cm^2 is shown in figure 8. It shows that the intensity is linear function of electron energy.

In conclusion, it was found that the intensity of radiation varies linearly with current and voltage. A surprising result was that the intensity followed an exponential decay through the entire sample rather than having a peak in the region where the mean electron ranges (Bethe ranges) have predicted. Beside measurements with Si-doped GaAs, optical studies with SI GaAs have been performed. The cathodoluminescence from undoped GaAs was found to be much lower in magnitude, as expected from our modeling results.

FIGURES

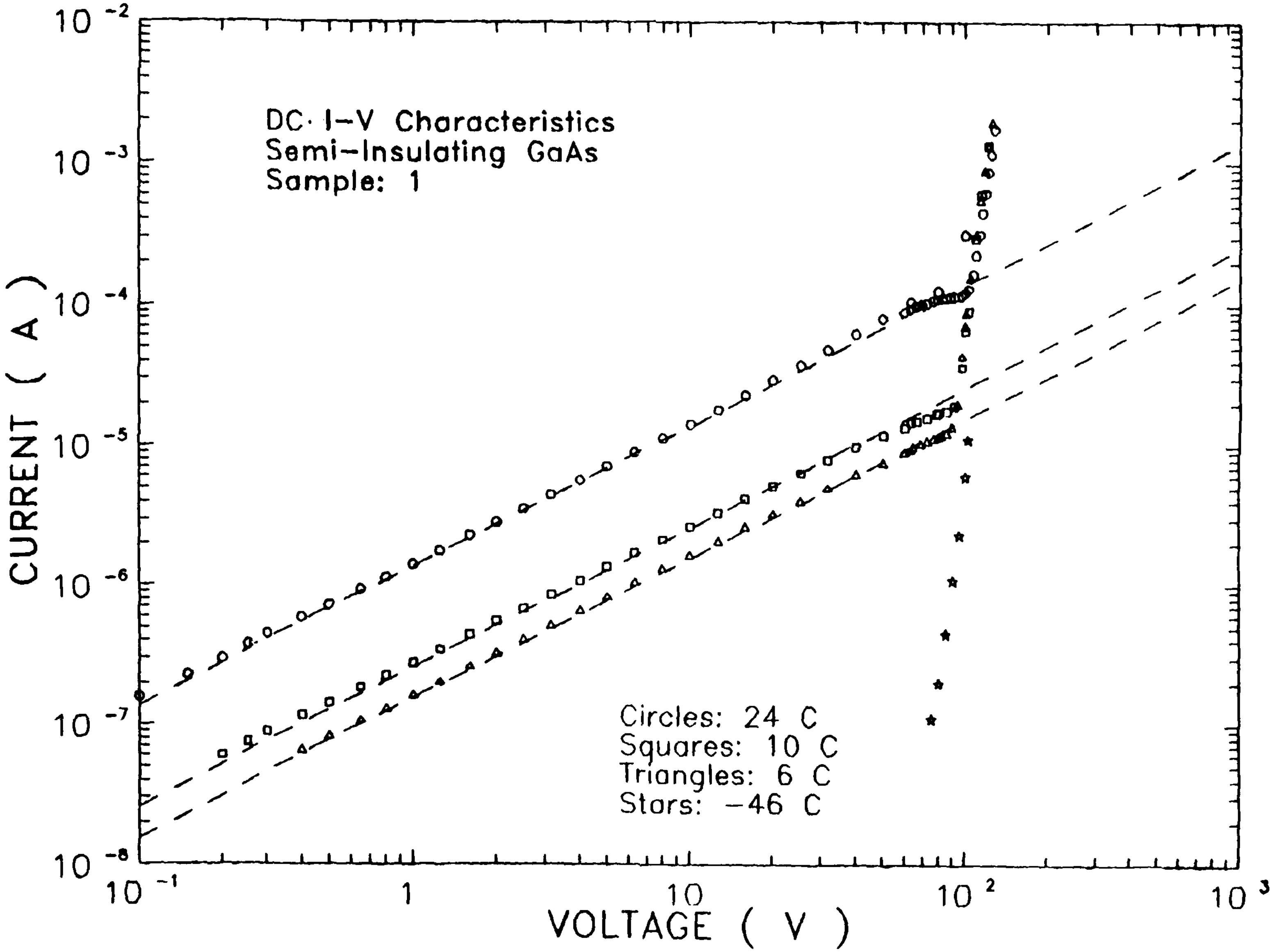

Fig. 1 DC I–V characteristics of sample 1 (SI GaAs) with temperature as the variable parameter.

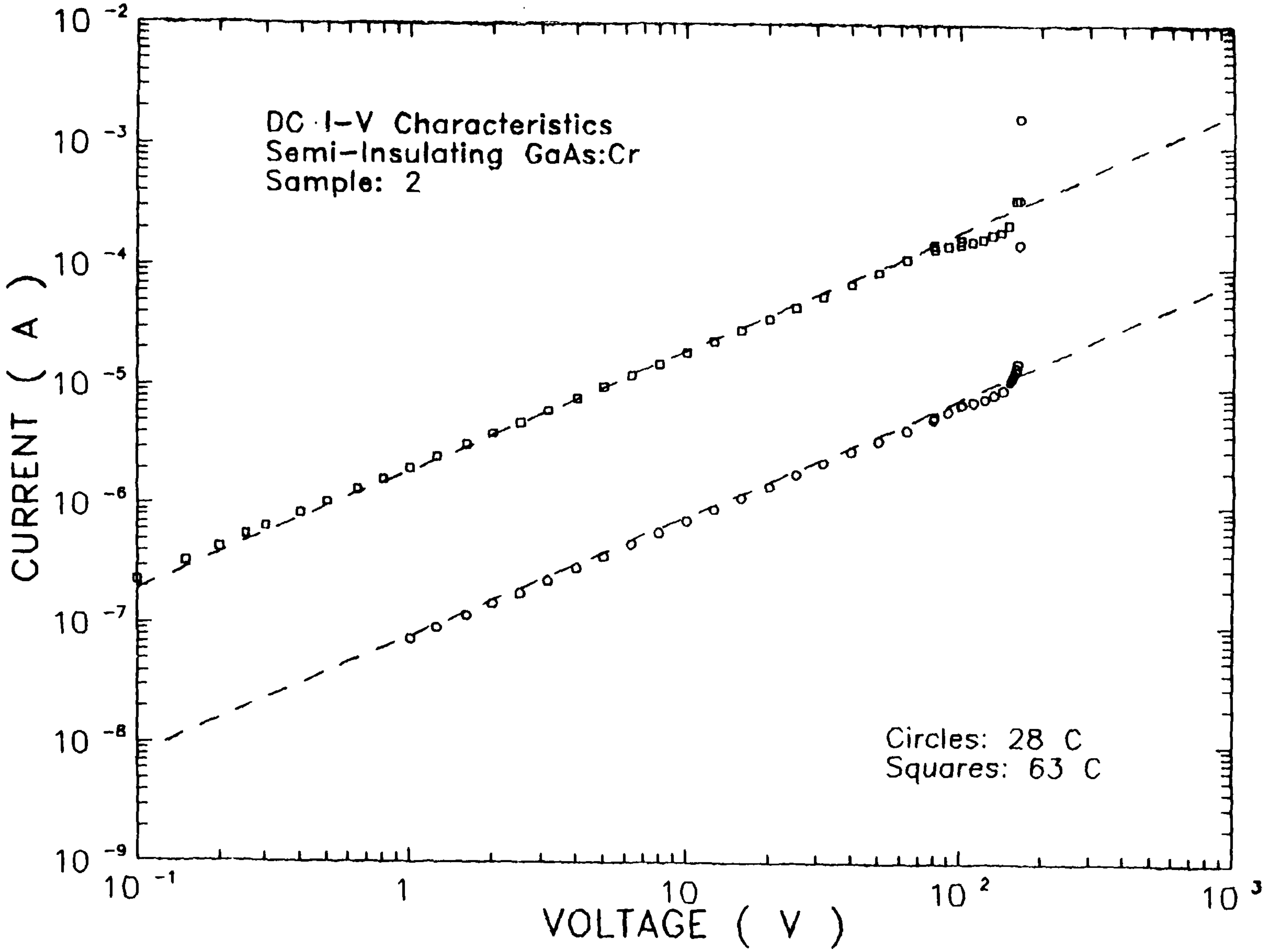

Fig. 2 DC I–V characteristics of sample 2 (SI GaAs:Cr) with temperature as the variable parameter.

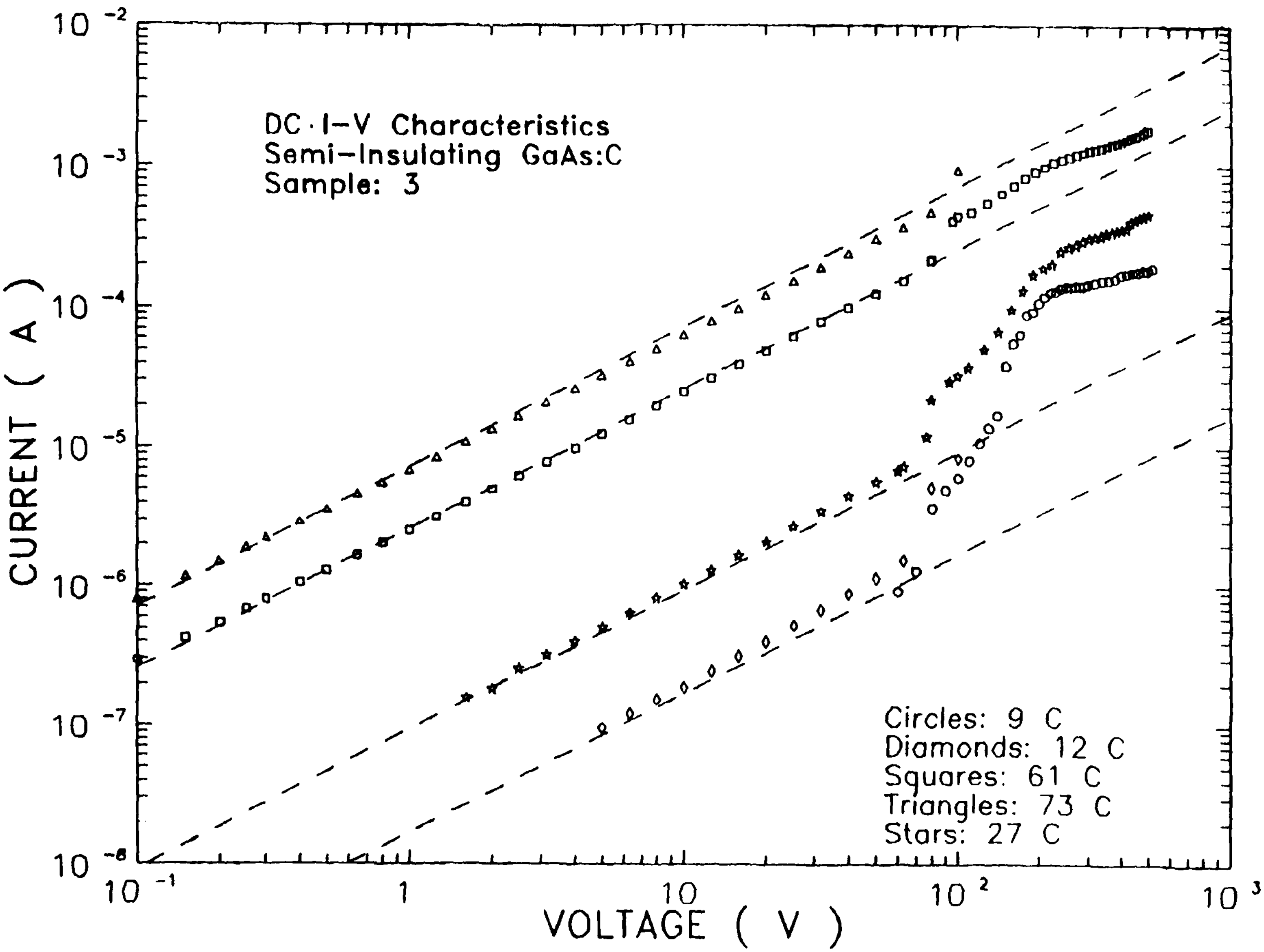

Fig. 3 DC I–V characteristics of sample 3 (SI GaAs:C) with temperature as the variable parameter.

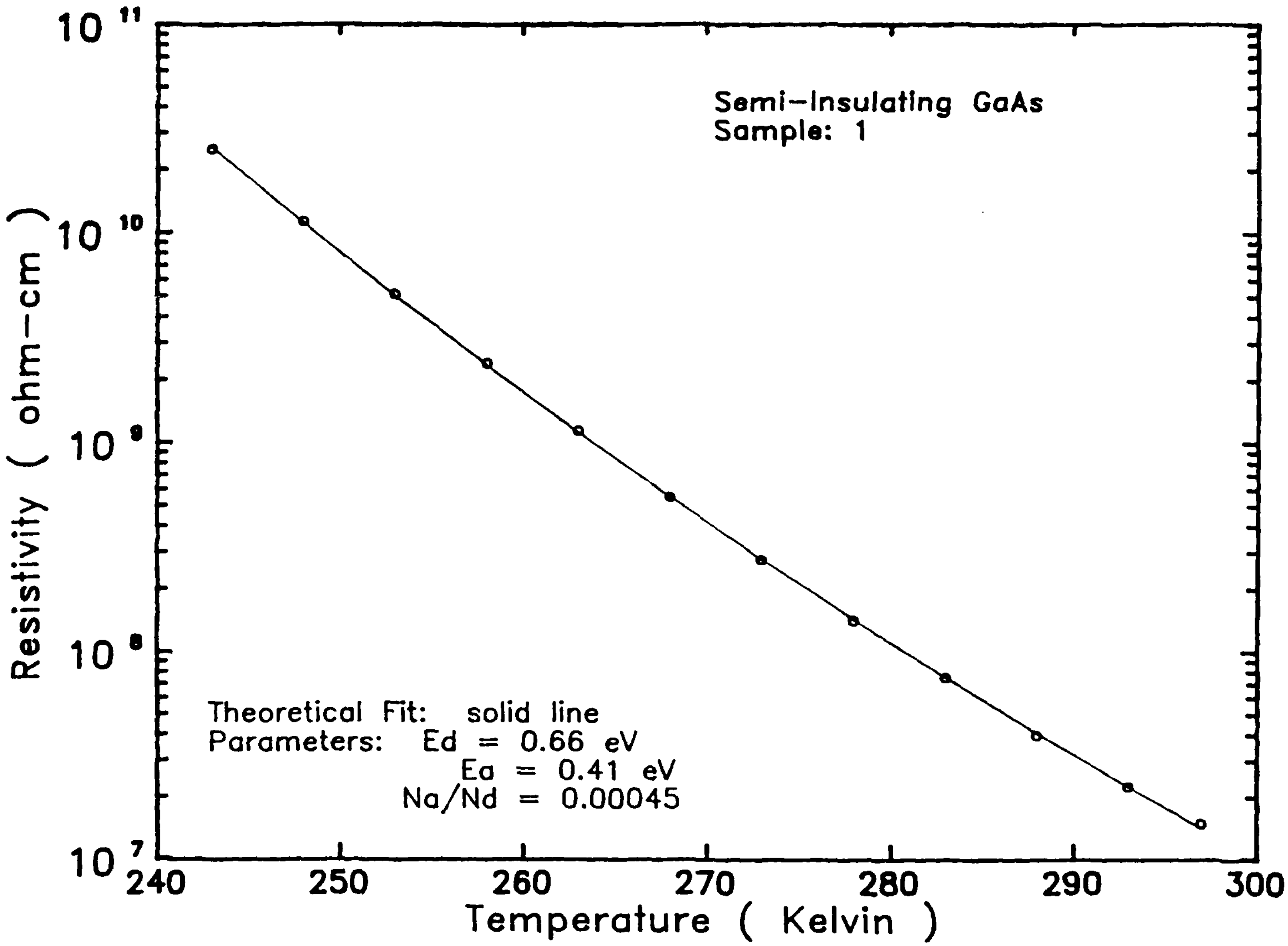

Fig. 4 Resistivity-temperature characteristics of sample 1 for an applied field of 630 V/cm.

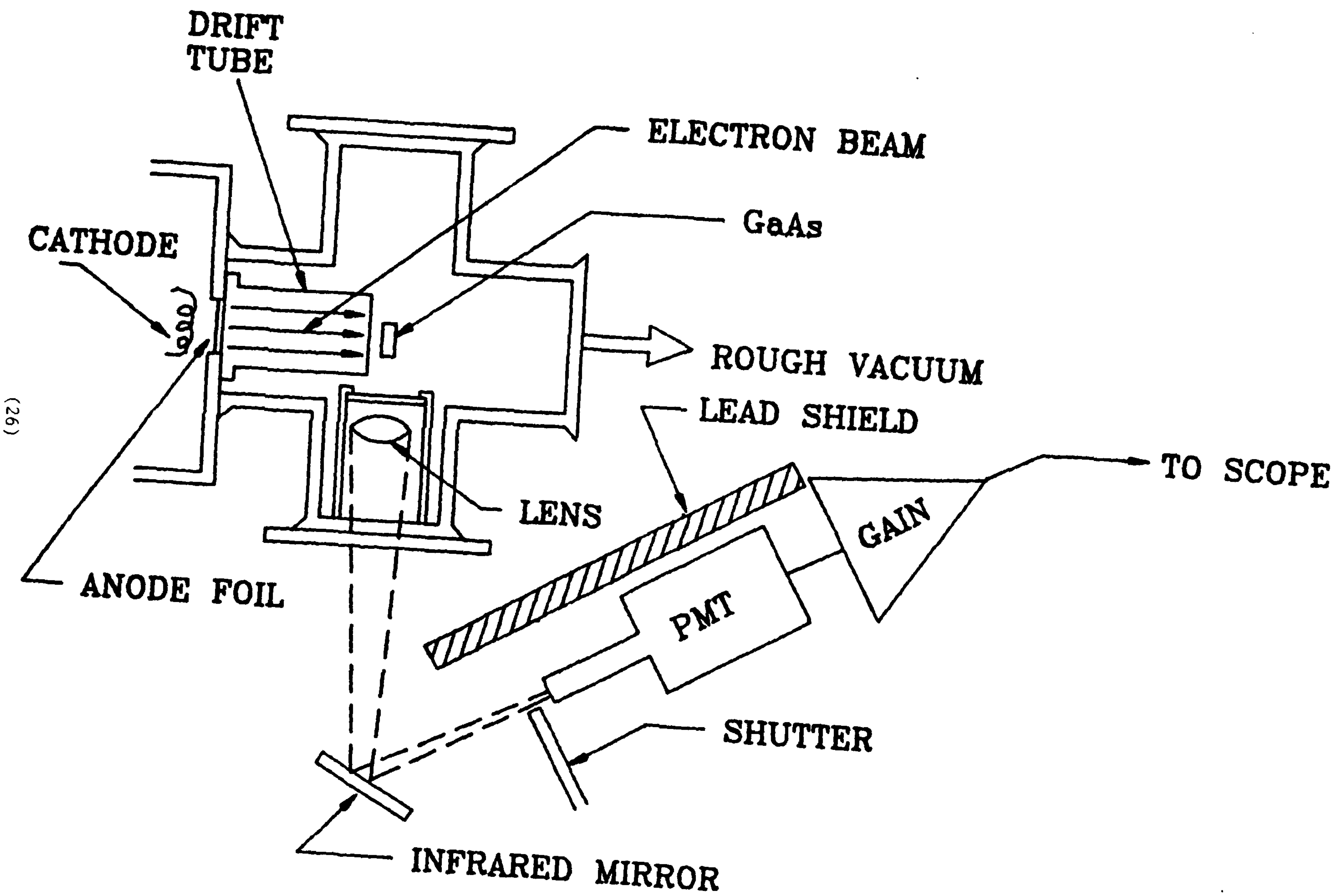

Fig. 5 Diagnostic System used to measure Cathodoluminescense.

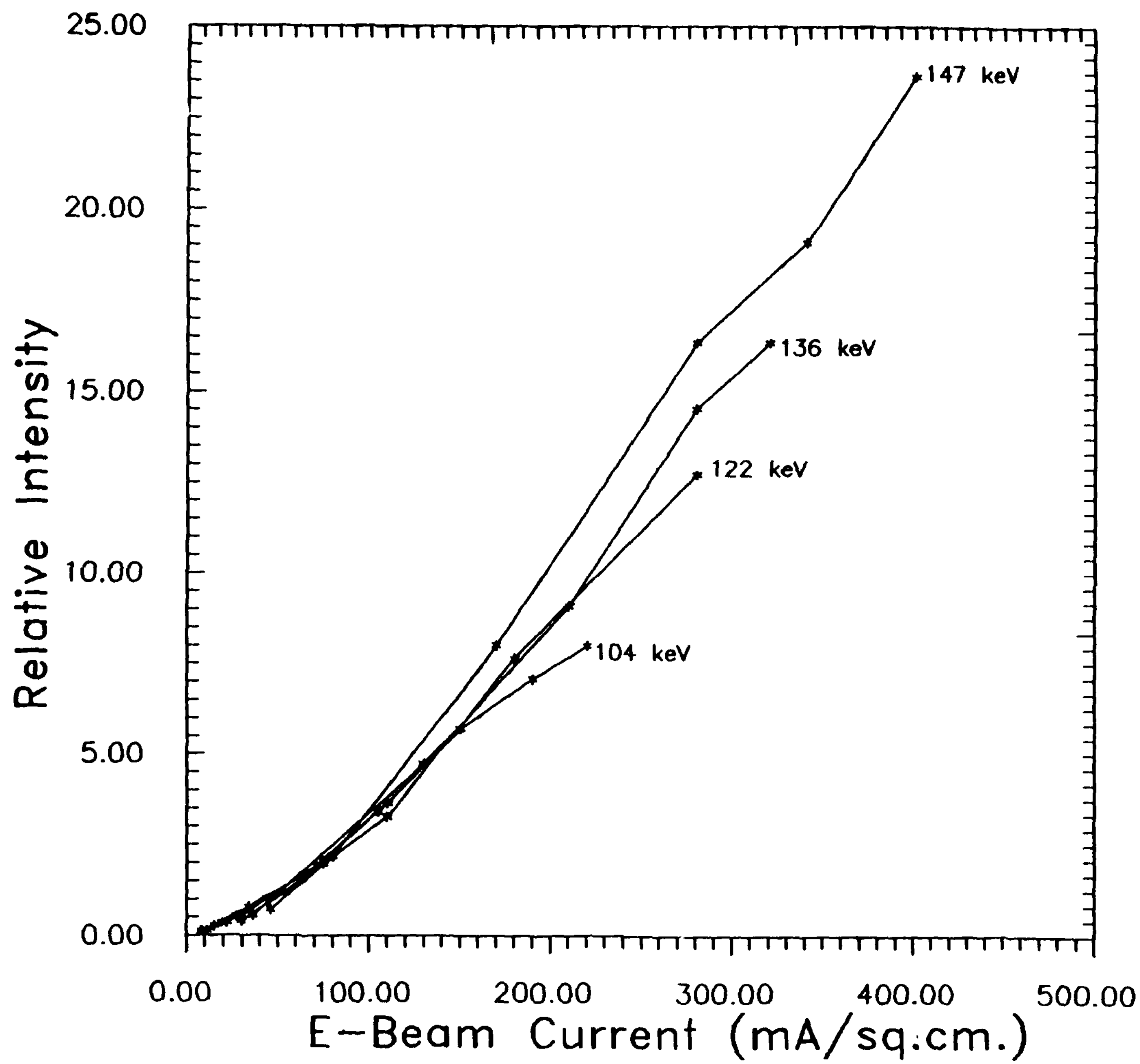

Fig. 6 Integrated Cathodoluminescense versus the Electron-Beam Current Density for Constant Electron Energies.

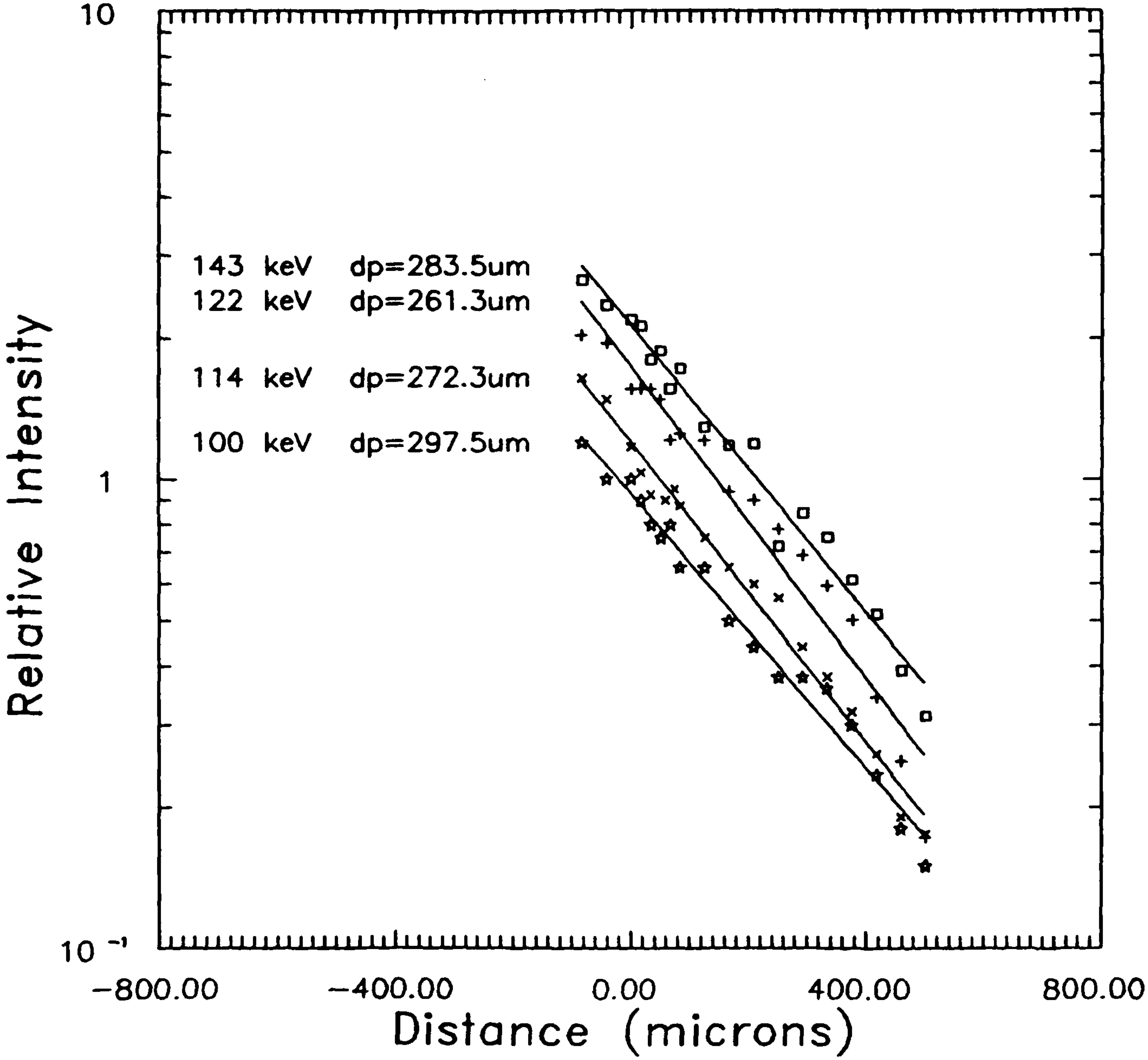

Fig. 7 Spatially resolved Cathodoluminescense intensitv for various Electron Energies with a Current Density of 75 mA/sq cm.

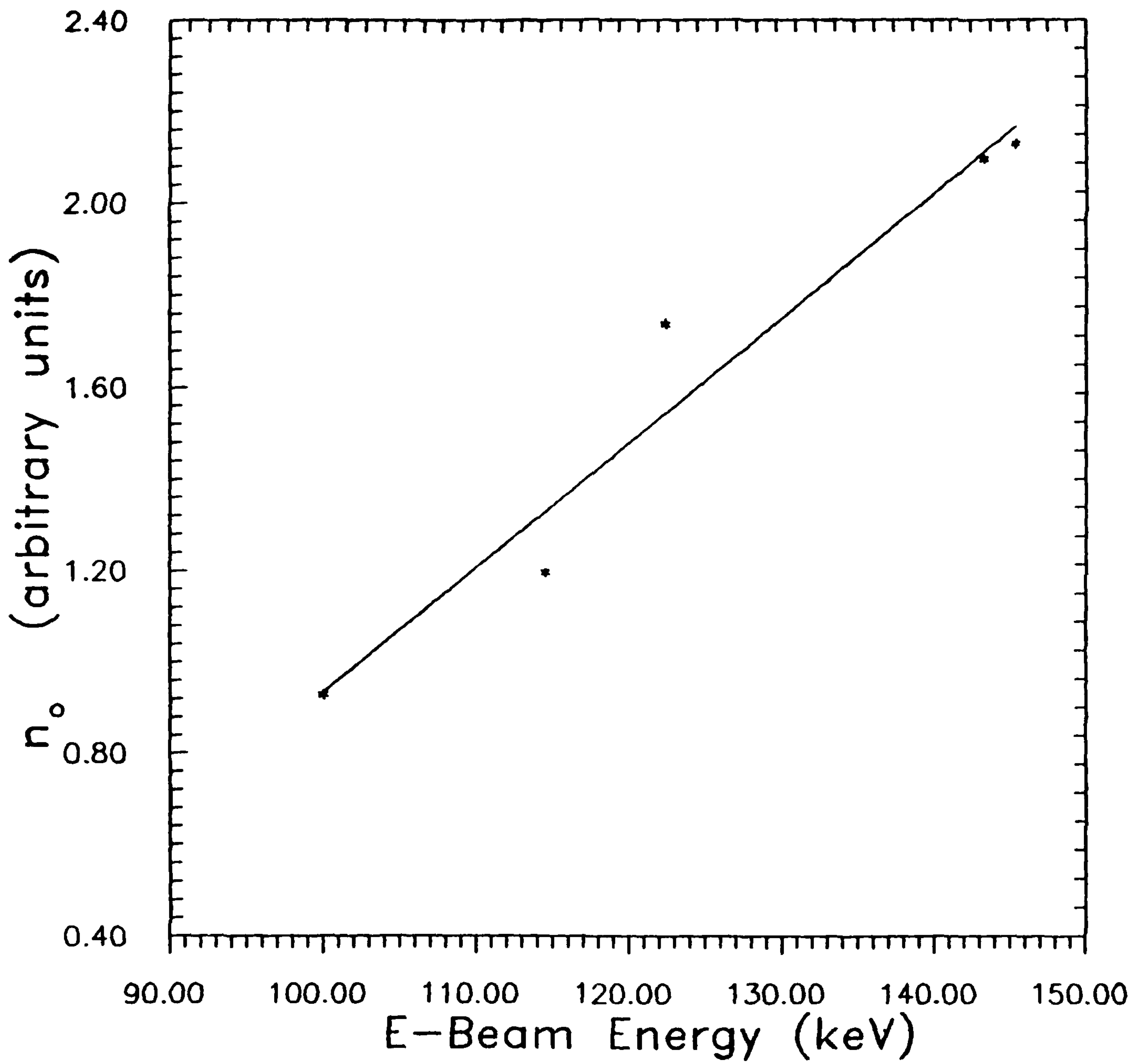

Fig. 8 n_o versus Electron Energy for a Constant Current Density of 75 mA/cm^2.

TABLE 1 MATERIAL PARAMETERS GIVEN BY THE MANUFACTURER

SAMPLE	1	2		3	
	Tail [a]	Seed	Tail	Seed	Tail
Resistivity (Ω-cm)	$6x10^6$	$1.28x10^9$	$5.11x10^8$	$2x10^8$	$4x10^8$
μ_H^6 ($cm^2V^{-1}sec^{-1}$)	6653	3911	5315	6086	5181
Type	n	n		n	
n (cm^{-3})	$1.9x10^8$	$1.25x10^6$	$2.3x10^6$	$5.13x10^6$	$3.01x10^6$
Thickness (cm)	0.065	0.063		0.052	
Added compensating impurity	None	Chromium		Carbon	
Impurity Concentration (cm^{-3})	***	$10^{15}-10^{16}$	$10^{15}-10^{16}$	$2.11x10^{15}$	$4.12x10^{15}$
Manufacturer	Spectrum Tech Inc.	MA/Com		Spectrum Tech Inc.	

a) Only tail information was given.
b) A hole mobility of 400 was assumed for this work. Also μ_e was considered to be equal to μ_H.

TABLE 2 VALUES OBTAINED FROM THE APPLICATION OF LAMPERT'S THEORY TO THE EXPERIMENTAL CURRENT vs VOLTAGE CHARACTERISTICS.

SAMPLE	1	2	3
Material	SI GaAs	Si GaAs: cr	SI GaAs: C
V_{TFL} (V)	100	$\approx$ 160	72
P_{to} (cm^{-3})	$3.4x10^{11}$	$5.8x10^{11}$	$3.8x10^{11}$
n (cm^{-3})	$5.8x10^{7}$	$5x10^{6}$	$6.2x10^{6}$
$E_c - F$ (eV)	0.580	0.656	0.649
N_t [a] (cm^{-3})	$9.6x10^{15}$	$7.8x10^{14}$	$6.8x10^{14}$
T (K)	297	301	300

a) EL2 Trap assumed at $E_c - E_t = 0.825$ eV (21)

TABLE 3 CALCULATED RESULTS USING A NONLINEAR LEAST-SQUARES FIT OF EQUATION (28) TO THE MEASURED RESISTIVITY vs TEMPERATURE DATA USING E_d, E_a and N_a / N_d AS FITTING PARAMETERS.

(Results evaluated at T = 298 K)

SAMPLE	1	2	3
Material	SI GaAs	SI GaAs:Cr	SI GaAs: C
$E_c - E_d$ (eV)	0.759	0.755	0.733
$E_a - E_v$ (eV)	0.410	0.810	0.004
N_a / N_d	4.5×10^{-4}	0.090	0.022
$E_c - F$ (eV)	0.579	0.652	0.653
n (cm^{-3})	7.4×10^{7}	4.3×10^{6}	4.1×10^{6}
p (cm^{-3})	3.7×10^{4}	6.3×10^{5}	6.7×10^{5}
Resistivity (Ω-cm)	1.3×10^{7}	3.1×10^{8}	3.9×10^{8}
Deviation of fit from experiment	0.6%	3.9%	3.2%

REFERENCES

[1] Mott, N.F. and Gurney, R.W., Electronic Processes in Ionic Crystals, Oxford Univ. Press (Clarendon), New York, p.62, 1940.

[2] Landsberg, P.T., "A Note on the Theory of Semiconductors, "Proc. Phys, Soc. London, A 65, p.604, 1952.

[3] Zucca, R., "Electrical Compensation in Semi-Insulating GaAs", Journal of Applied Physics, 48, p.1988, 1977.

PUBLICATIONS

Concepts for electron-beam and optical control of bulk semiconductor switches

K. Schoenbach, R. Germer, V. Lakdawala, K. Schmitt, and S. Albin
Department of Electrical and Computer Engineering, Old Dominion University
Norfolk, Virginia 23508-8546

Abstract

Two concepts for externally controlled bulk semiconductor switches are discussed. One concept is based on electron-beam ionization of direct semiconductors with a negative differential electron mobility region in their velocity-field strength characteristic (e.g. GaAs). The e-beam is injected through one of the contacts in direction of the applied electric field, similar to e-beam controlled diffuse discharge switches.[1] Because of the very high value of the source function (number of electrons generated per second and cubic centimeter) compared to diffuse discharge switches, the ratio of switch current to sustaining e-beam current can reach values of 10^5. Generation of excess charge carriers in the region beyond the range of the electrons is provided by absorption of recombination radiation and bremsstrahlung emanating from the e-beam excited zone. Opening of the switch is obtained by turning the e-beam off. If the switch is part of an inductive discharge circuit, the increasing field strength during opening drives the semiconductor through a negative differential mobility region into a low conductivity range, a mechanism which supports switch opening. A second switch concept is based on optical control of semiconductors, where lasers are used to drive the switch into and out of the conductive state using two different wavelengths. The direct semiconductor is doped with material which generates deep acceptor levels and is compensated with donors in shallow levels. Increase of conductivity - closing of the switch - is obtained through excitation of electrons from the occupied deep traps. Reduction of conductivity - opening of the switch - is achieved through optical hole excitation from the deep centers and subsequent direct recombination of electron-hole pairs.

Introduction

Energy storage for pulsed power devices commonly implies capacitive storage for which the state of art is relatively well developed. The components of capacitor banks, including capacitors and switches, are commercially available and relatively inexpensive. However, in terms of energy density, capacitor banks are inefficient compared to inductive storage systems. Ratios of inductive to capacitive energy density on the order of 100 seem to be obtainable by stressing the technology of coil design. The key technological problem in developing a successful inductive energy storage system with its potentially high-energy storage capability, especially if it has to be operated with a high repetition rate (≥ 10 kHz) is the opening switch.[2] Semiconductor junction devices were considered as opening switches for large inductive storage systems.[3] However, with the present solid-state opening switches (junction devices), large arrays of devices would be required, with concomitant problems in jitter, speed degradation, reliability, and cost.[4] Pulsed power semiconductor devices, where the conductivity of the bulk material is modulated through external excitation have so far been operated only as closing switches.[5]

Closing is obtained by optical generation of electron-hole-pairs through band-to-band transitions. This method allows fast on-switching. However, the use of this method for fast opening-by turning off the light source-requires short recombination life times in the semiconductor material. The correspondingly high losses during conduction, which must be compensated by means of "expensive" laser photons, limits the efficiency of such an opening switch considerably and make it useful probably only for applications where energy considerations are of secondary importance. However, if it becomes possible to use the advantages of bulk semiconductors for off-switching (scalability and reliability) and, on the other hand, increase their efficiency, these switches would become serious competitors to presently used rep-rated opening switches.

In the following, two concepts will be discussed which could lead to the use of bulk semiconductors in repetitively operated pulsed power switches: the electron-beam controlled and the laser controlled semiconductor switch.

Electron-beam controlled semiconductor switch

The earliest recorded experiments of conductivity changes in a semiconductor due to electron irradiation were published by Kronig in 1924.[6] The use of this effect for microwave power tubes and amplifiers in so-called "electron-bombarded semiconductor devices" (EBS devices) was proposed by Norris in 1968.[7] In the 1970's such tubes were developed by the Watkins-Johnson Company, Palo Alto, CA. The principle of operation is analogous to that of a semiconductor photodiode with electrons instead of photons used to generate electron-hole pairs in a reverse biased p-n junction. The electron beam is injected into the depletion region and causes carrier multiplication at the edge of the junction (cathode) to close the switch. Removal of the e-beam terminates the electron generation at the "cathode" and the switch opens. The diode is reverse biased to typically 10 to 15 percent of the hold-off voltage if it is to be used as a switch.[8] The correspondingly high field in the junction causes a rapid separation of electrons and holes. The electrons are swept across the depletion region, which extends throughout the chip, resulting in a current flow in the external circuit. The maximum current is determined by the space charge limited current condition. The holes have no effect but to provide continuity of charge. Considering the current carrier movement, the EBS device has essentially the same characteristics as vacuum tubes: a very fast response for both closing and opening; however, it is inefficient as a switch due to the large forward voltage.[8]

The experimental set up for an e-beam controlled bulk semiconductor switch as we propose it is similar to that of EBS devices. However, whereas EBS devices are related to cathode controlled vacuum tubes, where the current is carried by electrons only, our system is closely related to a diffuse plasma switch.[1] High current densities at low forward voltage drops can be obtained at very high current gains. As in diffuse discharge switches, it is possible to choose switch materials with a negative differential conductivity region which allow for forced opening in inductive energy storage systems.[2]

An experimental setup is shown in Figure 1. An electron-beam with beam energy in the 100 keV range is used to control the conductivity in a wafer of semiconducting material. The semiconductor material should have a resistivity which is high enough to prevent appreciable current flow when the electron beam is off. During a switching cycle the switch current and switch voltage vary in the following way: When the e-beam is turned on (closing phase) the semiconductor carries a large current at relatively low voltage. When the e-beam is turned off (opening phase), the conductivity decreases due to electron-hole recombination. If the semiconductor switch is part of an inductive energy storage circuit, then the voltage across the switch increases drastically during this stage.

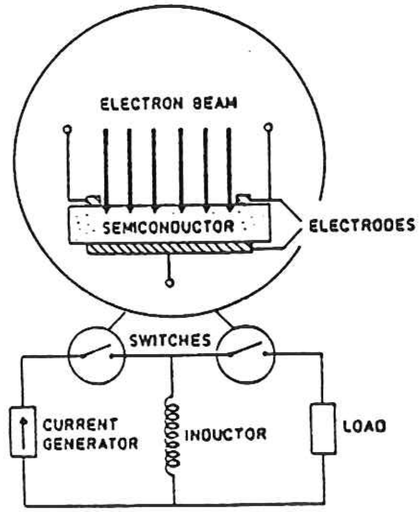

Figure 1. Electron beam controlled semiconductor switch as part of an inductive energy storage system

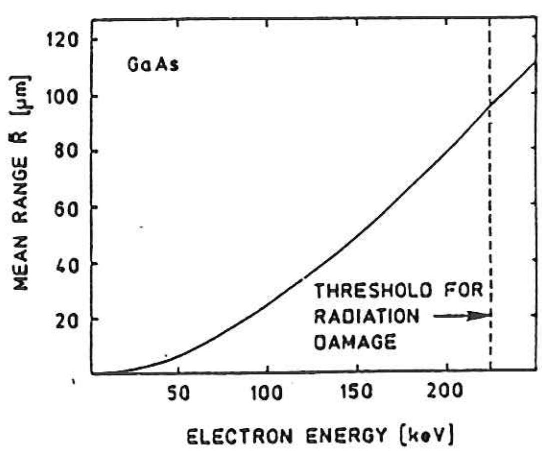

Figure 2. Electron range in GaAs as a function of electron energy

A. Steady state characteristics

In order to analyze the operation of an e-beam sustained semiconductor switch, a direct, intrinsic semiconductor (GaAs) is considered as switching material. The penetration depth or mean range of the electrons is given by[9]

$$R_o = B*E_o^{\ n} \qquad (1)$$

where E_o is the electron energy and B and n are material constants. The resultant range in GaAs is plotted versus E_o in Figure 2. The upper limit for the electron energy is given by the threshold for radiation damage in GaAs.[10]

The energy dissipation of the electron-beam in the semiconductor is not uniform. For the following analysis, however, the stopping power dW/dl is assumed to be constant (E_o/R_o). The source function S, the number of electron-hole pairs created per volume and time, is

$$S = (dW/dl)\ (J_b/eW_i) \qquad (2)$$

where J_b is the electron current density in the electron-beam and W_i is the effective ionization energy. W_i is about 5 eV for GaAs.

With present technologies the equilibrium carrier density of "pure" GaAs can be made as low as $10^{14}\,cm^{-3}$. A further reduction can be achieved through cooling. The excess electron density δn and hole density δp generated by the electron-beam can be determined by the continuity equation for a spatially homogeneous semiconductor

$$d\,\delta n/dt = d\,\delta p/dt = S - \alpha\ [(n_o + p_o)\,\delta n + \delta n^2] \qquad (3)$$

where n_o and p_o are equilibrium densities, and α is the recombination coefficient. For large excess carrier concentrations equation (3) reduces to:

$$d\,\delta n/dt = S - \alpha\,\delta n^2 \qquad (4)$$

The steady-state excess electron and hole density is

$$\delta n_o = (S/\alpha)^{1/2} \qquad (5)$$

With electrons of E_o = 150 keV in GaAs, and assuming that the recombination coefficient for direct recombination in GaAs is $10^{-7}\ cm^3/s$, the excess carrier density is given as

$$\delta n_o = 1.5 * 10^{16}\ J_b^{\ 1/2} \qquad (6)$$

with δn_o in cm^{-3} and J_b in A/cm^2. For a moderate e-beam current density of 5 mA/cm^2, the carrier density would be about $10^{15}\ cm^{-3}$. This is the density of electron-hole pairs in the layer defined by the range of electron penetration (Figure 2). Excitation of electron hole pairs in the region adjacent to this layer is obtained optically. The recombination radiation emitted in direct semiconductors is partially reabsorbed in this layer and provides for conductivity outside the electron range. Calculations on this process have been performed using GaAs emission and absorption data[11] and the results are shown in Figure 3. Another mechanism which provides for electron-hole generation in the region beyond the electron range is excitation by X-rays, which are produced when the primary electrons are slowed down in the semiconductor material. Their effect on the bulk conductivity has been calculated assuming an isotropic distribution of the thick target bremsstrahlung. The effect of the bremsstrahlung is smaller by more than one order of magnitude compared to that of recombination radiation.

The switch current density under steady-state conditions is given by

$$J_s = e\,\delta n_o\ (\mu_n + \mu_p)E \qquad (7)$$

where μ_n and μ_p are the electron and hole mobility, respectively, and E is the electric field intensity. For GaAs the electron mobility is 8000 cm^2/Vs and the hole mobility is 400 cm^2/Vs.[12] The value for the electron mobility holds in the field strength range below E = 3 kV/cm only. Above this threshold the electron mobility is approaching the value 180 cm^2/Vs due to the Ridley-Watkins-Hilsum mechanism.[13,14] Operating the semiconductor switch at a field intensity just below this threshold results in a switch current density of

$$J_s = 1.7 * 10^3 * J_b^{\ 1/2} \qquad (8)$$

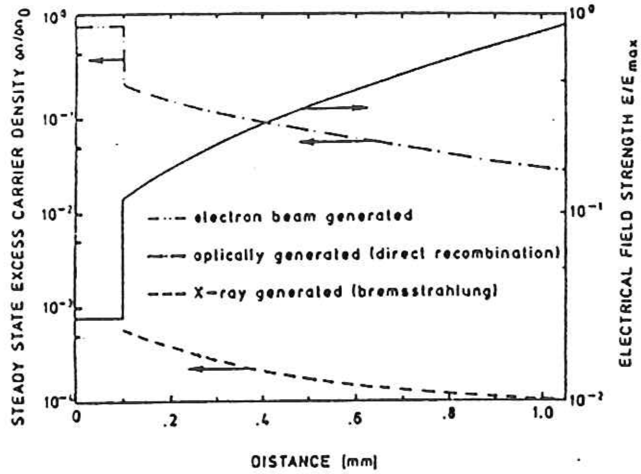

Figure 3. Spatial distribution of charge carrier density in a GaAs wafer for $J_b = 5 mA/cm^2$ and corresponding field strength E ($E \sim 1/\delta n$). It is assumed that an electron beam of about 200 keV generates a constant charge density δn over a mean range of 100 μm.

This current density is calculated by using the value of the carrier density at the edge of the semiconductor wafer of 1 mm thickness opposite to the e-beam irradiated face. At this point the electric field is maximum (see Figure 3). With J_b being 5 mA/cm^2 the switch current density is $J_s = 120\ A/cm^2$. The current gain J_s/J_b in this case is $2.4 * 10^4$, a value which exceeds the current gains obtained in diffuse discharge switches[1] by orders of magnitude.

For a thickness of 1 mm and a field of 3 kV/cm at the edge of the semiconductor, the forward voltage drop across the semiconductor wafer during conduction is $V_f = 150$ volts. The dielectric strength of the semiconductor is about 1 MV/cm for pure material, that means it should be possible to increase the voltage across the wafer to about 100 kV before the breakdown occurs. The actual hold off voltage is, however, on the order of 10 kV due to defects and thermal breakdown in the semiconductor.

B. Opening phase

For an initially high carrier concentration, the decay of the carrier density after the e-beam is turned off can be calculated by the following equation:

$$d\,\delta n/dt = -\alpha\delta n^2 \quad (9)$$

The solution of this differential equation is

$$n(t) = n_o/(1-\delta n_o \alpha t). \quad (10)$$

The 1/10 decay time T (time for n to decay to 10 percent of n_o) is, according to equation (10)

$$T = 9/(\alpha\delta n_o). \quad (11)$$

With δn_o being $10^{15}\ cm^{-3}$ in the e-beam excited range, the opening time (1/10-time) is 90 ns. It is comparable to that of the fastest, presently studied opening switches.[15]

If the GaAs semiconductor switch is part of an inductive energy storage circuit, the opening time is even shorter due to the negative differential conductivity effect in this semiconductor. When the switch opens, the voltage across it is increasing due to the increasing induced voltage across the inductance.[16] This effect drives the semiconductor through a region of negative differential mobility into a state of low electron mobility ($\mu_n = 180\ cm^2/Vs$) (Figure 4a). This effect is similar to that obtained in diffuse discharge switches (Figure 4b) with attachers having an increasing attachment rate coefficient with increasing field strength.[2] Besides reducing the opening time, an important parameter for opening switches, it also lowers the conductivity of the semiconductor in the open state.

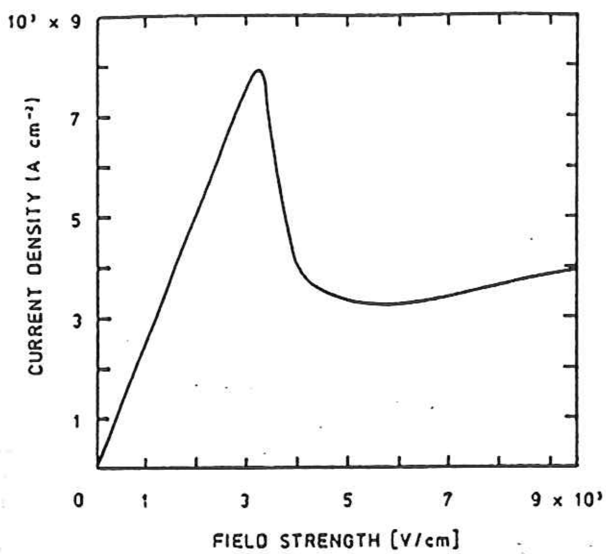

Figure 4a. Current density vs electrical field strength for GaAs.[17] The electron density is $n_e = 2*10^{15}\ cm^{-3}$.

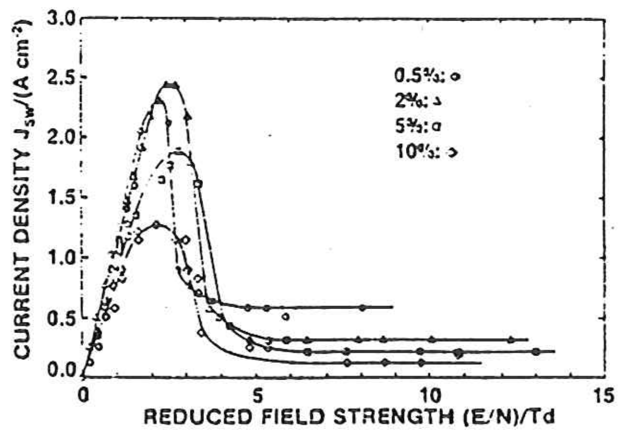

Figure 4b. Current density J vs reduced field strength E/N for an e-beam sustained discharge in argon with admixtures of C_2F_6.[18] The source function is $S = 1.3*10^{20}\ cm^{-3}\ s^{-1}$. The variable parameter is the C_2F_6 fraction.

Laser controlled semiconductor switch

The potential of photoconductive semiconductor switches for pulsed power applications is studied extensively.[5,19,20,21] Common to all these studies is that optical band to band electron-hole excitation is used to provide for high conductivity of the bulk semiconductor. If used as an opening switch, the laser has to sustain the conductivity during the time of current flow. The fundamental problem with this type of semiconductor (opening) switch is its inability to obtain both, long (microsecond) conduction and fast (nanosecond) opening with reasonable laser systems.

A concept where laser radiation is used only to turn the conductivity in the semiconductor material on and off, not to sustain it, is discussed in the following. As switch material a direct semiconductor is used (GaAs, InP). The semiconductors will be doped with material which generates deep acceptor levels and will be compensated with donors in shallow levels in order to fill the traps before switching action. An increase in the conductivity-closing of the switch-is obtained through photoexcitation of electrons into the conduction band from deep acceptor levels and subsequent electron-hole pair generation by two-photon excitation via the deep centers. Such processes have been studied at deep levels in ZnS.[22] After an initially fast drop of carrier density due to direct electron-hole recombination, the decay of electron density due to trapping is relatively slow. That means, the conductivity remains high for times long compared to the turn-on time. The opening of the switch is induced by low energy photons, which can excite the trapped holes to the valence band and stimulate their recombination with the electrons in the conduction band. Recently the existence of this switching mechanism has been proved in II-VI compound photoresistors.[23] It is planned to use copper as the material to generate deep acceptor levels. Copper is one of the most frequent impurities in III-V compounds. Studies of the direct semiconductor materials GaAs and InP show two dominant copper-related deep level defects, Cu_A and Cu_B.[24] Their position in the energy diagram is shown in Figure 5. The Cu_B levels, which are of main interest for our concept, are at 0.64 eV above the valence band for InP and at 0.40 eV above the valence band for GaAs. The band-gap energy is 1.28 eV for InP and 1.43 eV for GaAs at room temperature.

The photoionization cross sections of holes and electrons for the Cu -level were measured by Kullendorf et al.[24] They are shown in Figures 6a and 6b for InP and in Figures 7a and 7b for GaAs. For InP the onset for hole ionization is at about 0.55 eV and for electron ionization at about 0.3 eV at 112° K. Both cross sections have a peak value

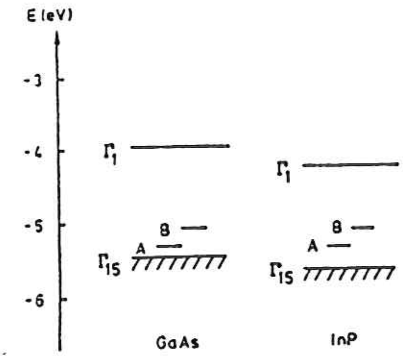

Figure 5. Summary of the Cu-related energy levels in GaAs and InP drawn on an absolute energy scale.[24]

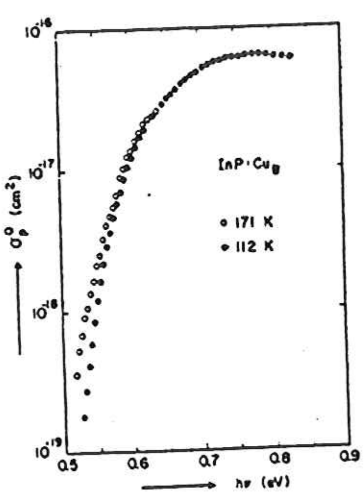

Figure 6a. Photoionization cross section of holes σ_p^o for InP:Cu_B.[24]

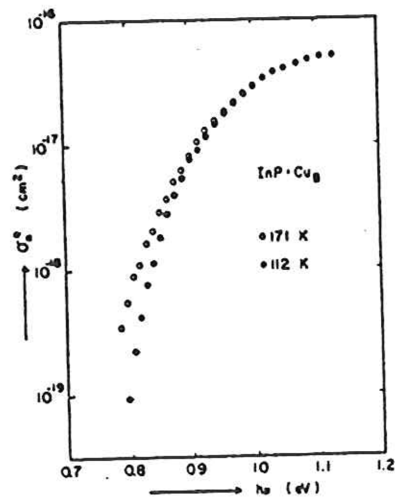

Figure 6b. Photoionization cross section of electrons σ_n^o for InP:Cu_B.[24]

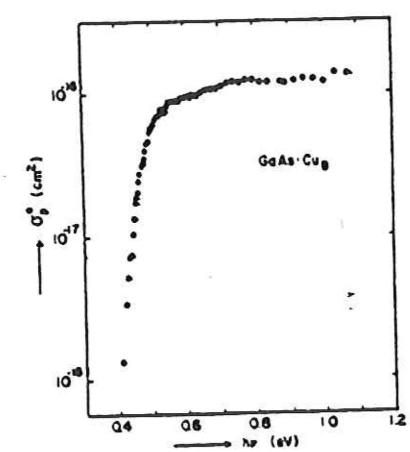

Figure 7a. Photoionization cross section of holes σ_p^o for GaAs:Cu_B at 60°K.[24]

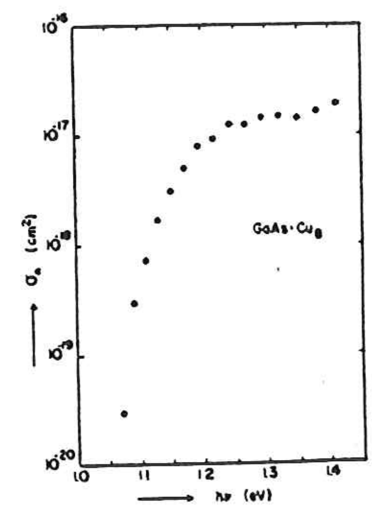

Figure 7b. Photoionization cross section of electrons σ_n^o for GaAs:Cu_B at 60°K.[24]

of about 5 * 10^{-17} cm^2. For GaAs the onset for hole ionization is at 0.4 eV, that for electron ionization is at 1.07 eV, with a peak electron cross section smaller by one order of magnitude ($10^{-17}cm^2$) than the hole ionization cross section ($10^{-16}cm^2$).

The capture cross sections for holes and electrons are 1.3 * $10^{-13}cm^2$ and 6 * $10^{-20}cm^2$ for InP:Cu_A , respectively (at T = 120° K) the hole capture cross section for InP: Cu_B is 6 x 10^{-15} cm^2 . For GaAs:Cu_B, they are 3 * $10^{-14}cm^2$ at 300 K°(decreasing slowly with increasing temperature) and 8 * 10^{-21} cm^2 at 250°K respectively (exhibiting a weak temperature dependance). For both semiconductor materials Cu generates deep acceptors.

Transient behavior of the laser controlled switch

The conductivity of the compensated semiconductor will be increased, that means the switch is turned on, by photoexcitation into the conduction band from the Cu_B level (Figure 8). The photon energy required for this process is according to Figures 6 and 7, ≥ 0.8 eV for InP and ≥ 1.1 eV for GaAs. Through this process the Cu_B level is partially depleted from electrons. For a short laser pulse (ns-range), used for the photoexcitation, the electron density in the conduction band will show a time response as sketched in Figure 9. After an initially fast decay caused by direct recombination, the remaining electron concentration, n_o , will decay with a time constant determined by the occupancy of the Cu_B centers and the electron capture cross section σ_n. The capture cross section, σ_n , is small compared to the cross section for direct electron-hole recombination. That means that the electron capture rate, $\Delta n/\tau$, is small, even for high concentrations of deep Cu_B-centers, necessary to obtain a large value of n_o during the on-state.

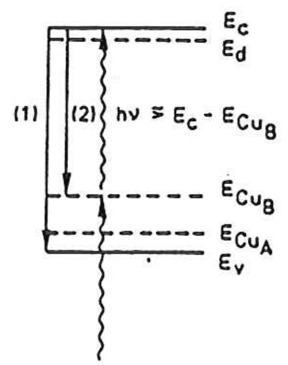

Figure 8. Two-step excitation and subsequent decay of electron density through direct recombination(1) and recombination of electrons with bound holes in the Cu_B energy level(2).

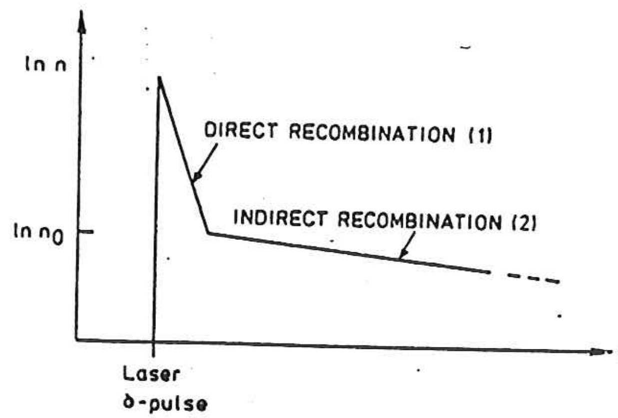

Figure 9. Decay of electron density after two-step excitation.

The conductivity of the semiconductor is decreased, that means the switch is turned off, by hole photoexcitation from the Cu_B level (Figure 10). The photon energy required for this process is according to Figures 6 and 7, 0.55 eV ≤ h ≤ 0.8 eV for InP:Cu_B and 0.4 eV ≤ hν ≤ 1.05 eV for GaAs:Cu_B . The hole excitation opens a channel for direct band-to-band recombination, a fast process which is determined by the direct recombination cross section, σ_d , and by the density of generated holes p_1 and available electrons n_1 :

$$(\Delta n/\tau) \sim \sigma_d * n_1 * p_1 \qquad (12)$$

The laser-induced initial increase in the current carrier concentration through the generation of holes should not contribute too much to the conductivity of the semiconductor, because of the relatively small mobility of holes compared to that of the electrons in InP and GaAs. The electron mobility is 8,500 cm^2/Vs in GaAs and 4,000 cm^2/Vs in InP. The hole mobility is only 400 cm^2/Vs and 100 cm^2/Vs in GaAs and InP, respectively (all values are for room temperature). The decay of the electron density is sketched in Figure 11.

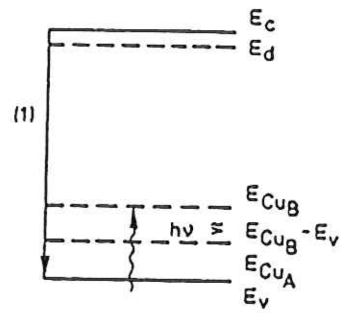

Figure 10. Optical one-step excitation and subsequent decay of hole (and electron) density through direct recombinations(1).

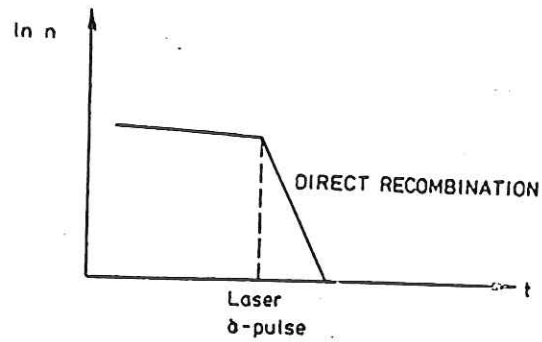

Figure 11. Decay of electron density after one-step hole photoexcitation.

Numerical calculations on the transient behavior of the optically controlled switch were performed using an algorithm similar to one developed by Hwang et al.[25] Two characteristic time constants were employed to define the electron hole recombination during the conductive phase namely: T_{MR} the main recombination time constant and T_{RA} the time needed for readjustment of charges on the recombination centers to a condition enabling equal capture rates of electrons and holes.[26,27] The deep level impurity (Cu) concentration was assumed to be 10^{17} cm^{-3}. Counter doping with Si was considered, which has a shallow donor energy level of 0.0058 eV below E_C in GaAs. Using the charge neutrality criterion it is seen that, under thermal equilibrium, the number densities of electrons are $n_o = 4 * 10^9$ cm^{-3}, of holes $p_o = 1.38 * 10^3$ cm^{-3} and of trapped electrons $n_T = 10^{17}$ cm^{-3} . The sample is therefore very weakly n-type. The resistivity of the sample at this concentration is approximately 10^6 Ωcm.

Turning on is accomplished by two step photoexcitation as described earlier in this section. The cross section for optical hole ionization is one order of magnitude higher than that for electron ionization for the copper level. Therefore, of the 10^{17} cm^{-3} electrons generated, $9 * 10^{16}$ cm^{-3} electrons will be excited from the valence band, leaving $9 * 10^{16} cm^{-3}$ holes. $1 * 10^{16} cm^{-3}$ will be excited from the impurity level. These conditions were used as initial conditions for the turn-on, turn-off calculations.

Of the initially generated 10^{17} cm^{-3} electrons, $9 * 10^{16}$ cm^{-3} electrons recombine rapidly (in about 20 ns) with valence band holes. The remaining 10^{16} electrons per cm^3 decay much slower with a recombination time constant in the order of 1 ms. The switch therefore remains in conductive state for times long compared to the turn on time. The current density obtained at an electron concentration of 10^{16} cm^{-3} is $8 * 10^3$ A/cm^2 , assuming a field strength of 500 V/cm and an electron drift velocity of $5 * 10^6$ cm/s.[28] Turn off time calculations were performed assuming a direct recombination coefficient of 10^{-7} cm^3 s^{-1}. In about 70 ns the electron concentration decays by three orders of magnitude resulting in an opening action.

It should be noted that these values of turn on and turn off times are calculated neglecting any radiation process which could lead to subsequent excitation and therefore increase the times for turn on and turn off. The large values of current densities might also cause instabilities which will not allow conduction for long time periods. In the analysis performed these effects are neglected. However, with all these constraints the type of switch is still very promising for pulsed power applications. The advantages of this type of laser-controlled switch are as follows:

1. High control efficiency, since the control processes are resonant and the laser is only used to drive the switch in or out of the conductive state, not to sustain the current carrier density;

2. High opening speed of the switch, determined by direct photoluminescence processes; and

3. Possibility of using commercially available rep-rated, high-power infrared lasers for the optical control.

Summary

Both semiconductor switches, discussed is this paper, are characterized by a very high control efficiency. In the case of the e-beam controlled switch, e-beam currents of less than 1 A are required to sustain switch currents of tens of kA. For the proposed laser controlled switch, laser energy is only needed to turn the switch on and off. In order to design these switches and to determine their limitations, it is necessary to study carrier generation and transport processes in direct semiconductors at high carrier concentrations and elevated temperatures. Furthermore more extensive investigation of deep level impurities at high concentrations have to be performed. If these studies show that the proposed schemes can be extrapolated and engineered in the high-power, high-repetition-rate, long-life regimes, this research on externally controlled bulk semiconductors could lead to a new generation of pulsed power switches.

Acknowledgement

This work is supported by the U. S. Army Research Office, the Air Force Office of Scientific Research and the Office of Naval Research.

References

1. Schaefer, G., Schoenbach, K. H., "A Review of Diffuse Discharge Opening Switches," IEEE Trans. Plasma Sci., Vol. PS-14, pp. 561-574. 1986.

2. Schoenbach, K. H., Schaefer, G., Kristiansen, M., Hatfield, L. L., Guenther, A. H., "Concepts for Optical Control of Diffuse Discharge Opening Switches," IEEE Trans. Plasma Sci., Vol. PS-10, pp. 246-251. 1982.

3. Parsons, W. M., "A Comparison between an SCR and a Vacuum Interrupter System for Repetitive Opening," Proc. Workshop on Repetitive Opening Switches, pp. 246-258. 1981.

4. Weiner, M., "Group Report on Solid State Opening Switches," Proceedings, Solid State Switches for Pulsed Power, ed. by W. Portnoy and M. Kristiansen, Tamarron, CO, pp. 189-201. 1983.

5. Nunnally, W. C., "Photoconductive Pulse Power Switches: A Review," Proc. 5th IEEE Pulsed Power Conf., Arlington, VA, pp. 235-241. 1985.

6. Kronig, R. L. de, "Change of Conductance of Selenium due to Electronic Bombardment," Phys. Rev., Vol. 24, pp. 377-382. 1924.

7. Norris, C. B., Jr., "The Capabilities of Electron-Beam Semiconductor Active Devices," Proc. IEEE Tube Tech. Conf., New York. 1968.

8. Burkes, T. R., A Critical Analysis and Assessment of High Power Switches, 2nd ed., NSWC, Dahlgren, VA, to be published (personal communication). 1986.

9. Katz, L., Penfold, A. S., "Range-Energy Relations for Electrons and the Determination of Beta-Ray End-Point Energies by Absorption," Rev. Mod. Phys., Vol. 24, pp. 28-44. 1952.

10. Ehrenberg, W., Gibbons, D. J., Electron Bombardment Induced Conductivity, Academic Press 1981.

11. Seeger, K., Semiconductor Physics, Springer Verlag 1973.

12. Liao, S. Y., Microwave Devices and Circuits, Prentice-Hall 1980.

13. Ridley, B. K., Watkins, T. B., "The Possibility of Negative Resistance Effects in Semiconductors," Proc. Phys. Soc., Vol. 78, pp. 293-304. 1961.

14. Hilsum, C., "Transferred Electron Amplifiers and Oscillators," Proc. IEEE, Vol. 50, pp. 185-189. 1962.

15. Schoenbach, K. H., Schaefer, G., Kristiansen, M., Krompholz, H., Harjes, H. C., Skaggs, D., "An Electron-Beam Controlled Diffuse Discharge Switch," J. Appl. Phys., Vol. 57, pp. 1618-1622. 1985.

16. Schoenbach, K. H., Kristiansen, M., Schaefer, G., "A Review of Opening Switch Technology for Inductive Energy Storage," Proc. IEEE, Vol. 72, pp. 1019-1040. 1984.

17. Butcher, P. N., Fawcett, W., "The Intervally Transfer Mechanism of Negative Resistivity in Bulk Semiconductors," Proc. Phys. Soc., Vol. 86, pp. 1205-1219. 1965.

18. Schaefer, G., Schoenbach, K. H., Kristiansen, M., Strickland, B. E., Korzewa, R. A., Hutcheson, G. Z., "Influence of the Circuit Impedance of an Electron-Beam Controlled Diffuse Discharge with a Negative Differential Conductivity," Appl. Phys. Lett., Vol. 48, pp. 1776-1779. 1986.

19. Morse, J. D., Pocha, M. D., "Characteristics and Modeling of High Voltage Photoconductive Switching Deivices," IEEE Conference Record of the Seventeenth Power Modulator Symposium, Seattle, WA, pp. 211-213. 1986.

20. Zutavern, F. J., O'Malley, M. W., "Engineering Limits of Photoconductive Semiconductor Switches in Pulsed Power Applications," IEEE Conference Record of the Seventeenth Power Modulator Symposium, Seattle, WA, pp. 214-218. 1986.

21. Bovino, L., Youmans,R., Weiner, M., Burke, T., "Optically Controlled Semiconductor Switch for Multi-Megawatt Rep-Rated Pulsers," IEEE Conference Record of the Seventeenth Power Modulator Symposium, Seattle, WA, pp. 219-223. 1986.

22. Broser, I., Germer, R., Seliger, F., Schulz, H.-J., "Luminescence of an M Center in ZnS," J. Phys. Chem. Solids, Vol. 41, pp. 101-107. 1980.

23. Germer, R., Pronko, S. and Schoenbach, K. H., to be submitted to Appl. Phys. Lett.

24. Kullendorf, N., Jansson, L., Ledebo, L.-A., "Copper-Related Deep Level Defects in III-V Semiconductors," J. Appl. Phys., Vol. 54, pp. 3203-3312. 1983.

25. Hwang, B.-Y., Lindholm, F. A., Hammond, R. B., "Methodology for Calculating Turn-Off Transients of Photoconductive Circuit Elements in Picosecond Optoelectronics," IEEE J. of Quantum Electronics, Vol. QE-19, pp. 648-657. 1983.

26. Sandiford, D. J., "Carrier Lifetime in Semiconductors for Transient Conditions," Phys. Rev., Vol. 105, p. 524. 1957.

27. Wertheim, G. K., "Transient Recombination of Excess Carriers in Semiconductors," Phys. Rev., Vol. 109, pp. 1087-1091. 1958.

28. Sze, S. M., Physics of Semiconductor Devices, John Wiley and Sons 1981.

SIMILARITIES BETWEEN CAVITATION EXPERIMENTS AND ELECTRICAL BREAKDOWN

R. GERMER* and K.-H. SCHOENBACH
DEPARTMENT OF ELECTRICAL AND COMPUTER ENGENEERING
OLD DOMINION UNIVERSITY
NORFOLK, VA 23508, USA

Cavitation has been produced in several liquids using ultrasound of 37 to 100 kHz and shockwaves. The spatial distribution of the bubbles has been investigated with stroboscopic tv-techniques using 20 ns spark flashes and with soft X-ray flash (100 ns) photography. Depending on the type of liquid and certain experimental control parameters, the bubbles arrange either in a periodic pattern or they are distributed chaotically. Fig.1 shows an X-ray flash shadow photograph of two exploding wires (W-bright) in a liquid (L-dark) between solid plates. The plates are accelerated by the explosion and the volume between them is enlarged. The enlarged volume cannot be filled with the liquid. At a distance of >10mm to the explosion, cavitation is induced by the seperating plates. One control parameter of the experiment is the speed of local volume increase between the plates. This increase depends on the energy density of the explosion and on the distance to it. The picture shows that outside the bubble-free liquid L bright bubbles appear with different density. This can be seen by differences in the average brightness throughout the bubble area. Furthermore the symmetry and regularity of the more or less bright areas should be noticed. Detailed studies show/1/, that the distance between neighboring bubbles may be constant, change in steps or change irregularly. A simple model which explains periodic and chaotic behaviour has been developed. The idea is that a bubble appears if streaming in the liquid to fill the expanding volume reaches acceleration values that adhesive forces between the liquid molecules cannot balance. In a one dimensional system like a sawtooth generator this idea leads to periodic oscillations. In systems with more dimensions chaotic behaviour is possible. The cavitation model can be represented by an electrical equivalent circuit consisting of coupled R-C oscillators (see Fig.2). The constant charge current is equal to the volume increase. The capacitance and the resistor represent the ability of the liquid to fill the volume by expansion and streaming. The breakdown voltage of the discharge device is equal to the cavitation threshold. Numerical studies have been performed to understand the properties of the circuit. This is of interest to describe the breakdown mechanism and filamentation in gases and semiconductors with respect to their application in pulsed power switches. Fig. 3 shows the result for the approximated iteration formula

$$X(n+1) = (X(n)*(1+B^2)-X(n)^{2/3}*B*A*2+X(n)^{1/3}*A^2)^{1/2} *2$$

The hysteresis characteristic disappears for another system, represented by

$$X(n+1) = (X(n)*(X(n)*(1+B^2)-X(n)^{2/3}*B*A*2+X(n)^{1/3}*A^2))^{1/2} *2$$

Then the limits move to zero or infinity, if the iteration of the initial conditions do not result in a series which convert to the chaotic branch.

* Author is on leave of absence from Fritz-Haber Institut/MPG and Technische Universitaet Berlin, GERMANY

Acknowledgement :

The authors thank Prof. G.Hildebrandt (FHI/MPG) and Prof. M.Heckl(ITA/TUB) for their support. The work was furthermore supported by the U.S. Air Force Office of Scientific Research

References :

1 R. Germer, Structure and Chaos in the spatial Arrangement of Seeds of a Phase Transition, submitted to Phys.Rev.

Figures :

Figure 1
X-ray flash photography of wire explosions in layers of liquid between solid plates. a) Experimental arrangement, b) Shadow photography, showing the explosion plasma (W-bright) of two crossed wires, compressed liquid (L-dark) and liquid with cavitation bubbles (B) in the surrounding

Figure 2
Coupled RC-sawtooth oscillators used for numerical studies

Figure 3
Chaotic behaviour of a two parameter system

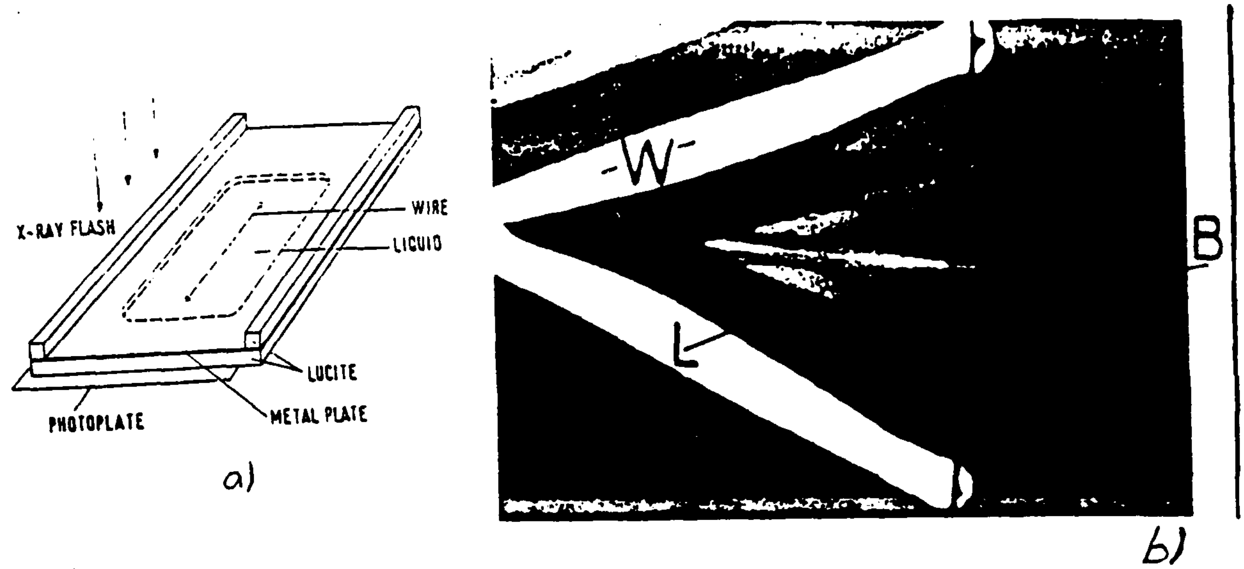

Figure 1
X-ray flash photography of wire explosions in layers of liquid between solid plates. a) Experimental arrangement, b) Shadow photography, showing the explosion plasma (bright) of two crossed wires, compressed liquid (dark) and liquid with cavitation bubbles in the surrounding

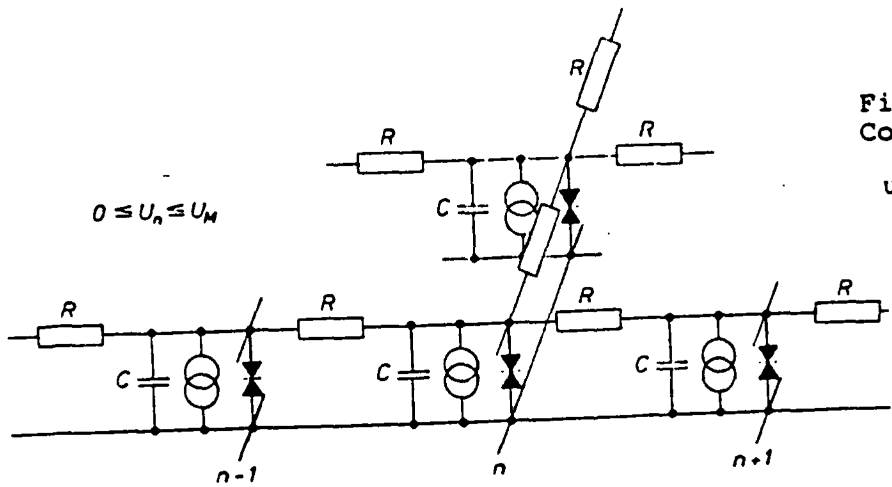

Figure 2
Coupled RC-sawtooth oscillators used for numerical studies

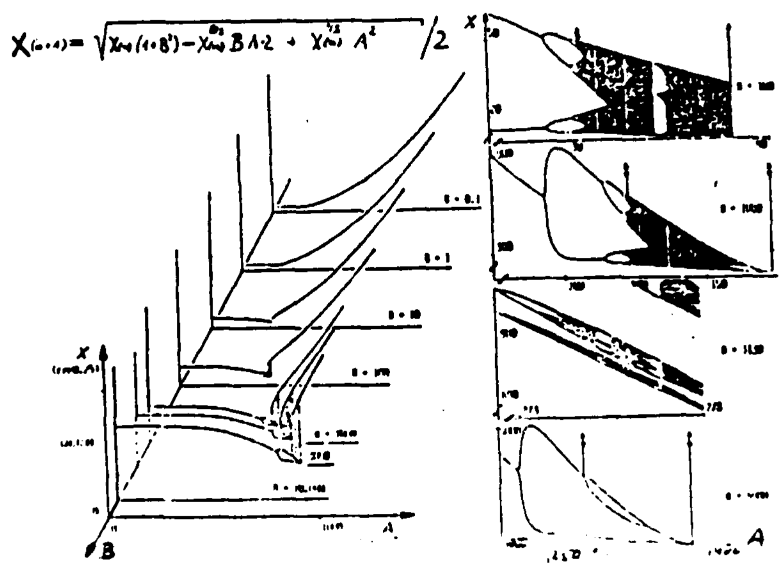

Figure 3
Chaotic behaviour of a two parameter system

Nuclear Physics B (Proc. Suppl.) 2 (1987) 569
North-Holland, Amsterdam

SIMILARITIES BETWEEN CAVITATION EXPERIMENTS AND ELECTRICAL BREAKDOWN

R. Germer and K.-H. Schoenbach

Old Dominion Univ. Dept. ECE, Norfolk, VA 23508 & Fritz-Haber Inst./TUB, D-Berlin

Cavitation has been produced in several liquids using ultrasound of 37–100 kHz and shockwaves. The spatial distribution of the bubbles has been investigated with stroboscopic tv-techniques and with soft X-ray flash photography. The bubbles arrange either in a periodic pattern or they are distributed chaotically. Fig. 1 shows an X-ray flash shadow photograph of 2 exploding wires (W-bright) in a liquid (L-dark) between solid plates. The plates are accelerated perpendicular to the photoplate by the explosion. At a distance of >10mm to the explosion, cavitation is induced by the separating plates. One control parameter of the experiment is the speed of local volume increase, which depends on the distance to the explosion. Outside the dense liquid L bright bubbles B appear with different density. Magnification shows that the distance between neighboring bubbles may be constant, change in steps or change irregularly. The idea of a simple model is that a bubble appears if streaming in the liquid to fill the expanding volume reaches acceleration values that adhesive forces between the liquid molecules cannot balance. In sawtooth generators (d=t=1) the breakdown leads to periodic oscillations, in systems with higher dimension d chaotic behaviour is possible. The cavitation model can be represented by an electrical equivalent circuit consisting of coupled R-C oscillators. This circuit is of interest to describe the breakdown mechanism and filamentation in gases and semiconductors used for pulsed power switches. Fig. 2 shows numerical results for the distance between bubbles or breakdowns.

ACKNOWLEDGMENT: The authors thank Prof. G. Hildebrandt (FHI/MPG) and Prof. M. Heckl (ITA/TUB) for their support and furthermore the U.S. A.R.O. and A.F.O.S.R.

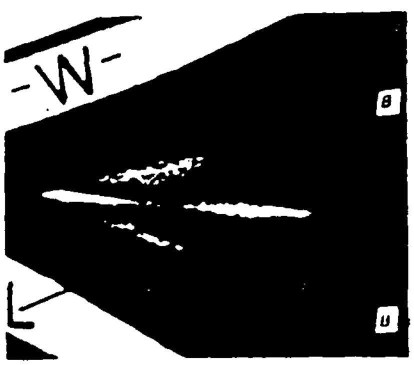

Fig. 1

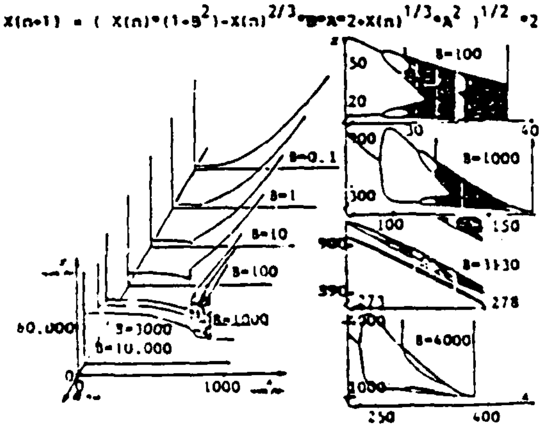

Fig. 2

0920-5632/87/$03.50 © Elsevier Science Publishers B.V.
(North-Holland Physics Publishing Division)

ELECTRON-BEAM CONTROLLED SEMICONDUCTOR OPENING/CLOSING SWITCH

Klemens B. Schmitt, Karl H. Schoenbach, Thomas J. Powers, and Rudolf K.F. Germer
Department of Electrical and Computer Engineering
Old Dominion University, Norfolk, VA 23529-0246

Abstract

The concept of an electron-beam controlled high power semiconductor switch is discussed. A high energy electron-beam (E_0 = 50 to 200 keV) is injected through one of the contacts (cathode) of a direct semiconductor wafer and generates an electron-hole plasma in a layer of typically 10 to 100 μm thickness. Generation of electron-hole pairs in the bulk of the semiconductor is provided by recombination radiation from the electron-beam excited layer and by X-rays (bremsstrahlung). The bulk ionization allows to overcome space-charge limitation in the semiconductor switch and to attain large current densities at low forward voltages. Current and voltage characteristics of GaAs and CdS samples were measured, with emphasis on GaAs. A current gain (ratio of switch current to electron-beam current) of 10^3 was obtained for GaAs when irradiated with 200 keV electrons. In this configuration the current was still space-charge limited. It is shown that the space-charge limitation can be overcome by proper doping of the electron-beam activated shallow layer in the semiconductor sample.

Introduction

Experiments on conductivity changes in semiconductors due to electron irradiation were first published by Kronig in 1924 [1]. This effect was used for microwave power tubes and amplifiers in so-called "Electron-Bombarded Semiconductor (EBS) Devices" [2]. The operation is based on the external injection of electrons into a reverse biased junction, generating electron-hole pairs (EHP's) at the edge of the junction (cathode). The high field in the junction causes a rapid separation of electrons and holes. The electrons are swept across the depletion region, resulting in a current flow in the external circuit. The holes have no effect but to provide continuity of charge. Due to the fact that in an EBS device the current is space-charge limited, relatively large forward voltages are needed to obtain high current densities.

The principle of operation of the electron beam controlled semiconductor switch discussed in this paper is based on EHP generation in the bulk of the semiconductor material by recombination radiation. This eliminates the space-charge limitation for the current. In this aspect it is closely related to a diffuse plasma switch [3].

The switch concept is shown in Figure 1. In the switch 'off state' the semiconductor should have a resistivity which is high enough to prevent appreciable current flow. Semi-insulating GaAs can be used, which has a resistivity of about 10^6 Ωm. In order to close the switch, an electron-beam is injected into a semiconductor wafer generating EHP's by impact ionization within the range of the electrons. In case of GaAs, the electron energy should be less than 220 keV due to the threshold for radiation damage in this material [4]. This limits the range for direct impact generation of EHP's to a region of about 100 μm depth.

Generation of EHP's in the region adjacent to this region can be obtained optically by using direct semiconductors (i.e. GaAs). The recombination radiation emanating from the electron-beam excited layer is partially reabsorbed in the bulk of the material, generating an electron-hole plasma beyond the range of the electron-beam. Additional ionization is provided by X-rays, which are produced when the beam electrons are slowed down in the semiconductor. By ionizing the entire bulk of the semiconductor, the space-charge limitation is abolished. This means that the semiconductor can carry large currents at relatively low voltages (closing phase). The indirect (optical) generation of EHP's also allows for larger thickness of the bulk material far in excess of the electron range thus allowing high hold-off voltages.

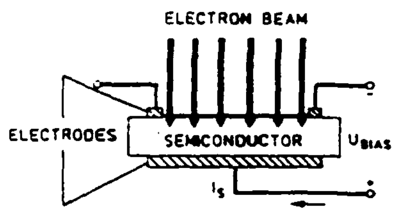

Figure 1. Electron-beam controlled bulk semiconductor switch.

When the electron-beam is turned off, the conductivity of the bulk material decreases due to electron-hole recombination (opening phase). Due to its negative differential mobility region, GaAs is a suitable material for opening switches which are part of an inductive storage circuit. When the switch opens, the voltage across it increases due to the increasing induced voltage across the inductance [5]. This effect drives the semiconductor from a region of high electron mobility to a state of low mobility. The effect is similar to that obtained in diffuse discharge switches where attacher gases are used which have an increasing attachment rate coefficient with increasing field strength [6].

Design Considerations

Bulk Ionization by Electron Impact In order to evaluate the operation of the switch, the basic equations for the generation of charge carriers in the irradiated semiconductor (GaAs) are discussed. The mean range R_0 of electrons in the target is given by [7]

$$R_0 = B * E_0^n \quad (1)$$

where E_0 is the electron energy and B and n are material constants. The range R_0 as a function of E_0 is plotted in Figure 2 for GaAs.

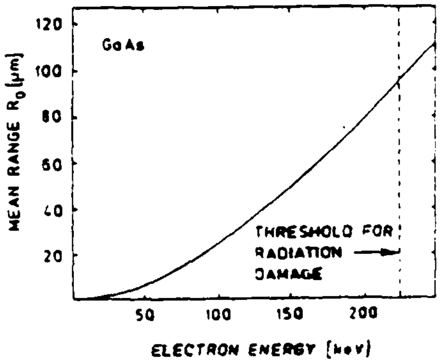

Figure 2. Mean electron range in GaAs as a function of initial electron energy, E_0.

The source function S_b, the number of electron-hole pairs created per volume and time by the electron beam, is

$$S_b = (dW/dx) * (J_b/e\ W_i) \qquad (2)$$

where e is the electron charge, J_b is the electron-beam current density and W_i the effective ionization energy. W_i is 4.3 eV for GaAs [8].

Assuming that the differential energy loss, dW/dx, is constant within the mean range R_o leads to the following expression for the source function:

$$S_b = (E_o/R_o)*(J_b/e\ W_i) \qquad (3)$$

The excess charge carrier density δn can be approximated by the following rate equation for a spatially homogenous semiconductor.

$$d\delta n/dt = S - \alpha_{rd}*\delta n*\delta p - \alpha_{ri}*\delta n*n_{ri} \qquad (4)$$

S is the source function, δn and δp are the excess electron and hole density respectively, n_{ri} is the density of the recombination centers.

n_{ri} is about $10^{15} cm^{-3}$ [9] for the semi-insulating GaAs samples used in the experiments. α_{rd}, α_{ri} are the recombination coefficients for direct and indirect recombination. The value of α_{rd} is about $10^{-10} cm^3/s$ [10]. Measurements revealed a value of about $10^{-7} cm^3/s$ for α_{ri}. This means that recombination due to recombination centers is the dominant process and the term which describes direct recombination can be neglected in equation (4). For steady state the excess charge carrier density can therefore be approximated by:

$$\delta n_o = S/(\alpha_{ri} * n_{ri}) \qquad (5)$$

For a moderate electron-beam current density of $10\ mA/cm^2$ and $E_o = 200$ KeV the corresponding excess charge carrier density δn_o in the layer defined by the range R_o of the electrons is about $4*10^{15} cm^{-3}$. The switch current under steady state conditions is given by

$$J_s = e*\delta n_o*(\mu_n+\mu_p)*E \qquad (6)$$

where μ_n and μ_p are the electron and hole mobility, respectively, and E is the electric field strength. For GaAs the electron mobility is $8000\ cm^2/Vs$, and the hole mobility is $400\ cm^2/Vs$ [11]. The value for the electron mobility holds in the field strength range below $E = 3kV/cm$. Above this threshold μ_n is approaching the value $180\ cm^2/Vs$ [11].

Bulk Ionization by Recombination Radiation In direct semiconductors like GaAs, the recombination radiation emanating from the electron beam excited layer is partially absorbed in the bulk of the semiconductor. This provides an electron-hole plasma. The spectral distribution of the recombination radiation and quantum efficiency is drastically influenced by doping [12]. This has been confirmed experimentally by irradiating n-doped GaAs wafers having different doping levels with 200 keV electrons. With undoped semi-insulating GaAs wafers recombination radiation emitted from the wafer surface opposite to the electron-beam irradiated surface was not observed. This means radiation does not provide for sufficient conductivity in the bulk of the wafer.

Figure 3 shows the optical absorption coefficient α for undoped GaAs. The absorption length $1/\alpha$ near the bandgap changes by more than three orders of magnitude within an interval of 0.05 eV. Calculations have been performed on the absorption of recombination radiation "matched" to the absorption coefficient of undoped material to provide EHP generation up to a depth of about ten times the range of the electrons. The recombination spectrum considered, which corresponds to p-doped GaAs with a doping concentration, $n_d = 10^{18} cm^{-3}$ [13], is shown in Figure 3.

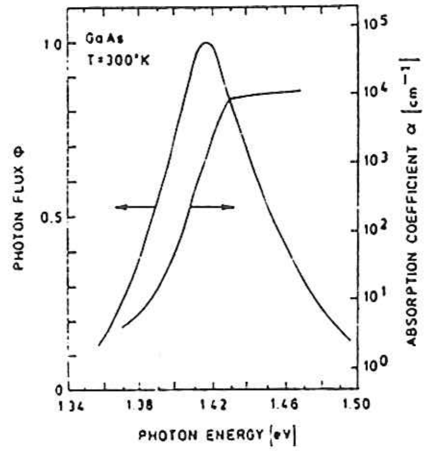

Figure 3. Recombination spectrum of p-doped GaAs, $n_d = 10^{18}\ cm^{-3}$, [13], and absorption coefficient of undoped GaAs [14].

It is assumed that the semi-insulating GaAs wafer is doped to a depth which corresponds to the mean range of the electrons. For the calculation it is further assumed that the internal quantum efficiency in the doped material is one and that absorbed photons are not again converted into optical energy. Figure 4 shows the corresponding spatial distribution of the excess charge carrier density δn_o.

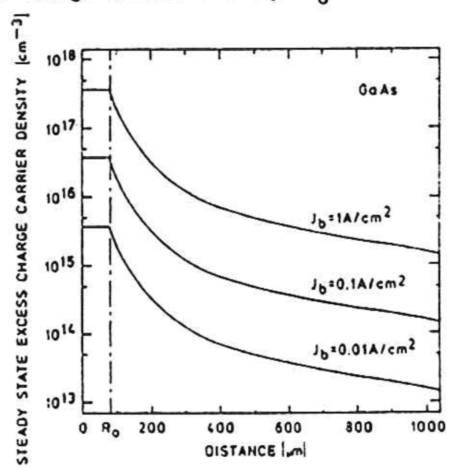

Figure 4. Spatial distribution of charge carrier density due to electron impact and absorption of recombination radiation for $E_o = 200$ keV.

Calculations show that the additional EHP density generated by bremsstrahlung is smaller by more than one order of magnitude compared to that which is optically generated.

Experimental Set-Up

The experimental set-up is shown in Figure 5. The electron-beam is produced by a pulsed thermionic diode. The high voltage pulse is generated by a pulse forming network (PFN) consisting of a LC-chain and is stepped up in a ratio 1:11 by a pulse transformer. The pulse duration can be adjusted between $1 \mu s$ and $20\ \mu s$ by varying the number of PFN segments. The diode voltage is limited to 220 kV by the pulse transformer rating.

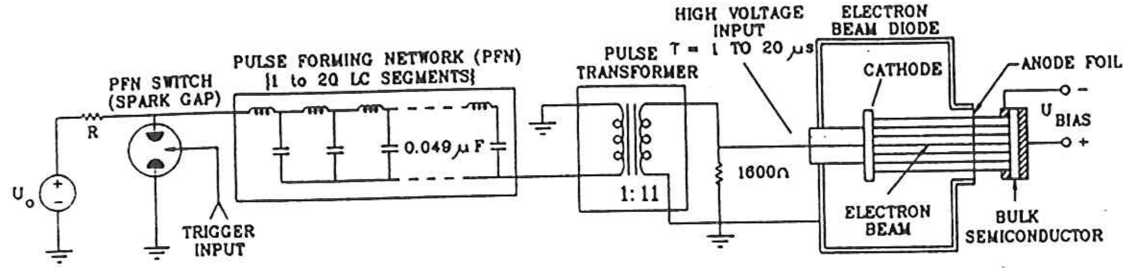

Figure 5. Experimental set up of the 200 kV electron-beam system.

A 200 keV electron-beam is transmitted through an anode foil (1 mil titanium) and irradiates the semiconductor target which is placed outside the diode vacuum chamber. The average electron energy, after passing the foil, is greater than 80% of the initial energy [15]. Figure 6a shows the electron beam current measured with a 50 Ω Faraday Cup. The rise and fall time of the electron-beam current is limited to about 400 ns due to the frequency characteristics of the pulse transformer.

Since it is desirable to use a high resistivity material, so that the switch current in the off-state is low, undoped semi-insulating GaAs is used for the bulk of the semiconductor. The material is semi-insulating due to a relatively large concentration of deep-level impurities. Wafers up to 4" diameter and between 0.4 and 0.6 mm thickness are commercially available. GaAs wafers with Schottky contacts (Al) and ohmic contacts (Au:Ge:Ni) have been tested. Additionally CdS samples have been used. The current voltage characteristics and the temporal response of different irradiated bulk semiconductors have been investigated.

Experimental Results

Figure 6b and 6c show the bulk currents, I_S, of GaAs and CdS samples generated by an electron-beam pulse shown in Figure 6a. For both samples the leading edge of the bulk current signal follows closely the electron-beam current (within 100 ns). The switch current in GaAs decreases within 150 ns of the decrease in the electron-beam current, indicating a fast recombination of EHP's. The decay of conductivity after laser irradiation of the same material was measured to be less than 50 ns. In the case of CdS, the bulk current initially drops in less than 500 ns to about 50% of its peak value and then decays exponentially with a time constant of greater than 10 μs. This slow decay is due to the traps in the material.

GaAs with ohmic contacts showed the highest switch current values. Figure 7 shows the switch current density J_S as a function of the biasing voltage for different electron-beam current densities J_b. The data are obtained by irradiating an undoped GaAs target with an area of 1 cm^2 and a thickness of 0.5 mm. For J_b=0, the current density J_S is determined by the intrinsic resistance of the GaAs wafer which is about 25 kΩ. For J_b = 16 mA/cm^2, J_S is about 10 A/cm^2 at 300V. This corresponds to a change in resistance due to irradiation of almost three orders of magnitude. However, the switch current is still space-charge limited. This is indicated by the current-voltage curves, which show a nonlinear behavior characteristic for space-charge limited currents [16], and also by the absolute value of the current. According to equation (6) the current density in case of a homogeneous bulk ionization with $\delta n_o = 10^{15} cm^{-3}$, U_{Bias} = 100V and d = 0.5mm should be $J_S > 2*10^3 A/cm^2$, whereas the actually measured value is more than two orders of magnitude smaller.

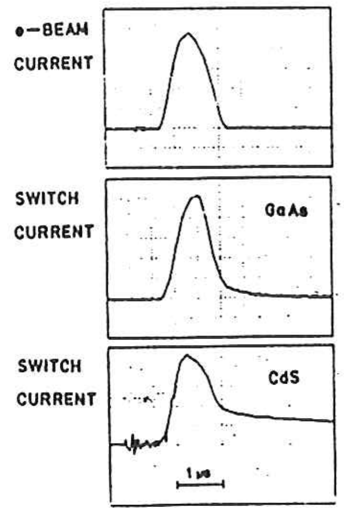

Figure 6. a) Electron-beam current and corresponding switch currents for b) GaAs and c) CdS.

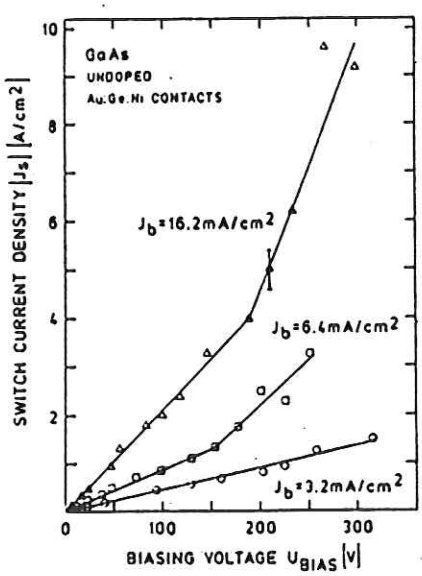

Figure 7. Current density vs. bias voltage for a GaAs switch (0.5 mm thickness) with the electron-beam current as a variable parameter.

The space-charge limitation is also confirmed by optical experiments. For electron-beam irradiated semi-insulating wafers (d = 0.04 cm - 0.06 cm) no recombination radiation was emitted from the wafer surface opposite to the one which was irradiated by a 200 kV electron-beam. N-doped GaAs wafers with doping levels of $5*10^{16} cm^{-3}$ and $2*10^{17} cm^{-3}$ have been tested in the same experimental configuration. The measured optical emission intensity increases linearly with the injected electron-beam current density in the range between $1 mA/cm^2$ and $20 mA/cm^2$ and is about one order of magnitude greater for the higher doped wafer. Figure 8 shows the optical emission detected with a photomultiplier tube (PMT) and the corresponding signal of the electron beam current. The optical signal is delayed by about 100 ns with respect to the electron-beam, due to the transit time in the PMT.

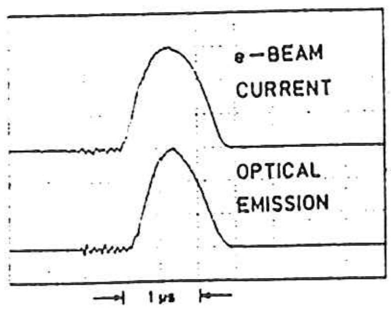

Figure 8. Electron-beam current and corresponding emission of recombination radiation.

Summary and Conclusion

With electron-beam irradiated GaAs switches opening and closing times (90 % to 10 %) less than 500 ns have been obtained. This time is determined by the turn off time of the electron-beam current. The actual decay time was measured to be less than 50 ns. For electron-beam current densities in the order of $10 mA/cm^2$, switch current densities were up to $10 A/cm^2$. The corresponding change in the switch resistance between ON and OFF state is about three orders of magnitude.

In the present configuration the switch current is space-charge limited, due to insufficient bulk ionization. To overcome this obstacle the semiconductor should have a surface layer of highly doped material with a thickness comparable to the range of the beam electrons. Experiments with Si doped GaAs samples have shown that the recombination emission increases drastically with increasing doping level.

An electron-beam controlled semiconductor switch, where the space charge limitation is eliminated, can be operated at high current densities with a high control efficiency (current gain) compared to electron-beam controlled gas discharge switches. The efficiency of such a closing and opening switch also exceeds that of conventional photoconductive semiconductor switches.

Additional advantages of the electron-beam controlled semiconductor switch are:

- Wide bandgap material with correspondingly small dark current can be used.

- A response in the nanosecond range for semiconductors with high recombination rates can be obtained with fast electron beam diodes. The switching speed can be increased into the picosecond range with appropriate semiconductors (GaAs : Cr) by sweeping the electron beam across the switch. Current rise times of about 100 ps have been obtained with this method [17].

- If the switch is part of an inductive energy storage circuit, opening can be enforced when semiconductors with a negative differential conductivity are used (i.e. GaAs).

- The limitation of the hold-off voltage due to surface flashover can be overcome because electron beam injection through the contacts allows to radially extend the semiconductor switch, and therefore to increase the distance between the electrodes along the surface.

Acknowledgments

This work is supported by the U.S. Army Research Office and the Air Force Office of Scientific Research.

The authors wish to thank Drs. A. Guenther and J. P. O'Loughlin, Kirtland Air Force Base, New Mexico, for contributing the electron-beam system.

References

[1] R. L. de Kronig, "Change of Conductance of Selenium Due to Electronic Bombardment," Phys. Rev., Vol. 24, pp. 377 - 382, 1924.

[2] C. B. Norris, Jr., "The Capabilities of Electron-Beam Semiconductor Active Devices", Proc. IEEE Tube Tech. Conf., New York, 1968.

[3] G. Schaefer, K. H. Schoenbach, "Review of Diffuse Discharge Opening Switches", IEEE Trans. Plasma Sci., Vol. PS-14, pp. 561 - 574, 1986.

[4] W. Ehrenberg, D. J. Gibbons, Electron Bombarded Induced Conductivity, Academic Press, 1981, Ch. 2, p. 72.

[5] K. H. Schoenbach, M. Kristiansen, G. Schaefer, "A Review of Opening Switch Technology for Inductive Energy Storage", Proc. IEEE, Vol. 72, pp. 1019 - 1040, 1984.

[6] K. H. Schoenbach, G. Schaefer, M. Kristiansen, L. L. Hatfield, A. H. Guenther, "Concepts for Optical Control of Diffuse Discharge Opening Switches", IEEE Trans. Plasma Sci., Vol. PS-10, pp. 246 - 251, 1982.

[7] L. Katz, A. S. Penfold, "Range - Energy Relations for Electrons and the Determination of Beta-Ray End-Point Energies by Absorption", Rev. Mod. Physics, Vol. 24, pp. 28 - 44, 1952.

[8] R. C. Alig, S. Bloom, "Electron-Hole-Pair Creation Energies in Semiconductors", Phys. Rev. Lett., Vol. 35, pp. 1522 - 1525, 1975.

[9] Morgan Semiconductor Division, Garland, Texas, private communication.

[10] M. J. Howes, D. V. Morgan, Ed., Gallium Arsenide, John Wiley & Sons, 1985, Ch. 11, p. 434.

[11] K. Seeger, Semiconductor Physics, Springer Verlag, 1973.

[12] D. A. Cusano, "Radiative Recombination from GaAs Directly Excited by Electron Beams", Solid State Com., Vol. 2, pp. 353 - 358, 1964.

[13] W. N. Carr, J. R. Biard, "Optical Generation Spectrum for the Electron Thermal Injection Mechanism in GaAs Diodes", J. Appl. Phys., Vol. 35, pp. 2777 - 2779, 1964.

[14] M. Schulz, H. Weiss (Ed.), Landolt-Boernstein Vol. 17, Springer Verlag, 1984, Ch. 6, p. 351.

[15] S. M. Seltzer, M. J. Berger, "Transmission and Reflection of Electrons by Foils", Nucl. Instr. and Meth., Vol. 119, pp. 157 - 176, 1974.

[16] G. Sh. Gildenblat, A. R. Rao, "Pulsed Space-Charge Limited Currents in GaAs", IEEE, Vol. EDL-8, pp. 135 - 136, 1987.

[17] G. Mourou, "Optically Induced High Power Switching in Bulk Semiconductors", Proc. Workshop on Solid State Switches, 1983, p. 114.

A Reprint from the

PROCEEDINGS

Of SPIE-The International Society for Optical Engineering

Volume 871

Space Structures, Power, and Power Conditioning

11-13 January 1988
Los Angeles, California

Electron-beam controlled semiconductor switches

K. H. Schoenbach, V. K. Lakdawala, K. B. J. Schmitt, T. J. Powers
Old Dominion University, Department of Electrical and Computer Engineering
Norfolk, Virginia 23529-0246

Electron-beam controlled semiconductor switches

K. H. Schoenbach, V. K. Lakdawala, K. B. J. Schmitt, and T. J. Powers
Old Dominion University, Department of Electrical and Computer Engineering
Norfolk, Virginia 23529-0246

ABSTRACT

A high power closing and opening bulk semiconductor switch is discussed where a high energy electron-beam (e-beam) is used to control the switch conductivity. The electrons are injected through a contact into the cathode region of a direct semiconductor switch. They generate a high concentration of electron-hole pairs over a distance of several micrometers to several hundred micrometers, depending on the electron energy. Ionization of the bulk of the semiconductor is provided by recombination radiation and X-ray Bremsstrahlung. The optical generation of an electron-hole plasma in the bulk region of the semiconductor switch overcomes the space charge limitation on the switch current and therefore allows external control of high current densities. Current and voltage measurements of e-beam irradiated semi-insulating GaAs samples were performed. A change of resistance of more than three orders of magnitude was obtained with e-beam current densities of some tens of mA/cm^2, corresponding to current gains (switch current/e-beam current) of up to 600. Closing and opening times of less than 50 ns seem to be achievable with these GaAs switches. An improvement in current gain by more than an order of magnitude can be obtained by proper doping of the cathode region of the semiconductor switch.

1. INTRODUCTION

Bulk semiconductor switches for both closing and opening applications have gained the attention of the pulsed power community. Externally controlled semiconductor switches have fast response times, allow jitter-free triggering, and may be scaled to high voltages and currents.[1-5] The conductivity in the semiconductor material, generally silicon (Si) or gallium arsenide (GaAs) is modified either by photo generation or annihilation[6] of electron-hole pairs or by e-beam ionization of the bulk material. In order to use photoconductive or e-beam controlled semiconductors as opening switches the electron-hole recombination time needs to be of the same order or less than the decay time of the ionizing beam.

E-beam controlled semiconductor switches have several advantages over optically controlled switches:

- The overall efficiency of e-beam control exceeds that of optical control.
- Wide bandgap, low dark current materials, which would for electron-hole pair generation require multi-photon processes with commonly used lasers, can easily be ionized with electrons.
- The limitation of the hold-off voltage, which is presently determined by surface flashover[4], can be overcome for e-beam injection through the contact. The semiconductor switch geometry can be shaped so that the breakdown voltage is determined by the intrinsic dielectric strength, rather than by the surface properties.

The major disadvantage of e-beam controlled compared to laser controlled semiconductors seems to be the small penetration depth of the electrons. The electron range is, for example, 1.5 micrometer for 10 keV electrons in Si. For switches, where the electrons are injected through the contact, and the distance between the contacts is large compared to the electron range, the current density is space charge limited, that means relatively large voltages are needed to obtain high current densities. The so called EBS-Devices (Electron Bombarded Semiconductor Devices), which were developed in the late sixties and in the seventies[7] as microwave power tubes and amplifiers, are examples for this mode of operation.

If used for high power closing and opening switches, the switch impedance in the conduction phase should be very small compared to the load impedance, which is generally not the case for electron beam controlled switches operated in the EBS mode. A way to keep the advantages of e-beam control, but without space charge limitation, is to utilize the e-beam generated radiation to ionize the bulk of the semiconductor. This concept uses cathodoluminiscence, rather than direct electron-hole pair generation by electron bombardment as the mechanism for controlling the current flow through a bulk semiconductor switch. Details of this concept and experimental results are discussed in the following.

2. SWITCH CONCEPT

The switch concept is shown in Figure 1. In the switch "off state" the semiconductor should have a resistivity which is high enough to prevent appreciable current flow. Semi-insulating GaAs can be used which has a resistivity of up to 10^7 Ω cm. In order to close the switch, an e-beam is injected through the cathode contact of the semiconductor switch and generates electron-hole pairs by impact ionization within the range of the primary electrons. For GaAs as switch material, the energy of the primary electrons should be less than 220 keV, which is the threshold for radiation damage in this material.[8] This limits the range for direct impact generation of electron-hole pairs to a depth of about 100 μm. Generation of electron-hole pairs in the bulk region can be obtained optically, using cathodoluminiscence of a direct semiconductor, such as GaAs.

When the e-beam is turned off, the conductivity of the bulk material decreases due to electron-hole recombination (switch opening phase). Because of its negative differential mobility region, GaAs is a suitable material for opening switches, which are part of an inductive energy storage circuit. When the switch opens, the voltage across it increases due to the increasing induced voltage across the inductance. This effect drives the semiconductor from a region of high electron mobility into a state of low mobility, and hence low conductivity.

The spatial charge carrier distribution in a 1 mm thick, semi-insulating GaAs-wafer due to impact of 200 keV electrons and recombination radiation was calculated by Schmitt et al.[9] Electron-hole pairs were assumed to be generated in a layer of doped p-type GaAs, corresponding to the electron range. Doping of GaAs with an acceptor material such as zinc (Zn) increases the probability for radiative recombination in this region.[10] For the calculation the quantum efficiency was assumed to be one. Experimentally obtained values for GaAs p-n junction devices are 0.083 in external efficiency at room temperature, which corresponds to a value of 0.88 for internal quantum efficiency.[11] For the undoped bulk material it was assumed that recombination through the recombination centers, rather than direct recombination is the dominant carrier loss process. The resulting charge distribution over a depth of 1 mm is shown in Figure 2 for an e-beam density of J_b = 0.1 A/cm².

Besides recombination radiation, X-radiation (Bremsstrahlung) plays an important role at high electron energies. The X-ray intensity (I) scales with the square of the electron energy (E). At an E of 200 keV the energy efficiency I/E is $4.5 * 10^{-3}$. The X-ray induced charge distribution is plotted in Figure 2, for an electron energy of 200 keV, and an e-beam current density of J_b = 0.1 A/cm². The energy efficiency for Bremsstrahlung is much less than that for recombination radiation. However, its influence on the carrier generation at distances large compared to the electron range could, due to its small absorption coefficient, become comparable to that of recombination radiation. However, since our calculations describe a one dimensional switch, they do not include the decay of intensity with increasing distance. The X-radiation decays as one over square of the distance (for nonrelativistic electrons). The IR recombination radiation, however, can be confined to a large extent in the GaAs switch, because of its high index of refraction and the metal contacts at both ends. In other words, a cylindrical GaAs switch with a length large compared to its radius acts as a waveguide for recombination radiation and almost all the radiative energy is dissipated in the bulk of the semiconductor.

For the GaAs wafers of thickness 1 mm and less, which we have used in our experiments, the one dimensional treatment is valid. The bulk resistance per cm², R_b, as derived from the carrier density values in Figure 1 is 0.2 Ω for J_b = 0.1 A/cm². It scales linearly with the e-beam current density. The resistivity of semi-insulating GaAs is given as 10^7 Ω cm by the manufacturer (Morgan Semiconductor Division, Garland, TX). Using these data, conductance ratios (e-beam generated conductance/dark conductance) of $2 * 10^7$ can be expected in 1 mm wafers for J_b = 0.1 A/cm². Even if we only take X-ray generated conductivity into account, ratios of several thousand should be obtainable. The current gain, G, the ratio of switch current to e-beam current, is another figure of merit for e-beam controlled switches. It is given as:

$$G = (E_b*d)/(R_b*J_{eb}) \qquad (1)$$

where E_b is the electric field intensity in the bulk material and d the thickness of the wafer. For values of E_b = 3 kV/cm, corresponding to the maximum of the drift velocity in GaAs, the current gain according to our calculations could be as high as $7.5 * 10^3$ (d = 0.5 mm, J_{eb} = 0.1 A/cm²).

2. SWITCH CONCEPT

The switch concept is shown in Figure 1. In the switch "off state" the semiconductor should have a resistivity which is high enough to prevent appreciable current flow. Semi-insulating GaAs can be used which has a resistivity of up to 10^7 Ω cm. In order to close the switch, an e-beam is injected through the cathode contact of the semiconductor switch and generates electron-hole pairs by impact ionization within the range of the primary electrons. For GaAs as switch material, the energy of the primary electrons should be less than 220 keV, which is the threshold for radiation damage in this material.[8] This limits the range for direct impact generation of electron-hole pairs to a depth of about 100 μm. Generation of electron-hole pairs in the bulk region can be obtained optically, using cathodoluminiscence of a direct semiconductor, such as GaAs.

When the e-beam is turned off, the conductivity of the bulk material decreases due to electron-hole recombination (switch opening phase). Because of its negative differential mobility region, GaAs is a suitable material for opening switches, which are part of an inductive energy storage circuit. When the switch opens, the voltage across it increases due to the increasing induced voltage across the inductance. This effect drives the semiconductor from a region of high electron mobility into a state of low mobility, and hence low conductivity.

The spatial charge carrier distribution in a 1 mm thick, semi-insulating GaAs-wafer due to impact of 200 keV electrons and recombination radiation was calculated by Schmitt et al.[9] Electron-hole pairs were assumed to be generated in a layer of doped p-type GaAs, corresponding to the electron range. Doping of GaAs with an acceptor material such as zinc (Zn) increases the probability for radiative recombination in this region.[10] For the calculation the quantum efficiency was assumed to be one. Experimentally obtained values for GaAs p-n junction devices are 0.083 in external efficiency at room temperature, which corresponds to a value of 0.88 for internal quantum efficiency.[11] For the undoped bulk material it was assumed that recombination through the recombination centers, rather than direct recombination is the dominant carrier loss process. The resulting charge distribution over a depth of 1 mm is shown in Figure 2 for an e-beam density of J_b = 0.1 A/cm^2.

Besides recombination radiation, X-radiation (Bremsstrahlung) plays an important role at high electron energies. The X-ray intensity (I) scales with the square of the electron energy (E). At an E of 200 keV the energy efficiency I/E is 4.5 * 10^{-3}. The X-ray induced charge distribution is plotted in Figure 2, for an electron energy of 200 keV, and an e-beam current density of J_b = 0.1 A/cm^2. The energy efficiency for Bremsstrahlung is much less than that for recombination radiation. However, its influence on the carrier generation at distances large compared to the electron range could, due to its small absorption coefficient, become comparable to that of recombination radiation. However, since our calculations describe a one dimensional switch, they do not include the decay of intensity with increasing distance. The X-radiation decays as one over square of the distance (for nonrelativistic electrons). The IR recombination radiation, however, can be confined to a large extent in the GaAs switch, because of its high index of refraction and the metal contacts at both ends. In other words, a cylindrical GaAs switch with a length large compared to its radius acts as a waveguide for recombination radiation and almost all the radiative energy is dissipated in the bulk of the semiconductor.

For the GaAs wafers of thickness 1 mm and less, which we have used in our experiments, the one dimensional treatment is valid. The bulk resistance per cm^2, R_b, as derived from the carrier density values in Figure 1 is 0.2 Ω for J_b = 0.1 A/cm^2. It scales linearly with the e-beam current density. The resistivity of semi-insulating GaAs is given as 10^7 Ω cm by the manufacturer (Morgan Semiconductor Division, Garland, TX). Using these data, conductance ratios (e-beam generated conductance/dark conductance) of 2 * 10^7 can be expected in 1 mm wafers for J_b = 0.1 A/cm^2. Even if we only take X-ray generated conductivity into account, ratios of several thousand should be obtainable. The current gain, G, the ratio of switch current to e-beam current, is another figure of merit for e-beam controlled switches. It is given as:

$$G = (E_b * d)/(R_b * J_{eb}) \tag{1}$$

where E_b is the electric field intensity in the bulk material and d the thickness of the wafer. For values of E_b = 3 kV/cm, corresponding to the maximum of the drift velocity in GaAs, the current gain according to our calculations could be as high as 7.5 * 10^3 (d = 0.5 mm, J_{eb} = 0.1 A/cm^2).

3. EXPERIMENTAL RESULTS

The e-beam, which is used to irradiate the semiconductor sample is produced by a pulsed thermionic diode. The diode voltage is less than 220 kV. The measurements described in the following were performed with 200 keV electrons. The pulse duration can be varied between 1 μs and 20 μs with rise and fall times of 400 ns. The 200 keV e-beam is transmitted through an anode foil (1 mil, titanium) and irradiates the semiconductor target, which is placed outside the diode vacuum chamber. The e-beam current is measured with a 50 Ω Faraday-cup. The semiconductor material which was mainly studied was undoped GaAs because of its high intrinsic resistivity (10^7 Ω cm). Au:Ge:Ni and Au:Ge were used to obtain ohmic contacts.

Figure 3 shows the temporal current response of GaAs and CdS to the e-beam irradiation. For both samples the leading edge of the bulk current signal follows the e-beam current. The switch current in GaAs decreases with about the same slope as the e-beam current. The decay of conductivity after 10 ns laser irradiation of the same material was found to be less than 50 ns. In the case of CdS, the bulk current drops initially in less than 500 ns to about 50% of its peak value, and then it decays exponentially with a time constant of greater then 10 μs. This slow decay is because electron capture in deep traps is the main current carrier loss mechanism.

Figure 4 shows the switch current density J_s in a 0.5 mm thick GaAs wafer as a function of the biasing voltage for different e-beam current densities J_b. The curves with J_b < 16.2 mA were obtained with one sample (sample 1), the curve with J_b = 36 mA with a different sample (sample 2) but the same semiconductor material. The slope of the curve, which represents the switch conductance per cm^2 area, varies linearly with the e-beam current density. For J_b = 36 mA/cm^2 the switch conductance was 0.05 Ω^{-1} cm^{-2}, corresponding to a resistance of 20 Ω for one cm^2. Figure 5 shows the switch current-voltage characteristics of sample 2 with no e-beam irradiation. The sample shows the typical behavior of an insulator with a discrete trapping level.[12] Based on these data the resistance ratio for the 36 mA/cm^2 curve is 6 * 10^3 for the range below V = 60 V, a voltage which corresponds to an electric field of about 1 kV/cm in the bulk of the semiconductor.

4. DISCUSSION

The closing and opening time of the e-beam controlled GaAs switches were in our experiment limited by the rise and fall time of the e-beam current. The actual opening time of the proposed bulk semiconductor switch, its response to a step-function of the e-beam current, is determined by recombination processes. In semi-insulating GaAs the recombination time constant was measured to be less than 50 ns. With Cr-doped GaAs the opening time should be in the nanosecond and subnanosecond range.[13]

The linear dependance of the switch current on the e-beam current demonstrates that the switch current is not space-charge limited. Also the obtained current density is far above the space charge limited current density which for a trap-free insulator, which represents the optimum condition for space charge limited current flow, is given by the Mott-Gurney square law:

$$J = \frac{8}{9} \epsilon\mu \frac{V^2}{d^3} \qquad (2)$$

V is the applied voltage, d the thickness of the semiconductor sample, ϵ the permittivity, and μ the mobility of electrons. For a 0.5 mm GaAs sample biased at 60 V, the maximum current density according to Mott-Gurney's law would be 0.25 A/cm^2, far below the 3 A/cm^2 obtained in the experiment (J_b = 36 mA/cm^2). The experimental results actually point to a bulk ionization by the e-beam generated X-rays. The resistance values of the switch material agree with resistance values obtained with our model. For a sample of d = 0.5 mm (J_b = 36 mA/cm^2, E = 200 keV) the calculated X-ray generated conductance is 2.16 * 10^{-2} Ω^{-1} cm^{-1}, compared to a measured conductance of 5 * 10^{-2} Ω^{-1} cm^{-1}.

The experimental results also indicate that recombination radiation does not play a role in our presently used semi-insulating GaAs switches. This was confirmed by optical experiments[9] where an S1 photomultiplier tube was placed behind the e-beam irradiated wafer to measure the recombination radiation transmitted through the 0.5 mm thick semiconductor. No recombination radiation was detected in the case of undoped, semi-insulating GaAs. In Si-doped (5 *10^{16} cm^{-3} and 2 * 10^{17} cm^{-3}) GaAs however, optical emission was observed, the intensity being linearly dependent on the e-beam current density. At constant J_b the

emission was more intense by about one order of magnitude for the higher doped wafer. This observation is in agreement with measurements of recombination radiation from doped GaAs excited by e-beams[10] where a steady increase of recombination radiation with doping density was measured for zinc (Zn) as the dopant. This correlation was valid for Zn doping densities below $5 * 10^{18}$ cm^{-3}.

These results indicate that it is possible to increase the conductance of an e-beam controlled semiconductor switch drastically by doping the semiconductor heavily at the e-beam irradiated face over a depth corresponding to the range of the electrons. E-beam control will, if the quantum efficiency in the cathode region can be increased, be a very efficient switch mechanism. It may become a competitor for photoconductive switching even with respect to switching speed. A way to get nanosecond and even subnanosecond e-beam pulses is to use photoelectrons. The electrons are generated by a laser at a photocathode. They are subsequently accelerated in the electric field of a vacuum diode, and are able, because of their high energy, to generate a large number of electron-hole pairs in the semiconductor switch.

The efficiency of this switching method is higher than by just using photoconductive methods, where one photon creates not more than one electron-hole pair. The gain G of e-beam controlled, photo assisted switching is given as:

$$G = \gamma_1 (E_{eb}/E_{eff})\ \gamma_2 \qquad (3)$$

where γ_1 is the photoelectric yield, E_{eb} the energy of an electron in the e-beam, E_{eff} the effective energy necessary to generate an electron-ion pair, and γ_2 the quantum efficiency for radiative recombination in the semiconductor. Assuming photoelectric yields of 0.1 (GaAs:Cs), an E_{eb} of 0.2 MeV, an E_{eff} of 5 eV (GaAs), and a quantum efficiency of 0.5, a gain of 2000 compared to laser switching could be attained.

The current rise time in semiconductor switches, obtained with such a photoelectronic method, was shown to be on the order of 0.1 ns.[14] Besides the high gain compared to laser switching, the photoelectronic and any method, which is based on e-beam control, offers as an additional advantage the possibility to generate multiple electric pulses with well defined rise times and temporal spacing between subsequent pulses by sweeping the electron beam across an array of semiconductor switches.

5. SUMMARY

With e-beam irradiated GaAs switches opening and closing times (90% to 10%) of less than 500 ns have been obtained. This time is determined by the turn-off time of the e-beam current. The actual decay time was measured to be less than 50 ns. For e-beam current densities in the order of 10 mA/cm^2, switch current densities were up to 10 A/cm^2. The corresponding change in the switch resistance between on and off states is about three orders of magnitude.

In the present configuration the switch current density is not space-charge limited, but is determined by the e-beam induced X-ray ionization of the bulk of the switch. In order to increase the conductivity of the bulk material (i.e., to increase the current gain) it is planned to utilize recombination radiation for further bulk ionization. A reasonable efficiency for the conversion of electron energy into photon energy requires doping of the cathode region of the GaAs switch. Experiments with Si doped GaAs samples have shown that the level of cathodoluminiscence increases drastically with increasing doping.

6. ACKNOWLEDGEMENTS

This work is supported by the U. S. Army Research Office and the Air Force Office of Scientific Research.

7. REFERENCES

1. G. Mourou, W. H. Knox, and S. Williamson, "High Power Picosecond Switching in Bulk Semiconductors," in Picosecond Optoelectronic Devices, Chi H. Lee, ed., Academic Press. Inc., pp. 219-248 (1984).

2. W. C. Nunnally, "Photoconductive Pulse Power Switches: A Review," Proc. 5th IEEE Pulsed Power Conf., Arlington, VA, pp. 235-241 (1985).

3. J. D. Morse, and M. D. Pocha, "Characteristics and Modeling of High Voltage Photoconductive Switching Devices," Conf. Record, 17th Power Modulator Symposium, Seattle, WA, pp. 211-213 (1986).

4. F. J. Zutavern, and M. W. O'Malley, "Engineering Limits of Photoconductive Semiconductor Switches in Pulsed Power Applications," Conf. Record, 17th Power Modulator

Symposium, WA, pp. 214-218 (1986).
5. L. Bovino, R. Youmans, M. Weiner, and T. Burke, "Optically Controlled Semiconductor Switch for Multi-Megawatt Rep-Rated Pulsers," Conf. Record, 17th Power Modulator Symposium, WA, pp. 219-223 (1986).
6. K. H. Schoenbach, V. K. Lakdawala, R. Germer, and S. T. Ko, "An Optically Controlled Closing and Opening Semiconductor Switch," accepted for publication in J. Appl. Phys. (March 1988).
7. D. J. Bates, R. I. Knight, S. Spinella, and A. Silzars, "Electron-Bombarded Semiconductor Devices," Adv. El. El. Phys. 44, pp. 221-281 (1977).
8. W. Ehrenberg, and D. J. Gibbons, Electron-Bombardment Induced Conductivity, Academic Press, New York (1981).
9. K. B. Schmitt, K. H. Schoenbach, T. J. Powers, and R. K. F. Germer, "E-Beam Controlled Semiconductor Opening/Closing Switch," to be published in the Proc. 6th IEEE Pulse Power Conf., Arlington, VA (1987).
10. D. A. Cusano, "Radiative Recombination from GaAs Directly Excited by Electron Beams," Solid State Communications 2, pp. 353-358 (1964).
11. W. N. Carr, "Characteristics of a GaAs Spontaneous Infrared Source with 40 Percent Efficiency," IEEE Trans. Electron Devices ED-12, pp. 531-535 (1965).
12. R. W. Haisty, and P. L. Hoyt, "Investigation of Voltage Breakdown in Semi-Insulating GaAs," Solid State Electronics 10, pp. 795-800 (1967).
13. Chi H. Lee, "Devices Based on Optically Injected Plasma," in Picosecond Optoelectronic Devices, Chi H. Lee, ed., Academic Press, New York (1984).
14. G. Mourou, "Optically Induced High Power Switching in Bulk Semiconductors," Proc. Workshop on Solid State Switches, W.M. Portnoy and M. Kristiansen, editors, Tamarron, CO, p. 114 (1983).

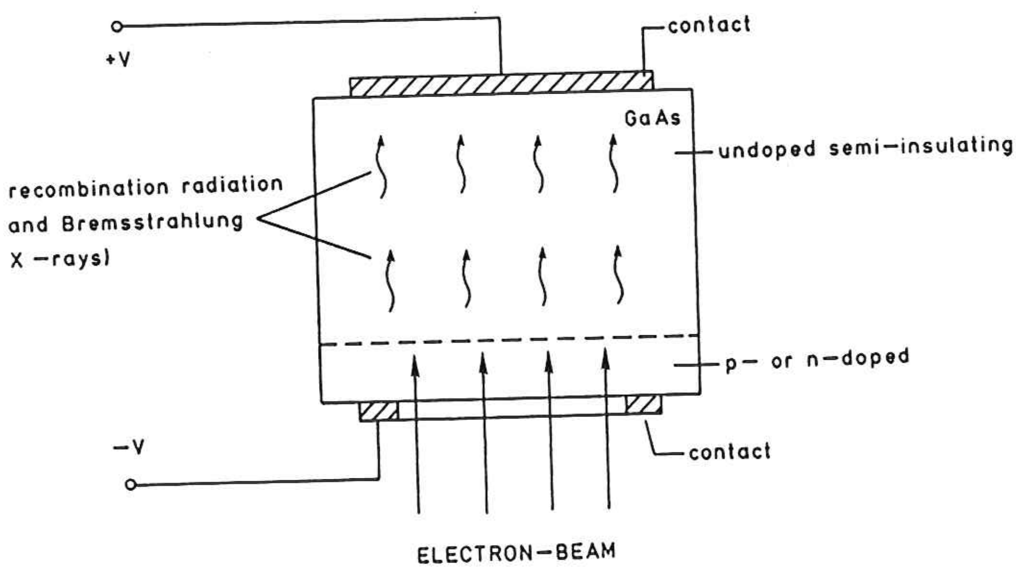

Figure 1. Electron-beam controlled semiconductor switch.

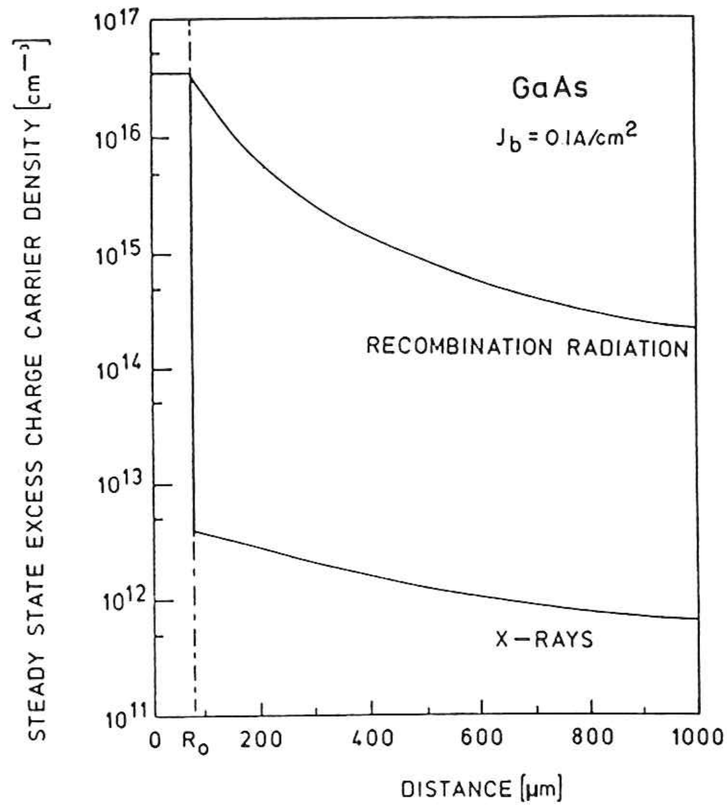

Figure 2. Spatial distribution of charge carrier density due to ionization by recombination radiation and due to X-ray ionization.

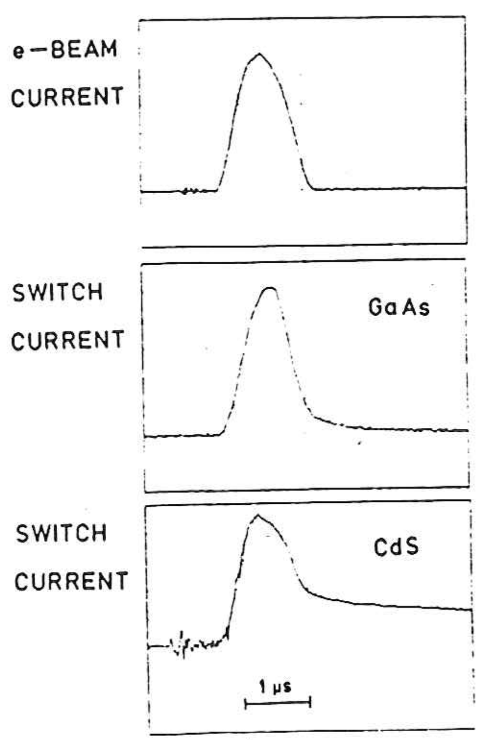

Figure 3. Electron-beam pulse and corresponding switch currents for GaAs and CdS.

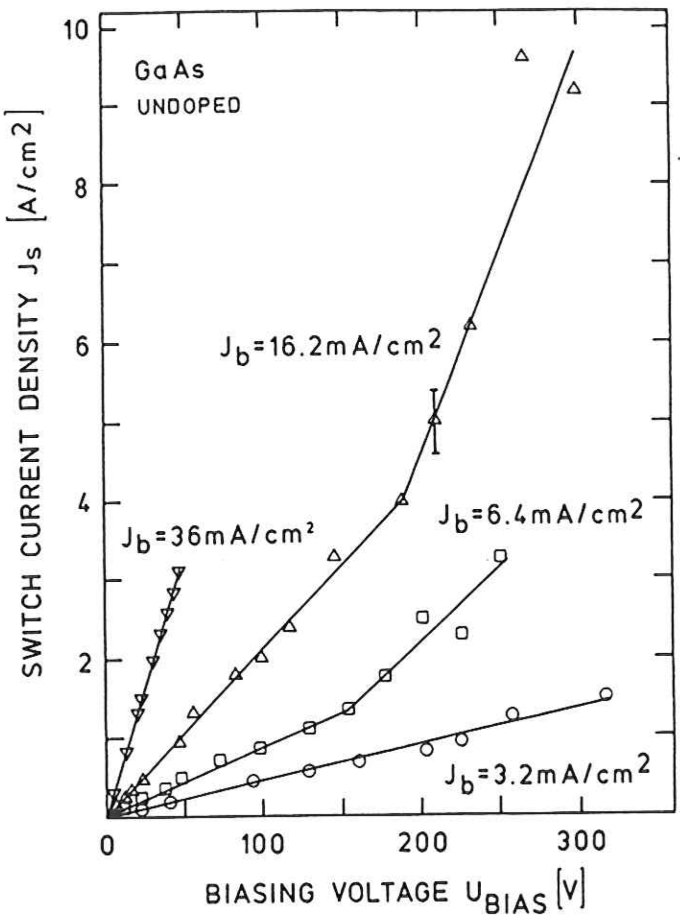

Figure 4. Current density versus bias voltage for a GaAs Switch (d = 0.5 mm) with electron-beam current as variable parameter.

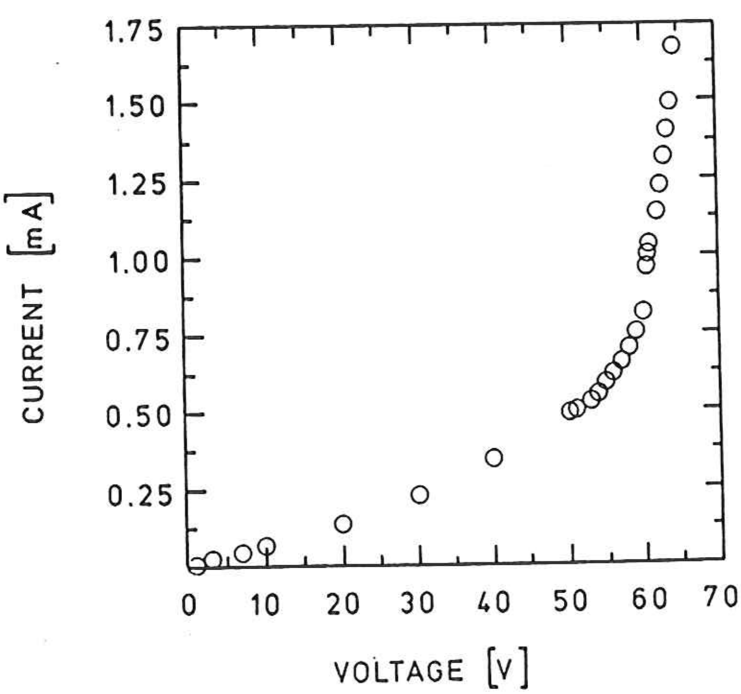

Figure 5. Current-voltage characteristic of a GaAs switch (J_B = 0).

WORKSHOP PROCEEDINGS

" OPTICALLY AND ELECTRON BEAM CONTROLLED SEMICONDUCTOR SWITCHES "

May 23-24, 1988

NORFOLK, VA

K. H. SCHOENBACH AND M. WEINER
WORKSHOP CO-CHAIRMEN

SPONSORED BY
THE PHYSICAL ELECTRONICS RESEARCH INSTITUTE AT OLD DOMINION UNIVERSITY, NORFOLK, VA, AND THE U.S. ARMY LABCOM,ELECTRONICS TECHNOLOGY AND DEVICES LABORATORY, FORT MONMOUTH, N.J.

WORKSHOP PROCEEDINGS
"OPTICALLY AND ELECTRON-BEAM CONTROLLED SEMICONDUCTOR SWITCHES"
MAY 23-24, 1988
NORFOLK, VIRGINIA

E-BEAM CONTROLLED SEMICONDUCTOR SWITCH

Karl H Schoenbach, Vishnu K Lakdawala, David Stoudt and Tyler Smith

Department of Electrical and Computer Engineering
Old dominion University, Norfolk, VA 23529

A concept is presented which utilizes e-beam ionization of bulk semiconductors is followed. This allows the control of the semiconductor conductivity in the temporal range (μs) where the operation of the photoconductive switches is limited. Long e-beam pulses (tens of μs's) at current densities in the tens of mA's range can easily be obtained with e-beam diodes (with a heated thoriated tungsten cathode). Other advantages of e-beam control of bulk semiconductors compared to photoconductive switching are: wide band gap material (such as diamond) can be activated, hold-off voltage limitation (surface flashover for example) can be overcome by using a switch configuration where the e-beam is injected through the contact. The major disadvantage of e-beam controlled semiconductor switches, the small penetration depth of the electrons, can be overcome by using cathodoluminiscent processes to provide for an electron-hole plasma in the bulk of semiconductor.

The switch concepts are based on e-beam controlled ionization of the semiconductor material. The switch closes when the e-beam is turned on and generates free charges in the semiconductor. When the e-beam is turned off, the conductivity of the semiconductor decreases due to electron-hole recombination, trapping of free charge carriers, and diffusion.

There are two basic switch configurations. In one configuration (I) the contacts are coplanar and the ionizing electrons are injected in the direction perpendicular to the applied electric field (Fig. 1a). In the second configuration (II) the electrons are injected through one of the contacts in electric field direction (Fig. 1b). Assuming that free charges are generated only in a layer corresponding to the range R of primary electrons the current in configuration I is limited to values on the order of ten amps even at current densities of 10^3 A/cm^2.

In configuration II, the principle of operation is analogous to that of a vacuum photodiode with electrons instead of photons used to generate electron-hole pairs adjacent to one of the contacts (cathode). The so-called Electron Bombarded Semiconductor Devices (EBS-Devices), which were developed in the late sixties and the seventies[1] as microwave power tubes are examples for this mode of operation. The high field in the region between the contacts causes a rapid separation of electrons and holes. The electrons are swept across the highly resistive region. The holes have no effect but to provide continuity of charge. This device has a nanosecond response to changes in the source function (e-beam). However, since the current density is space charge limited, relatively high voltages are needed to obtain reasonably high current densities. For a trap free insulator, which represents the optimum condition for space charge limited current flow in solids, the space charge limited current density is given by Mott-Gurney's square law:

Experimental Set Up

Two types of switches were investigated: one, where the switch material was completely undoped GaAs; and a second one, again using GaAs as the basic material, but with a surface layer of highly Zn-doped material. In both cases the GaAs used was semi insulating, LEC grown. The resistivity of this material was given as 7×10^6 ohm cm (Spectr.). The shallow layer of p-type GaAs was generated by diffusion of Zn for two hours at a temperature of 750° C. According to Ref. 5, this procedure creates a p-type layer of about 10 μm thickness with an acceptor concentration of 10^{19} cm^{-3}. Au:Ge contacts of about 0.1 μ255255Dm thickness were evaporated onto both faces of 0.5 mm wafers with a contact area of 0.8 cm^2 and annealed at 400° C for 15 minutes.

The experimental set up is shown in Fig. 3. The e-beam is produced by a pulsed thermionic diode. The diode voltage is generated by a pulse forming network (PFN) consisting of a LC-chain and is stepped up in a ratio 1:11 by a pulse transformer. The pulse duration can be adjusted between 1 μs and 15 μs by varying the number of PFN segments. The rise and fall time of the voltage pulse is 500 ns. The maximum diode voltage is 220 kV, determined by the pulse transformer rating. The e-beam current density can be varied in the range up to 100 mA/cm^3 by varying the temperature of the thoriated tungsten cathode. In our experiments we have used a 150 keV e-beam to irradiate the semiconductor sample outside the diode chamber. The energy losses in the anode-foil of the diode (1 mil titanium) are about 20% at this e-beam energy. [6]

In order to get the current density-voltage characteristics of the semiconductor switches, a dc voltage was applied to the sample. The current flowing through the semiconductor, when it was irradiated with high energy electrons was measured by means of a Pearson coil. The temporal development of the e-beam diode voltage was recorded simultaneously at each shot. This signal was obtained by measuring the total PFN current flowing into the 2600 Ω load resistor and, parallel to it, the e-beam diode. The variable parameter in all the measurements was the e-beam current density at a fixed electron energy of 150 keV.

Experimental Results

The temporal current response of semi insulating GaAs-switch of 0.5 mm thickness to e-beam irradiation is shown in Fig. 4 for an e-beam current density of J_e = 36 mA/cm^2 and a bias voltage of 135 V. Also shown is the e-beam diode voltage for this particular switch event. The e-beam irradiated face is the cathode of the switch. The switch current signal follows closely the e-beam pulse. The switch current density in this case was J_S = 9.4 A/cm^2, that means that the current gain J_S/J_e is about 260.

The values of switch current density versus biasing voltage, with the e-beam current density as variable parameter are plotted in Fig. 5 for 0.5 mm semi insulating GaAs wafers. The curves with J_e 16.2 mA/cm^2 were obtained with one sample, the curve with J_e = 36 mA/cm^2, with a different sample, but the same semiconductor material. The slope of the curves, which represents the switch conductance per cm^2 area, varies linearly with the e-beam current density. For J_e = 36 mA/cm^2 the switch conductance is 0.05 Ω^{-1} cm^{-2}, corresponding to a resistance of 20 Ω/cm^2. Compared to the initial resistance of the sample,

$$J = (8/9)\ \varepsilon\mu\ V^2/d^3 \qquad (1)$$

where V is the applied voltage, d the thickness of the semiconductor sample, ε the permittivity, and μ the mobility of the electrons. For a 0.5 mm GaAs sample, biased at 60 V, the maximum current density according to Mott-Gurney's law is 0.15 A/cm^2.

A way to overcome the space charge limitation, without sacrificing the advantages of e-beam control, is to convert the electron energy E into photon energy I and use the e-beam generated radiation to ionize the bulk of the semiconductor (Fig. 2). The radiation generated directly and indirectly by the e-beam is Bremsstrahlung (X-rays) and band edge radiation due to radiative recombination of electron-hole pairs in the e-beam activated layer. It is generated in region I, whose depth is given by the electron range, and is absorbed in region II where it generates an electron-hole plasma.

The energy efficiency for Bremsstrahlung I/E is relatively small for the electron energy range of interest. It scales linearly with the electron energy and the atomic charge Z:[2]

$$I/E = 7*10^{-4}\, Z\, E \qquad (2)$$

with E in MeV. For GaAs and an electron energy of 200 keV, I/E is about 0.5%. The energy efficiency for band edge radiation with a photon energy around 1.4 eV can exceed that of Bremsstrahlung by more than an order of magnitude. The effective ionization energy for GaAs is 4.3 eV. The external quantum efficiency, the number of photons emitted per electron-hole recombination process, in GaAs p-n junction devices was measured to be 0.083, corresponding to an internal quantum efficiency of 0.88 at room temperature.[3] Hence, the total energy efficiency for cathodoluminiscence could be about 35% under optimum conditions.

The efficiency of bulk ionization with band edge radiation is, unlike the ionization by X-rays, independent of the energy of the primary electrons. This allows to use relatively low energy electrons to provide for the generation of electron-hole pairs in the luminescent layer. An additional advantage of this method is the fact that the cathodoluminiscent layer in the semiconductor switch is highly conductive and therefore can be used to carry the switch current to contacts, which are placed outside the e-beam irradiated region. This way electron losses in contacts, which at low electron energies can be substantial, are avoided. The cathodoluminiscent layers near contact region can be realized by doping with shallow donors or acceptors (such as Zn) for a thickness corresponding to the electron range.

It could be shown by using a rate equation model that the combined effect of Bremsstrahlung and recombination radiation on electron-hole generation in the bulk of the semiconductor, could lead to an extention of the current density range of electron-bombarded semiconductor switches to hundreds of amps/cm^2.[4] This is an improvement in current density of two to three orders of magnitude over EBS-devices. Experimental results with semi insulating GaAs as base material have proven the feasibility of the concept.

0.35 MΩ/cm^2 the reduction in resistance due to e-beam irradiation is more than four orders of magnitude.

The temporal response of the second type of switches; semi insulating GaAs switches with a shallow layer of Zn-doped material in the cathode region, is shown in Fig. 6. Zn was used to generate a high cathodoluminiscent zone in the cathode area of the switch. Calculations[4] and measurements[7] have shown that doping GaAs with Zn at levels of 10^{18} to 10^{19} cm^{-3} increases the rate for radiative recombination drastically. The cathode face of the semiconductor switch is irradiated by the e-beam. Contrary to the results with homogeneous switch material, the temporal response does not follow the e-beam pulse over the entire length of the pulse. After an initial linear response, whose duration is increasing when the e-beam intensity is lowered, a more or less linear rise of the switch current is observed. The current flow is terminated when the e-beam is turned off. That the current termination is controlled by the e-beam is even more clearly shown in Fig. 7 where, due to a breakdown in the diode, the e-beam was turned off very rapidly. The switch current followed the e-beam current instantaneously. That means that opening of the switch is fully controllable by the e-beam. The maximum switch current density, obtained at the end of the current pulse, is, at voltages above 125 V, about twice as large as the current density in homogenous switch material. This is shown in Fig. 8. The maximum switch current density obtained in our experiments with Zn-doped GaAs was 53 A/cm^2, at a voltage of 185 V across the switch. This number corresponds to a current gain J_s/J_e of 1472.

Acknowledgements

This work is funded by ARO and AFOSR.

References

[1] D.J. Bates, R.I. Knight, S. Spinella, and A.Silzars, "*Electron-bombarded Semiconductor Devices*", Adv. El. Phys., 44, 221 (1977)

[2] R.D. Evans, **The Atomic Nucleus**, pp 615, McGraw-Hill Book Company Inc., (1955)

[3] W.N. Carr, "*Characteristics of a GaAs Spontaneous Infrared Source with 40 Percent Efficiency*", IEEE Trans. on Electron Devices, ED-12, No. 10, 531 (1965)

[4] K.H. Schoenbach, V.K. Lakdawala, D.C. Stoudt, and T.S. Smith, "*Electron-Beam Controlled High Power Semiconductor Switches*", (to be published)

[5] H.C. Casey, **Atomic Diffusion in Semiconductors**, pp 351, D. Shaw, Ed., Plenum Press, New York, (1973)

[6] S.M. Seltzer and M.J. Berger, "*Transmission and Reflection of Electrons by Foils*", Nnd. Insts. and Meth., 119, 157 (1974)

[7] D.A. Cusano, "*Radiative Recombination From GaAs Directly Excited by Electron Beams*", Solid State Comm., 2, 353 (1964)

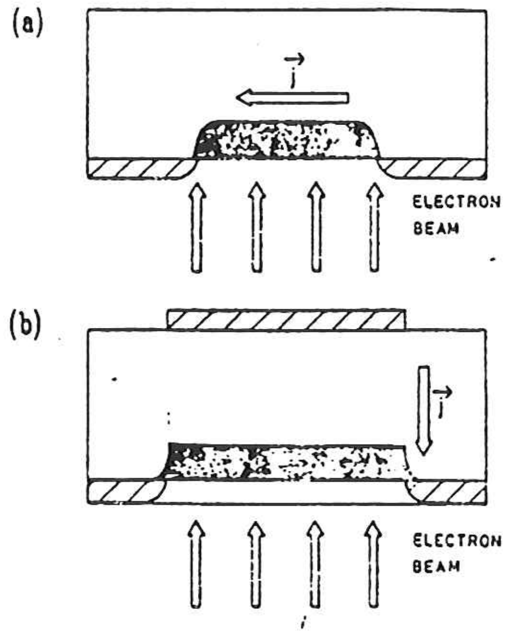

Fig. 1 High energy electron injection: a) perpendicular and b) parallel to the electric field in a semiconductor switch.

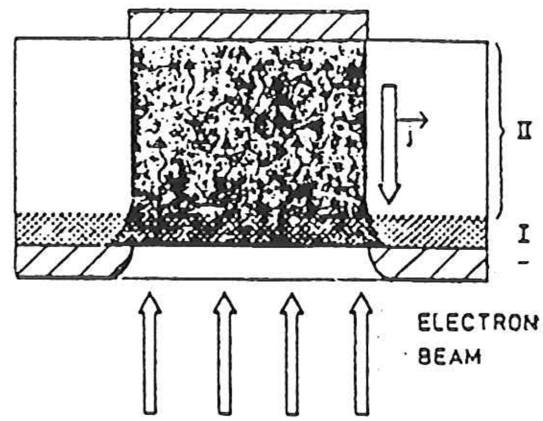

Fig. 2 E-beam controlled semiconductor switch with bulk ionization by cathodoluminescence.

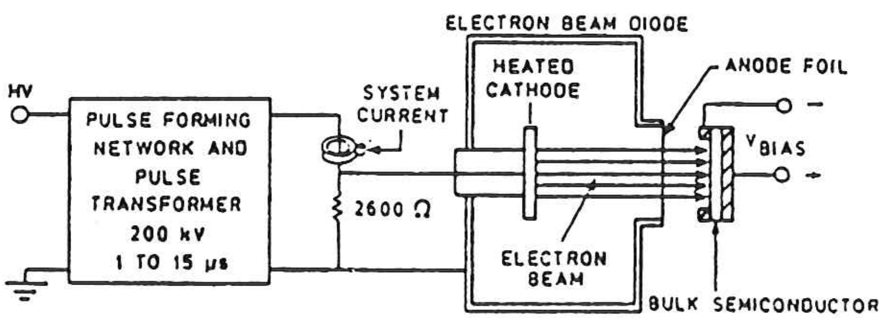

Fig. 3 Experimental set up of the 200 kV e-beam system.

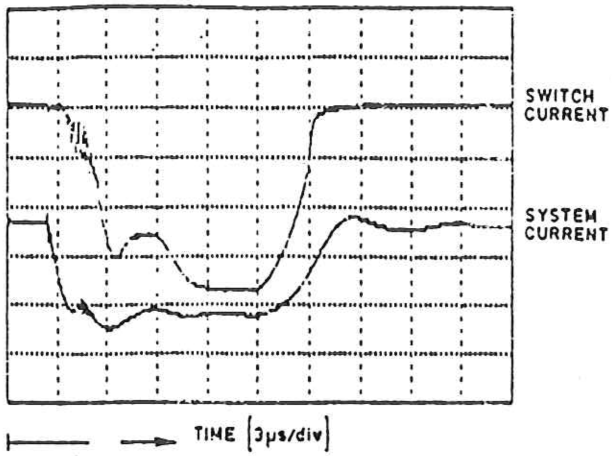

Fig. 4 Temporal behavior of switch current in undoped semi-insulating GaAs with system current as a reference (Switch current: 2 A/div.).

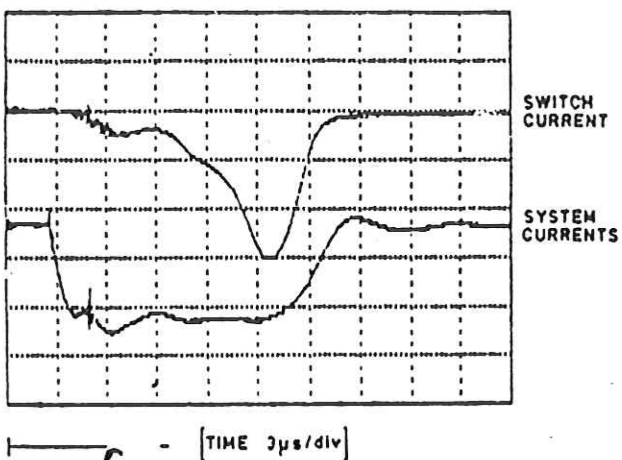

Fig. 6 Temporal behavior of switch current in semi-insulating GaAs containing a layer of highly Zn-doped material (Switch current: 4 A/div.).

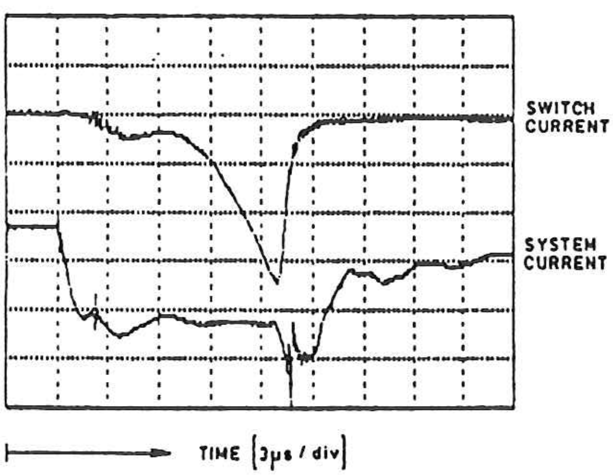

Fig. 7 Temporal behavior of switch current for same sample as in Fig. 12. This figure clearly shows the response of switch current to the termination of the e-beam due to a breakdown in the diode.

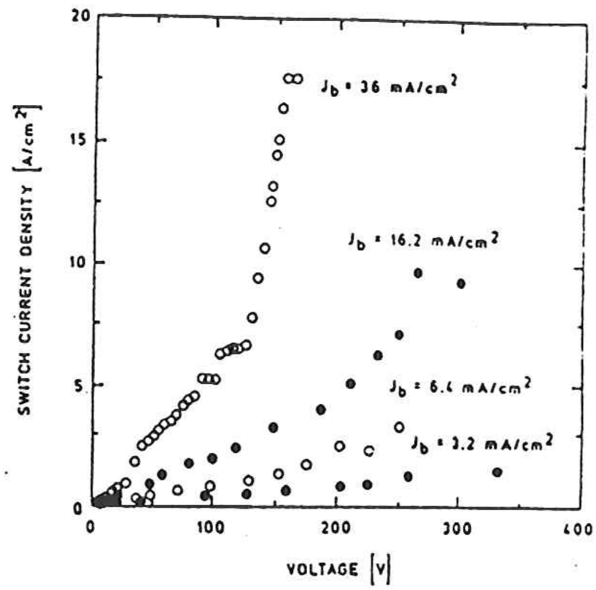

Fig. 5 Current density vs bias voltage for a GaAs switch (0.5 mm thickness) with the e-beam current density as a variable parameter.

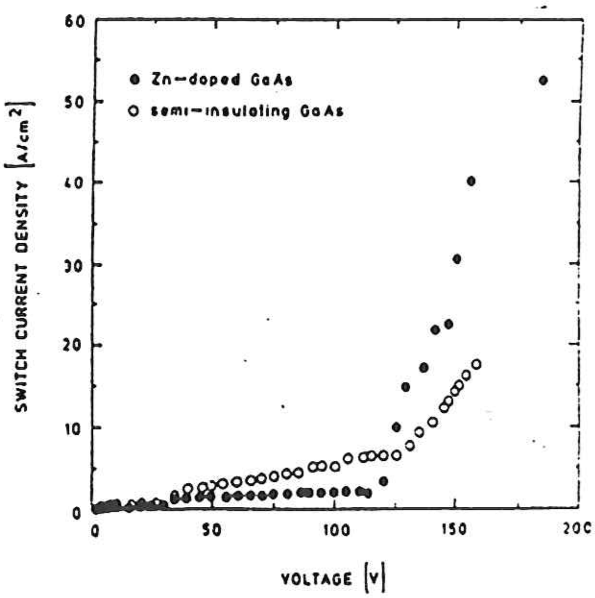

Fig. 8 Switch current-voltage characteristics for semi-insulating GaAs and for the same material containing a highly doped layer of Zn at the cathode.

WORKSHOP PROCEEDINGS
"OPTICALLY AND ELECTRON-BEAM CONTROLLED SEMICONDUCTOR SWITCHES"
MAY 23-24, 1988
NORFOLK, VIRGINIA

Subnanosecond Photoelectron Beam Closing Switches

Glenn Gerdin, K. H. Schoenbach, V. K. Lakdawala, and A. N. Dharamsi

Department of Electrical and Computer Engineering

Old Dominion University

Norfolk, VA 23529–0246

I. Introduction

Solid state fast closing switches could be a replacement for thyratrons and spark gaps if they can be scaled to high voltage and current operation. As such they could be used in a wide variety of applications such as Marx banks, pulse–forming networks, frozen–wave generators,[1] and in pulse generators for time–domain analysis[2]. The latter require subnanosecond pulses and presently employ step–recovery diodes which can be stacked to achieve a 200V step pulse with 200ns rise time[3]. Thus, while an improvement of several orders of magnitude would be required to replace thyratrons and spark gaps in conventional pulsed power applications[4], more modest increases could have an impact on time domain analysis in the near term.

The concept considered here is shown in Figure 1. A laser shines on the photocathode with a light pulse of subnanosecond risetime to generate a photoelectron beam having the same risetime which is then accelerated to between 10 and 200kV. The beam then strikes the cathode of a semiconductor diode (SCD) creating electron–hole pairs as the electrons in the beam slow down in a thin layer next to the cathode. If the electrons are then drawn off to the anode of the SCD, this would resemble a version of the electron bombarded switch, EBS, which were developed in the 60's and 70's and tested for over 2500 hours of life on CW r.f. amplifiers[5]. However the EBS was current limited by space charge effects in the bulk of the SCD so that prospects for the replacement of thyratrons using the EBS concept would not be promising.

To overcome this problem, it is proposed to explore a concept conceived by K. H. Schoenbach and V. K. Lakdawala[6] to enhance the recombination radiation from the layer where the beam electrons slow down by specially doping this layer. The recombination radiation then spreads out into the bulk material and creates electron hole pairs in this

region through absorption. The bulk electron hole pairs eliminate space charge and permit the flow of much higher currents than those in the EBS. Preliminary experiments indicate this technique will work[7], so in the rest of this paper, the prospects of scaling this photoelectron beam switch to higher power levels will be explored for purposes of design.

II. Design Criteria

As a first approach to the subject, the feasibility of scaling of the photoelectron beam driven switches (PEBS) to high operating voltage and power levels will be explored keeping the risetime τ_R and characteristic line impedence Z_L fixed. Since one of the applications of these switches is time–domain radar,[2] where the power transmitted by the antenna scales as $(di/dt)^2$, the scaling of operating power requirements and i, the current carried by the switch, is clearly of interest as is the scaling of this power with risetime. However since these latter two are inversely related, it is a simple matter to convert the results obtained here for $\tau_R \sim 300$ps to other risetimes.

It will be attempted in this study to introduce the essential phenomena governing the various parts of the PEBS (Fig. 1) to determine those most likely to limit performance and those areas where the lack of sufficient data creates the greatest uncertainties. Also it will be attempted to survey the status of the technology to see which components of the PEBS are commercially available and which are in need of development.

Before proceeding it should be noted that two other restrictions are imposed on the scope of this study: the geometry of the semiconductor diode (SCD) and its material compositon.

Two configurations are possible as shown in Fig. 2. One is the side–on illumination by the photoelectron beam (PEB), Fig. 2a, and the other is the end–on illumination or 'shine–through' configuration of Fig. 2b. For side–on illumination, the depth of the current channel is basically the penetration depth of the PEB, which is limited to less than 100μm by the damage limit for the semiconductor material ($E_e \leq 220$keV for GaAs[8]). This

small channel width forces the current densities to be prohibitively high for low Z_L (~50Ω), high–power systems and so this configuration (Fig. 2a) was rejected at the initial stage of this study. Thus only the 'shine–through' geometry of Fig. 2b will be considered.

The SCD material is restricted to GaAs. Part of this decision is due to the authors' experience with this material and is also due to its several advantages. Its properties of high resistivity, high electron mobility, and of being a direct bandgap semiconductor give it distinct advantages for the high power PEBS over the now extensively used silicon and germanium. On the other hand, it has been investigated for a much longer period than the other more 'exotic' materials and hence has a much better data base on which to make predictions.

With these restrictions in mind, the phenomena that need to be explored in a PEBS feasibility study consist of the circuit, the semi–conductor, the PEB, and the photocathode–laser conbination (Fig. 1). The circuit imposes the magnitude of the current required, risetime limitations and the load which impact the driving power neccessary to close the PEBS properly. Next the physics of the semiconductor imposes restrictions as to the maximum current and minimum risetime which in turn have a strong influence on the switch driving power requirements. Third, vacuum space charge places limits on the PEB which supplies the driving power for the SCD. Finally the efficiency of the photocathode at laser wavelengths has a strong effect on the power requirements of the laser which could have a significant effect on the degree of compactness and cost that a PEBS could achieve. These four topics are the subject of a report.[9]

References

1. H.M Cronson, IEEE Trans. Microwave Theory Tech. MMT–23, 1048 (1975) and J.M. Proud and S.L. Norman, IEEE Trans. Microwave Theory Tech. MMT 26, 137 (1978).
2. C.L. Bennett and G.F. Ross, Proc. IEEE 66, 299 (1978).
3. J.R. Andrews, "Fast Pulse Generator Survey", in Time–Dome in Measurements in Electromagnetics, Ed. Edmund K. Miller, Van Nostrand Reinhold, New York, 1986, chap. 4.
4. I. Vitkovitsky, High Power Switching, Van Nostrand Reinhold, New York, 1987.
5. D.J. Bates, R.I. Knight and S. Spinella, "Electron–Bombarded Semiconductor Devices", Adv. Electrical and Electron Phys. 44, 221 (1977).
6. K.H. Schoenback, V.K. Lakdawala, K.B.J. Schmitt,and T.J. Powers, Proc. SPIE 871, "Space Structure, Power, and Power Conditioning (1988)," 133 (1988).
7. K.H. Schoenbach, V.K. Lakdawala, D.C. Stoudt, and T.F. Smith, "Electron–Beam Controlled High Power Semiconductor Switches", submitted to IEEE Trans. on Electron Devices, July, 1988.
8 W. Ehrenberg and D.J. Gibbons, Electron Bombardment Induced Conductivity Academic Press, 1981, 72.
9. G. A. Gerdin, K. H. Schoenbach, V. K. Lakdawala, and A. N. Dharamsi. "Subnanasecond Photoelectron Beam Closing Switches," Physical Electronics Research Center Report No. PERC 8801, Old Dominion University, Norfolk, VA. 23529–0246, October 1988.

Figure Captions

Fig.1. Overall schematic of the photoelectron beam switch. The laser drives the photocathode PC generating the photoelectron beam I_B. This beam is accelerated by the beam potential V_B into the cathode of the semiconductor diode, SCD. Recombination radiation generated in the Zn doped layer ionizes the bulk of SCD to overcome space charge and closes the SCD so the voltage V_o can drive the load Z_L.

Fig.2. Two possible illumination schemes for the photoelectron beam. a) The photoelectrons strike across the anode cathode gap of the SCD in side–on illumination and the circuit current flows through the region of beam penetration on the surface of the SCD. b) The photoelectrons strike the cathode (cathodolumenescense) of the SCD (region I) and the circuit current flows across the SCD through the bulk.

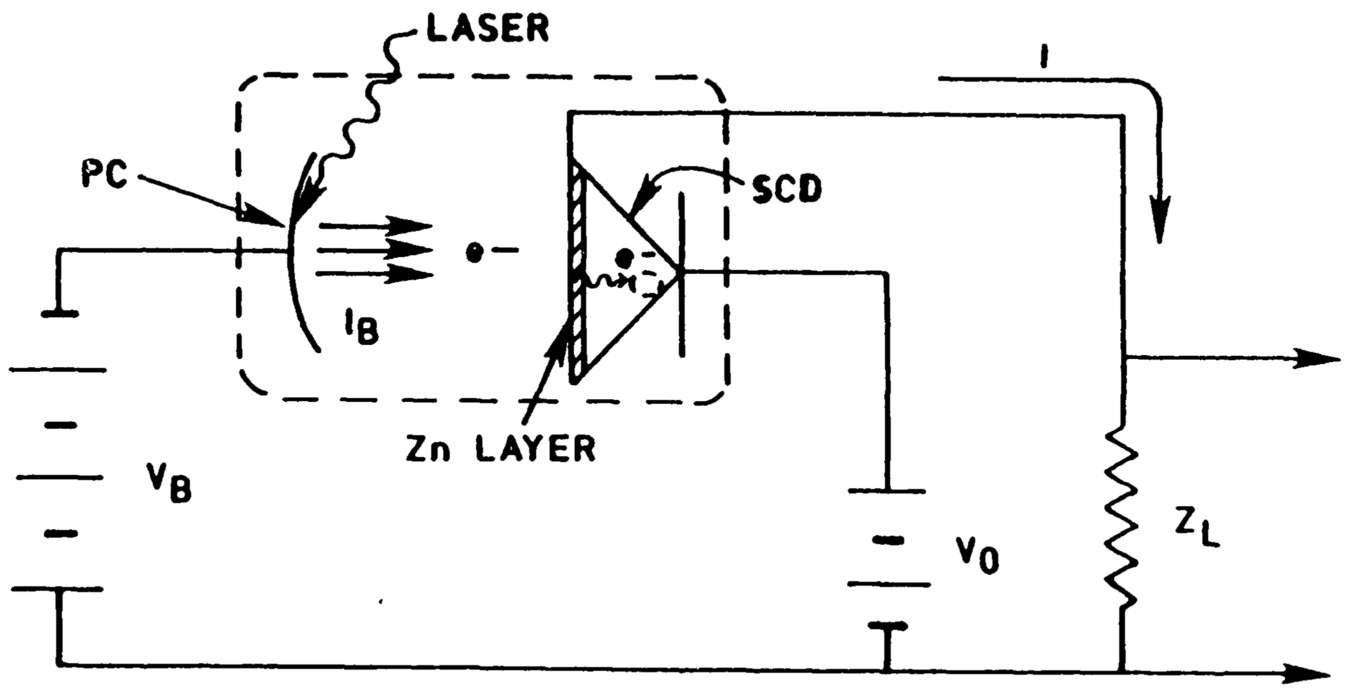

LASER
I
PC
SCD
I_B
Zn LAYER
V_B
V_0
Z_L

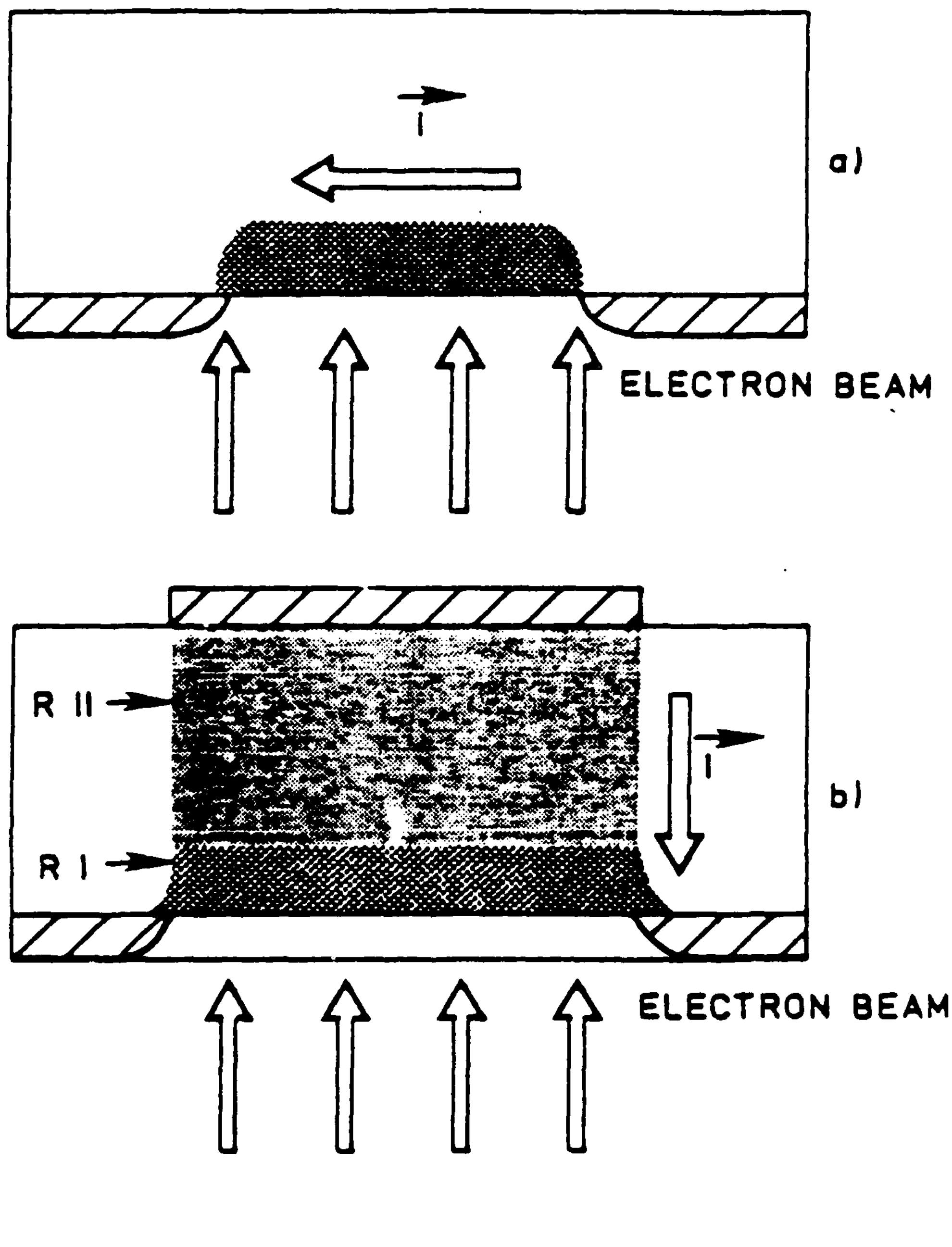

I
a)
ELECTRON BEAM
R II
R I
I
b)
ELECTRON BEAM

OPTICAL AND ELECTRON-BEAM CONTROL OF SEMICONDUCTOR SWITCHES

K. Schoenbach, V. Lakdawala, S. Ko, M. Mazzola, D. Stoudt and T. Smith

Department of Electrical and Computer Engineering
Old Dominion University
Norfolk, VA 23529-0246

Abstract

Currently at Old Dominion University there are two ongoing research projects on bulk semiconductor switches which can be closed and opened on command. Both types of switches have the advantage of requiring small energies to support the conductivity and switching action on a nanosecond time scale is possible.

The switch mechanism in one of the projects is based on laser quenching of photoconductivity in semiconductors containing certain deep level impurities.[1] Investigations in GaAs and CdS crystals have demonstrated the quenching effect.

The second project deals with electron-beam (e-beam) control of semiconductor switch. The electrons are injected through a contact into the cathode region of a semiconductor switch. Through cathodoluminiscence processes it is possible to obtain bulk ionization thereby overcoming the space charge limitations. Switch current/e-beam current ratio of more than 1500 at current densities of 60 A/cm^2 has been achieved so far. Improvements by an order of magnitude in the current gain seems to be possible by proper choice of cathodoluminiscent material.

Introduction

Bulk semiconductor switches - both optically and e-beam controlled - switches have gained the attention of the pulsed power community for a number of reasons, such as, fast rise time, jitter free operation, high energy efficiency, low inductance and high repetition rates.

In optically controlled switches the closing is obtained by optical generation of electron-hole pairs through band-to-band transitions. This method allows fast-on switching. The use of this method for fast opening - by turning the light source off - requires short recombination life times in the semiconductor material. The correspondingly high losses during conduction, which must be compensated by means of "expensive" laser photons, limits the efficiency of such an opening switch considerably and make it useful probably only for applications where energy considerations are of secondary importance. However, if it becomes possible to use the advantages of bulk semiconductors for off-switching (scalability and reliability) and, on the other hand, increase their efficiency, these switches would become serious competitors to presently used rep rated switches.

A concept where laser radiation is used only to turn the conductivity in the semiconductor material on and off, not to sustain it, is presented. As a switch material a direct semiconductor material (such as GaAs, CdS) doped with deep level impurities (such as Cu) is used. The laser is used to modulate the population of the deep levels and hence, depending on the wavelength, generate either free electrons or free holes. The second process leads to increased recombination and serves as opening mechanism.

A second concept which utilizes e-beam ionization of bulk semiconductors is followed. This allows the control of the semiconductor conductivity in the temporal range (μs) where the operation of the photoconductive switches is limited. Long e-beam pulses (tens of μs's) at current densities in the tens of mA's range can easily be obtained with e-beam diodes (with a heated thoriated tungsten cathode). Other advantages of e-beam control of bulk semiconductors compared to photoconductive switching are: wide band gap material (such as diamond) can be activated, hold-off voltage limitation (surface flashover for example) can be overcome by using a switch configuration where the e-beam is injected through the contact. The major disadvantage of e-beam controlled semiconductor switches, the small penetration depth of the electrons, can be overcome by using cathodoluminiscent processes to provide for an electron-hole plasma in the bulk of semiconductor.

Laser Controlled Semiconductor Switch

A semiconductor material which has a large electron-hole recombination coefficient is used as base material. The semiconductor is doped with a material which generates deep acceptor levels below the middle of the band gap. The deep centers are assumed to have electron capture cross sections very small compared to hole capture cross sections. The semiconductor is counterdoped with donors in shallow levels in order to fill the deep centers before switching action.

An increase in conductivity - closing of the switch - is obtained through photoionization of trapped electrons from the deep acceptor level into the conduction band by means of a short laser pulse. In addition, electron-hole pairs are generated by two-photon ionization via the vacant deep centers [Fig. 1(a)]. After an initially fast drop of carrier density due to recombination of free electrons and holes, the decay of electrons due to capture into the deep centers is relatively slow [Fig. 1(b)]. Hence, the conductivity remains high for times long compared to the turn-on time. The opening of the switch - reduction of the conductivity - is induced by low-energy photons which ionize the trapped holes into the valence band and stimulate their recombination with the electrons in the conduction band [Fig. 1(c)].

A material which has the required features for the described optically triggered switch is GaAs, doped with copper and counterdoped with silicon.[2] Copper generates deep

CH2662-5/88/0000-0318$01.00 © 1988 IEEE

acceptors in GaAs and Si is a shallow donor impurity. Copper is one of the well-known impurities in III-V compounds. Studies of the direct semiconductor material GaAs show two dominant copper related deep level defects Cu_A and Cu_B.[3] The Cu_B level, which is of main interest for our concept, is at 0.44 eV above the valence band. At room temperature the band-gap energy is 1.42 eV for GaAs.

Modeling

Modeling of the temporal variation of electron and hole densities in the bulk of the semiconductor when irradiated with two subsequent laser pulses of equal intensity, but different wavelengths, was done by using rate equations for different levels.[5] The results of the theoretical calculations are shown in Fig. 2. The photon fluxes are assumed to be gaussian in the simulation. The three distinct phases of the switch operation , i.e., the turn-on, the on state and the turn-off phase, are shown in the figure. It is clearly seen from these results that the switch can stay on for periods much longer (indicated by the flat region of the free electron density) than the duration of the turn-on and turn-off pulses (10 ns FWHM) and the laser radiation is not required to sustain the conductivity.

Experimental Results

Optogalvanic measurements to demonstrate the feasibility of the concept were conducted on CdS crystals containing Cu and some natural defects and Si doped GaAs crystals diffused with copper. LEC grown GaAs samples with a Si doping density of $2 \times 10^{16} cm^{-3}$ supplied by Morgan Semiconductors were used as host material.

For CdS experiments simple contacts were used. Instead of evaporating ohmic contacts on each sample, an electrolytic $CuSO_4$-water solution was used to realize electrodes. For GaAs a more detailed process was used. The low resistivity Si doped GaAs wafers supplied by the manufacturers were compensated by doping the bulk with copper using the method of thermal diffusion. First, a thin layer of copper was vacuum deposited onto one side of the sample. The sample was then annealed at 750°C for 40 minutes for copper to diffuse uniformly throughout the sample. The measured sample resistance increased by three orders of magnitude as compared with a control sample that did not undergo copper diffusion. A sample resistance of about 1 kΩ was obtained. This result is in good agreement with the results of Blanc et al.[2] Their results show that it is possible to obtain a resistivity of 10^8 ohm-cm by copper compensation. Au-Ge contacts were deposited on the sample in a planar geometry. They were found to be ohmic.

Experimental Set Up

Optogalvanic measurements (turn on and turn off) were performed with the prepared sample. The experimental set up used is shown in Fig. 3. The sample was dc biased and the fast photoinduced transient signals were coupled to a 50 Ω diagnostic system through a capacitor. Because of the dc bias and finite resistance of the sample, there was a significant dark current. This dark current was augmented by the flash lamp which induced photocurrents on the order of another few mA. The sample was then irradiated with a 8 ns FWHM laser pulse produced by a tunable laser system based on a Nd:YAG laser. The flashlamp pulse width (a few μs) was long compared to the laser pulse, thus the photoexcitation was quasi dc.

Turn On Experiments

In order to study the turn-on phase and the conductive phase of the semiconductor switch, laser radiation at 1064 nm wavelength was used (pulse duration 3 ns FWHM, 30 mJ pulse energy). The GaAs sample was illuminated through a 1 mm wide slit which allowed the activation of just the center part of the semiconductor between the contacts. A typical signal is shown in Fig. 4. It clearly shows the expected initial fast decay of photon induced current, due to the electron hole recombination and the subsequent slow change in current caused by trapping of electrons into Cu_B level. The results demonstrate that compensated GaAs:Cu:Si, if used as a photoconductive switch, can be activated by using Nd:YAG laser radiation at 1064 nm. The decay time of the conductivity is, after an initial drop with 1/e time of about 10 ns, in the range of few tens of μs. These time constants are only slightly dependant on the temperature in the range of $77°K \leq T \leq 370°K$. The initial strong decay of photoconductivity can be reduced by using photoconductors with similar band structure and deep level configuration but higher ratios of electron photoionization versus hole photoionization for the dominant deep level (eg: InP:Cu). The dark resistivity, which was at room temperature in the range of 10 ohm cm for the prepared samples is strongly increasing for the p type (overcompensated) sample with reduced temperature. A value of 10^5 ohm cm was measured at 77°K. Higher values, exceeding those for Si switches by orders of magnitude can be obtained by proper compensation.[2] These high values would allow to dc-charging of pulse power devices which use photoconductive switches.

Turn-off Experiments

A response of a CdS sample to irradiation with white light and subsequent illumination with IR-light is shown in Fig. 5. The upper trace shows the turn on phase only. The lower trace depicts part of the turn on phase (left) and the turn off phase. The initial increase in the conductivity for a period of about 50 ns is due to generation of free holes by the laser pulse. Subsequently the conductivity decreases due to electron-hole recombination with a time constant of about 250 ns. A more detailed discussion of results in CdS can be found elsewhere.[4]

The results of the optogalvanic experiments with GaAs samples is shown in Fig. 6. Low intensity laser radiation at 1300 nm was incident on the sample superimposed on flashlamp irradiation. A negative current pulse with a fast fall time can be clearly observed from the figure. The flashlamp induced current is shown superimposed on the trace. It is seen that all of the flashlamp current is interrupted (optical quenching) as well as a portion of the dark current. The partial dark current interruption is an effect known as negative photoconductivity.[6] The conditions for the negative photoconductivity to occur are discussed by Bube.[7] Based on DLTS experiments in our laboratory, it seems likely that these conditions are met in our samples. The optogalvanic measurements demonstrate the feasibility of our concept.

E-Beam Controlled Semiconductor Switch

The switch concepts are based on e-beam controlled ionization of the semiconductor material. The switch closes when the e-beam is turned on and generates free charges in the semiconductor. When the e-beam is turned off, the con-

ductivity of the semiconductor decreases due to electron-hole recombination, trapping of free charge carriers, and diffusion.

There are two basic switch configurations. In one configuration (I) the contacts are coplanar and the ionizing electrons are injected in the direction perpendicular to the applied electric field (Fig. 7a). In the second configuration (II) the electrons are injected through one of the contacts in electric field direction (Fig. 7b). Assuming that free charges are generated only in a layer corresponding to the range R of primary electrons the current in configuration I is limited to values on the order of ten amps even at current densities of 10^3 A/cm^2.

In configuration II, the principle of operation is analogous to that of a vacuum photodiode with electrons instead of photons used to generate electron-hole pairs adjacent to one of the contacts (cathode). The so-called Electron Bombarded Semiconductor Devices (EBS-Devices), which were developed in the late sixties and the seventies[8] as microwave power tubes are examples for this mode of operation. The high field in the region between the contacts causes a rapid separation of electrons and holes. The electrons are swept across the highly resistive region. The holes have no effect but to provide continuity of charge. This device has a nanosecond response to changes in the source function (e-beam). However, since the current density is space charge limited, relatively high voltages are needed to obtain reasonably high current densities. For a trap free insulator, which represents the optimum condition for space charge limited current flow in solids, the space charge limited current density is given by Mott-Gurney's square law:

$$J = (8/9) \ \varepsilon\mu \ V^2/d^3 \qquad (1)$$

where V is the applied voltage, d the thickness of the semiconductor sample, ε the permittivity, and μ the mobility of the electrons. For a 0.5 mm GaAs sample, biased at 60 V, the maximum current density according to Mott-Gurney's law is 0.15 A/cm^2.

A way to overcome the space charge limitation, without sacrificing the advantages of e-beam control, is to convert the electron energy E into photon energy I and use the e-beam generated radiation to ionize the bulk of the semiconductor (Fig. 8). The radiation generated directly and indirectly by the e-beam is Bremsstrahlung (X-rays) and band edge radiation due to radiative recombination of electron-hole pairs in the e-beam activated layer. It is generated in region I, whose depth is given by the electron range, and is absorbed in region II where it generates an electron-hole plasma.

The energy efficiency for Bremsstrahlung I/E is relatively small for the electron energy range of interest. It scales linearly with the electron energy and the atomic charge Z:[9]

$$I/E = 4 \cdot 10^{-5} \, Z \, E \qquad (2)$$

with E in MeV. For GaAs and an electron energy of 200 keV, I/E is about 0.5%. The energy efficiency for band edge radiation with a photon energy around 1.4 eV can exceed that of Bremsstrahlung by more than an order of magnitude. The effective ionization energy for GaAs is 4.3 eV. The external quantum efficiency, the number of photons emitted per electron-hole recombination process, in GaAs p-n junction devices was measured to be 0.083, corresponding to an internal quantum efficiency of 0.88 at room temperature.[10] Hence, the total energy efficiency for cathodoluminiscence could be about 35% under optimum conditions.

The efficiency of bulk ionization with band edge radiation is, unlike the ionization by X-rays, independent of the energy of the primary electrons. This allows to use relatively low energy electrons to provide for the generation of electron-hole pairs in the luminescent layer. An additional advantage of this method is the fact that the cathodoluminiscentlayer in the semiconductor switch is highly conductive and therefore can be used to carry the switch current to contacts, which are placed outside the e-beam irradiated region. This way electron losses in contacts, which at low electron energies can be substantial, are avoided. The cathodoluminiscent layers near contact region can be realized by doping with shallow donors or acceptors (such as Zn) for a thickness corresponding to the electron range.

It could be shown by using a rate equation model that the combined effect of Bremsstrahlung and recombination radiation on electron-hole generation in the bulk of the semiconductor, could lead to an extention of the current density range of electron-bombarded semiconductor switches to hundreds of $amps/cm^2$.[11] This is an improvement in current density of two to three orders of magnitude over EBS-devices. Experimental results with semj insulating GaAs as base material have proven the feasibility of the concept.

Experimental Set Up

Two types of switches were investigated: one, where the switch material was completely undoped GaAs; and a second one, again using GaAs as the basic material, but with a surface layer of highly Zn-doped material. In both cases the GaAs used was semi insulating, LEC grown. The resistivity of this material was given as 7×10^6 ohm cm (Spectr.). The shallow layer of p-type GaAs was generated by diffusion of Zn for two hours at a temperature of 750° C. According to Ref. 12, this procedure creates a p-type layer of about 10 μm thickness with an acceptor concentration of 10^{19} cm^{-3}. Au:Ge contacts of about 0.1 μm thickness were evaporated onto both faces of 0.5 mm wafers with a contact area of 0.8 cm^2 and annealed at 400° C for 15 minutes.

The experimental set up is shown in Fig. 9. The e-beam is produced by a pulsed thermionic diode. The diode voltage is generated by a pulse forming network (PFN) consisting of a LC-chain and is stepped up in a ratio 1:11 by a pulse transformer. The pulse duration can be adjusted between 1 μs and 15 μs by varying the number of PFN segments. The rise and fall time of the voltage pulse is 500 ns. The maximum diode voltage is 220 kV, determined by the pulse transformer rating. The e-beam current density can be varied in the range up to 100 mA/cm^3 by varying the temperature of the thoriated tungsten cathode. In our experiments we have used a 200 keV e-beam to irradiate the semiconductor sample outside the diode chamber. The energy losses in the anode-foil of the diode (1 mil titanium) are less than 20% at this e-beam energy.[13]

In order to get the current density-voltage characteristics of the semiconductor switches, a dc voltage was applied to the sample. The current flowing through the semiconductor, when it was irradiated with high energy electrons was measured by means of a Pearson coil. The temporal development of the e-beam diode voltage was recorded simultaneously at each

shot. This signal was obtained by measuring the total PFN current flowing into the 2600 Ω load resistor and, parallel to it, the e-beam diode. The variable parameter in all the measurements was the e-beam current density at a fixed electron energy of 200 keV.

Experimental Results

The temporal current response of semi insulating GaAs-switch of 0.5 mm thickness to e-beam irradiation is shown in Fig. 10 for an e-beam current density of $J_e = 36$ mA/cm^2 and a bias voltage of 135 V. Also shown is the e-beam diode voltage for this particular switch event. The e-beam irradiated face is the cathode of the switch. The switch current signal follows closely the e-beam pulse. The switch current density in this case was $J_s = 9.4$ A/cm^2, that means that the current gain J_s/J_e is about 260.

The values of switch current density versus biasing voltage, with the e-beam current density as variable parameter are plotted in Fig. 11 for 0.5 mm semi insulating GaAs wafers. The curves with J_e 16.2 mA/cm^2 were obtained with one sample, the curve with $J_e = 36$ mA/cm^2, with a different sample, but the same semiconductor material. The slope of the curves, which represents the switch conductance per cm^2 area, varies linearly with the e-beam current density. For $J_e = 36$ mA/cm^2 the switch conductance is 0.05 Ω^{-1} cm^{-2}, corresponding to a resistance of 20 Ω/cm^2. Compared to the initial resistance of the sample, 0.35 MΩ/cm^2, the reduction in resistance due to e-beam irradiation is more than four orders of magnitude.

The temporal response of the second type of switches; semi insulating GaAs switches with a shallow layer of Zn-doped material in the cathode region, is shown in Fig. 12. Zn was used to generate a high cathodoluminiscent zone in the cathode area of the switch. Calculations[11] and measurements[14] have shown that doping GaAs with Zn at levels of 10^{18} to 10^{19} cm^{-3} increases the rate for radiative recombination drastically. The cathode face of the semiconductor switch is irradiated by the e-beam. Contrary to the results with homogeneous switch material, the temporal response does not follow the e-beam pulse over the entire length of the pulse. After an initial linear response, whose duration is increasing when the e-beam intensity is lowered, a more or less linear rise of the switch current is observed. The current flow is terminated when the e-beam is turned off. That the current termination is controlled by the e-beam is even more clearly shown in Fig. 13 where, due to a breakdown in the diode, the e-beam was turned off very rapidly. The switch current followed the e-beam current instantaneously. That means that opening of the switch is fully controllable by the e-beam. The maximum switch current density, obtained at the end of the current pulse, is, at voltages above 125 V, about twice as large as the current density in homogenous switch material. This is shown in Fig. 14. The maximum switch current density obtained in our experiments with Zn-doped GaAs was 53 A/cm^2, at a voltage of 185 V across the switch. This number corresponds to a current gain J_s/J_e of 1472.

Conclusions

Two concepts - optical and e-beam control of semiconductor switches - which utilize deep level impurities for switching action are described. The switches can be closed and opened on command. Both types of switches have the advantage of requiring small energies to support conductivity and fast switching action (ns) is possible. Experimental results demonstrating the feasibility of the concept are presented.

Acknowledgements

The laser controlled semiconductor switch work is funded by SDIO/IST and manged by ONR under contract # N00-14-86-k-560. The e-beam controlled semiconductor switch work is funded by ARO and AFOSR.

References

[1] K.H. Schoenbach, V.K. Lakdawala, R. Germer and S.T. Ko, "*An Optically Controlled Closing and Opening Semiconductor Switch*", J. Appl. Phys., 63, 2460 (1988)

[2] J. Blanc, R.H. Bube and H.E. McDonald, "*Properties of Gallium Arsenide Compensated with Diffused Copper*", J. Appl Phys., 32, 1666 (1961)

[3] N. Kullendorf, L. Jansson and L.A. Ledebo, "*Copper Related Deep Level Defects in III-V Semiconductors*", J. Appl. Phys., 54, 3202-3312 (1983)

[4] S.T. Ko, V.K. Lakdawala and K.H. Schoenbach, "*Kinetics of Photoconductivity in Bulk GaAs with Deep Traps*", (to be published)

[5] R.F.K. Germer, K.H. Schoenbach and S.G.E. Pronko, "*A Bulk Optically Controlled Semiconductor Switch*", J. Appl. Phys., J. Appl. Phys., to appear in July 1988 issue.

[6] F. Stockmann, "*Negative Photoeffekte in Halbleitern*", Z. Physik, 143, 348 (1955)

[7] R.H. Bube, **Photoconductivity of Solids**, pp [illegible]-406, John Wiley & Sons, New York (1960)

[8] D.J. Bates, R.I. Knight, S. Spinella, and A.Silzars, "*Electron-bombarded Semiconductor Devices*", Adv. El. Phys., 44, 221 (1977)

[9] R.D. Evans, **The Atomic Nucleus**, pp 615, McGraw-Hill Book Company Inc., (1955)

[10] W.N. Carr, "*Characteristics of a GaAs Spontaneous Infrared Source with 40 Percent Efficiency*", IEEE Trans. on Electron Devices, ED-12, No. 10, 531 (1965)

[11] K.H. Schoenbach, V.K. Lakdawala, D.C. Stoudt, and T.S. Smith, "*Electron-Beam Controlled High Power Semiconductor Switches*", (to be published)

[12] H.C. Casey, **Atomic Diffusion in Semiconductors**, pp 351, D. Shaw, Ed., Plenum Press, New York, (1973)

[13] S.M. Seltzer and M.J. Berger, "*Transmission and Reflection of Electrons by Foils*", Nnd. Insts. and Meth., 119, 157 (1974)

[14] D.A. Cusano, "*Radiative Recombination From GaAs Directly Excited by Electron Beams*", Solid State Comm., 2, 353 (1964)

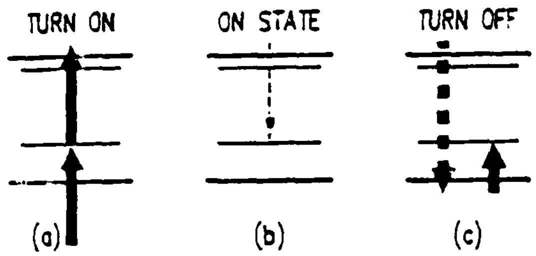

Fig. 1 Optical ionization processes (solid lines) and recombination processes (dashed lines) during different stages of the switch.

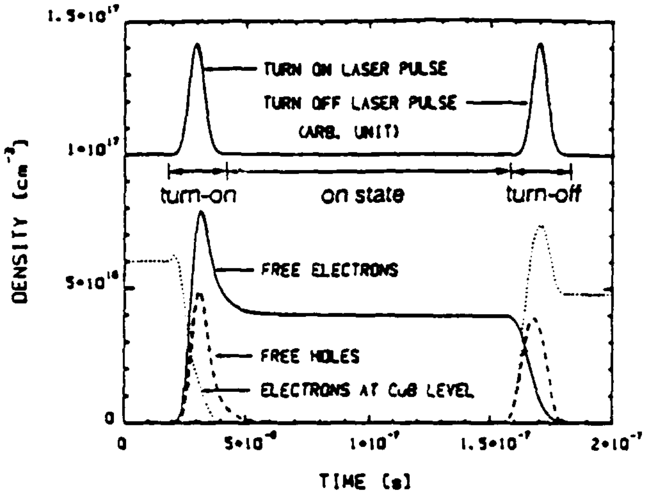

Fig. 2 Computed temporal variations of the charge carrier densities during different stages of GaAs:Cu:Si switch.

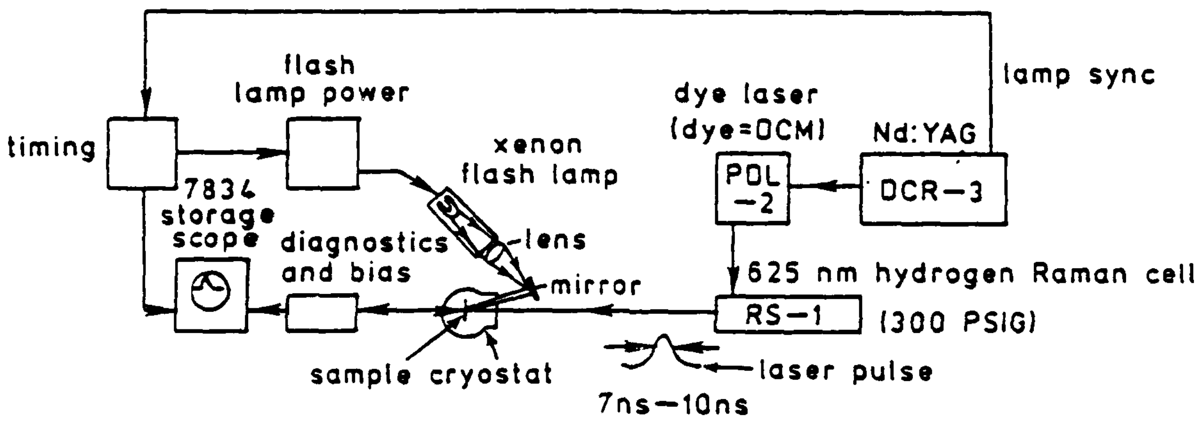

Fig. 3 Schematic diagram of the experimental set up for the laser controlled switch experiments.

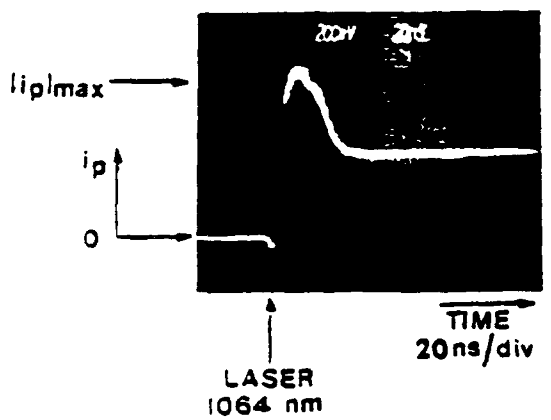

Fig. 4 A typical response of GaAs:Cu:Si sample to 1064 nm radiation (turn-on response).

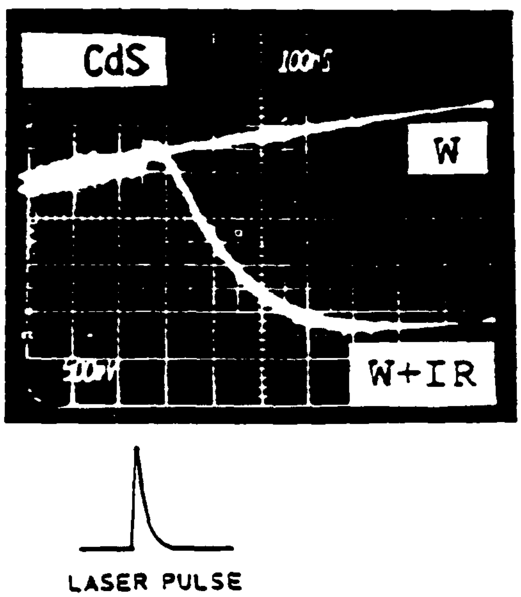

Fig. 5 A typical response of a CdS sample.

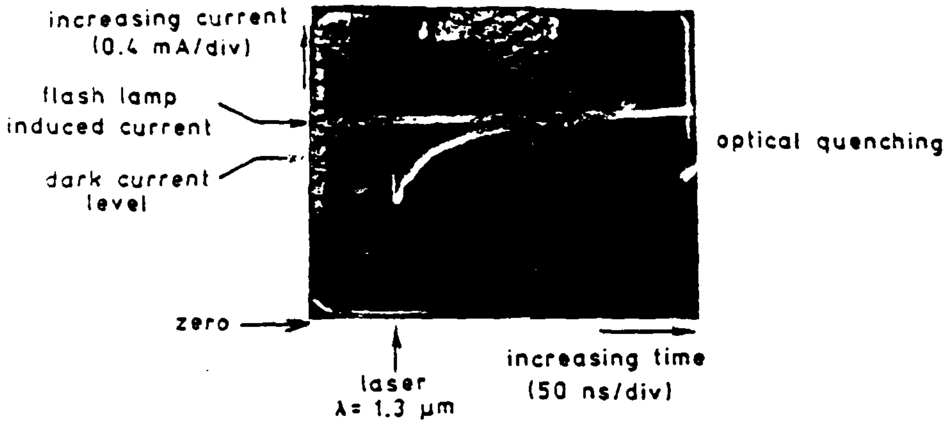

Fig. 6 A typical response of GaAs:Cu:Si sample to 1300 nm excitation superimposed on flashlamp excitation (turn-off - optical quenching).

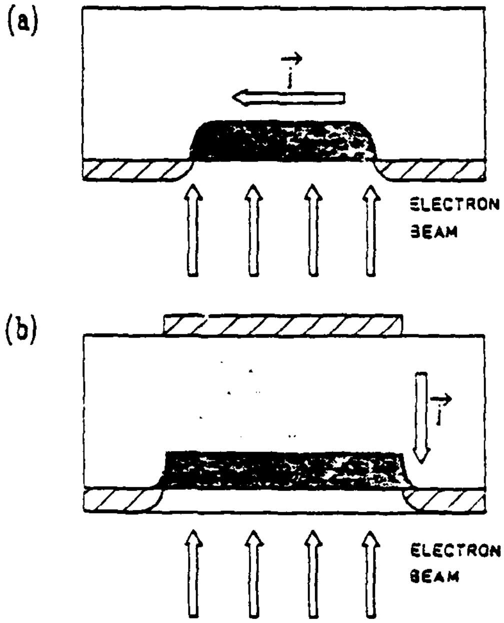

Fig. 7 High energy electron injection: a) perpendicular and b) parallel to the electric field in a semiconductor switch.

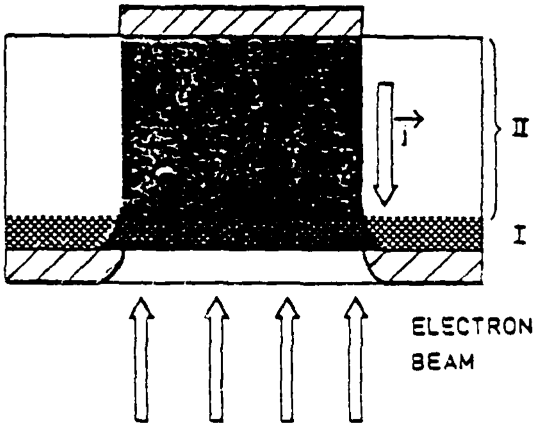

Fig. 8 E-beam controlled semiconductor switch with bulk ionization by cathodoluminescence.

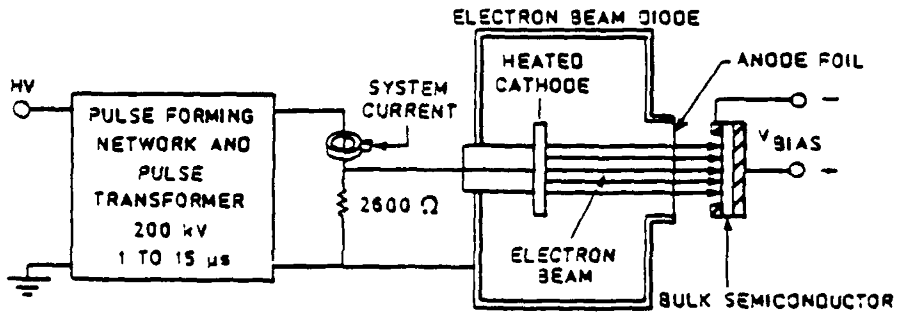

Fig. 9 Experimental set up of the 200 kV e-beam system.

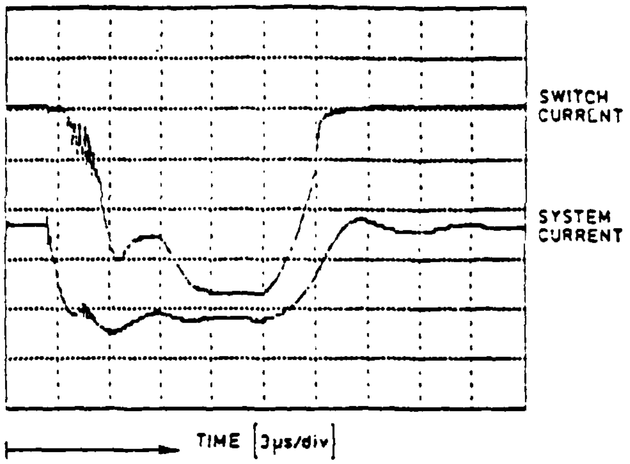

Fig. 10 Temporal behavior of switch current in undoped semi-insulating GaAs with system current as a reference (Switch current: 2 A/div.).

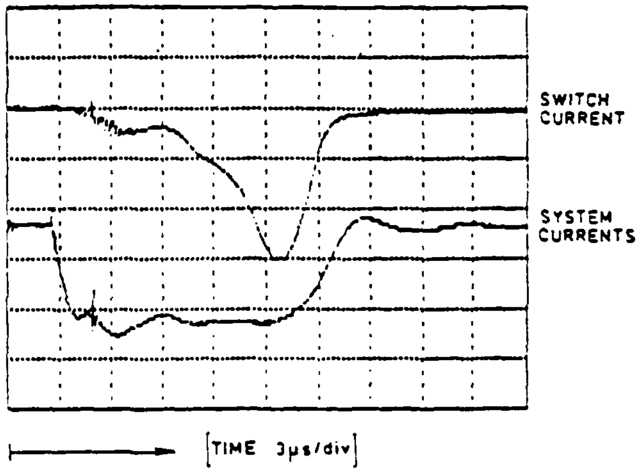

Fig. 12 Temporal behavior of switch current in semi-insulating GaAs containing a layer of highly Zn-doped material (Switch current: 4 A/div.).

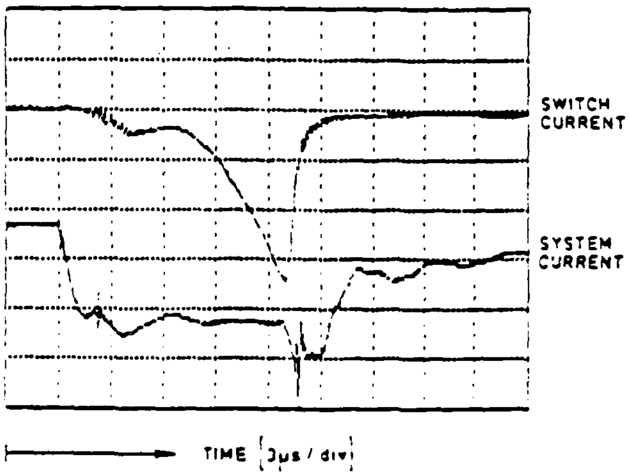

Fig. 13 Temporal behavior of switch current for same sample as in Fig. 12. This figure clearly shows the response of switch current to the termination of the e-beam due to a breakdown in the diode.

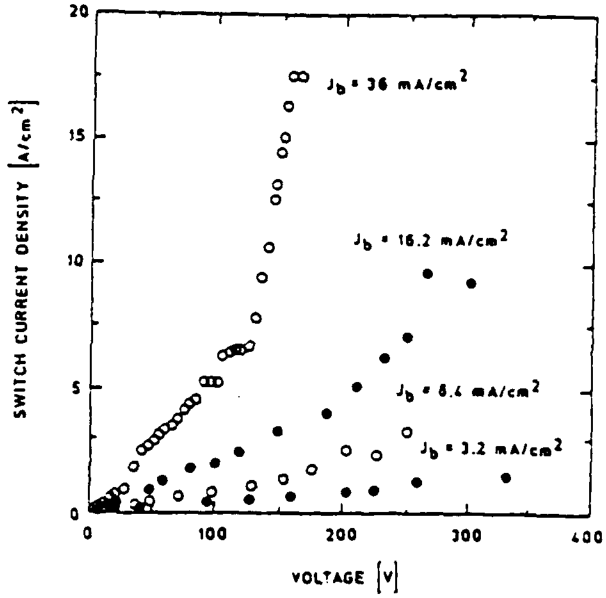

Fig. 11 Current density vs bias voltage for a GaAs switch (0.5 mm thickness) with the e-beam current density as a variable parameter.

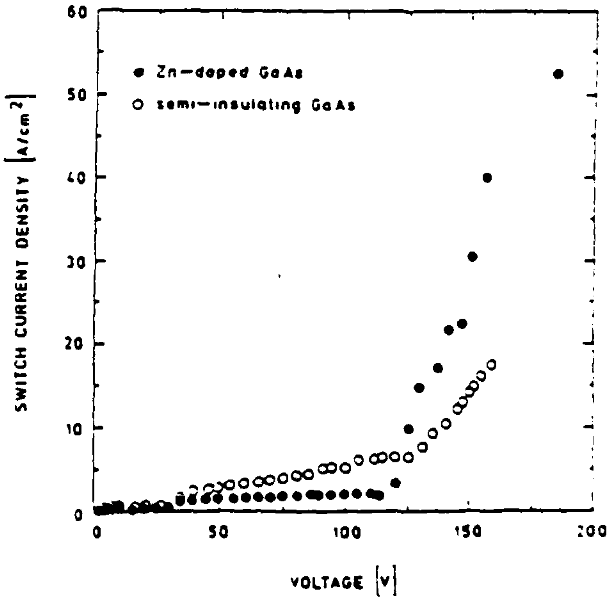

Fig. 14 Switch current-voltage characteristics for semi-insulating GaAs and for the same material containing a highly doped layer of Zn at the cathode.

Abstract Submitted
for the
May 1 - 4, 1989 Meeting
American Physical Society

Investigations into Chaotic Oscillations in GaAs substrate* -- D. Stoudt, R. Brinkmann, L. Vahala, K. Schoenbach and V. Lakdawala, Old Dominion University. The behavior of semi-insulating GaAs is investigated in the pulsed mode under strong electric fields. In particular, in the voltage range where there occurs a strong change in the dc current, one finds the onset of what appears to be chaotic oscillations. The onset of these oscillations and the dependence on experimental parameters is investigated. Power spectra will be exhibited. A simple model is constructed in an attempt to explain these oscillations. An analysis is performed which distinguishes between chaotic oscillations and microscopic fluctuations. In particular, a Grassberger-Procaccia time series analysis is performed on both the experimental and theoretical data to determine the dimensionality of the attractor.

*Work supported by the ARO & AFOSR: DAAL03-86-K-0078

Signature of APS Member

Dr. Linda L. Vahala
Same Name Typewritten

Old Dominion University
Address

THE ELECTRICAL CHARACTERISTICS OF SEMI-INSULATING GaAs FOR HIGH POWER SWITCHES*

D.C. Stoudt, K.H. Schoenbach, V.K. Lakdawala

Department of Electrical and Computer Engineering
Old Dominion University, Norfolk, Virginia 23529-0246

Abstract

Experimental studies on electron-beam controlled, high power semiconductor switches have been performed. In experiments on semi-insulating GaAs switches, current densities of 57 A/cm^2 have been obtained with an electron-beam current density of 26 mA/cm^2. Switch resistances of 1 ohm-cm^2 are possible with an electron-beam current density of 1 A/cm^2 and for a load resistance of 50 ohms. The dark current was found to be a function of voltage and time with response times in the μs to ms range. The dielectric strength exceeds 140 kV/cm for 3.5 μs FWHM voltage pulses. The measured electrical characteristics and the fast response of semi-insulating GaAs make it a promising material for pulse power switches.

Introduction

Research on photoconductive and electron-beam controlled semiconductor switches has evolved rapidly during the past few years. With the exception of one type of bulk semiconductor switch, where lasers with different wavelengths are used to turn the switch conductance on and off [1], the conductivity in these types of switches must be sustained by external ionization: lasers or electron-beams. The inability to produce a high power laser pulse with a pulse width in the μs range severely limits the conduction time of the photoconductive switch. Electron-beam ionization of bulk semiconductors, however, allows the control of the switch conductivity well into the tens of μs range.

Other advantages of electron-beam control of bulk semiconductors compared to direct photoconductive switching are:

- Wide band gap materials with a very high dark resistance, such as diamond, can be activated.
- The limitation in hold-off voltage, which in photoconductive switches is determined by surface flashover, can be overcome by using a switch configuration where the electron-beam is injected through the contact. In such a configuration, the breakdown voltage is determined by the intrinsic dielectric strength, rather than by the surface properties.
- The ability to generate a train electron-beam pulses, by using a triode or tetrode configuration [2], would allow the use of these switches in a high power modulator.

A major disadvantage of electron-beam control compared to laser control of semiconductor switches is the small penetration depth of electrons (tens of μm) as opposed to the long absorption depth of photons with energies less than the band gap (1000 μm at 1.1 eV). A way to overcome this disadvantage is to use direct semiconductors such as GaAs and convert the electron energy into optical energy. The band gap radiation generated in the electron-beam activated layer is used to ionize the bulk of the semiconductor switch over distances of up to a cm. The conversion of electron energy into radiation energy (cathodoluminescence) can be optimized by doping the base material, semi-

* This research is supported by the ARO and AFOSR under contract number: DAA L03-86-K-0078.

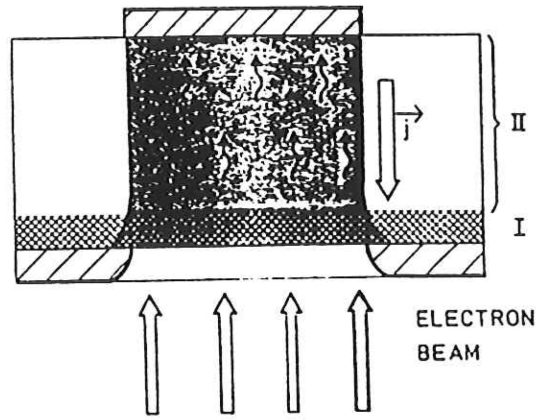

Fig. 1 Electron-beam controlled semiconductor switch with bulk ionization by cathodoluminescence.

insulating GaAs, with a shallow donor or acceptor material over the depth corresponding to the electron-beam range [3]. In this doped region (I), the direct radiative recombination rate is greatly increased there by providing an efficient source function for electron-hole generation in region II shown in figure 1 [4].

Experiments

Experiments were conducted to measure the electron-beam induced conductivity (EBIC) for several different semi-insulating (SI) GaAs samples. The as-grown SI GaAs had resistivities of 6×10^6 ohm-cm (Spectrum Technology, Inc.) and 3×10^7 ohm-cm (Morgan Semiconductor Division) while the carbon compensated material (GaAs:C) had a resistivity of 4×10^8 ohm-cm (Spectrum Technology, Inc.). The sample thickness for all of the switches was 0.05 cm with a contact area of about 1 cm^2. The sample configuration was similar to that shown in figure 1 with the exceptions that there was no doped, cathodoluminescent layer (region I) and the contacts were identical parallel plates on both sides of the bulk material. The contacts were made by thermal deposition of Au:Ge to a thickness of 0.1 μm. The experimental set-up used to measure the EBIC is shown in figure 2. The circuit was used to apply a 15 μs voltage pulse across the sample, during which the sample is irradiated with a 10 μs electron-beam pulse through the cathode. A pulsed voltage was used to reduce the problem of heating due to dark current at voltages greater than 100 V. A second circuit was built to determine the dark current characteristics of the samples. It consisted of a storage capacitor and a high voltage (3500 V) vacuum tube which was used to switch a voltage across the sample for durations of up to 500 ms.

Electron-Beam Induced Conductivity

The first experiments were done without the 50 ohm load resistance (figure 2). Figure 3 shows a typical voltage and current waveform for this "no load" condition. The switch current closely follows the electron-beam pulse (not shown). The observed reduction in the switch voltage is the result of

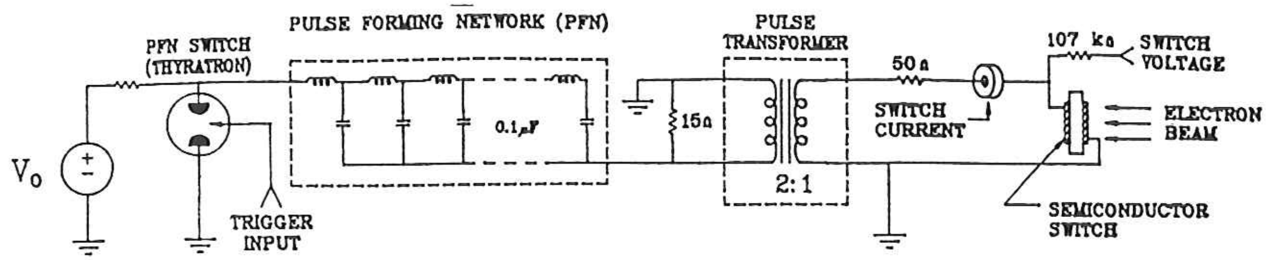

Fig. 2 Experimental set-up of the system used to measure the EBIC.

saturation effects in the inverting transformer shown in figure 2. The results of these measurements for three different samples are shown in figure 4. The maximum pulsed voltage applied to the 6×10^6 ohm-cm sample was 400 V which yielded a switch current density of 57 A/cm^2. The initial switch resistance before the electron-beam irradiation was about 600 kohms. This corresponds to a change in resistance due to irradiation of more than four orders of magnitude. The electron-beam current density used in these measurements was 26 mA/cm^2. Therefore, a maximum current gain (j_{switch}/j_{beam}) of 2200 was achieved. As shown in figure 4, for samples with increasing resistivities, the amount of current that can be switched decreases for a constant electron-beam energy and electron-beam current density. This results from the presence of deep levels in the material. Some of these deep levels can represent losses in the switch by acting as recombination centers. Therefore, as the losses are increased, the resistivity is increased which results in a reduction of the EBIC.

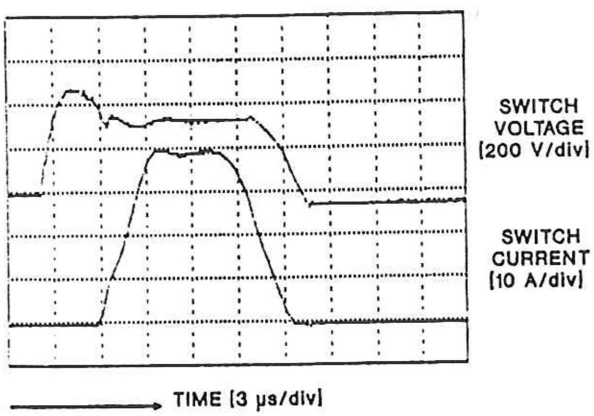

Fig. 3 Temporal behavior of the switch current and the applied switch voltage for the "no load" condition.

The next measurements were conducted on the 6×10^6 ohm-cm material with the 50 ohm load resistance in the circuit. The electron-beam pulse width was reduced to about 4 μs to observe the recovery of the switch. For an electron-beam energy of 175 keV and a current density of 26 mA/cm^2, the switch resistance stayed relatively constant at an average value of 35 ohms while the amplitude of the applied voltage pulse was varied from 80 V (1.6 kV/cm) through 400 V (8 kV/cm). The applied voltage across the switch and the electron-beam energy were then held constant at 250 V and 175 keV, respectively, while the electron-beam current density was varied between 0.1 and 26 mA/cm^2. The results of these measurements are shown in figure 5. The switch conductance was found to be roughly proportional to the electron-beam current density. This indicates that a switch resistance of a few ohms could be produced with an electron-beam current density of about 1 A/cm^2.

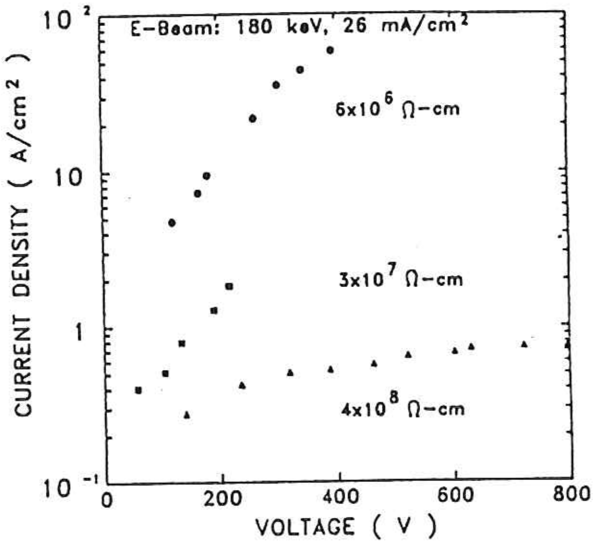

Fig. 4 Switch current density versus pulsed bias voltage with the sample resistivity as the variable parameter.

A change in the switch recovery was noted when the applied voltage reached 265 V (5.3 kV/cm). After the electron-beam terminated, the voltage only returned to a value of 245 V (4.9 kV/cm) or 93% of the initial value. At the same time the dark current - the current through the switch without electron-beam activation - rose to a peak value of 0.4 A/cm^2. An

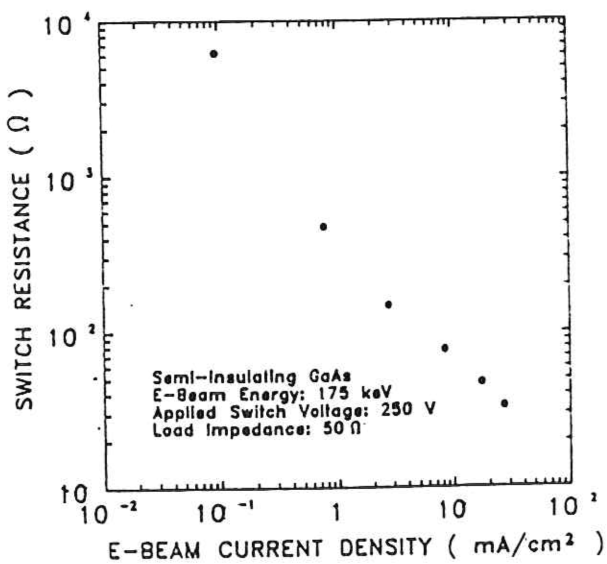

Fig. 5 Switch resistance versus electron-beam current density.

example of the switch voltage and current waveforms is shown in figure 6 where the final dark current was 16% of the switch current during irradiation. As the applied voltage across the switch was increased, the dark current after irradiation also increased. At an applied voltage of 340 V, the final dark current was about 2 A after 4.5 A were carried by the switch during irradiation. The switch recovered to a voltage of 240 V after the electron-beam was terminated. The peak in the dark current was found to increase after irradiation by a factor of 6 over that measured without irradiation.

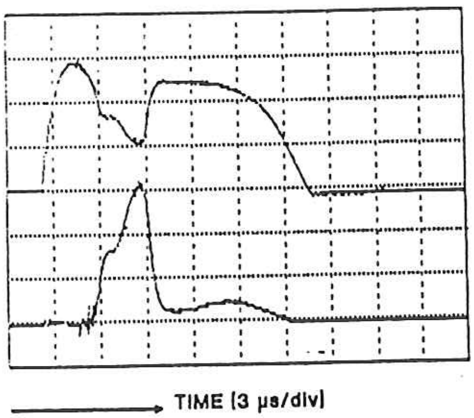

Fig. 6 Temporal behavior of switch current and the applied switch voltage for a 50 ohm load.

Dark Current

In order to investigate the temporal characteristics of the dark current in SI GaAs, a hard tube pulse generator was used which could apply up to a 3000 V pulse for a duration of up to 500 ms. An example of a typical voltage and current waveform is shown in figure 7 for the 6×10^6 ohm-cm SI GaAs sample. The figure shows that for a voltage pulse of 200 V, the time delay for the initial increase in the dark current, or onset time, was about 600 µs. The onset time is strongly dependent on the resistivity or deep level configuration of the material as observed when long voltage pulses were applied to a SI GaAs:C sample. The temporal response was very similar to that shown in figure 7, however, the time delay was more than two orders of magnitude longer.

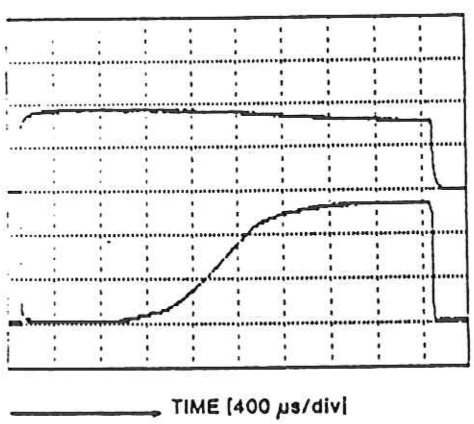

Fig. 7 Temporal development of the switch dark current.

Figure 8 shows the dark current density vs. voltage (j-V) characteristics obtained with the SI GaAs:C sample, which according to the manufacturer (Spectrum Technology, Inc.) had a resistivity of 3×10^8 ohm-cm. This corresponds to the slope of the j-V curve at relatively low voltages. For the dc curve (circles), at voltages above 100 V (E>2kV/cm) a drastic change in slope is observed [5], and the current density eventually approaches values which are determined by the electron drift velocity saturation [6]. At the highest dc voltage, the current density was still more than two orders of magnitude below the trap free limit. The dark current in the pulsed mode for 1 ms pulse widths (open squares), was up to three orders of magnitude below the dc value. The onset time for this material was greater than 100 ms and the steady state or dc value of the current was reached after approximately 300 ms (solid squares) for an applied voltage of about 570 V (11.4 kV/cm).

For the case of SI GaAs (Morgan Semiconductor Division), the onset of seemingly chaotic current oscillations was observed [7]. These oscillations are thought to be the result of microchannel formation in conjunction with field enhanced trapping effects.

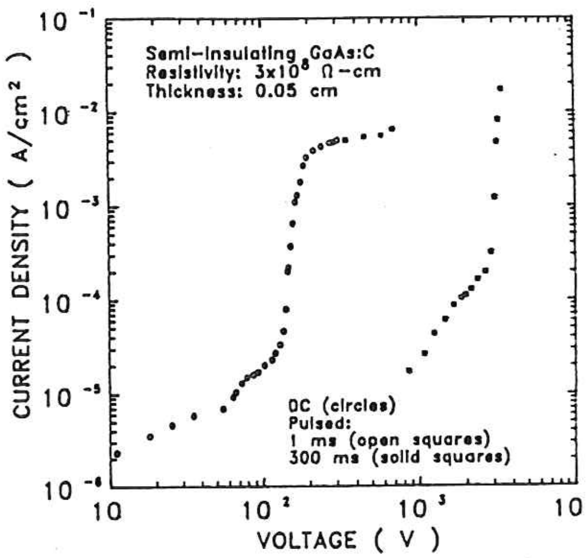

Fig. 8 Dark current density versus applied voltage for a SI GaAs:C sample.

Hold-Off Voltage

Measurements were conducted to determine the dielectric strength of the material. A circuit very similar to that shown in figure 2 was used. A field strength of 140 kV/cm was sustained, for about 3.5 µs FWHM, by chromium compensated SI GaAs (GaAs:Cr) which had a resistivity of 9×10^8 ohm-cm (Macom, Inc.). The medium surrounding the sample was N_2 at 40 psig. The application of higher fields was not possible because of the occurrence of a surface breakdown around the sample. The SI GaAs:C sample sustained a field of 104 kV/cm for 15 µs at atmospheric pressure, however, the same sample broke down at 70 kV/cm when a 1 ms pulse was applied. This low field breakdown for long pulses is thought to be caused by thermal processes in the bulk of the material.

Discussion of Results

The observed high current gain and the large value of the switch current density show that the space charge limitation is greatly exceeded in the

electron-beam controlled switch because of the creation of both electrons and holes in the bulk of the material. The maximum switch current density obtained in our experiments with SI GaAs (6×10^6 ohm-cm) was 57 A/cm^2 at an applied voltage of 400 V. For the same voltage, the space charge limited current density resulting from Poisson's equation and for the case of drift velocity saturation is about 4 A/cm^2. As illustrated in figure 4, samples with higher resistivities carried less switch current for the same electron-beam energy and current density. This results from increased losses in the bulk of the material. Preliminary results indicate a trade-off in that the samples with higher losses will respond faster to the termination of the electron-beam.

One parameter which determines the application of the switch is the dark current. The dark current was explored both independent of the electron-beam and after irradiation with the electron-beam. The fact that the dark current is higher after irradiation may be the result of increased hole trapping in the bulk of the material due to the generation of electron-hole pairs by the electron-beam. This effect and the temporal development of the dark current without irradiation (figure 7) can be qualitatively explained with the use of a model which contains two deep levels. One level is an electron trap (possibly EL2) and the other level is a hole trap (possibly Cr). During the initial part of the voltage pulse, electrons injected at the cathode are trapped in EL2. These trapped charges are immobile and constitute a negative space charge. The space charge limit as previously described is independent of whether the charge is free or trapped. Also during this initial phase of the dark current, holes are being injected at the anode and subsequently drift in the material towards the cathode. These holes are then trapped in the Cr level with a time constant which is dependent on the hole capture cross section, the concentration of the deep level and the hole concentration in the material. As the holes are trapped, they will compensate the negative space charge contained in EL2 and therefore, allow more electrons to be injected at the cathode. Once the hole trap is full, a steady state condition will be reached. The value of the current which is measured at steady state should then be equivalent to the value which is measured when a dc voltage is applied.

The increase in the onset time for the case of SI GaAs:C can also be explained with the two level model discussed above. The EL2 and Cr levels are both located near the middle of the band gap in GaAs. The carbon level is located very close to the valence band and is a shallow acceptor. The role of the carbon acceptor is to lower the Fermi level and therefore decrease the equilibrium occupation of EL2. This results in a higher resistivity material. Because the occupation of EL2 is reduced, the amount of time required to fill the trap is increased. This results in a longer onset time because the injected electrons will not stay in the conduction band long enough to carry a current if there are still unoccupied electron traps. This model also offers a possible explanation as to why the trap free limit was not reached by the dark current. For the trap free limit to be reached, there can be no trapped space charge in the bulk of the material. This condition is not possible unless the trapped negative charge is exactly compensated by the trapped positive space charge.

Conclusion

Experimental studies have shown that the electron-beam controlled semiconductor switch has a high potential for use in high power rep-rated systems. Switch hold-off fields of 140 kV/cm and 107 kV/cm have been sustained by GaAs:Cr and GaAs:C samples, respectively, for times in the µs range. With an electron-beam current density of 1 A/cm^2, a switch resistance of a few ohms could be achieved. These experiments were done without optimizing the cathodoluminescence in the switch. Therefore, much better results with a doped cathodoluminescent layer can be expected. Planar electron tubes with plate voltages up to 100 kV and dc electron currents of 1.5 A are commercially available (EIMAC). Gate voltages for the tube are in the range of 100 V. Replacing the anode by the GaAs switch will allow the control of currents in the range of several kA to tens of kA.

The dark currents, although high, are less than one percent of the switch current for 1 kA/cm^2. The temporal development of the dark current is the result of trapping effects in the semiconductor material. For the case of repetitive operation, the initial delay in the dark current would only effect the first few pulses. A possible way to reduce the dark current would be to provide the sample with non-injecting or blocking contacts [8]. This is not a problem during irradiation because the electron-beam will generate electron-hole pairs in the bulk of the material and does not require additional injection at the contacts.

References

[1] K.H. Schoenbach, V.K. Lakdawala, R. Germer and S.T. Ko, "An Optically Controlled Closing and Opening Semiconductor Switch," J. Appl. Phys., vol. 10, pp.2460-2463, April 1988.

[2] C.H. Harjes, K.H. Schoenbach, G. Schaefer, M. Kristiansen, H. Krompholz and D. Skaggs, "Electron-Beam Tetrode for Multiple Submicro-second Pulse Operation," Rev. Sci. Instrum., vol. 55, pp.1684-1686, October 1984.

[3] K. Schoenbach, R. Germer, V. Lakdawala, K. Schmitt, and S. Albin, "Concepts for Electron-Beam and Optical Control of Bulk Semiconductor Switches," in Proceedings of SPIE Conference on Pulse Power for Lasers, 1987, pp.85-94.

[4] K.H. Schoenbach, V.K. Lakdawala, D.C. Stoudt, T.F. Smith and R.P. Brinkmann, "Electron-Beam Controlled High Power Semiconductor Switches," to be published in IEEE Trans. Electron Devices, scheduled to appear in the September 1989 issue.

[5] M.A. Lampert and P. Mark, Current Injection in Solids, New York: Academic Press, 1970, ch. 2, pp.14-25.

[6] G.SH. Gildenblat and A.R. Rao, "Pulsed Space-Charge-Limited Currents in GaAs," IEEE Electron Device Lett., vol. EDL-8, pp.135-136, April 1987.

[7] D.C. Stoudt, R.P. Brinkmann, L.L. Vahala, K.H. Schoenbach and V.K. Lakdawala, "Investigations Into Chaotic Oscillations in GaAs Substrate," presented at the Spring APS Conference, Baltimore, Maryland, May 1-4, 1989.

[8] R.P. Brinkmann, "Analytical and Numerical Modeling of Electron-Beam Controlled Semiconductor Switches," 7th IEEE Pulsed Power Conference, Monterey, CA, June 1989.

ANALYTICAL AND NUMERICAL MODELING OF ELECTRON-BEAM CONTROLLED SEMICONDUCTOR SWITCHES

R.P. Brinkmann
Department for Electrical and Computer Engineering
Old Dominion University, Norfolk, VA 23508

ABSTRACT

The subject of this paper is the mathematical modeling of a recently proposed[1] class of electron-beam controlled high power semiconductor switches which are able to overcome the space-charge limitation of conventional EBS (electron bombarded semiconductor) devices by utilizing the secondary ionization effects of cathodoluminiscence and bremsstrahlung. Current densities of several kA/cm^2 at forward voltages of tens of volts can be controlled with an electron-beam of 100 keV and 1 A/cm^2; hold-off voltages of more than 100 kV/cm and dark currents as small 10 $\mu A/cm^2$ are possible. The concept allows for fast and repetitively closing and opening under load and is therefore suitable for inductive energy storage applications.

I. INTRODUCTION

In terms of weight and energy density, inductive energy storage systems are superior to capacitive systems by more than two orders of magnitude. However, two major problems have to be overcome before a technological realization of this concept will become feasable: The problem of resistive losses in the storing inductivity, and the lack of appropriate opening switches which can interrupt a sufficiently high electrical current in the presence of an induced counter voltage.

The first difficulty seems to be solvable by applying the concept of superconductivity, either by using the well-established conventional technology or the new ceramic high T_c materials. In this work we are concerned with the second problem, the realization of a high power switch which allows fast repetitive closing and openings cycles under load. We present analytical and numerical investigations into the concept of electron-beam controlled semiconductor switches as recently proposed by [1].

Fig.1: Geometry of the Configuration

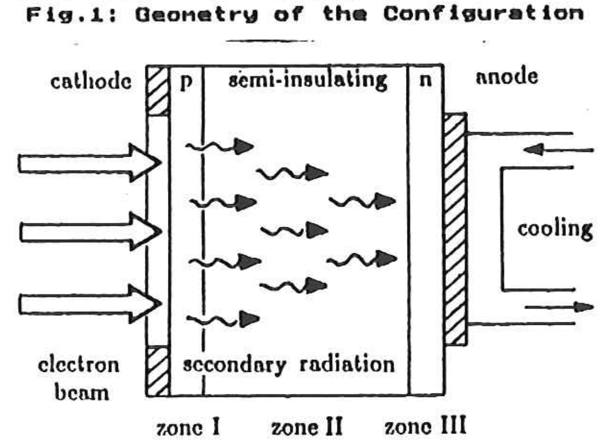

II. CONCEPT OF THE SWITCH

The concept of electron-beam controlled semiconductor switches is based on irradiating a body of well-compensated direct semiconductor material with a high energy electron-beam just below the radiation damage threshold. Both direct and indirect ionization processes are utilized to create a high density of free charge carriers. A schematic sketch of the geometry of the proposed device is given in figure 1.

The configuration consists of a semi-insulating (compensated) gallium arsenide body of a thickness L up to 1 cm (zone II), provided with a highly p-doped surface layer of $d \approx 25\,\mu m$ extension (zone I) at the cathode and a similiar but n-doped layer at the anode (zone III). Appropriate doping materials are for instance zinc and silicon, respectively.

In the open state, the bulk material of the switch is highly resistive and can hold off a voltage of up to 400 kV/cm depending on the break-down field strength of the material.[2] The highly doped surface layers reduce drastically the electrical field at the contacts and the concentration of minority carriers (i.e., of electrons at the cathode and holes at the anode), this prevents any current injection in the bulk zone and insures therefore a low dark current (determined by the intrinsic conductivity).

To turn the switch in the conducting state, an electron-beam with energy up to 250 keV (the radiation damage threshold of GaAs)[3] is injected into the cathode side of the sample. Due to the very small penetration depth of the electrons (e.g., about 25 μm for a 100 keV beam),[4] the beam is entirely stopped within the surface zone I where it creates a high concentration of electron-hole pairs by direct ionization. Subsequently, these charge carriers recombine under emission of band-edge radiation which then can penetrate deeper into the material to ionize the bulk zone II of the switch. Also, the abrupt stopping of the energetic electrons generates a beam of bremsstrahlung emitted in forward direction which creates secondary free charge carriers as well. By these means, also the bulk zone becomes conductive and the ususal space charge limitation of conventional EBS (electron bombarded semiconductor) devices is overcome.

The strong p-type doping of the stopping zone I has two different beneficial effects. First, it enhances considerably the efficiency of converting the direct beam energy into secondary band-edge radiation by increasing the relative fraction of direct over indirect (non-radiative) recombinations, and secondly, it changes the spectral characteristic of the emitted radiation towards lower energies.[5] As the absorption coefficient κ near the fundamental edge is a very rapidly varying function of the photon energy,[2] this allows a deeper penetration of light into the bulk zone II.

III. THE MATHEMATICAL MODEL

The operation of electron-beam controlled switches involves the interaction of many different physical processes in the semiconductor material, among which are:

- Absorption of the primary electron-beam and generation of electron-hole pairs as well as bremsstrahlung.
- Generation, absorption and emission of band-edge radiation.
- Secondary generation of electron-hole pairs due to absorption of band-edge radiation and bremsstrahlung.
- Direct recombination of electron-hole pairs, as well as indirect recombination via trapping or Auger interaction.
- Drift and diffusion of both types of free charge carriers.

A mathematical modeling of the switch configuration leads to a system of nonlinearly coupled partial differential equations, consisting of drift equations for the free charge carriers and balance equations for the trapped, Poission's equation for the electrical field, and of radiation transport equations for both bremsstrahlung and band-edge radiation. It is clear *a priori* that an analytical solution of this model will be impossible to obtain, so that an appropriate numerical code has to be developed. However, a direct implementation of the equations is also not feasible, the dynamical range between the different modes of the switch (open vs. closed) would demand an unreasonably high numerical resolution.

For that reason, we will present in the following sections a separate discussion of the closed and the open state of the switch configuration. Both regimes allow a number of well-motivated (but different) approximations which facilitate the mathematical treatment considerably.

A. THE CLOSED STATE

From the qualitative description given above, it is clear that the switch configuration can be conceptionally seperated into two regions with different purposes and different physical behavior, namely in a) the highly doped region I which stops the electron-beam and transforms its energy partially in band-edge radiation and bremsstrahlung, and b) the semi-insulating zone II which absorbs this radiation creating secundary electron-hole pairs.

First, we turn to the description of the transport processes in the region I. Due to the heavy p-doping in this region, $N_a \approx 10^{19}\mathrm{cm}^{-3}$, the hole density p is always much higher than the electron density n, even compared to the number of charge carriers generated by the e-beam irradiation. This fact has the following consequences:

i) The density of holes is so high that quasi-neutrality applies, $p - p_{eq} - n + n_{eq} - \sum_i N_i(r_i - r_{i,eq}) \approx p - N_a = 0$.

ii) The electrical current (essentially carried by the holes) is not influenced by the small voltage drop in zone I.

iii) The occupation number r_i of the trap levels is close to zero.

iv) Because of the small field strength in zone I the transport processes are linear, i.e., the drift velocity is $v_d = \mu E$ and the diffusion coefficent is $D = \mu k_B T/e$.

vi) Thermal rates can be neglected as they are not detectable against the dominant dynamical processes.

Employing all these approximations (which are valid up to a very high accuracy), and using especially (i) and (ii) to express the electrical field by the current density j and the acceptor concentation N_a, we can establish the following equations for the transport of the minority carrier density n:

$$\frac{\partial n}{\partial t} + D_n \frac{\partial}{\partial x}\left(\left[\frac{j/e}{D_p N_a} - \frac{\partial \ln N_a}{\partial x}\right]n - \frac{\partial n}{\partial x}\right) = S - L \qquad (1)$$

On the right hand side of equation (1), the electron loss term $L = k_a N_d n + \sum_i k_i N_i n + k_a N_a^2 n$ represents the losses due to direct, deep level and Auger recombination; the source function $S = S_{\mathrm{beam}} + S_{\mathrm{be}}$ denotes the generation of charge carriers due to direct beam ionization and the reabsorption of band-edge radiation, respectively. (The contribution of bremsstrahlung can be neglected because of the deep penetration depth of x-rays.) The beam-generated number of electron-hole pairs is

$$S_{\mathrm{beam}} = \frac{I_{\mathrm{beam}}}{e}\frac{dE}{dx}/\chi, \qquad (2)$$

where I_{beam} is the current density of the e-beam, $\chi \approx 4.3\mathrm{eV}$ the mean ionization energy of gallium arsenide and $\frac{dE}{dx}$ the electron dissipation function (interpolated for GaAs from Cu and Sn[4]). Figure 2 shows S_{beam} for a beam of 100 keV and 1 A/cm^2.

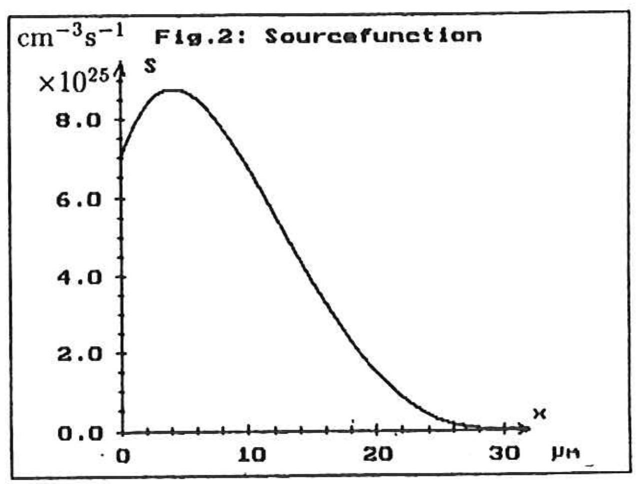

Fig.2: Sourcefunction

To calculate the contribution from the emission and reabsorption of band-edge energy, we have to solve the radiation transport equation for the photon flux $F(x, h\nu, \vartheta)$,

$$\cos\vartheta \frac{\partial F}{\partial x} = -\kappa F + \sigma, \qquad (3)$$

where κ and $\sigma = k_d N_a n \hat{\sigma}$ denote the spectral absorption and emission coefficient, respectively, and ϑ the angle to the x-axis. The reabsorption source function can then be written as

$$S_{\mathrm{abs}}(x) = 2\pi \int_{h\nu_{\mathrm{min}}}^{h\nu_{\mathrm{max}}} \int_0^{\pi} F\,\eta_{\mathrm{abs}}\kappa\, dh\,\nu \sin\vartheta d\vartheta, \qquad (4)$$

where η_{abs} is the ratio of the actually generated electron-hole pairs over the absorbed photons. (Free carrier absorption gives rise to photon losses of about 10%.)

Finally, we demand as boundary conditions the electron density n to vanish at $x = 0$ (to model enhanced surface recombination) and its derivative $\frac{\partial n}{\partial x}$ to remain finite at $x \to d$ where $N_a \to 0$ (regularity condition).

With these premises, equation (1) can be solved numerically. Figure (3) shows the steady state electron density result for a beam irradiation of 100 keV and 1 A/cm^2 and a switch current of 1 kA/cm^2. Within reasonable accurary, all quantities in the stopping zone I scale linearly on the electron-beam current I_{beam}, in particular the number $k_d N_a n$ of the recombination events generating secondary photons which appear as the source function in region II. (Note that (1) is not a linear equation in a strict sense, the current j depends on the conductance of zone II and therefore indirectly on n.)

The typical reaction time of zone I on the electron-beam irradiation can be estimated by the constant in the loss term, $\tau^{-1} = k_a N_d + \sum_i k_i N_i + k_a N_a^2$. For the values we have assumed in our calculations, τ is less than 1 ns. In view of the much greater time constant of region II, the response of zone I can therefore be regarded as effectively instantaneous.

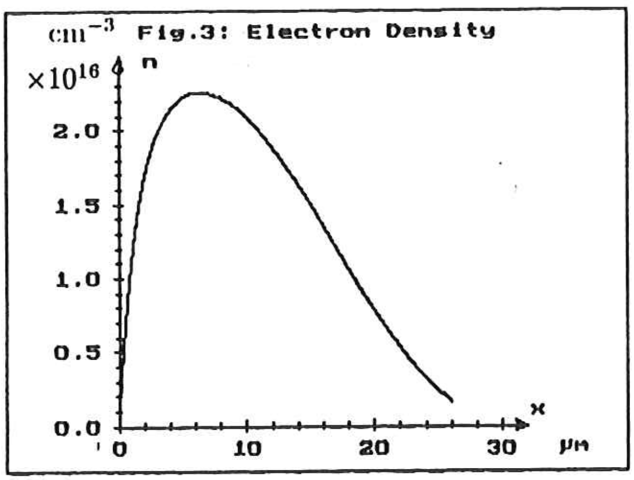

Next we describe the bulk zone II of the switch, where we have to take into account the dynamics of both electrons and holes as well as the influence of the trapped charges. The carrier densities are relatively low so that direct and Auger recombination can be neglected. Again omitting the thermal rate coefficients, the motion of the free charge carriers in the conduction and the valence band are then given by the following drift and diffusion equations

$$\frac{\partial n}{\partial t} + \frac{\partial}{\partial x}(-D_n \frac{\partial n}{\partial x} + n v_n) = S - \sum_i k_{Ci} N_i (1 - r_i) n \quad (5)$$

$$\frac{\partial p}{\partial t} + \frac{\partial}{\partial x}(-D_p \frac{\partial p}{\partial x} - p v_p) = S - \sum_i k_{Vi} N_i r_i p, \quad (6)$$

the bound electrical charges are governed by the rate equations

$$\frac{\partial r_i}{\partial r} = k_{Ci}(1 - r_i) n - k_{Vi} r p, \quad (7)$$

and the system is completed by the quasi-neutrality condition $p - n - \sum_i N_i (r_i - r_{i,eq}) = 0$.

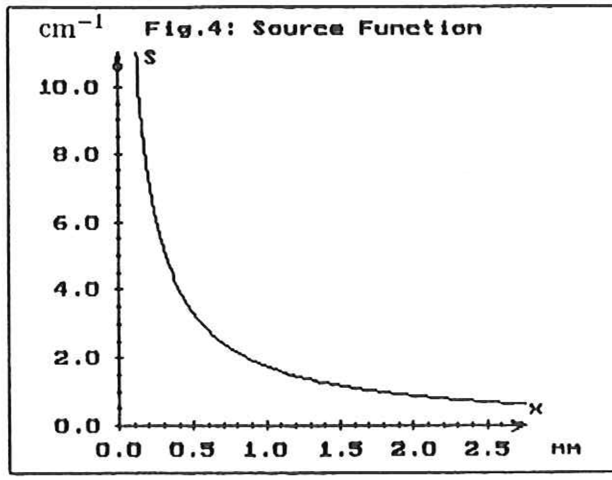

The source function S represents the secondary ionization of the bulk material by absorption of band-edge radiation and bremsstrahlung. As apposed to zone I, re-emission of radiation is negligible and we can formulate the function in a closed form. Utilizing the dimensional separation between the zone I and II ($L \gg d$), the band-edge radiation part is (see figure 4)

$$S_{be}(x) = 2\pi \int_{h\nu_{min}}^{h\nu_{max}} \tilde{\sigma} \kappa E_1(\kappa x)\, dh\nu \times \int_0^d k_d n p\, dx'. \quad (8)$$

E_1 denotes the exponential integral, it results from carrying out the integration over the emission angle ϑ. The contribution of the bremsstrahlung can be formulated in a similar manner, it turns out that it is small compared to (8).

The reaction rates in equations (5 - 7) involve the cross sections and densities of the deep levels which depend considerably on the details of the semiconductor manufacturing process. We will assume in the following the existence of only one level with density $N = 10^{17}$ cm^{-3} in middle of the band gap, $r_{i,eq} = 0.5$. Furthermore, we take the electron and hole capture coefficients to be equal, $k_{Ci} = k_{Vi} = k$.

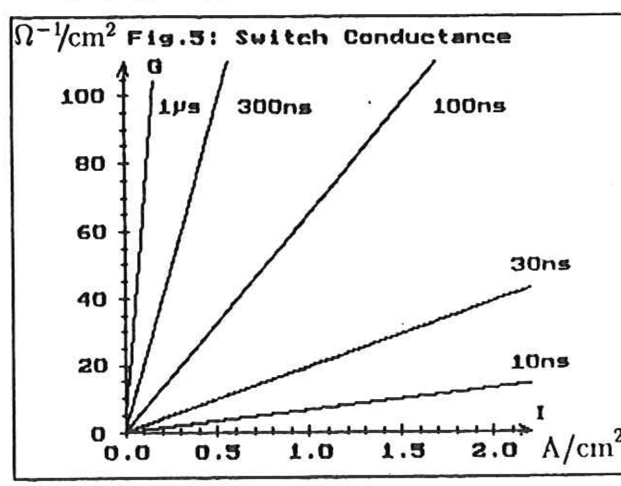

Figure 5 shows the essential result of a numerical calculation, the conductance as a function the electron-beam current and the free carrier lifetime $\tau = \frac{1}{kN}$. The beam energy is 100 keV and the switch length $L = 0.25$ cm. The result can be expressed as $G = 6.5\, \Omega^{-1}\text{cm}^{-2} \times I_{beam}/1\text{Acm}^{-2} \times \tau/10\,\text{ns}$.

B. THE OPEN STATE

In evaluating the performance of the electron-beam controlled switch, information on the open state behavior are as important as those on the closed state. To control a high power application effectively and to achieve a reasonable efficiency, a low dark current and a high hold-off voltage are neccessary.

The short-time (peak) hold-off voltage U_p is essentially determined by the breakdown field strength E_b of the switch material. GaAs has an E_b of about 400 kV/cm, above which field emission and impact ionization lead to charge carrier multiplication and avalanche breakdown.[2] Assuming an approximately homogeneous electrical field (which can be confirmed by numerical calculations), this translates into a short-time hold-off voltage of $U_p = 400\,\mathrm{kV/cm} * L = 100\,\mathrm{kV}$ for $L = 0.25\,\mathrm{cm}$.

For applications in which the switch has to hold off a steady state voltage U, dissipation has to be taken into account. For the configuration shown in figure 1, the overheating equals $\Delta T = PL/2\lambda$ with $P = Uj_d$ as the Ohmic losses and $\lambda = 0.46\,\mathrm{W/cmK}$ as the heat conduction coefficient.[2] For $L = 0.25\,\mathrm{cm}$, this gives $\Delta T = 2.7 \times 10^5\,\mathrm{K} \times U/100\,\mathrm{kVcm}^{-1} \times j_d/\mathrm{Acm}^{-2}$.

Clearly, any dark current of the order of the space charge limit, $I_d = \frac{1}{2}\epsilon_0\epsilon_r U v_d/L^2 \approx 0.8\,\mathrm{Acm}^{-2} \times U/100\,\mathrm{kV}$, would lead to totally unacceptable results. In the presented configuration, however, the dark current is reduced by several orders of magnitude compared to that value: The heavily doped contact zones decrease the concentration of minority charge carriers at the cathode and the anode drastically, and they also reduce the current injection by locally shielding the high electrical field. Therefore, only charge carriers that are generated in the intrinsic bulk zone contribute to the electrical current.

A numerical simulation of the open state starts from equations (5) and (6). The source function is zero, but thermal emission has to be taken into account. Completed with Poisson's equation, the system has been solved numerically. Figure 6 shows the result of a calculation for a slightly n-type material with ($n_{eq}/p_{eq} \approx 7$), it demonstrates that in well compensated material dark currents of less than $10\,\mu\mathrm{Acm}^{-2}$ are feasable.

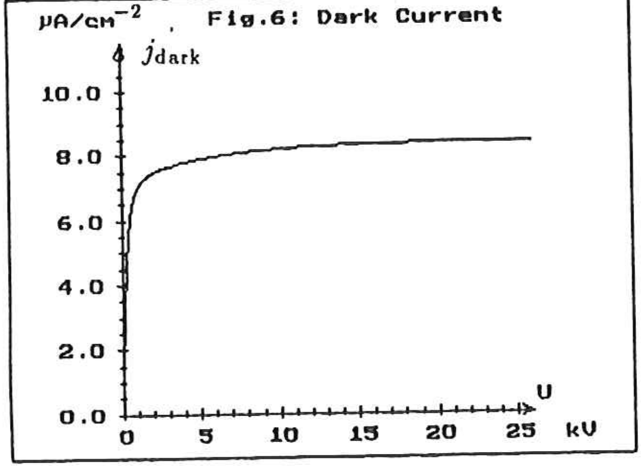

Fig.6: Dark Current

IV. DISCUSSION

The theoretical investigations presented in this paper (and also the corresponding experimental results of [1] and [6]) have shown that the concept of electron-beam controlled semiconductor switches is indeed very promising. It seems possible that devices based on this principle will be able to control currents of several kA and voltages up to 100 kV within time spans in the order of tens of ns. In evaluating possible applications, the following points may be of particular interest:

- For constant beam irradiation, the switch behaves like a linear Ohmic conductor. This characteristic (which is valid for fields up to 3 kV/cm) is very beneficial in order to achieve a stable device operation.
- The conductivity of the switch is in a linear relationship of the controlling e-beam current. This fact – which is based on the linear behavior of both zone I and II – promises to be useful in the fields of high-power modulation.
- Also, it is interesting to note that the steady state conductivity G is inversly proportional to the free carrier lifetime $\tau = 1/kN$, i.e., to the effective response time of the switch. This indicates a trade-off between efficiency and speed.

We conclude the discussion with two examples. Consider, for instance, an extremely pure sample with an effective free carrier lifetime of, say, of 1 µs. Here, we can expect for a 100 keV and 1 A/cm^2 electron-beam a steady state switch conductivity of nearly 1kS/cm^2. Coupled with a standard technology vacuum triode, this configuration might be a very attractive alternative to conventional thyratrons. On the other hand, in a highly perturbated crystal τ can be as low as 1 ns. Controlled by a high speed electron-beam as provided, e.g., by the PEBES-concept,[7] response times down to the nanoseconds may be obtainable. Obviously, such a device will be very interesting for inductive energy storage applications.

V. Acknowledgements

This work was supported by the U.S. Army Research Office and the Air Force Office for Scientific Reasearch under Contract DAA L03-86-K-0078.

VI. REFERENCES

[1] K.H. Schoenbach, V.K. Lakdawala, D.C. Stoudt, T.F. Smith and R.P. Brinkmann, to be published in *IEEE Trans. Electron Devices*, (1989)

[2] S.M. Sze, Physics of Semiconductor Devices, (Wiley, 1981).

[3] A.G. Chynoweth, W.L. Feldman, and R.A. Logan, *Phys. Rev.* 121, 684 (1961)

[4] L.V. Spencer, Energy Dissipation by Fast Electrons, NBS Monograph 1, (NBS, Washington, 1959)

[5] D.A. Cusano, *Solid State Communications* 2 353 (1964)

[6] D.C. Stoudt, K.H. Schoenbach and V.K. Lakdawala, this conference

[7] S.G. Pronko and G.A. Gerdin, this conference

A SHORT-PULSE, LASER-DRIVEN PHOTOELECTRON DIODE

Steven G.E. Pronko and Glenn A. Gerdin

Old Dominion University
Department of Electrical and Computer Engineering
Norfolk, Virginia 23529-0246

Abstract

We report a laser-driven photoelectron diode which is capable of producing an electron beam pulse whose shape is determined by the shape of the laser pulse. A tungsten dispenser cathode impregnated with Ba and Sc is used as the photoemitter. Space-charge limited photoelectron current of just under 1 A with 10 ns duration has been achieved with modest laser-driver power. Performance of the photoelectron diode is classified into three regimes based on the characteristics of the generated electron beam and the input laser-driver power. The photoelectron dominated regime (PDR), the transition regime (TR), and the diode closure regime (DCR) are qualitatively discussed based on the electron current data. Compliance of the peak photoelectron current with the Child-Langmuir law is also shown.

Introduction

The need for a short-pulse source of moderate energy (50-200 keV) electrons for electron beam controlled semiconductor switching research [1] has led to the design of a laser-driven photoelectron diode. Other laser-driven diodes have been reported using the laser power to generate thermionic emission [2], produce a plasma (followed by plasma-assisted field emission) [3], and to generate photoelectrons (photoelectric effect) [4]. Generation of electrons via the photoelectric effect is particularly interesting since the temporal response of the diode is given by that of the incident laser pulse. It then becomes feasible for the formation of ultra-short e-beam pulses in a temporal regime where high-power electrical pulse-forming tecniques are not possible.

The photoelectron beam system (PEBES) described in this paper is centered around a low aspect ratio planar diode with a special cathode material. A pulsed laser is used to irradiate the cathode when an electric field is applied to the diode. Electrons produced by the laser-cathode interaction are then accelerated across the diode gap by the field. If the interaction is purely photoelectric, then the resulting electron beam will have a temporal shape identical to the laser pulse. The amplitude of the e-beam is related to the laser wavelength and intensity through the work function and photoelectric efficiency of the cathode material. The ultimate limit on the maximum photoelectron current is set by space-charge limitations.

In order to make PEBES practical, the cathode material should have a reasonably high photoelectric efficiency at a laser wavelength that is readily available and not too costly. Conventional photocathodes such as cesium-antinomide and cesiated gallium-arsenide offer high efficiencies but require ultra-high vacuum and are difficult to work with. A possible alternative is the tungsten dispenser cathode impregnated with barium (Ba) and scandium (Sc). When properly activated a layer of Ba and Sc forms over the surface [5] yielding a work function <2.0 eV. This low work function would allow the use of lasers operating in the visible portion of the spectrum. The main advantage of dispenser cathodes over the cesiated types is that they can survive in a modest vacuum (10^{-7} torr) and are relatively inexpensive. In the experiments presented here, type 311H tungsten dispenser cathode buttons [6] were used. Experiments were performed on both unactivated and activated samples.

Experimental Set-up

The PEBES diode is a demountable vacuum chamber mated to an oil-filled, high-voltage bushing. The cathode is of cylindrical geometry with a diameter of 4.3 cm and has a removable stainless steel tip. The cathode tip has a 1.2 cm bore in which the dispenser cathode buttons are held near flush to the slightly cupped front surface. The anode-plate has a 5.1 cm diameter vacuum port to which transmission foils, collector plates, or diagnostics can be attached. In the experiments presented here, the graphite charge collector of a Faraday cup served as the anode electrode. With the Faraday cup installed, the anode-cathode gap is 6.5 cm. Also provided on the anode-plate is a laser transmission window. The entire PEBES assembly is mounted atop an oil-diffusion vacuum system that pulls down to an operating pressure of <10^{-7} torr. A schematic diagram of the experimental set-up is shown in figure 1.

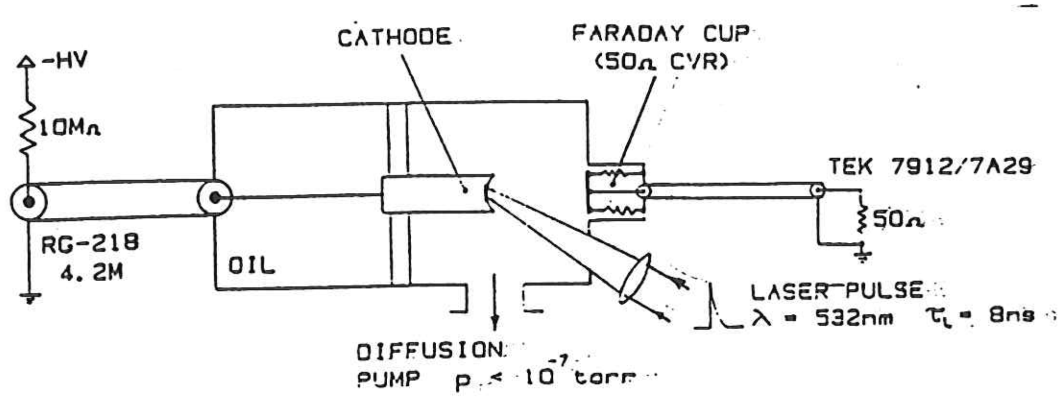

Figure 1. A schematic diagram of the experimental set-up

The electrical system presently used to supply PEBES is simply a DC-charged coaxial cable. The cable is a 4.2 m length of 50 ohm RG-218 and is used more or less as a low-inductance capacitor (not a PFL). The DC power supply is capable of charging the cable to 50 kV. Experiments at higher voltages are at present prohibited due to triggering problems and insulator failure.

The laser-driver is a Q-switched Nd:YAG system which is frequency-doubled to yield a laser pulse at λ= 532 nm and a pulsewidth of τ_L= 8 ns (FWHM). The laser beam is focused by a lens through the anode-plate window onto the center of the cathode. The laser spot size on the cathode is approximately 0.75 cm. The area of illumination is then 0.44 cm^2 which is about one third of the available cathode area. This is limited by the clear aperature of the laser window.

The main diagnostic is a Faraday cup with a graphite charge collector. The electron current is determined by measuring the voltage developed across an internal 50 ohm shunt resistance (CVR). The risetime of the cup was calibrated with a 50 ohm pulse generator and found to be <2 ns. Hence the bandwidth is sufficiently wide to perform the required measurements. The Faraday cup signals are processed using a PC-based TEK 7912/7A29 transient digitizer system.

Results

The results from experiments performed with an activated dispenser cathode installed in PEBES are presented here. The response of PEBES to the laser-driver was measured over a range of laser intensities and diode voltages. For reference, a typical laser pulse is shown in figure 2. The laser pulse has a risetime of about 3 ns (10-90%).

The electron current as measured by the Faraday cup is shown in figures 3, 4, and 5 (the output was inverted so as to display a positive pulse). The e-beam pulse shown in figure 3 is typical of the "photo-detector" like response observed at the lower laser intensities. The peak electron current is 74 mA at a diode voltage of 45 kV and an incident laser intensity of approximately 1 MW/cm^2. The pulse shape is essentially identical to the laser pulse, however, if any sub-nanosecond structure had been present on the e-beam pulse it would not have been resolved by the Faraday cup (bandwidth limited). For the same diode voltage but a higher laser intensity of 1.5 MW/cm^2, the PEBES response is shown in figure 4. The peak electron current on this shot is 160 mA. Again, the e-beam pulse rises and peaks just like the laser. However, at the higher laser intensity the tail of the e-beam broadens. As the laser intensity is increased, the broadening of the e-beam tail is also increased until the diode apparently closes. A typical electron current pulse during an apparent diode closure is shown in figure 5. The inception of this behavior occurs for laser intensities near and above 2 MW/cm^2 for all diode voltages used. It must be noted, however, that <u>ALL</u> e-beam pulses rise and peak with the laser-driver before broadening and diode closure occur. In addition, the repeatability of the e-beam pulses at any given diode voltage and laser intensity is very good. A plot of the peak electron current versus the percent laser intensity for a range of diode voltages is shown in figure 6. Note that the data points correspond to the peak electron current which is temporally correlated with the laser-driver pulse. The inception of diode closure occurs around 65% laser intensity (about 2 MW/cm^2). It is seen that for laser intensities above 75% the peak electron current saturates.

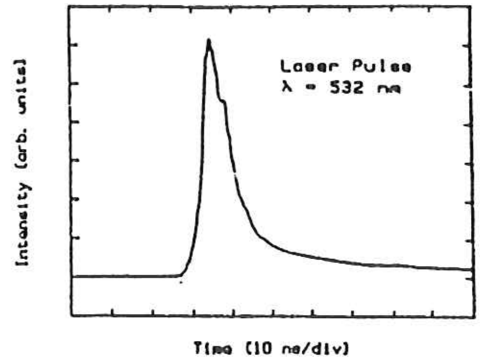

Figure 2. Photodetector signal of the laser pulse.

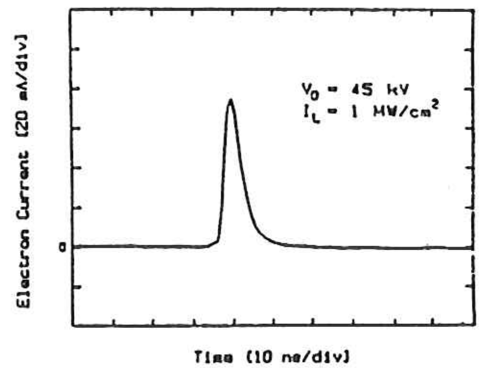

Figure 3. Faraday cup signal of the e-beam in the PDR. The peak current is 74 mA.

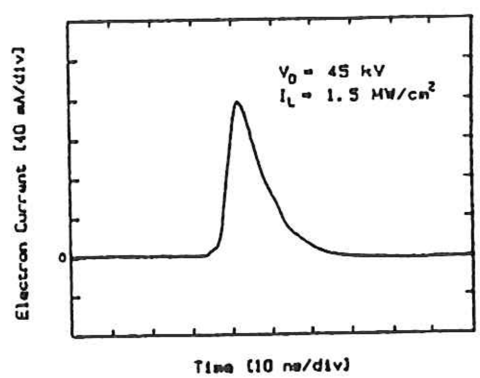

Figure 4. Faraday cup signal of the e-beam in the TR. The peak current is 160 mA.

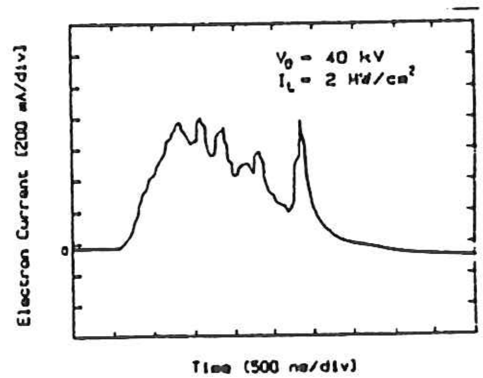

Figure 5. Faraday cup signal of the e-beam during diode closure.

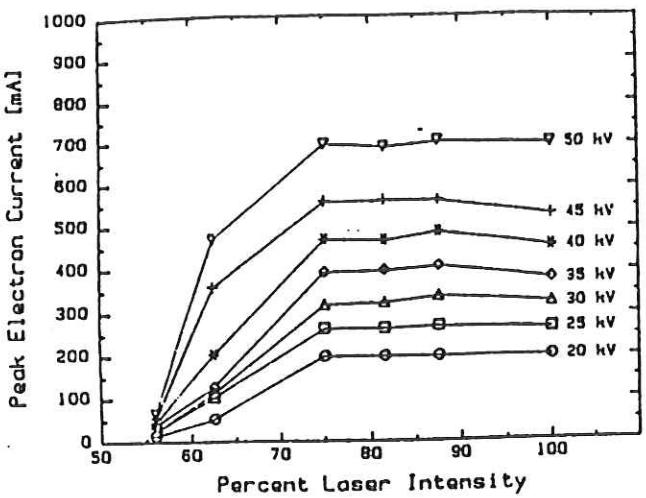

Figure 6. The peak electron current/relative laser intensity curve family.

Discussion

The performance of PEBES can be classified into three regimes depending on the intensity of the laser-driver. The three regimes are

1) the photoelectron dominated regime (PDR) which occurs at low laser intensities,

2) the transition regime (TR) which begins at slightly higher laser intensities and leads to

3) the diode closure regime (DCR) requiring the higher laser intensities.

The e-beam pulse shown in figure 3 typifies the performance of PEBES in the PDR. The fact that the e-beam pulse is very well correlated with the laser pulse is strong evidence that the beam is composed of photoelectrons produced by the laser at the cathode (the photoelectric effect). This is a very important result since it shows that the e-beam can indeed be temporally shaped by the laser-driver. The efficiency of converting the laser power into electron current can be determined from knowledge of the laser energy deposited on the cathode and the peak electron current. Without proper (and complicated) calorimetry, however, the incident laser power that is reflected, absorbed (converted into heat), or converted into electrons (photoelectric effect) is difficult to discriminate. At any rate, order of magnitude assumptions can be made about the incident laser power leading to an estimate of the photoelectric efficiency

$$\eta_{PE} = (I_e/P_L)h\nu \quad \text{[electrons/photon]}$$

where I_e is the peak electron current in amps, P_L is the estimated useable laser power in watts, and $h\nu$ is the photon energy in electron volts. The e-beam pulse shown in figure 3 implies a conversion efficiency on the order of 10^{-7} [electrons/photon]. The photoelectric efficiency for BaO at $\lambda = 532$ nm (2.34 eV) has been found to be approximately 5×10^{-6} [electrons/photon] [7].

With increasing laser intensity, the operating regime moves into the transition regime (TR). The TR gets its name from the fact that it lies between the other two, very distinct regimes. The e-beam pulse shown in figure 4 is typical of the TR. The broadening of the pulse tail is thought to be caused by two processes occuring either singly or simultaneously. One possibility is that at the increased laser intensities the temperature of the cathode can reach thermionic levels within a few nanoseconds. Since the thermal diffusion in the cathode is slower than the fall time of the laser pulse, thermal electrons can still be generated, thus contributing to the tail of the e-beam. The other possibility is due to gas liberation at the anode caused by e-beam heating. Once the initial photoelectron beam deposits enough energy in the anode material, a gas layer can form in the region of beam impact. This gas layer is subsequently ionized by the remaining photoelectrons and possibly any thermal electron contributions. Electrons produced in the gas layer due to this ionization are collected by the Faraday cup and measured as if they were beam electrons. Consequently, an error is produced in the measurement of the actual beam current.

As the laser intensity is further increased, the e-beam pulse tail continues to broaden and then the current slowly increases above the level of the first peak. This is the onset of the third regime which is characterized by closure of the diode (DCR). Since the photoelectron current saturates (figure 6) at a level which corresponds to the Child-Langmuir space-charge limit, diode closure is indicated by the increase of current above this limit. During high intensity laser shots, the diode current can grow to several amps. Figure 5 is an example of the electron current during diode closure. The processes responsible for causing the diode closure are the same as those acting in the TR. At the higher beam currents and laser intensities the effects of these processes are more drastic. In addition to the anode outgassing and the thermionic emmission, the high laser intensity can evaporate some of the cathode material and create a plasma. Ionization of the anode outgassing provides space-charge neutralization for the beam electrons and those supplied by the cathode plasma. The structure along the pulse in figure 5 is probably due to fluctions in the density of the gas layer in the region of the anode.

The saturation in the peak electron current (figure 6) is confirmed to be space-charge limited by the following argument. The nonrelativistic, steady-state, Child-Langmuir law for space-charge limited current density is given by [5]

$$J_{CL} = 2.33 \times 10^{-6}(V^{1.5}/d^2) \quad [\text{A/cm}^2]$$

where d is the anode-cathode gap in cm. The total current is found by multiplying through by the cross-sectional area of the electron beam. Taking the logarithm of both sides yields

$$\text{Log}(I_{CL}) = 1.5\text{Log}(V) + \text{Log}(2.33 \times 10^{-6}A_e/d^2)$$

A Log-Log plot of the saturated electron current versus the diode voltage for a laser intensity (75%) well into the saturation region is shown in figure 7. The least squares fit of the data yields a slope of n=1.51 and an intercept such that

$$d/\sqrt{A_e} = 6.51$$

Since the gap spacing is known to be 6.5 cm, then the electron beam cross-sectional area is approximately 1 cm^2. In a previos experiment, a titanium foil window with a thin layer of evaporated brass showed evidence of e-beam "cleaning" or etching. The spot-size was slightly larger than 1 cm^2. Thus the data and the measured parameters (gap space) are in reasonable agreement with the Child-Langmuir law.

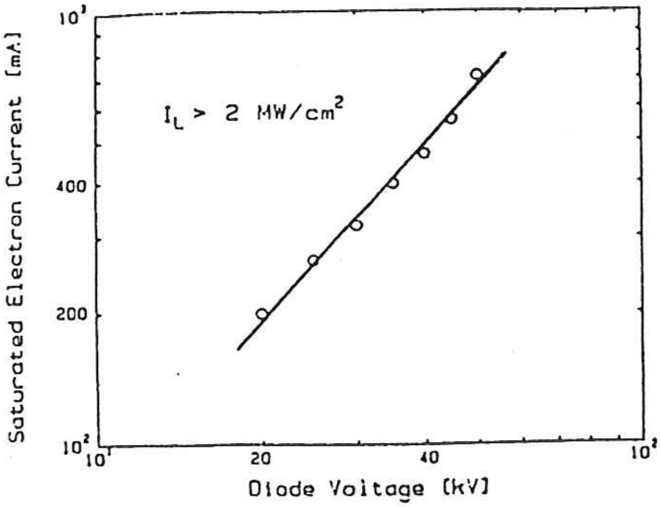

Figure 7. Log-Log plot of the peak e-beam current versus the diode voltage indicating a 3/2 power law.

Conclusions

Experiment has shown that tungsten dispenser cathodes can be used as photocathodes to produce laser controlled electron beam pulses. Increasing the photoelectric efficiency for the present system seems to be a matter of achieving a higher level of cathode activation. At present, comparison of the unactivated cathode to the activated sample is difficult since a complete set of data has not yet been obtained for the unactivated sample. However, it has been observed that the inception of the DCR occurs erraticly from shot to shot for the unactivated sample. Also, the shape and amplitude of the e-beam pulse in the PDR is not nearly as repeatable as in the case with the activated cathode. Use of shorter laser wavelengths can only increase the efficiency [7], however, the cost per photon usually scales inversely with wavelength.

The diode closure phenomenon can be suppressed by doing two things. First, a properly outgassed anode and careful vacuum assembly will reduce considerably the effect of adsorbed gases. Second, the laser power can be maintained below a level such that thermionic emission and evaporation are negligable. This limitation on the laser power forces the need for higher photoelectric efficiencies and/or shorter laser wavelength.

As it stands, PEDES is capable of producing peak photoelectron currents just under 1 A with nanosecond duration at moderate laser power. With higher voltages (up to 200 kV), space-charge limited photoelectron currents of several amps are possible.

Acknowledgement

The authors would like to acknowledge Randy Roush for his technical assistance during the course of the experiments.

This work is supported by the Air Force Office of Scientific Research and the Army Research Office under contract number DAA L03-86-K-0078.

References

[1] K.H. Schoenbach, V.K. Lakdawala, D.C. Stoudt, T.F. Smith, R.P. Brinkmann, "Electron-Beam Controlled High Power Semiconductor Switches," to be published in IEEE Trans. on Electron Devices, scheduled to appear in the September 1989 issue.

[2] C. Lee and P. Oettinger, "Beam Characteristics of Laser-Excited High-Emission Cathodes", Appl. Surface Sci. 16 (1983) 250-56.

[3] P. Krehl, "Pulse compression effect in a laser driven flash x-ray tube", Appl. Phys. Lett. 52(5), 1 Feb. 1988, 354-55.

[4] K.T. McDonald, "Design of the Laser Driven RF Electron Gun for the BNL Accelerator Test Facility", IEEE Trans. on Electron Devices, 35(11) (1988) 2052-59.

[5] A.S. Gilmour, Jr., Microwave Tubes. Dedham, MA: Artech House, Inc., 1986, Chap. 5, pp. 107-130.

[6] Spectra-Mat, Inc., Watsonville, CA.

[7] A.H. Sommer, Photoemissive Materials, New York: John Wiley and Sons, Inc., 1963, Chap. 12, pp. 195-197.

A BAND EDGE RADIATION GENERATOR FOR PULSED POWER*

Glenn Gerdin, K.H. Schoenbach,
V.K. Lakdawala, T.F. Smith, and R.P. Brinkmann
Department of Electrical and Computer Engineering
Old Dominion University
Norfolk, Va. 23529–0246

ABSTRACT

The band edge radiation generator (BERG) concept consists of using an electron beam to drive a direct band gap semiconductor (DBGSC); the electron–hole plasma thus generated in the DBGSC recombines to produce band edge radiation which may be enhanced by doping the DBGSC with a shallow donor or acceptor. The band edge radiation is then coupled to photoconductive switches by optical fibers which cause the switches to conduct as if driven by a conventional laser. The advantage of the BERG concept is that since high power gridded electron beam tubes exist, that photoconducting switches could be driven without lasers. In addition, if the electron beam is being generated by a laser incident on a photocathode, the laser power can be reduced by a factor of a thousand over that required to drive the photoconductive switches for typical photocathodes (bialkali), lasers (532nm) and DBGSCs (GaAs). The results of experiments supporting this concept and near term practical applications will be presented.

I. INTRODUCTION

The band edge radiation generator (BERG) concept consists of using an electron beam to drive a direct band gap semiconductor (DBGSC); the electron–hole (e–h) plasma thus generated in the DBGSC recombines to produce band edge radiation which may be enhanced by doping the DBGSC with a shallow donor or acceptor. The band edge radiation is then coupled to photoconductive switches by optical fibers which cause the switches to conduct as if driven by a conventional laser. The doping of the DBGSC also makes it a good conductor so the charge of the electron beam can be easily drained to avoid charge build up.

The advantages of the BERG concept are that since high power gridded electron beam tubes exist [1] that photoconductive switches could be driven without lasers. In addition if the electron beam is being generated by a laser incident on a photocathode, the laser power can be reduced by a factor of a thousand over that required to drive a photoconductive switch for typical photocathodes (bialkali), lasers (532nm) and DBGSCs (GaAs). By changing the DBGSC a wide range of wavelengths could be achieved from 6889nm (InSb) to 344nm (ZnS). Since the band gap energy is a function of temperature, the wavelengths could be varied by heating or cooling this material.

In the following sections, the overall efficiency, an example, a comparison with other sources, and preliminary experimental results will be examined.

II. Overall Efficiency

This concept is in principle an electron beam driven light emitting diode[2] so the electrical efficiency of the system, η_s, as compared with another light source, is basically that of the electron beam generation and its focusing to the DBGSC (η_{EB}), the conversion efficiency of the electron beam energy to band–edge radiation (internal coupling efficiency) η_i, and the external coupling efficiency to the fiber optic cable, η_x or

$$\eta_s = \eta_{EB}\,\eta_i\,\eta_x \qquad (1)$$

*Research supported in part by a grant from AFOSR, and ARO.

In the next three subsections the expected ranges of these three efficiencies will be explored.

IIa. Electron–Beam Generation and Focusing

To avoid having surface recombination dominate the internal conversion efficiency, the energy of the beam electrons, E_B, should be at least 20 keV and less than 110–340 keV to avoid damage to the material.[3] Electron beam tubes in this range of voltages have been manufactured [1,4] and tested for 3500 hours of continuous operation at efficiency greater than ninety percent. Hence the electron beam efficiency does not play a limiting role in the overall efficiency of the system. Because of space charge restrictions, higher voltage beams are preferred for higher current applications and very fast beam rise times can be achieved through beam deflection.

IIb. Internal Conversion Efficiency

As the fast beam electrons slow down in the DBGSC, the electron's energy is converted to electron–hole pairs. The amount of fast electron energy required to create one electron–hole pair in a given material, W_b, has been fitted to the following formula:[3]

$$W_b = 2.1 \cdot E_g + 1.3 \qquad (2)$$

where E_g is the band gap energy for the material. If all the electron–hole pairs are converted to band–edge radiation photons (maximum conversion) then the internal conversion efficiency $\eta_{i_{MAX}}$ would be

$$\eta_{i_{MAX}} = \frac{h\nu}{W_b} \simeq \frac{E_g}{W_b} \qquad (3)$$

which would approach 0.48 for large E_g.

Potential DBGSC materials are listed in Table I, where E_g, W_b, λ, and $\eta_{i_{MAX}}$ are shown. While a wide range of wavelengths are possible for a BERG device, the longer wavelengths suffer in efficiency as expected from equation (3). While not all the electron–hole pairs are converted to band edge radiation, the coupling efficiency can be quite high; it is estimated[5] to be ≥ 0.76 for GaAs. Therefore $\eta_{i_{MAX}}$ will be taken for the internal coupling efficiency in the following estimates.

IIc. External Coupling Efficiency: Theoretical Considerations.

Two major problems with the BERG concept as with light emitting diodes are the high index of refraction of the material in which the photons are produced and reabsorption of the photons by the material. The former results in a significant portion of the photons to suffer total internal reflection back into the DBGSC where they were produced; the latter can prevent photons reflected from other surfaces from being transmitted out of the DBGSC.

Total internal reflection will occur if the incident angle α_c (with respect to the surface normal) is greater than a critical angle given by:

$$\sin\alpha_c = n_2/n_1 = n^{-1} \qquad (4)$$

where n_2 is the medium into which the light would be transmitted and n_1 is that of the DBGSC. For a planar interface, the ratio of transmitted power to incident power for an isotropic source can be shown[6] to be given by:

$$P_t/P_i = \frac{1}{n(n+1)^2} \qquad (5)$$

For a hemispherical source, where an irradiated source disk of diameter d sits on the center of it's flat surface, the total internal reflection at the hemispherical interface can be eliminated if[6]:

$$nd \leq D \qquad (6)$$

where D is the diameter of the hemisphere. In this case the ratio can be shown to be[6]:

$$P_t/P_{in} \approx \frac{2n}{(n+1)^2} \qquad (7)$$

If the reabsorption by the material can be neglected and a non–lossy reflecting surface can be placed on the surface opposite the transmission interface then, the transmission efficiencies given by equations (5) and (7) can be increased by a factor of two.

These efficiencies [equations (5) and (7)] and indices of refraction with respect to air as the second medium for the DBGSC materials of Table I are given in Table II. If one were to couple to a fiber optic cable instead of air then the relative refractive indices would be reduced by a factor of 1.45 (typical index of refraction of such cable[8]). In this case the planar efficiencies of Table II improve by a factor of about 2.5 since the acceptance angle [equation (4)] of total internal reflection is significantly increased. However, the efficiencies for the hemispherical source are only increased by about 20% due to improvement in the percent transmitted at normal incidence:

$$T = \frac{4n}{(n+1)^2} \qquad (8)$$

This factor can be made to approach 1 if a quarter wavelength coating can be placed on the transmitting surface where the index of refraction of the surface layer n_s is given by :

$$n_s = \sqrt{n_1 n_2} \qquad (9)$$

For a GaAs – air interface $n_s = 1.9$, whereas for a GaAs – fiber optic interface $n_s = 2.3$ and a quarter wavelength in these media would correspond to a thickness of 0.114 μm and 0.094μm respectively. Potential coating materials include SiO having $n = 1.89$ and ZnS or CdS having $n = 2.3$. These materials can be deposited in such layers by sputtering deposition[9]. This would increase the efficiencies in Table II by a factor of $(n+1)^2/4n$ for the planar case and raise all the hemispherical efficiencies to 0.5. Thus if reabsorption were negligible the addition of a non–lossy reflecting surface on the flat interface of the hemispherical interface would cause the external coupling efficiency to approach 1.0; For the planar case these efficiencies would vary between 6 and 20%. Thus theoretically it should be possible to achieve external coupling efficiencies between 0.1 and 1.0 using these strategies.

IIc. External Coupling Efficiency: Experimental Results

The use of a hemispherical shaped n type GaAs light emitting diode (tin doped to $10^{17}/cm^3$) with a circular source (p type from diffusion) in it's center was demonstrated by W.N. Carr[5] in 1965. Carr also used a quarter wavelength layer of SiO_x to eliminate partial internal reflection at the GaAs–air interface. He found external quantum efficiencies $\eta_e = \eta_i \eta_x$ of 40.5, 32 and 7.3% for the diode at temperatures of 20, 77, and 295oK respectively. The optical losses were attributed to bulk absorption and imperfect reflection from the alloyed metal contracts. The higher yields at lower temperatures are indicative of bulk absorption since at lower temperatures the emission peak of the band edge radiation is narrower so that it overlaps the absorption band to a lesser degree. This is also indicated by the higher external coupling efficiencies when Si is used as the dopant material[10]. Here emission peak of the –doped diode is shifted to longer wavelengths away from the absorption peak; the resulting diode efficiencies were as high as 32% for diodes in high–index glass hemisphere ($n \sim 1.57$)[10] Thus high external coupling efficiency appears possible by either cooling the diode to liquid nitrogen temperature or by changing the dopant. Cooling has the additional advantage of shortening the rise time of the light pulse (from 1.6 ns to 0.6 ns for a reduction in diode temperature from 295oK to 77oK [5]). Thus in the following example the external coupling efficiency will be taken to be 0.3 for the purpose of illustration.

III. Example

As an example of how the BERG concept could be implemented in the near term, there are commercially available[1] gridded thermionic electron beam tubes which can be biased to 150kV, have a peak current of 15–20A with a 15μsec wide pulse. Such tubes have nanosecond rise time and cost on the order of $6K. If the anode of such were modified into a BERG, 300kW could be delivered to a photoconductive switch assuming 30% external radiation coupling. Assuming direct drive of the photoconductive switch (one photon/e–h) and a corresponding turn–on energy of 1–10mJ/cm^2, a rise time of 3–30 ns could be obtained. This would make the BERG competitive with lasers for driving photoconductive switches in the near future.

IV. Comparison With Other Sources

The major competing light sources at these wavelengths and power levels are lasers, which certainly can match these power levels although they may have difficulty in matching the potentially fast rise times in some cases. Perhaps the area where these sources could make the most impact would be as competitors to pulsed junction semi conductor lasers (JSCL), where 800W pulses have been achieved in a stacked array with 30–40% electrical efficiency.[11] The JSCL are potentially useful as pumps for solid state lasers having wavelengths in the range of 1.06μm to 2.8μm [11], but at present are too low power to be used to drive switches. The high powers achievable from a BERG GaAs source (see example) could be used to achieve much greater power levels from these solid state lasers with much more rapid rise times for the pump source. The relative compactness of the gridded accelerator tube proposed for the BERG, roughly a cylinder 20 cm long and 13 cm in diameter,[1] means the pumping system including power supply could be relatively compact: on the order of a beer keg.

Perhaps the greatest disadvantage of the BERG versus the semi conductor laser would be in electrical efficiency, i.e. 10% versus 30–40%. While the BERG would have the advantage of

higher power levels and shorter rise times with respect to the present generation of junction semi conductor lasers (JSCLs),[11] in the longer term the JSCL may be developed to overcome this disadvantage. However, the electron beam of the BERG could be used to pump a lasing DBGSC (Table I). In fact almost all the DBGSC materials listed in Table I were first made to lase using electron beam pumping,[12] and one material (CdS) was shown to exhibit an overall electrical efficiency[13] of 26.5%. The corresponding internal conversion efficiency was estimated[13] to approach 35% which is close to the theoretical limit given by Equation (3). The much greater directionality of the lasing DBGSC emission permits much higher external coupling efficiencies[10]. If this percentage efficiency could be achieved for GaAs, lasing BERGs would be competitive with JSCLs in power, rise time, and efficiency and thus be competitive with them even in the long term.

V. Preliminary Experimental Results

Recent experiments in our laboratory [14] with an thermionic electron beam driven by a pulse forming network with a wide pulse have proven the feasibility of the generation of band edge radiation to eliminate space charge effects in the semiconductor diode (SCD) in the configuration shown in Figure 1. The current and voltage waveforms are shown in Figure 2. The resulting SCD current densities were higher by a factor of 50 over the Mott–Gurney space–charge limit for the SCD. The increase is achieved by the production of an electron–hole plasma throughout the SCD by band edge radiation generated in a SCD driven by a BERG drive.

The band edge radiation intensity has been shown to increase with doping level by the observation of a Si doped semi–insulating GaAs wafer under irradiation by an electron beam with a CCD camera[15]. For GaAs, Si acts like a donor as does the Zn dopant in our electron beam driven switched experiments discussed above.

To measure the band edge radiation intensity emitted from various DBGSC the following experimental apparatus has been constructed to be coupled to our thermionic electron beam facility[14]. Electrons, accelerated up to a voltage of 220keV with currents in excess of 30mA are coupled to a drift tube through a thin titanium foil[14] (Figure 3). The DBGSC sample to be radiated, typically a 1 cm^2 square, 0.5 mm thick sample of GaAs, is placed at the end of the drift tube which is evacuated to a rough vacuum to promote better coupling between the beam and the sample. The radiation being emitted from the sample edge is focused by the lens (Figure 3) onto the photocathode of a photomultiplier tube (PMT) with S–1 characteristics. The infrared mirror is used to deflect the band gap radiation away from the X rays generated by the electron beam interacting with the sample and the drift chamber. Direct coupling of the X rays with the PMT is prevented by the lead shielding shown. The output of the PMT is amplified by an operational amplifier with a band width of 40 MHz.

Some preliminary results are shown in Figure 4; the sample is a Zn–doped (10^{18}–$10^{19} cm^{-3}$ in a 100μm layer) of semi–insulating GaAs (0.5cm thick). As can be seen in the figure, the infrared light intensity appears to follow the electron beam voltage after a short delay (Figure 2). In the next few months, we plan to vary the electron beam voltage and current to see if the emission intensity varies in the expected manner to further test the feasibility of the BERG concept.

VI. Conclusions

In summary, the band edge radiation generator (BERG) concept appears to have the potential to fill an important demand for high power, compact, efficient drivers for photoconductive switches and for solid state lasers. Since the idea to use electron beams as drivers for direct band gap semiconductor lasers is not new,[12] a considerable body of experimental and theoretical evidence exists[12] to support this concept. What is new are the technologic advances permitting a compact electron beam driver[1] and the possibility of a fast rise time electron beam through the use of a photocathode in the electron beam tube driven by a fast low–power laser[16]. We hope to couple these concepts in the near future to test the feasibility of this promising idea.

REFERENCES

[1] Ei–mac–Varian Catalog, 1988.

[2] E.W. Williams and R. Hall, Luminescence and The Light Emitting Diode, Oxford: Pergamon Press, 1978, Ch.9, pp. 183–214.

[3] W. Ehrenberg and D.J. Gibbons, Electron Bombardment Induced Conductivity, London: Academic Press, 1981, Ch. 2, pp. 65–79.

[4] D.J. Bates, R.I. Knight and S. Spinella, "Electron Bombarded Semiconductor Devices", Adv. Electrical and Electron Phys., 1977, Vol. 44, pp. 221–281.

[5] W.N. Carr, "Characteristics of a GaAs Spontaneous Infrared Source with 40 Percent Efficiency", IEEE Trans On Electron Devices, October, 1965, Vol. ED–12, pp. 531–535.

[6] C.H. Gooch, Injection Electroluminescent Devices, London: J. Wiley and Sons, 1973, Ch. 3, pp. 58–64.

[7] B.G. Streetman, Solid State Electronic Devices, Englewood Cliffs, NJ: Prentice–Hall, 1980, App.III, p. 443.

[8] J.C. Palais, Fiber Optic Communications. Englewood Cliffs, NJ: Prentice–Hall, 1984, Ch. 6, pp. 121–140.

[9] S. Albin, Dept of Electrical and Computer Engineering, Old Dominion University, Norfolk, VA. 23529, Private Communication, June 1989.

[10] I. Ladany, "Electroluminescence Characteristics and Efficiency of GaAs: Si Diodes", J. Appl. Phys., February 1971, Vol. 42, pp. 654–656.

[11] W. Streifer, D.R. Scifres, G.L. Harnagel, D.F. Welch, J. Berger, and M. Sakamoto, "Advances in Diode Laser Pumps", IEEE J. Quantum Electronics, June, 1988, Vol. 24, pp. 883–894.

[12] M.I. Nathan, "Semiconductor Lasers", Proc. of the IEEE, October, 1966, Vol. 54, pp. 1276–1290.

[13] C.E. Hurwitz, "High Power and Efficiency in CdS Electron Beam Pumped Lasers", Appl Phys. Lett., 15, December, 1966, Vol. 9, pp. 420–423.

[14] K.H. Schoenbach, V.K. Lakdawala, D.C. Stoudt, T.F. Smith, R.P. Brinkmann "Electron–Beam Controlled High Power Semiconductor Switches", accepted for publication in IEEE Trans. on Electron Devices.

[15] R. Germer, Fritz Haber Inst. Berlin, FRG, Private Communication, 1988.

[16] S.G.E. Pronko and G.A. Gerdin, "A Short–Pulse, Laser–Driven Photoelectron Diode", these proceedings.

Table I

Direct Bandgap Materials To Be Used to Generate Bandedge Radiation

Material	E_g(eV)	W_b(eV)	λ(nm)	η_{iMAX}
InSb	0.18eV	1.678eV	689Onm	0.1073
InAs	0.36eV	2.056eV	344Snm	0.1751
GaSb	0.7eV	2.77eV	177Onm	0.2527
InP	1.28eV	3.99eV	969nm	0.321
GaAs	1.43eV	4.30eV	867nm	0.332
CdTe	1.58eV	4.618eV	785nm	0.342
CdSe	1.73eV	4.933eV	717nm	0.351
ZnTe	2.25eV	6.02SeV	551nm	0.373
CdS	2.42eV	6.382eV	512nm	0.379
ZnSe	2.7eV	6.97eV	459nm	0.387
ZnS	3.6eV	8.86eV	344nm	0.406

Table II

Relative Refractive Indices and the Planar and Hemispherical External Coupling Efficiencies (to Air) for the DBGSC Materials of Table I.

Material	Relative Refractive Index (to Air)[7]	Planar η_x $\frac{1}{4n^2}$	Planar η_x Eqn.(5)	Hemispherical η_x Eqn.(7)
InSb	4.2	$1.4.10^{-2}$	$8.8.10^{-3}$	0.31
InAs	3.8	$1.7.10^{-2}$	$1.1.10^{-2}$	0.33
GaSb	4.0	$1.6.10^{-2}$	$1.0.10^{-2}$	0.32
InP	3.4	$2.2.10^{-2}$	$1.5.10^{-2}$	0.35
GaAs	3.6	$1.9.10^{-2}$	$1.3.10^{-2}$	0.34
CdTe	2.7	$3.4.10^{-2}$	$2.7.10^{-2}$	0.39
CdSe	2.5	$4.0.10^{-2}$	$3.3.10^{-2}$	0.41
ZnTe	2.7	$3.4.10^{-2}$	$2.7.10^{-2}$	0.39
CdS	2.3	$4.7.10^{-2}$	$4.0.10^{-2}$	0.42
ZnSe	2.4	$4.3.10^{-2}$	$3.6.10^{-2}$	0.42
ZnS	2.3	$4.7.10^{-2}$	$4.0.10^{-2}$	0.42

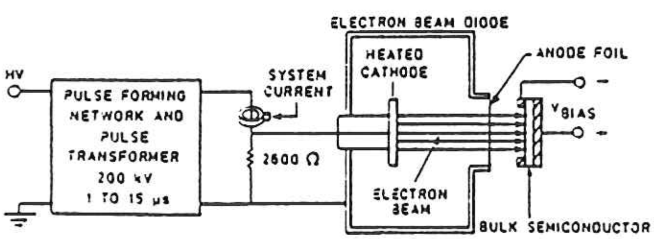

Fig.1: The ODU Thermionic Electron Beam Generator

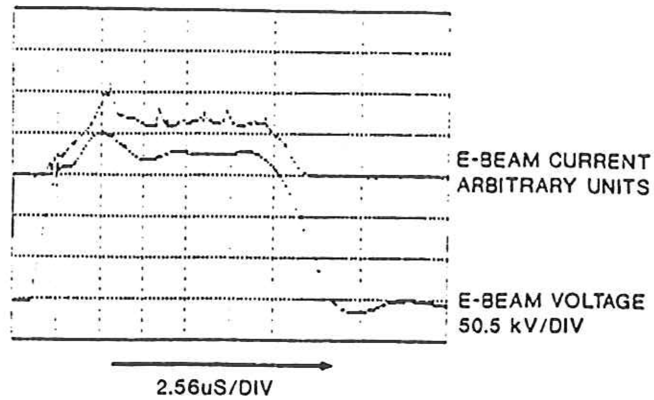

Fig.2: Typical Voltage and Current Waveforms From The ODU Thermionic Electron Beam Generator

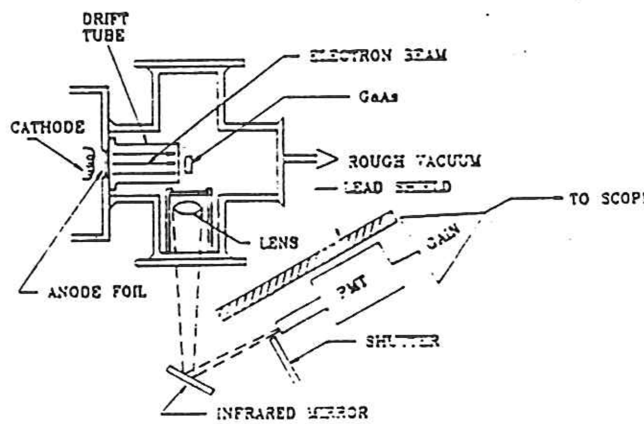

Fig.3: Experimental set-up for Measuring Band-Edge Radiation

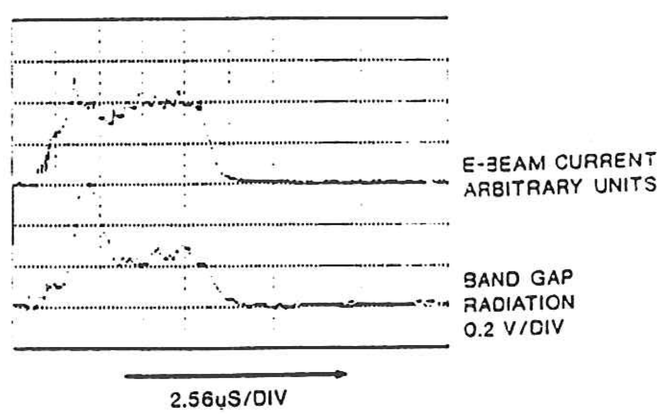

Fig.4: Typical Electron Beam Current and Band-Edge Radiation Waveforms.

T-ED/36/9//28680

Electron-Beam-Controlled High-Power Semiconductor Switches

Karl H. Schoenbach
Vishnukumar K. Lakdawala
David C. Stoudt
Tyler F. Smith
Ralf P. Brinkmann

Reprinted from
IEEE TRANSACTIONS ON ELECTRON DEVICES
Vol. 36, No. 9, September 1989

Electron-Beam-Controlled High-Power Semiconductor Switches

KARL H. SCHOENBACH, SENIOR MEMBER, IEEE, VISHNUKUMAR K. LAKDAWALA, MEMBER, IEEE, DAVID C. STOUDT, TYLER F. SMITH, AND RALF P. BRINKMANN

Abstract—Theoretical and experimental studies on electron-beam-controlled high-power semiconductor switches have been performed. By using cathodoluminescence as a means to ionize the bulk of the semiconductor switch, it seems to be possible—according to the results of a rate equation model—to control current densities of several hundred amperes per square centimeter with electron-beam current densities in the tens of millamperes per square centimeter. In experiments on semi-insulating gallium arsenide switches with a zinc-doped cathodoluminescent layer, switch current densities of 53 A/cm^2 have been obtained with an electron-beam current density of 36 mA/cm^2. The resistance of the switch was lowered by more than four orders of magnitude after the electron-beam was turned on. The closing and opening times were 400 ns, determined by the temporal rise and fall of the thermionically generated electron current. By using laser-generated photoelectrons, closing and opening times in the nanosecond range are achievable.

I. Introduction

ENERGY storage for pulsed power devices commonly implies capacitive storage for which the state of art is relatively well developed. However, in terms of energy density, capacitor banks are inefficient compared to inductive energy storage systems. Ratios of inductive-to-capacitive energy density of one hundred seem to be obtainable by stressing the technology of the coil design. However, there are two major technological problems in inductive energy storage systems; the limited storage time of magnetic energy due to the energy dissipation in the coil and the development of repetitively operating switches that can carry high current (tens of kiloamperes) for long times (tens of microseconds), and on command interrupt the current flow through the coil in times of 1 μs and less [1].

With the advent of high T_c superconductors, the problem of limited storage time for inductive energy seems to be solvable. The more severe problem—the opening switch design, especially for repetitive operation of the discharge system—is far from being solved. Diffuse discharge switches [2] and bulk semiconductor switches [3] are two of the most promising candidates for fast repetitive opening switches. With the exception of one type of bulk semiconductor switch, where lasers with different wavelengths are used to turn the switch conductance on and off [4], the conductivity in these type switches must be sustained by external ionization sources: lasers or electron beams.

In order to obtain short opening times, which for semiconductors means a high electron–hole recombination rate, the sustainment of the conductivity through radiative electron–hole ionization requires a high-power light source operating for the entire duration of the current flow through the switch. The inability to attain both long conduction times and fast opening with reasonable laser power limits the application of photoconductive switches in the microsecond range. Electron-beam ionization of bulk semiconductors, however, allows the control of semiconductor conductivity in this temporal range. Long electron-beam pulses (tens of microseconds) at current densities in the tens of milliamperes range can easily be obtained with electron-beam diodes with a heated thoriated tungsten cathode. With dispenser-type thermionic cathodes, current density values of 300 A/cm^2 have been reached [5]. Thermionic emitters offer the additional advantage of decoupling the electron generation and electron acceleration with, in principle, unlimited pulse length. The generation of pulse trains is possible by using a triode or tetrode configuration [6].

Other advantages of electron-beam control of bulk semiconductors compared to direct photoconductive switching are:

1) Wide-bandgap materials with a very high dark resistance, such as diamond, can be activated.

2) The limitation in hold-off voltage, which in photoconductive switches is determined by surface flashover, can be overcome by using a switch configuration, where the electron beam is injected through the contact. In such a configuration, which is discussed in the following paragraph, the breakdown voltage is determined by the intrinsic dielectric strength, rather than by the surface properties. The dielectric strength of gallium arsenide (GaAs) is 400 kV/cm [7].

3) The generation of multiple electric pulses with well defined risetime and temporal spacing between subsequent pulses can be obtained by sweeping the electron-beam across an array of semiconductor switches.

4) By using photoelectrons, it is possible to combine the advantages of photoconductive switching—remote control and picosecond timing--with those of electron-

Manuscript received November 28, 1988; revised March 10, 1989. This work was supported by the U.S. Army Research Office and the Air Force Office for Scientific Research under Contract DAA L03-86-K-0078.

The authors are with the Department of Electrical and Computer Engineering, Old Dominion University, Norfolk, VA 23529-0246.

IEEE Log Number 8928680.

0018-9383/89/0900-1793$01.00 © 1989 IEEE

beam controlled switching. The current rise in photoelectronic switches can be almost as fast as in directly laser-controlled switches. Current rise times of 100 ps were obtained in a photoelectronically controlled switch [8].

A major disadvantage of electron-beam-controlled compared to photoconductive semiconductor switches is the small absorption depth of electrons compared to that of photons with a quantum energy below the bandgap energy. For GaAs the absorption depth for photons with a quantum energy of 1.1 eV (Nd:YAG-laser) is greater than 1000 μm [3]. The range for 100-keV electrons in GaAs, on the other hand, is only some tens of micrometers. A way to overcome this problem of limited activation depth and to use electron beams to ionize large switch volumes is discussed in the following.

II. Concept

The switch concept is based on electron-beam-controlled ionization of the semiconductor material. The switch closes when the electron beam is turned on and generates free charge carriers in the semiconductor. When the electron beam is turned off, the conductivity of the semiconductor decreases due to electron–hole recombination, trapping of free charge carriers, and diffusion.

There are two basic switch configurations. In one configuration (A), the contacts are coplanar and the ionizing electrons are injected in the direction perpendicular to the applied electric field (Fig. 1(a)). In the second configuration (B) the electrons are injected through one of the contacts in the direction of the electric field (Fig. 1(b)). Assuming that free charge carriers are generated only in a layer corresponding to the range R of primary electrons, which for GaAs is shown in Fig. 2, the current in configuration A is limited to values on the order of ten amperes per centimeter width even at current densities of 10^3 A/cm^2.

In configuration B, the principle of operation is analogous to that of a vacuum photodiode with electrons instead of photons used to generate electron–hole pairs adjacent to one of the contacts (cathode). The so-called electron-bombarded semiconductor (EBS) devices, which were developed in the late 1960's and the 1970's [9] as modulators for microwave power tubes, are examples for this mode of operation. EBS devices are reverse-biased p^+-n Si diodes. The 10- to 20-keV electron-beam acts as a control element by injecting carriers through the p^+-layer into the depletion region [9]. The high field in the depletion region causes a rapid separation of electrons and holes. The electrons are swept across the depletion region; the holes have no effect but to provide continuity of charge. This device has a nanosecond response to changes in the source function (electron beam). However, since the current density is space-charge limited, relatively high voltages are needed to obtain reasonably high current densities in thick samples with correspondingly high breakdown voltages. For a trap-free insulator, which represents the optimum condition for space-charge-limited current flow in solids, the space-charge-limited current

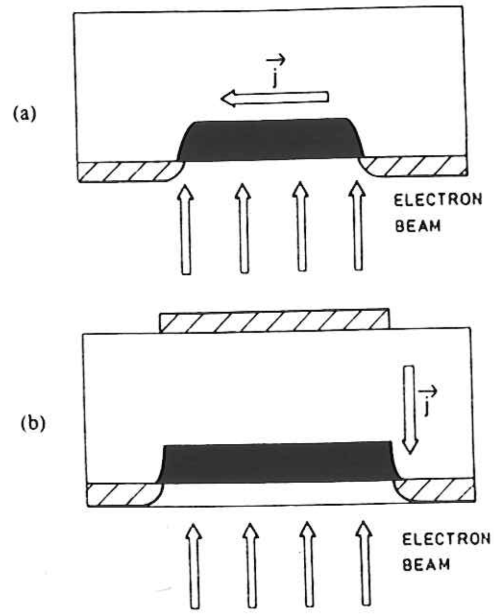

Fig. 1. High-energy electron injection: (a) perpendicular and (b) parallel to the electric field in a semiconductor switch. The darkly shaded region is the electron ionized part of the switch; the lightly shaded one in (b) is the electron drift region.

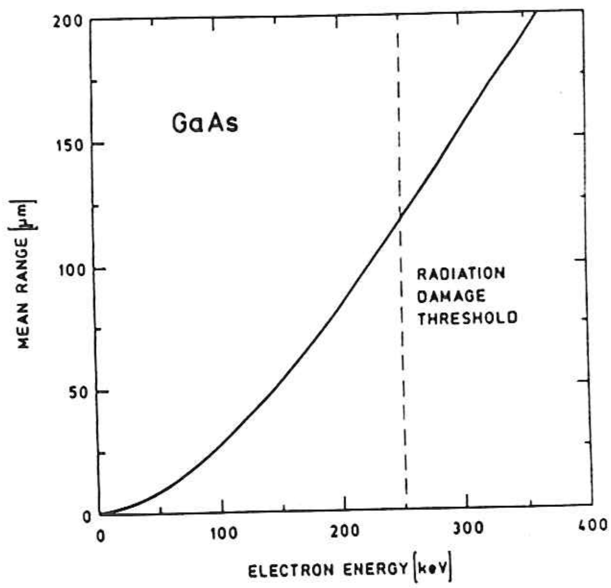

Fig. 2. Mean electron range in GaAs as a function of the electron energy.

density (J) is given by Mott–Gurney's square law

$$J = (9/8)\epsilon\mu V^2/d^3 \quad (1)$$

where V is the applied voltage, d the thickness of the semiconductor sample, ϵ the permittivity of the semiconductor material, and μ the mobility of the electrons. Equation (1) is valid for the electric field range where the electron drift velocity is proportional to the electric field intensity E. In GaAs, this is the range of E up to 3 kV/cm. For a 0.5-mm GaAs sample, biased at 100 V, the maximum current density that can be obtained according to Mott–Gurney's law is 0.4 A/cm^2.

A way to reduce the space-charge effect, without sacrificing the advantages of electron-beam control, is to

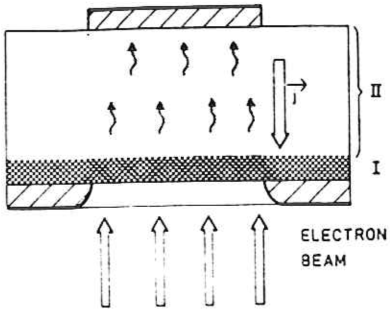

Fig. 3. Electron-beam-controlled semiconductor switch with bulk ionization by cathodoluminescence. The cross-hatched region consists of cathodoluminescent material, the darkly shaded part is the electron-penetration region, and the lightly shaded one is the region of the photon generated electron-hole plasma.

convert the electron energy (E) into photon energy (I) and use the electron-beam-generated radiation to ionize the bulk of the semiconductor (Fig. 3). The radiation generated by the electron-beam is Bremsstrahlung (X-rays) and band edge radiation due to radiative recombination of electron–hole pairs in the electron-beam activated layer. The radiation is generated in region I, whose depth is given by the electron range, and is absorbed in region II where it generates an electron–hole plasma.

The energy efficiency for Bremsstrahlung (I/E) is relatively small for the electron energy range of interest. It scales linearly with the electron energy and the atomic charge Z [10]

$$I/E = 7 \times 10^{-4} ZE \tag{2}$$

with E in megaelectronvolts. For GaAs and an electron energy of 200 keV, I/E is about 0.5 percent. The energy efficiency for band edge radiation with a photon energy around 1.4 eV can exceed that of Bremsstrahlung by more than an order of magnitude. The external radiation efficiency, the number of photons emitted per electron–hole recombination process, in GaAs p-n junction devices was measured to be 0.083, corresponding to an internal radiation efficiency of 0.88 at room temperature [11]. The effective ionization energy for GaAs is 4.3 eV. Hence, the total energy efficiency for cathodoluminescence could be about 30 percent under optimum conditions.

It is shown in the following sections that the combined effect of Bremsstrahlung and recombination radiation on electron–hole generation in the bulk of the semiconductor will allow us to extend the current density range of electron-bombarded semiconductor switches to hundreds of amperes per square centimeter. This is an improvement in the current density of two to three orders of magnitude over EBS devices. Experimental results with semi-insulating GaAs as the base material, which prove the feasibility of the concept, are discussed and interpreted using a rate equation model of the electron-beam-controlled semiconductor switch.

III. Characterization of Switch

A cross section of the semiconductor switch is shown in Fig. 3. The semiconductor wafer consists of semi-insulating GaAs. In order to model the switch, we have assumed that semi-insulating GaAs has two dominant deep centers [12]: EL2 and HL10. For EL2 the electron and hole capture cross sections are 4.67×10^{-16} cm^2 and 2×10^{-18} cm^2 [13], and for HL10, 3.7×10^{-16} cm^2 and 5×10^{-16} cm^2 [14], respectively. The concentration of EL2 centers for LEC-grown semi-insulating GaAs is in the range of 1.5×10^{16} cm^{-3} to 3×10^{16} cm^{-3} [15]. In our model the upper value was used. The concentration of HL10 centers was assumed to be 2×10^{16} cm^{-3}. At this concentration, the decay time constant of the free-electron concentration is in the range of 10 ns, a value that was experimentally obtained by irradiating the switch with a 10-ns Nd-YAG laser pulse. According to the data on LEC grown semi-insulating GaAs (Spectrum Technology, Inc.), the material is slightly n-type indicating the presence of residual donors, which are introduced during the growth process.

The rate coefficient for direct recombination k_d in GaAs is 7.5×10^{-10} cm^3 s^{-1} [16]. That means that electron–hole recombination in semi-insulating GaAs occurs for moderate electron–hole densities (10^{16} cm^{-3}) predominantly via the HL10 level. Such densities are typical for e-beam-generated electron–hole plasmas, where the electron-beam current is in the range of ten's of milliamperes per square centimeter. A way to increase the direct recombination rate, and therefore create a highly luminescent layer in the semi-insulating GaAs, is to dope the semiconductor with shallow donors or acceptors [17] to a depth corresponding to the electron range R, which for 125-keV electrons is 40 μm. In our model, the material in region I (Fig. 3), which has a depth of 40 μm, is therefore assumed to be doped with zinc (Zn), an acceptor material, at densities of 1×10^{18} cm^{-3} and 1×10^{19} cm^{-3}, respectively.

The electron source function S is assumed to be constant over the range I:

$$S = \left[\frac{dE}{dx}\right] \cdot \frac{J_b}{eW_i} \tag{3}$$

where dE/dx is the stopping power for electrons [18], J_b is the e-beam current density, e is the electronic charge, and W_i is the effective ionization energy. Since the p-doped region, with its high conductivity, carries the switch current radially to ring electrodes on the cathode face of the semiconductor, there is no need for contacts in the path of the electron beam. This way electron-beam losses in contacts, which at low electron energies are substantial, are avoided. Although such a configuration seems to allow the use of electron beams with arbitrary small electron energy E, there is a lower limit for E. For optimum radiation efficiency, the electron range needs to exceed a value that corresponds to the diffusion length for the ambipolar diffusion. The diffusion length is a measure for the boundary layer that is formed at the surface of the semiconductor. Diffusion lengths for GaAs doped with Zn at concentrations of 10^{18} to 10^{19} cm^{-3} are on the order of

micrometers [19]. The electron density decays over this distance from its equilibrium value to zero (for infinitely large surface recombination velocity). Consequently, the radiation efficiency becomes increasingly smaller when the electron range is reduced below the diffusion length. The condition that the electron range should exceed the diffusion length determines the minimum value of the electron-beam energy.

The material in region II (Fig. 2) is undoped semi-insulating GaAs. The depth of this region is related to the required hold-off voltage. Assuming a dielectric strength of greater than 10^5 V/cm [6], a switch that needs to hold off a voltage of 10 kV requires a thickness of 1 mm.

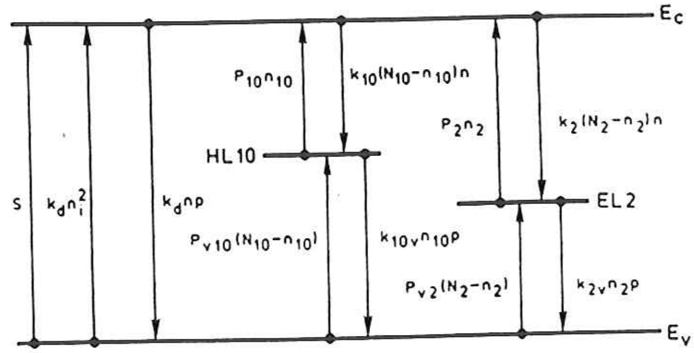

Fig. 4. Energy diagram of semi-insulating GaAs with relevant electron transitions.

IV. Rate Equation Model

Fig. 4 shows the four-level system with the transitions that were considered in our model. S is the source function for electron–hole generation. The electron-beam- or radiation-induced transition of electrons from the deep centers to the conduction band is assumed to be negligible compared to S because of the relatively low density of these centers. Recombination and trapping is characterized by recombination and trapping coefficients k_j. Thermal emission coefficients are characterized by P_j. Drift and diffusion of carriers has not been included in the model. We have assumed that the electric field during conduction is small: the switch has a small resistance in the on-state. Strong gradients in density, which occur at the highly doped region, affect the total resistance of the switch only slightly. Considering this, the rate equation system for electrons in the conduction band (n), in the electron trap EL2 (n_2), and in the recombination centers HL10 (n_{10}), and for holes (p) are given as

$$dn/dt = S - k_dnp + k_dn_i^2 - k_{10}(N_{10} - n_{10})n + P_{10}n_{10} - k_2(N_2 - n_2)n + P_2n_2 \quad (4a)$$

$$dn_{10}/dt = k_{10}(N_{10} - n_{10})n - P_{10}n_{10} - k_{10v}n_{10}p + P_{v10}(N_{10} - n_{10}) \quad (4b)$$

$$dn_2/dt = k_2(N_2 - n_2)n - P_2n_2 - k_{2v}n_2p + P_{v2}(N_2 - n_2) \quad (4c)$$

$$dp/dt = S - k_dnp + k_dn_i^2 - k_{10v}n_{10}p + P_{v10}(N_{10} - n_{10}) - k_{2v}n_2p + P_{v2}(N_2 - n_2). \quad (4d)$$

The charge densities are related via the quasineutrality condition:

$$p = n + n_{10} - (N_2 - n_2) + N_a. \quad (5)$$

In the above equations, k_2 and k_{2v} are the rate coefficients for electron and hole capture by EL2 centers, and k_{10v} characterize electron and hole capture by HL10 centers. The rate coefficients are obtained by multiplying the known cross sections with the thermal velocity of electrons and holes, respectively. P_2, P_{2v}, P_{10}, and P_{10v} are the thermal electron and hole emission coefficients for EL2 and HL10 centers. n_i is the intrinsic carrier density. The densities of electron traps, recombination centers, and acceptor atoms are N_2, N_{10}, and N_a, respectively. The above set of equations is valid for both regions I and II with N_a, the density of acceptors, always being zero in region II.

A. Semi-Insulating GaAs

The set of equations was solved for the steady-state case. At first it was assumed that the material both in regions I and II is undoped semi-insulating GaAs. In this case N_a is zero for both regions I and II. The steady-state free-electron density in region I was computed to be 2.4×10^{16} cm^{-3} for an e-beam current density of $J_b = 100$ mA/cm^2 and 2.1×10^{15} cm^{-3} for a J_b of 10 mA/cm^2. The ionization in the bulk of the semiconductor is caused by Bremsstrahlung and band edge radiation. The source function for electron–hole plasma generation by Bremsstrahlung in region II was calculated by using (2) for the total X-ray intensity and assuming a linear spectral distribution for the X-ray emission. The spectral dependence of the absorption coefficient was taken from Kaye and Laby [20].

The source function of electrons in region II due to band edge radiation was computed by using the emission and absorption data shown in Fig. 5. The measured absorption coefficient holds for undoped GaAs [21]. The emission coefficient was derived from the absorption coefficient by means of thermodynamic considerations [19]. The computed spectral distribution of the band edge radiation agrees well with the measured photon flux for Zn-doped GaAs [22]. Assuming a quantum efficiency of 100 percent for electron–hole generation, the source function for electron–hole generation by band edge radiation was then calculated and added to the Bremsstrahlung source function in region II. These data were then used to find the spatial electron distribution $n(x)$ in the bulk of the semiconductor for $J_b = 10$ mA/cm^2 (Fig. 6(a)) and $J_b = 100$ mA/cm^2 (Fig. 6(b)) by solving the set of rate equations for range II.

The spatial dependence of the conductivity can be obtained by multiplying the electron density with the elec-

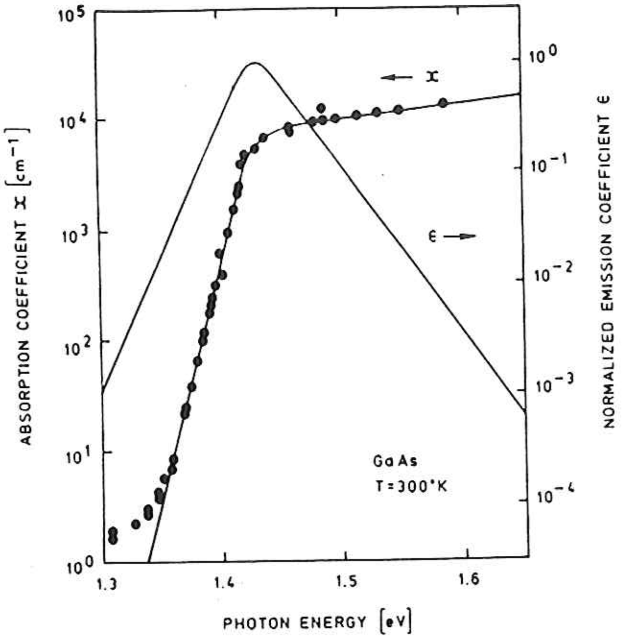

Fig. 5. The absorption coefficient κ of undoped GaAs [20] and the emission coefficient ϵ for band edge radiation [21]. The solid line through the experimentally obtained values for κ represents the fit that was used to calculate ϵ.

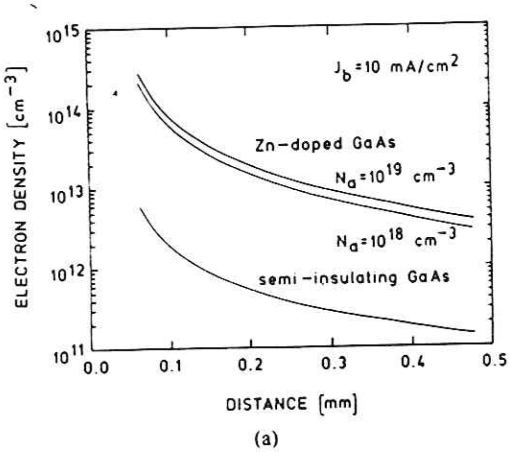

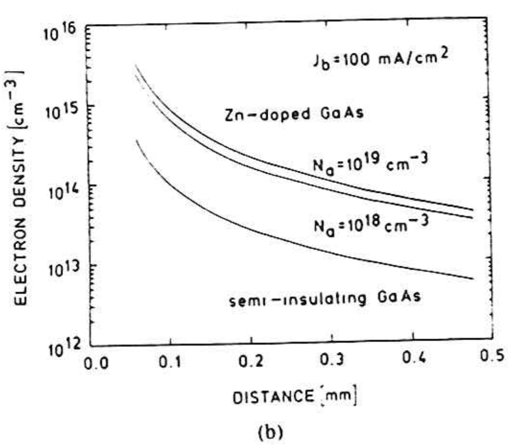

Fig. 6. Spatial dependence of the electron density in region II for semi-insulating GaAs and for the same material, but containing a highly doped, 40-μm-deep layer of Zn at the cathode. (a) J_b = 10 mA/cm^2. (b) J_b = 100 mA/cm^2.

tron mobility μ and the electronic charge e. The electron mobility was assumed to be 5500 Vs/cm^2 (Spectrum Technology, Inc.). The contribution by holes to the conductivity is neglected because of the relatively small hole mobility in GaAs. The conductance G of the switch per unit area is given by

$$G = \frac{e\mu}{\displaystyle\int_0^d \frac{dx}{n(x)}}. \tag{6}$$

The calculated conductance values for an undoped GaAs switch with width d = 0.5 mm are listed in Table I.

B. Semi-Insulating GaAs with Zn Layer at the Cathode

The radiation efficiency of the electron beam is increased by doping the base material, semi-insulating GaAs, with a shallow donor or acceptor material over the depth of the electron-beam range. In Zn-doped GaAs the direct recombination rate is enhanced due to the increased number density of holes ($p \approx N_a$), which generally is many orders of magnitude above the equilibrium value p_0. The calculated values for the electron density (n) in the Zn doped region I, the radiative recombination rate ($k_d np$), and the radiation efficiency (η) are listed in Table I. The variable parameters are the electron-beam current density and the Zn-doping concentration. The electron density is lower for higher doping densities. This is due to the increased electron loss by direct recombination. However, in spite of a reduced electron density, the recombination rate in Zn-doped GaAs, which is a measure of the radiative source function in region II, is considerably higher than in semi-insulating GaAs.

The radiation efficiency (the ratio of direct recombination rate to the sum of all electron loss rates) is for J_b = 10 mA/cm^2 more than an order of magnitude higher for Zn-doped GaAs compared to undoped GaAs. Consequently, for a 0.5-mm-thick semi-insulating GaAs switch with a Zn-doped layer at the cathode, the conductance per unit area can be increased by more than an order of magnitude for low electron-beam current densities (Table I). This shows that by utilizing cathodoluminescence it should be possible to generate switch conductances in the range of mhos per square centimeter with moderate electron-beam current densities of tens of milliamperes per square centimeter. The corresponding switch current densities in a cathodoluminescent system could exceed those of EBS systems with comparable dimensions and voltage by more than two orders of magnitude.

V. Experiments

Experiments have been performed to demonstrate the feasibility of the cathodoluminescence-controlled semiconductor switch. Two types of switches were investigated: one where the switch material was undoped semi-insulating GaAs and a second one, again using GaAs as the base material, but with a surface layer of highly Zn-doped material. In both cases LEC-grown semi-insulating

TABLE I
RESULTS OF RATE EQUATION CALCULATIONS FOR REGION I (CATHODOLUMINESCENCE REGION) AND REGION II (SWITCH REGION) OF AN ELECTRON-BEAM-CONTROLLED GaAs SWITCH

E-BEAM CURRENT DENSITY J_b[mA/cm^2]	Zn LAYER DOPING DENSITY N_a [cm^{-3}]	ELECTRON DENSITY REGION I n [cm^{-3}]	RECOMBINATION RADIATION RATE $k_d np$ [cm^{-3}s^{-1}]	RADIATION EFFICIENCY η	CONDUCTANCE PER UNIT AREA G [Ω^{-1}cm^{-2}]
10	undoped	2.1×10^{15}	9.7×10^{21}	0.02	9.55×10^{-3}
	10^{18}	4.4×10^{14}	3.3×10^{23}	0.73	2.19×10^{-1}
	10^{19}	5.8×10^{13}	4.4×10^{23}	0.96	2.88×10^{-1}
100	undoped	2.4×10^{16}	5.5×10^{23}	0.12	3.95×10^{-1}
	10^{18}	4.4×10^{15}	3.3×10^{24}	0.73	2.27
	10^{19}	5.8×10^{14}	4.4×10^{24}	0.96	2.99

GaAs was used. The resistivity of this material was given as 7×10^6 Ω-cm (Spectrum Technology, Inc.). The shallow layer of p-type GaAs was obtained by diffusion of Zn for 2 h at a temperature of 750°C. According to [23], the Zn-doped profile, which follows a complementary error function, has a peak value of 10^{20} cm^{-3} at the diffused surface. The acceptor concentration decays to about 10^{19} cm^{-3} over a distance of 50 μm and has a very steep diffusion front at this depth. Au:Ge contacts of about 0.1-μm thickness were evaporated onto both faces of 0.5-mm wafers with a contact area of 0.8 cm^2 and annealed at 400°C for 15 min.

The experimental set up is shown in Fig. 7. The electron beam is produced by a pulsed thermionic diode [24]. The diode voltage is generated by a pulse forming network (PFN) consisting of an LC chain and stepped up in a ratio 1:11 by a pulse transformer. The pulse duration can be adjusted between 1 and 15 μs by varying the number of PFN segments. The rise and fall times of the voltage pulse are 500 ns. The maximum diode voltage is 220 kV, determined by the pulse transformer rating. The electron-beam current density can be varied up to 100 mA/cm^2 by varying the temperature of the thoriated tungsten cathode.

In our experiments we have used a 150-keV electron beam to irradiate the semiconductor sample outside the diode chamber. The energy losses in the anode foil of the diode (1-mil titanium) are about than 20 percent at this electron-beam energy [25] and the maximum value of the electron energy is reduced to about 125 keV. The influence of the foil on the intensity of the electron beam is demonstrated in Fig. 8, where the temporal variation of the diode voltage is compared to the electron-beam current pulse, which was measured by means of a 50-Ω Faraday cup. Due to the fact that the electron-beam losses in the foil are higher at lower electron energies, we obtain a steepening in rise and fall of the electron-beam pulse compared to the voltage pulse. Generally, any variation in voltage appears more pronounced in the electron-beam pulse.

In order to get the current density–voltage characteristics of the semiconductor switches, a dc voltage was ap-

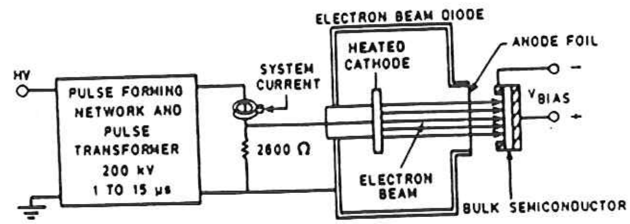

Fig. 7. Experimental setup of the 150-kV electron-beam system.

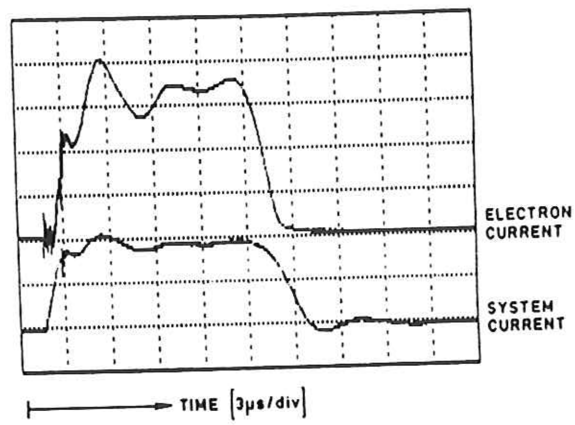

Fig. 8. Comparison of system current with electron-beam current density. (Electron current density: 4 mA/div. System current: 40 A/div.)

plied to the sample. The current flowing through the semiconductor (switch current), when it was irradiated with high-energy electrons, was measured by means of a Pearson coil. The temporal development of the electron-beam diode voltage was recorded simultaneously at each shot. This signal was obtained by measuring the total PFN current (system current) flowing into the 1200-Ω load resistor and, parallel to it, the electron-beam diode. The current and voltage signals were recorded by a Tektronix 7612 D transient digitizer. The variable parameter in all the measurements was the electron-beam current density at a peak electron energy of 125 keV.

VI. EXPERIMENTAL RESULTS

The temporal current response of the semi-insulating GaAs switch of 0.5-mm thickness to electron-beam irradiation is shown in Fig. 9 for an electron-beam current

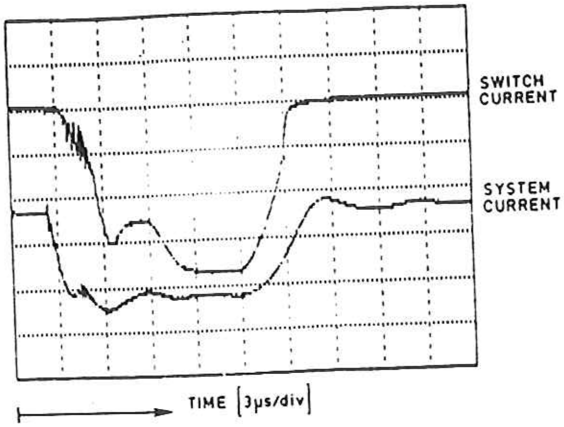

Fig. 9. Temporal behavior of switch current in undoped semi-insulating GaAs with system current as a reference. (Switch current: 2 A/div.)

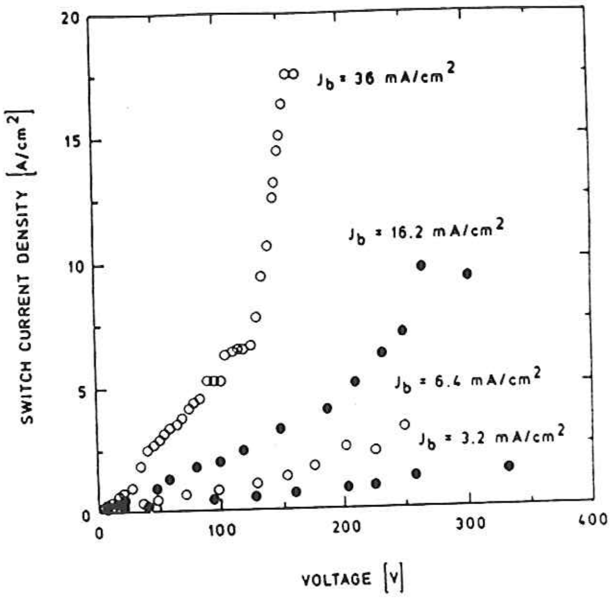

Fig. 10. Current density versus bias voltage for a GaAs switch (0.5-mm thickness) with the e-beam current density as a variable parameter.

density of $J_b = 36$ mA/cm^2 and a dc bias voltage of 135 V. Also shown is the electron-beam diode voltage for this particular shot. The switch current signal follows closely the electron-beam pulse. The switch current density in this case was $J_s = 9.4$ A/cm^2, which means the current gain J_s/J_b is about 260.

The values of switch current density versus biasing voltage with the electron-beam current density as a variable parameter are plotted in Fig. 10 for 0.5-mm semi-insulating GaAs wafers. The slope of the curves, which represents the switch conductance per unit area, varies linearly with the electron-beam current density. For J_b = 36 mA/cm^2 the switch conductance, at voltages below 130 V, is 0.05 Ω^{-1} cm^{-2}, corresponding to a resistance of 20 Ω/cm^2. Compared to the initial resistance of the sample, 3.5×10^5 Ω/cm^2, the reduction in resistance due to electron-beam irradiation is more than four orders of magnitude.

The temporal response of the second type of switch, semi-insulating GaAs with a shallow layer of Zn-doped material in the cathode region, is shown in Fig. 11. The cathode face of the semiconductor switch is irradiated by the electron beam with a current density of 36 mA/cm^2. Contrary to the results with homogeneous switch material, the temporal response does not follow the electron-beam pulse over the entire length of the pulse. After an initial linear response, whose duration increased when the electron-beam intensity was lowered, an approximately linear rise of the switch current is observed. The current flow is terminated when the electron beam is turned off. The current termination due to electron-beam turn-off is shown even more striking in Fig. 12 where, caused by a breakdown in the diode, the electron beam was turned off very rapidly. The switch current followed the electron-beam current instantaneously. This means that the opening of the switch is fully controllable by the electron beam.

The maximum switch current density obtained at the end of the current pulse is, at voltages above 125 V, about twice as large as the current density in homogeneous switch material. This is shown in Fig. 13. The change in the slope of the *I-V* characteristics at around 130 V is assumed to be caused by reaching a trap-filled limit. The

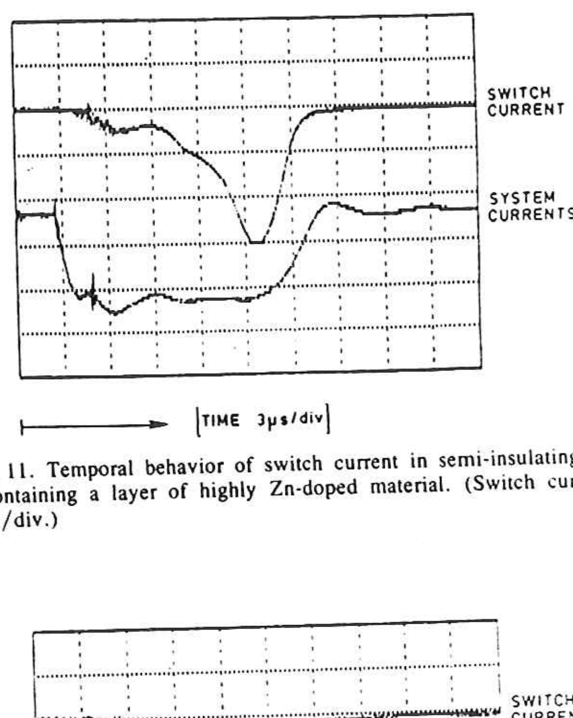

Fig. 11. Temporal behavior of switch current in semi-insulating GaAs containing a layer of highly Zn-doped material. (Switch current: 4 A/div.)

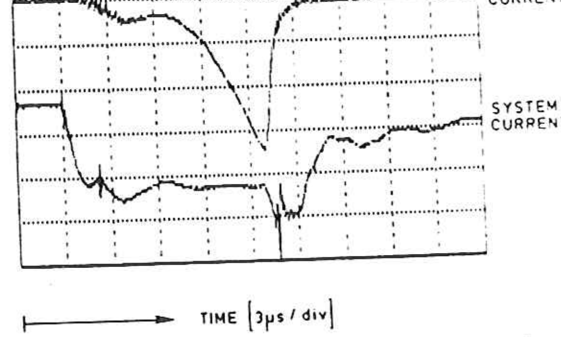

Fig. 12. Temporal behavior of switch current for same sample as in Fig. 11. This figure clearly shows the response of switch current to the termination of the electron beam due to a breakdown in the diode

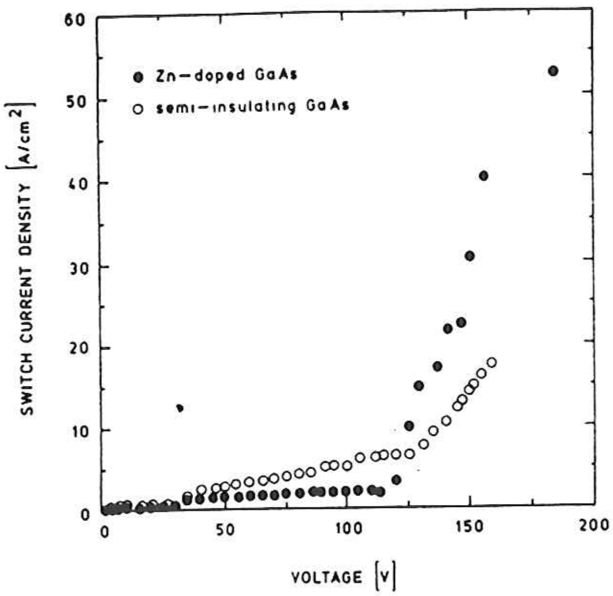

Fig. 13. Switch current–voltage characteristics for semi-insulating GaAs and for the same material containing a highly doped layer of Zn at the cathode.

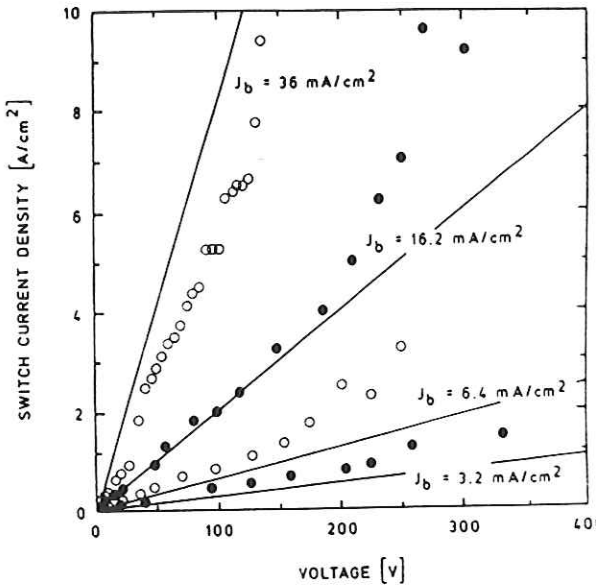

Fig. 14. Comparison of experimentally obtained J–V characteristics with computed J–V curves for 0.5-mm-thick semi-insulating GaAs switches. The modeling results hold for low voltages only.

maximum switch current density obtained in our experiments with Zn-doped GaAs was 53 A/cm^2, with an electron-beam current density of 36 mA/cm^2, at a voltage of 185 V across the switch. This corresponds to a current gain J_s/J_b of 1470.

VII. Discussion and Conclusion

The closing and opening times of the electron-beam-controlled GaAs switches were limited in our experiments by the rise and fall time of the electron-beam current to about 400 ns. The intrinsic closing time, i.e., the response of the switch to a step-function-like rise of the electron-beam current, is determined by the difference of the generation rate and the loss rate for electrons and holes in the switch volume. The generation rate is directly related to the electron-beam current and the loss rate is determined mainly by the electron and hole capture into deep traps. Using reasonable assumptions on the concentration and capture cross section of deep centers in semi-insulating GaAs [14], [15], the risetime of the switch conductance at electron-beam current densities of the order of 10 mA/cm^2 can be expected to be in the tens of nanosecond range for undoped semi-insulating GaAs. The actual opening time of the bulk semiconductor switches is determined mainly by recombination and trapping processes. Measurements of the current decay time of semi-insulating GaAs, which was ionized by a 10-ns laser pulse, gave time constants on the order of 10 ns for electron–hole recombination. With Cr-doped GaAs the opening time should be in the subnanosecond range [26].

The linear dependence of the switch current in homogeneous semi-insulating GaAs switches on the electron beam current demonstrates that these switches are not space-charge limited. This is also proven by the absolute values of the switch current density. The measured current densities are far above the space-charge-limited current density for a trap-free insulator, which represents the optimum condition for space-charge-limited current flow. In Fig. 14 the measured current–voltage characteristics for 0.5-mm-thick semi-insulating GaAs switches are compared with the computed curves. The measured values agree, by about a factor of two, with the computed results, which hold for small bias voltages. All experimental results were obtained on 0.5-mm-thick samples. The results of our model indicate that the switch resistance scales linearly with the sample thickness.

Recombination radiation and Bremsstrahlung play about an equal role in the generation of an electron–hole plasma in the bulk of the semi-insulating GaAs switch for electron-beam current densities of 10 mA/cm^2. With increasing electron-beam current density, Bremsstrahlung becomes less and less important. For Zn-doped GaAs, band edge radiation generated by the radiative decay of the electron-beam-created electron–hole concentration in region I is always the dominant ionization source in region II. Although steady state was obviously not reached in the Zn-doped switch, an increase in conductivity, by a factor of two,, over undoped semi-insulating material was observed at the end of the 15-μs pulse. Compared to the space-charge-limited current devices (EBS devices), the gain in current density is about two orders of magnitude.

A possible reason for the relatively slow growth of the current in the Zn-doped GaAs switch is the initially large trapping rate for electrons by ionized EL2 centers. The ionization of EL2 in the bulk of the semiconductor could be caused by Zn complexes, which form a shallow diffusion front beyond the steep front described by the complementary error function [27]. The time required to fill the ionized EL2 traps is proportional to the trap density and inversely proportional to the electron source function. The current rises after the traps are filled with a time con-

stant that is determined by direct and indirect electron–hole recombination processes. Our measured current profiles are in qualitative accordance with profiles calculated by means of a simple rate equation model [28].

For applications of electron-beam-controlled switches in inductive energy storage circuits, the observed slow rise of current density together with the fast decay of the current, after electron-beam turn-off, is desirable. In order to charge an inductor, that is, to build up a magnetic field, a constant rise of current up to a maximum value is required. The fast electron-beam-controlled increase of switch resistance after the current maximum is reached provides for high-power amplification in the inductive discharge circuit [1].

Because of the relatively small absorption length of band edge radiation in the semiconducting material, the resistance of the electron-beam-controlled switch is determined mainly by the region most distant from the cathodoluminescent layer. Doping the cathodoluminescent layer highly with Zn does not just increase the radiation efficiency but also causes a reduction of the bandgap energy and, consequently, a shift of the band edge emission characteristics toward longer wavelengths [17]. The light generated in the Zn-doped layer will therefore penetrate deeper into the bulk of the semiconductor switch. Although the reduced absorption causes the conductivity in the bulk of the semiconductor to decrease, the advantages of achieving ionization in large volumes outweigh the loss in conductivity. With large size switches of dimension (d) it is possible to keep the dark current low, which at high field strengths (E) is proportional to E/d. Secondly, the high breakdown voltage that can be obtained in large-size switches makes them attractive for applications in pulsed power systems. A second possibility to ionize the bulk more efficiently is to generate a temperature gradient between the anode and cathode. Lowering the temperature of the cathodoluminescent region causes, as with doping, a shift of the emission characteristics of this layer relative to the absorption profile of the bulk material. This method should allow a simple control of the optical depth and consequently the switch resistance.

In order to get nanosecond or subnanosecond pulses with an electron-beam-controlled switch, it will be necessary to use photoelectrons. Photoelectronic switching combines the advantages of photoconductive switching—remote control and picosecond timing—with those of electron-beam switching. The emission of electrons from a photocathode is controlled by a light source with photon energy exceeding the work function of the cathode material. The electrons gain enough energy in the electric field between anode and cathode to penetrate the anode foil and ionize the semiconductor. Compared to direct photoconductive switching, where one photon creates one electron–hole pair, in the photoelectronic switch the number of electron–hole pairs per photon (g) can be considerably higher. The gain g is given as

$$g = y(E_{eb}/W_i) \tag{7}$$

where y is the photoelectric yield, E_{eb} is the energy the electrons gained in the electric field between cathode and anode, and W_i is the effective energy necessary to create an electron–hole pair in the switch material. Assuming a photoelectric yield of 0.1, an E_{eb} of 100 kV, and a W_i of 4.3 eV for GaAs, a gain of about 2250 compared to direct photoconductive switching can be obtained. This high gain may allow the use of relatively low power light sources, e.g., semiconductor diodes, to control large currents through the electron-beam-activated semiconductor switch.

Acknowledgment

We thank G. Gerdin and H. Erkaya (ODU) for helpful discussions and R. Roedel (U. Arizona) for information on diffusion of Zn in GaAs.

References

[1] K. H. Schoenbach, M. Kristiansen, and G. Schaefer, *Proc. IEEE*, vol. 72, p. 1019, 1984.
[2] G. Schaefer and K. H. Schoenbach, *IEEE Trans. Plasma Science*, vol. PS-14, p. 561, 1986.
[3] W. C. Nunnally, in *Proc. 5th IEEE Pulsed Power Conf.* (Arlington, VA), 1985, p. 235.
[4] K. H. Schoenbach, V. K. Lakdawala, R. Germer, and S. T. Ko, *J. Appl. Phys.*, vol. 63, p. 2460, 1988.
[5] R. Petr and M. Gundersen, *Lasers and Particle Beams*, vol. 1, p. 207, 1983.
[6] C. H. Harjes *et al.*, *Rev. Sci. Instrum.*, vol. 55, p. 1684, 1984.
[7] S. M. Sze, *Physics of Semiconductor Devices.* New York: Wiley, 1981.
[8] G. Mourou, W. Knox, and S. Williamson, *Laser Focus Mag.*, p. 97, Apr. 1982.
[9] D. J. Bates, R. I. Knight, S. Spinella, and A. Silzars, *Adv. El. Phys.*, vol. 44, p. 221, 1977.
[10] R. D. Evans, *The Atomic Nucleus.* New York: McGraw-Hill, 1955, p. 615.
[11] W. N. Carr, *IEEE Trans. Electron Devices*, vol. ED-12, p. 531, 1965.
[12] T. Burke, M. Weiner, L. Bovino, and R. Youmans, in *Proc. 6th IEEE Pulsed Power Conf.* (Arlington, VA), 1987, p. 283.
[13] G. M. Martin, A. Mitonneau, and A. Mircea, *Electron. Lett.*, vol. 13, p. 191, 1977.
[14] A. Mitonneau, G. M. Martin, and A. Mircea, *Electron. Lett.*, vol. 13, p. 666, 1977.
[15] G. M. Martin, *Appl. Phys. Lett.*, vol. 39, p. 747, 1981.
[16] M. S. Demokan and M. S. Ozyazici, *Int. J. Electron.*, vol. 55, p. 699, 1983.
[17] D. A. Cusano, *Solid State Commun.*, vol. 2, p. 353, 1964.
[18] "Stopping powers for electrons and positrons," ICRU Rep. 37, Bethesda, MD, 1984, p. 90.
[19] R. P. Brinkmann, to be published.
[20] G. W. C. Kaye and T. H. Laby, *Tables of Physical and Chemical Constants.* New York: Longman, 1986, p. 326.
[21] M. Schulz and H. Weiss, Eds., *Landolt-Boernstein*, vol. 17. New York: Springer, 1984, ch. 6, p. 351.
[22] W. N. Carr and J. R. Biard, *J. Appl. Phys.*, vol. 35, p. 2777, 1964.
[23] H. C. Casey, *Atomic Diffusion in Semiconductors*, D. Shaw, Ed. New York: Plenum, 1973, p. 351.
[24] J. P. O'Loughlin and S. L. West, in *Proc. 3rd IEEE Int. Pulsed Power Conf.* (Albuquerque, NM), 1981, p. 59.
[25] S. M. Seltzer and M. J. Berger, *Nucl. Insts. Meth.*, vol. 119, p. 157, 1974.
[26] C. H. Lee, *Picosecond Optoelectronic Devices.* Orlando, FL: Academic, 1984, pp. 119–186.
[27] S. Reynolds, D. W. Vook, and J. F. Gibbons, *J. Appl. Phys.*, vol. 63, p. 1052, 1988.
[28] R. H. Bube, *Photoconductivity of Solids.* New York: Wiley, 1960, p. 276.

Karl H. Schoenbach (SM'82) was born in Peterswald, Germany, [redacted] He received the Diploma degree in physics and the Dr.rer.nat. degree in physics in 1966 and 1970, respectively, from the Technische Hochschule Darmstadt, Germany.

From 1970 to 1978, he was a Scientific Assistant and Docent with the Applied Physics Department at the Technische Hochschule Darmstadt, working in the areas of gas discharge physics and on dense plasma focus. From 1979 to 1985, he held a faculty position at Texas Tech University, Lubbock, where he was involved in research on fast opening switches, especially diffuse discharge opening switches. Since 1985, he has been a Professor in the Electrical Engineering Department at Old Dominion University, Norfolk, VA, where he is currently the Director of the Physical Electronics Research Institute. He is active in research on electron-beam and optically controlled bulk semiconductor switches and in modeling and experimental studies of low-pressure gas discharges. He has organized a number of workshops, most recently one on "Optically and e-beam controlled semiconductor switches."

Dr. Schoenbach is a member of the APS and the German Physical Society.

*

Vishnukumar K. Lakdawala (M'83) was born [redacted] in Bangalore, India. He received B.S. and M.S. degrees, both in electrical engineering, in 1972 and 1974, respectively, from Bangalore University, Bangalore, India, and the Indian Institute of Science, Bangalore, India. He received the Ph.D. degree in electrical engineering from The University of Liverpool, United Kingdom, in 1980.

From 1974 to 1977, he worked at the Research and Development Center of Jyoti Limited, Baroda, India, on the design and development of high-voltage instrument transformers. From 1980 to 1982, he was conducting research on ring laser gyroscopes. From 1982 to 1983, he worked as a Post-Doctoral Research Fellow in the Atomic, Molecular, and High Voltage Physics Group at Oak Ridge National Laboratory, Oak Ridge, TN. In 1983, he joined Old Dominion University, Norfolk, VA. Currently, he is an Associate Professor of Electrical Engineering. His current areas of research include high-power semiconductor switching, semiconductor characterization, and processing.

Dr. Lakdawala is a member of the IEEE Electrical Insulation Society and serves as a faculty advisor to the Eta Kappa Nu Electrical Engineering Honor Society (Zeta Epsilon Chapter). Currently he is also serving as Vice-Chairman of the IEEE Virginia Council Executive Committee.

*

David C. Stoudt was born in Abington, PA, on [redacted] He received the B.S. degree in electrical and computer engineering (*summa cum laude*) from Old Dominion University, Norfolk, VA, in 1987. He is currently working toward the M.S. degree in physical electronics in the area of high-power electron-beam-irradiated semiconductor switches at Old Dominion University.

He is also currently a Research Assistant at Old Dominion.

Mr. Stoudt has received several awards for academic achievement, including the Old Dominion Alumni Association Outstanding Scholar Award.

*

Tyler F. Smith was born in Washington, DC, on [redacted] He received the B.S. degree in electrical and computer engineering from Old Dominion University, Norfolk, Virginia, in 1987. He is currently working toward the M.S. degree in physical electronics in the area of high-power electron-beam-irradiated semiconductor switches at Old Dominion University.

He is also a Research Assistant at Old Dominion.

*

Ralf P. Brinkmann was born in Braunschweig, Germany, [redacted] He received the Diplom degree in physics in 1984, the Diplom degree in electrical engineering in 1985, and the doctoral degree in physics in 1986, all from the Ruhr-Universität Bochum.

Supported by a scholarship from the Studienstiftung des deutschen Volkes, he spent a year as a Post-Doctoral Fellow at the University of Chicago. He joined Old Dominion University in September 1988 to work at the Physical Electronics Research Institute. His current research interests are the analysis of current-carrying plasma configurations and the modeling of semiconductor devices.

MODELING OF ELECTRON-BEAM CONTROLLED SEMICONDUCTOR SWITCHES

R.P. Brinkmann
Department for Electrical and Computer Engineering
Old Dominion University, Norfolk, VA 23508

ABSTRACT

The subject of this paper is the mathematical modeling of a recently proposed class of electron-beam controlled high power semiconductor switches which are able to overcome the space-charge limitation of conventional electron bombarded semiconductor devices by utilizing the secondary ionization effects of cathodoluminiscence and bremsstrahlung. Current densities of several kA/cm^2 at forward voltages some 10 V can be controlled with an electron-beam of 100 keV and $1\,A/cm^2$; hold-off voltages of more than 100 kV/cm and dark currents as small as $10\,\mu A/cm^2$ are possible. The concept has several possible applications, its fast and repetitive closing and opening under load makes it suitable for inductive energy storage applications; its linear characteristics suggests a use as a high-power modulation device.

I. INTRODUCTION

In terms of weight and energy density, inductive energy storage systems are superior to capacitive systems by more than two orders of magnitude. However, two major problems have to be overcome before a technological realization of this concept: The problem of resistive losses in the storing inductivity, and the lack of appropriate opening switches which can interrupt a sufficiently high electrical current in the presence of an induced counter voltage.

The first difficulty seems to be solvable by applying the concept of superconductivity, either by using the well-established conventional technology or the new ceramic high T_c materials. In this work we are concerned with the second problem, the realization of a high power switch which allows fast repetitive closing and openings cycles under load. We present analytical and numerical investigations into the concept of electron-beam controlled semiconductor switches as recently proposed by Schoenbach et al. [1].

The paper is organized as follows. First, in section II, we will describe the proposed concept more extensively and discuss the interaction of the different physical processes involved. In section III, an appropriate description of these processes will be established in terms of a coupled set of one-dimensional transport equations. The results of a numerical calculation of both the conductive and the open state are presented in section IV. The paper concludes with a discussion of the obtained results and their significance for possible applications.

II. CONCEPT OF THE SWITCH

The concept of electron-beam controlled semiconductor switches is based on irradiating a body of well-compensated direct semiconductor material with a high energy electron-beam just below the radiation damage threshold. Both direct and indirect ionization processes are utilized to create a high density of free charge carriers. A schematic sketch of the geometry of the proposed device is given in figure 1.

The configuration consists of a semi-insulating (compensated) gallium arsenide body of a thickness L up to 1 cm (zone II), provided with a highly ($N_a \approx 10^{19}$) p-doped surface layer of $d \approx 25\,\mu$m extension (zone I) at the cathode and a similiar but n-doped layer at the anode (zone III). Appropriate doping materials are for instance zinc and silicon, respectively. The exact density profile depends on the details of the manufacturing process, for our simulation we have utilized the results of a theoretical calculation given by Weisberg and Blanc [2].

In the open state, the bulk material of the switch is highly resistive and can hold off a voltage of up to 400 kV/cm depending on the break-down field strength of the material [3]. The highly doped surface layers reduce drastically the electrical field at the contacts and the concentration of minority carriers (i.e., of electrons at the cathode and holes at the anode), this prevents any current injection in the bulk zone and insures therefore a low dark current (determined by the intrinsic conductivity).

To turn the switch in the conducting state, an electron-beam with energy up to 250 keV (the radiation damage threshold of GaAs [4]) is injected into the cathode side of the sample. Due to the very small penetration depth of the electrons (e.g., about 25 μm for a 100 keV beam) [5], the beam is entirely stopped within the surface zone I where it creates a high concentration of electron-hole pairs by direct ionization. Subsequently, these charge carriers recombine under emission of band-edge radiation which then can penetrate deeper into the material to ionize the bulk zone II of the switch. Also, the abrupt stopping of the energetic electrons generates a beam of bremsstrahlung emitted in forward direction which creates secondary free charge carriers as well. By these means the bulk zone becomes conductive and the space charge limitation of conventional EBS (electron bombarded semiconductor) devices is overcome.

The strong p-type doping of the stopping zone I has two beneficial effects. First, it enhances considerably the efficiency of converting the direct beam energy into secondary band-edge radiation by increasing the relative fraction of direct over indirect (non-radiative) recombinations, and secondly, it changes the spectral characteristic of the emitted radiation towards lower energies [6]. As the absorption coefficient κ near the fundamental edge is a rapidly varying function of the photon energy [3], this allows a deeper penetration of light into the bulk zone II.

III. THE MATHEMATICAL MODEL

It has become clear in the last section, that the operation principle of electron-beam controlled switches involves the interaction of many different physical processes in the semiconductor material. Among these are:

- Absorption of the primary high energy electron-beam and generation of electron-hole pairs as well as bremsstrahlung.
- Generation, absorption and re-emission of band-edge radiation.
- Secondary generation of electron-hole pairs due to absorption of band-edge radiation and bremsstrahlung.
- Direct recombination of electron-hole pairs, as well as indirect recombination via trapping and Auger interaction.
- Drift and diffusion of both types of free charge carriers.

A fully satisfactory description of these processes is only possible in the framework of a kinetic theory model, or equivalently, by the use of an extensive Monte-Carlo simulation. However, for our purposes it is sufficient to employ an effective macroscopic model based on a moment approximation of lowest order, where we can take account of the relevant physical processes in the form of semi-empirical reaction terms.

In the following, we assume a one-dimensional geometry and consider all quantities as functions of the time t and the x-axis of an appropriately chosen coordinate system. A mathematical modeling of the switch configuration then leads to a system of one-dimensional partial differential equations to describe the electrical conduction phenomena, interacting with transport equations for the radiation intensities. The electrical set consists of drift equations for the free electrons and holes as well as balance equations for the trapped charges, coupled to Poission's equation for the electrical field:

$$\frac{\partial n}{\partial t} + \frac{\partial}{\partial x}\left(-D_n \frac{\partial n}{\partial x} + n v_n\right) = S + \dot{n}^{r}_{cv} + \dot{n}^{nr}_{cv} + \sum_i N_i \dot{r}_{ci}, \tag{1}$$

$$\frac{\partial p}{\partial t} + \frac{\partial}{\partial x}\left(-D_p \frac{\partial p}{\partial x} + p v_p\right) = S + \dot{n}^{r}_{cv} + \dot{n}^{nr}_{cv} + \sum_i N_i \dot{r}_{vi}, \tag{2}$$

$$\frac{\partial r}{\partial t} = \dot{r}_{vi} - \dot{r}_{ci}. \tag{3}$$

$$\epsilon_0 \epsilon_r \frac{\partial^2 \Phi}{\partial x^2} = e\left(n - n_{eq} + \sum_i N_i (r - r_{eq}) - p + p_{eq}\right). \tag{4}$$

Here, n and p stand for the concentration of the free electrons and holes, respectively; N_i is the absolute value of the ith deep level and r_i its relative occupation number. The quantities with index eq refer to the local thermodynamic equilibrium values. The D's are the diffusion coefficients which in general depend on the electrical field $E = -\frac{\partial \Phi}{\partial x}$, the v's stand for the drift velocites which are field dependent as well. On the right hand side of eqs. (1) to (3) appear terms which denote the transitions between different energy levels; $S = S_{\mathrm{eb}} + S_{\mathrm{be}} + S_{\mathrm{bs}}$ represents the generation of electron-hole pairs due to beam-ionization and the absorption of band-edge radiation and bremsstrahlung, respectively, $\dot{n}_{cv}^{\mathrm{r}}$ and $\dot{n}_{cv}^{\mathrm{nr}}$ the radiative and non-radiative direct recombination, and $\dot{r}_{ci}$ and $\dot{r}_{vi}$ the processes of electron and hole capture. Finally, ϵ_0 and ϵ_r stand for the absolute and the relative dielectrical constant, and e for the electrical elementary charge.

Coupled to the electrical transport equations are radiation transport equations for the bremsstrahlung and the recombination radiation. The predominantly forward directed bremsstrahlung can be described in terms of a spectral quantum density $F_{\mathrm{bs}}(x, h\nu)$ which follows the equation

$$\frac{\partial F_{\mathrm{bs}}}{\partial x} = -\kappa_{\mathrm{bs}} F_{\mathrm{bs}} + \sigma_{\mathrm{bs}}. \tag{5}$$

The spectral emission rate σ_{bs} is given as a product of the local beam intensity $j_{eb}T/e$ - where $T = T(x)$ is the mean kinetic energy of the beam electrons - and the normalized spectral distribution $\hat{\sigma}_{\mathrm{be}}$ of the emitted X-ray quanta (for which we use a form reported by Evans [7]),

$$\sigma_{\mathrm{bs}}(h\nu, x) = \frac{j_{\mathrm{eb}}}{e} E(x) \hat{\sigma}_{\mathrm{bs}}(E, h\nu). \tag{6}$$

The spectral absorption coefficient κ_{bs} is related to the source function S_{bs} by

$$S_{\mathrm{bs}}(x) = \int_0^{eV} F_{\mathrm{bs}}\, \kappa_{\mathrm{bs}}\, d\, h\nu / \chi, \tag{7}$$

where $\chi = 4.3$ eV stands for the mean ionization energy of GaAs.

To describe the transport of the isotropily emitted band-edge radiation, we have to take an angular coordinate ϑ (the angle to the x-axis) into account and solve for the photon flux density $F_{\mathrm{be}}(x, h\nu, \vartheta)$,

$$\cos\vartheta \frac{\partial F_{\mathrm{be}}}{\partial x} = -\kappa_{\mathrm{be}} F_{\mathrm{be}} + \sigma_{\mathrm{be}}. \tag{8}$$

In this case, the relations between the spectral absorption and emission coefficients and the terms in the electrical transport equations are

$$S_{be}(x) = 2\pi \int_{h\nu_{min}}^{h\nu_{max}} \int_0^{\pi} F_{be}\, \eta_{be} \kappa_{be}\, d\,h\nu \sin\vartheta d\vartheta, \tag{9}$$

$$\sigma_{be}(h\nu, x) = \dot{n}^{r}_{cv}(x)\hat{\sigma}_{be}(h\nu) \tag{10}$$

where η_{be} is the ratio of the generated electron-hole pairs to the absorbed photons and $\hat{\sigma}_{be}$ is the spectral distribution of emitted photons. (Both functions can be inferred from data reported by reference 8.)

Finally, we specify the direct source function, i.e., the number of electron-hole pairs generated by ionization due to the electron beam itself, by writing it

$$S_{eb} = \frac{j_{eb}}{e}\frac{dE}{dx}/\chi. \tag{11}$$

Here again, j_{eb} is the current density of the e-beam, $\chi \approx 4.3$eV the mean ionization energy of gallium arsenide and $\frac{dE}{dx}$ the electron dissipation function (interpolated for GaAs from Cu and Sn after reference 4).

It is clear *a priori* that an analytical solution of the complete system of transport equations (1 - 11) will be impossible to obtain, so that an appropriate numerical code has to be developed. However, a direct implementation of the equations is also difficult, the dynamical range between the different modes of the switch (open vs. closed) would demand a very high numerical resolution and hence a considerable calculational effort. For that reason, we will restrict ourselves in the following sections to a discussion of the steady state modes of the switch, i.e., on the closed and the open state of the switch configuration. Both regimes allow a number of well-motivated (but different) approximations which facilitate the mathematical analysis considerably; a treatment of the fully time-dependent (transient) behavior will be presented elsewhere [9].

A. THE CLOSED STATE

We focus first on the closed state of the switch, where the semiconductor has been made highly conductive by the e-beam irradiation. From the qualitative description given above, it is clear that the configuration can be conceptionally seperated into two regions with different purposes and different physical behavior, namely in a) the highly doped region I which stops the electron-beam and transforms its energy partially in band-edge radiation and bremsstrahlung, and b) the semi-insulating zone II which absorbs this radiation creating secondary electron-hole pairs.

First, we turn to the description of the transport processes in the region I. Due to the heavy p-doping in this region, $N_a \approx 10^{19}\mathrm{cm}^{-3}$, the hole density p is always much higher than the electron density n, even when compared to the number of charge carriers generated by the e-beam irradiation. This fact has the following consequences:

i) The density of holes is so high that quasi-neutrality applies, i.e, Poissons equation (4) can be replaced by $p - p_{\mathrm{eq}} - n + n_{\mathrm{eq}} - \sum_i N_i(r_i - r_{i,\mathrm{eq}}) \approx p - N_a = 0$.

ii) The electrical current (essentially carried by the holes) is not influenced by the small voltage drop in zone I, in other words, the bulk zone II acts as a highly resistive current source for the stopping layer.

iii) The occupation number r_i of the trap levels is close to zero.

iv) Because of the small field strength in zone I the transport processes are linear, i.e. the drift velocity is $v = \mu E$ and the diffusion coeffient follows the Einstein relation $D = \mu k_B T/e$ where k_B denotes the Boltzmann constant and T the crystal temperature.

vi) Thermal rates can be neglected as they are not detectable against the dominant dynamical processes generated by the beam irradiation.

Employing all these approximations (which are valid up to a very high accuracy), and using especially (i) and (ii) to express the electrical field by the current density j and the acceptor concentation N_a, $E = j/\mu_p e N_a - (kT/e)\partial \ln N_a/\partial x$, we can establish the following equation for the transport of the minority carrier density n,

$$\frac{\partial n}{\partial t} + D_n \frac{\partial}{\partial x}([\frac{j/e}{D_p N_d} - \frac{\partial \ln N_d}{\partial x}]n - \frac{\partial n}{\partial x}) = S_{\mathrm{eb}} + S_{\mathrm{be}} - k_d N_a n - k_A N_a^2 n - \sum_i k_{ci} N_i n. \quad (12)$$

Here we have written the radiative electron loss term as $\dot{n}_{cv}^{\mathrm{r}} = -k_d N_d n$ with $k_d = 7.5 \times 10^{-10}$ $\mathrm{cm^3 s^{-1}}$ as the direct recombination time constant, and specialized the non-radiative as Auger recombinations, $\dot{n}_{cv}^{\mathrm{nr}} = -k_A N_a^2 n$, where the Auger constant has the value $k_A =$

$10^{-29}\ \mathrm{cm^6 s^{-1}}$. The k_{ci} are the electron capture coefficients for the ith level, we assume that the overall trapping rate $\sum_i k_{ci}$ is of the order of $10^{-8}\ \mathrm{s^{-1}}$. (The re-absorbtion of the radiation emitted during band-level transitions is neglected.) S_{ee} and S_{be} are calculated as explained above; the contribution of bremsstrahlung can be dropped because of the deep penetration depth of x-rays. Finally, we demand as boundary conditions the electron density n to vanish at $x = 0$ (to model enhanced surface recombination) and its derivative $\frac{\partial n}{\partial x}$ to remain finite at $x \to d$ where $N_a \to 0$ (regularity condition).

With these premises, equation (12) can be solved numerically. Figure (2) shows the steady state electron density result for a beam irradiation of 100 keV and $1\ \mathrm{A/cm^2}$ and a switch current of $1\ \mathrm{kA/cm^2}$. Within reasonable accurary, all quantities in the stopping zone I scale linearly on the electron-beam current j_{beam}, in particular the number $k_d N_a n$ of the recombination events generating secondary photons which appear as the source function in region II. (Note that (12) is not a linear equation in a strict sense, the current j depends on the conductance of zone II and therefore indirectly on n.) The typical time scale on which zone I reacts on the electron-beam irradiation can be estimated by the constant in the loss term, $\tau^{-1} = k_a N_a + \sum_i k_{ci} N_i + k_a N_a^2$. For the values we have assumed in our calculations, τ is less than 1 ns.

Next we describe the bulk zone II of the switch, where we have to take into account the dynamics of both electrons and holes as well as the influence of the trapped charges. The carrier densities are relatively low so that direct and Auger recombination can be neglected. Again omitting the thermal rate coefficients, the motion of the free charge carriers in the conduction and the valence band are then given by the following drift and diffusion equations

$$\frac{\partial n}{\partial t} + \frac{\partial}{\partial x}\left(-D_n \frac{\partial n}{\partial x} - \mu_n E n\right) = S_{\mathrm{be}} + S_{\mathrm{bs}} - \sum_i k_{ci} N_i (1 - r_i) n \tag{13}$$

$$\frac{\partial p}{\partial t} + \frac{\partial}{\partial x}\left(-D_p \frac{\partial p}{\partial x} + \mu_p E p\right) = S_{\mathrm{be}} + S_{\mathrm{bs}} - \sum_i k_{vi} N_i r_i p, \tag{14}$$

the bound electrical charges are governed by the rate equations

$$\frac{\partial r_i}{\partial r} = k_{ci}(1 - r_i) n - k_{vi} r p, \tag{15}$$

where k_{ci} and k_{vi} are the electron and hole capture coefficients, respectively. The system is completed by the quasi-neutrality condition

$$p - n - \sum_i N_i (r_i - r_{i,\mathrm{eq}}) = 0. \tag{16}$$

The source function S now represents the secondary ionization of the bulk material by the absorption of band-edge radiation and bremsstrahlung. As opposed to zone I, re-emission of radiation is negligible and we can formulate the function in a closed form. Utilizing the scale separation between the zone I and II ($L \gg d$), the band-edge radiation part is

$$S_{\text{be}}(x) = 2\pi \int_{h\nu_{\text{min}}}^{h\nu_{\text{max}}} \hat{\sigma}_{\text{be}} \kappa_{\text{be}} \eta_{\text{be}} E_1(\kappa_{\text{be}} x)\, dh\nu \times \int_0^d k_d n p\, dx'. \tag{17}$$

E_1 denotes the exponential integral which results from the integration over the emission angle ϑ. The contribution of the bremsstrahlung can be formulated in a similar manner, it is, however, small compared to S_{ne}.

The reaction rates in equations (13 - 16) involve the cross sections and densities of the deep levels which depend considerably on the details of the semiconductor manufacturing process. We will assume in the following the existence of only one level with density $N = 10^{16}\,\text{cm}^{-3}$ in middle of the band gap, $r_{i,\text{eq}} = 0.5$. Furthermore, we take the electron and hole capture coefficients to be equal, $k_{ci} = k_{vi} = k$.

Using these numerical values, we have calculated the steady state solution of equations (13 - 16) for several values of the electron beam current j_{beam} and the free carrier life time $\tau = 1/kNr_{i,\text{eq}}$. The latter gives an estimate of the reaction time of the configuration. Although it is not strictly true mathematically for the reason explained above, it turns out that the solution depended nearly linearly on both variables. Figure 4 shows the electron density for the values $j_{\text{beam}} = 1\text{Acm}^{-2}$ and $\tau = 10^{-8}$ s. (Again, the beam energy is 100 keV and the switch length is $L = 0.25\,\text{cm}$.)

Figure 5 displays the conductance G per area as a function of both variables j_{beam} and τ. The linear characteristic of the system is obvious, it can approximately be expressed as $G = 6.5\,\Omega^{-1}\text{cm}^{-1} \times j_{\text{beam}}/1\text{Acm}^{-2} \times \tau/10\,\text{ns}$. The conductance is also a nearly linear function of the e-beam energy; its dependence on the switch length can be expressed approximately as $G \sim L^{-1.3}$.

B. THE OPEN STATE

In evaluating the performance of the electron-beam controlled switch, information of the open state behavior are as important as that of the closed state. To control a high power application effectively and to achieve a reasonable efficiency, a low dark current and a high hold-off voltage are neccessary.

Let us first consider the case when the voltage pulses applied across the switch are short enough so that the effects of dissipative heating can be neglected. In this regime, the hold-off voltage V_p is essentially determined by the dielectrical strength (breakdown field strength) E_b of the switch material. Pure GaAs has an E_b of about 400 kV/cm above which field emission and impact ionization lead to charge carrier multiplication and avalanche breakdown [3], in technically availble material this value can be substantially less, $E_b \approx 100\,\mathrm{kV/cm}$ [10]. Assuming an approximately homogeneous electrical field (which can be confirmed by numerical calculations), this translates into short-time hold-off voltages $V_b = E_b L$ between 100 kV and 25 kV, respectively, for a switch length of $L = 0.25\,\mathrm{cm}$.

For voltage pulses which have a longer duration, dissipation and Ohmic heating have to be taken into account. For the configuration with anode side cooling shown in figure 1, the overheating equals $\Delta T = PL/2\lambda$ where $P = Vj_{\mathrm{dark}}$ descibes the Ohmic losses and $\lambda = 0.46\,\mathrm{W/cmK}$ the heat conduction coefficient [3]. For $L = 0.25\,\mathrm{cm}$, this leads to a steady state overheating $\Delta T = 2.7 \times 10^5\,\mathrm{K} \times V/100\,\mathrm{kVcm}^{-1} \times j_{\mathrm{dark}}/\mathrm{Acm}^{-2}$.

Clearly, any dark current of the order of the space charge limit, $j_{\mathrm{dark}} = \frac{1}{2}\epsilon_0\epsilon_r V v/L^2 \approx 0.8\,\mathrm{Acm}^{-2} \times V/100\,\mathrm{kV}$, would not be tolerable for steady state application and hence places rather strict limits on the maximal time duration of the voltage pulse. In the presented configuration, however, the dark current is reduced by several orders of magnitude compared to that value. The heavily doped contact zones decrease the concentration of minority charge carriers at the cathode and the anode drastically, and they also reduce the current injection by locally shielding the high electrical field. Therefore, only charge carriers that are generated in the intrinsic bulk zone contribute to the electrical current.

A numerical simulation of the open state starts from equations (1) to (4). The source function is zero so that thermal emission becomes important; furthermore, the nonlinearity of the transport processes has to be considered. Figure 5 shows the result of a calculation for a slightly n-type material with ($n_{eq}/p_{eq} \approx 7$), it demonstrates that in well compensated material dark currents of less than $10\,\mu\mathrm{Acm}^{-2}$ are feasable. It should be noted that the

processes of field-enhanced emission and impact ionization have not been taken into account, the result is therefore only valid for voltages that are below the (material dependent) breakdown voltage V_b.

IV. DISCUSSION

The theoretical investigations presented in this paper (and also the corresponding experimental results of reference [1] and [11]) have shown that the concept of electron-beam controlled semiconductor switches is very promising. It seems possible that devices based on this principle will be able to control currents of several kA and voltages up to 100 kV with electron beams of the order of one A. While we have not performed any simulations of the transient switch behavior so far, orders-of-magnitude estimates based on the effective recombination constants indicate the feasibility of reaction time spans of the order of tens of ns or even lower. In evaluating possible applications, the following points may be of particular interest:

- For constant beam irradiation, the switch reacts like a linear Ohmic conductor. This characteristic behavior (which is valid for on-state-fields up to 3 kV/cm) is very beneficial in order to achieve a stable device operation.
- The steady state conductance G is inversely proportional to the free carrier lifetime $\tau = 1/kN$, i.e., to the effective response time of the switch. This indicates a trade-off between efficiency and speed.
- The conductance of the switch is in linear relation to the controlling e-beam current. This fact – which is based on the linear behavior of both zone I and II – promises to be useful in the fields of high-power modulation.

We conclude the discussion with two examples. Consider, for instance, an extremely pure sample with an effective free carrier lifetime of 1 μs. Here, we can expect for a 100 keV and 1 A/cm^2 electron-beam a steady state switch conductance of nearly 1kΩ^{-1}/cm^2. Coupled with a standard technology vacuum triode, this configuration might be a very attractive alternative to conventional thyratrons. On the other hand, in a crystal with a high density of recombination centers, τ can be less than 1 ns. Controlled by a high speed electron-beam as provided, e.g., by high-voltage vacuum tubes, response times down to the nanoseconds may be obtainable. Such a configuration would be very promising in the field of high-power microwave modulation.

V. Acknowledgements

This work was supported by the U.S. Army Research Office and the Air Force Office for Scientific Research under Contract DAA L03-86-K-0078.

VI. REFERENCES

[1] K.H. Schoenbach, V.K. Lakdawala, D.C. Stoudt, T.F. Smith and R.P. Brinkmann, *IEEE Electron Devices*, **36**, 1793 (1989).

[2] Weisberg and Blanc, *Phys Rev.* **131**, 1548 (1963).

[3] S.M. Sze, Physics of Semiconductor Devices, (Wiley, New York, 1981).

[4] A.G. Chynoweth, W.L. Feldman, and R.A. Logan, *Phys. Rev.* **121**, 684 (1961).

[5] L.V. Spencer, Energy Dissipation by Fast Electrons, NBS Monograph 1, (NBS, Washington, 1959).

[6] D.A. Cusano, *Solid State Communications* **2**, 353 (1964).

[7] R.P. Evans, *The Atomic Nucleus*, (McGraw-Hill, New York, 1955).

[8] W.J. Turner and W.E. Reese, *J. Appl. Phys.* **35**, 350 (1963).

[9] R.P. Brinkmann, to be published

[10] D.C. Stoudt, to be published

[11] D.C. Stoudt, K.H. Schoenbach and V.K. Lakdawala, Proceedings of the Seventh IEEE Pulsed Power Conference, Monterey, CA, June 11-14, 1989.

Figure Captions

Figure 1: Schematic representation of the proposed device geometry.

Figure 2: Electron density in region I as a function of the spatial coordinate, evaluated for an electron beam of 100 keV and $1 \mathrm{A/cm^{-2}}$.

Figure 3: Electron density in region II as a function of the spatial coordinate, evaluated for an electron beam of 100 keV and $1 \mathrm{A/cm^{-2}}$.

Figure 4: Switch conductance G per area as a function of the electron beam current pear area and the free carrier life time τ, for an electron beam of 100 keV and a switch length of 0.25 cm.

Figure 5: Dark current per area in the off-state as a function of the hold-off voltage, for a switch length of 0.25 cm.

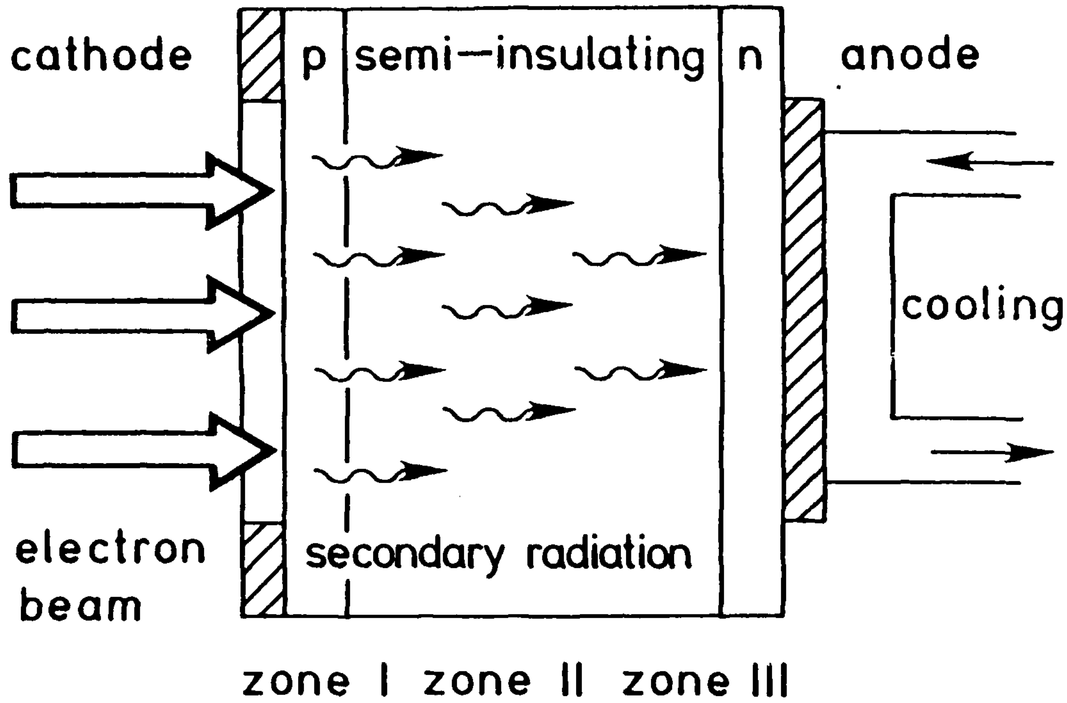
cathode
p
semi—insulating
n
anode
cooling
electron
beam
secondary radiation
zone I
zone II
zone III

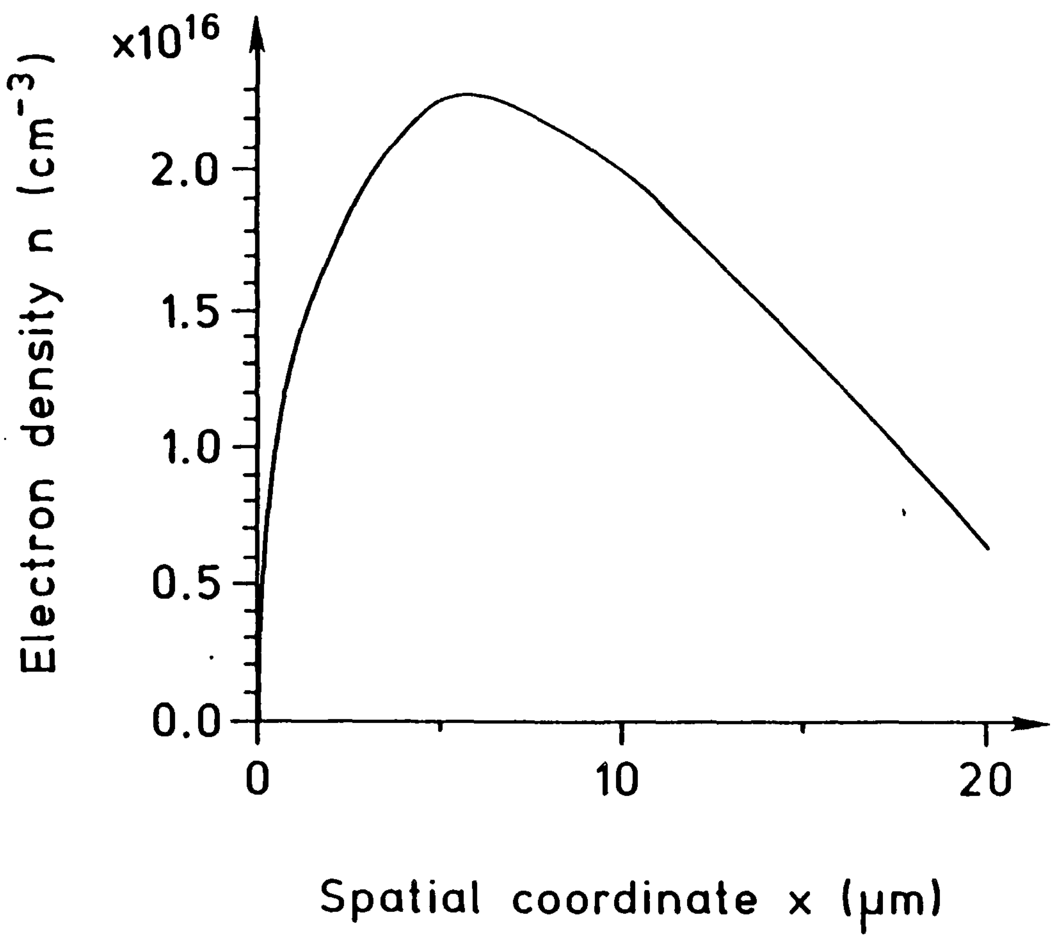
×10^16
2.0
1.5
1.0
0.5
0.0
0
10
20
Electron density n (cm^-3)
Spatial coordinate x (μm)

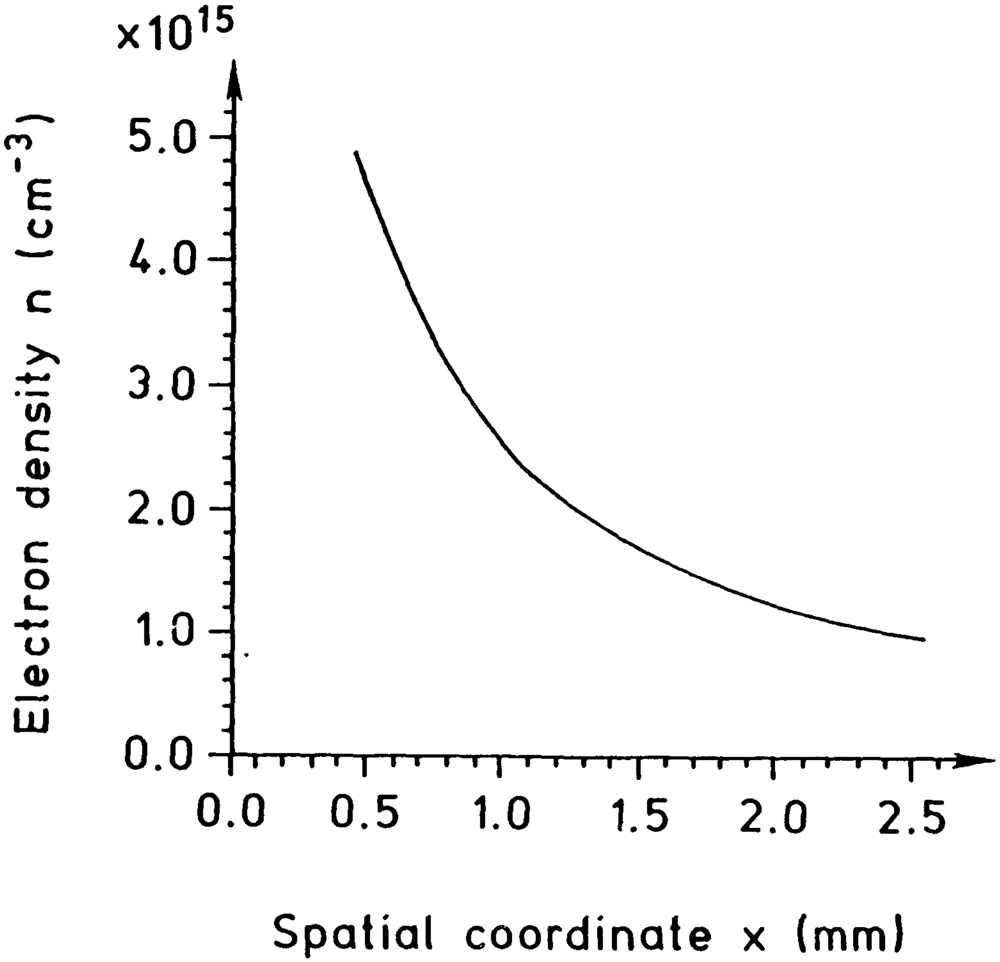
x10^15
Electron density n (cm^-3)
5.0
4.0
3.0
2.0
1.0
0.0
0.0
0.5
1.0
1.5
2.0
2.5
Spatial coordinate x (mm)

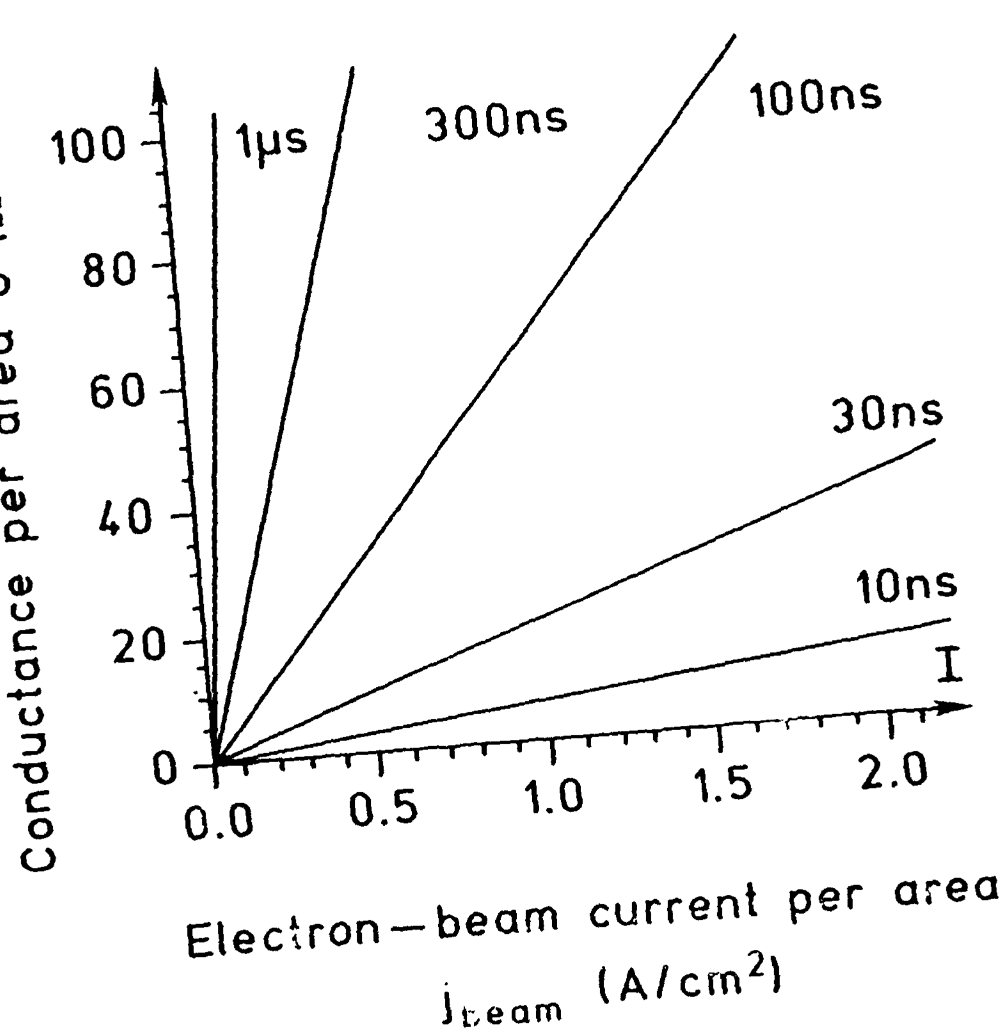

Conductance per area G (Ω^{-1}/cm^2)
100
80
60
40
20
0
1µs
300ns
100ns
30ns
10ns
I
0.0
0.5
1.0
1.5
2.0
Electron—beam current per area
j_{beam} (A/cm^2)

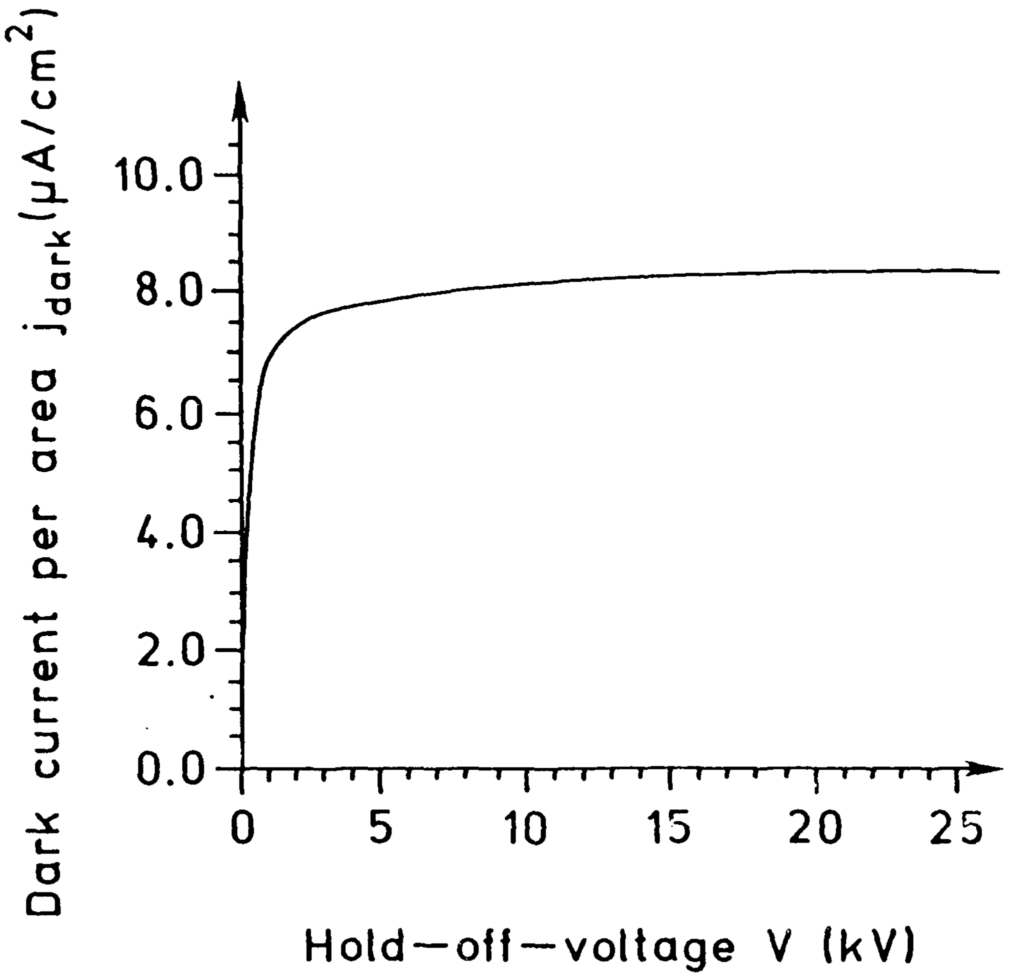
Dark current per area j_{dark} ($\mu A/cm^2$)
10.0
8.0
6.0
4.0
2.0
0.0
0
5
10
15
20
25
Hold—off—voltage V (kV)

PATENTS

United States Patent [19]

Schoenbach et al.

[11] **Patent Number:** **4,831,248**

[45] **Date of Patent:** **May 16, 1989**

[54] **ELECTRON BEAM CONTROLLED BULK SEMICONDUCTOR SWITCH WITH CATHODOLUMINESCENT ELECTRON ACTIVATION**

[75] Inventors: **Karl H. Schoenbach**, Norfolk; **Vishnukumar K. Lakdawala**, Virginia Beach, both of Va.; **Rudolf K. F. Germer**, Berlin; **Klemens B. Schmitt**, Rothenbach, both of Fed. Rep. of Germany

[73] Assignee: **Center for Innovative Technology**, Herndon, Va.

[21] Appl. No.: **184,680**

[22] Filed: **Apr. 22, 1988**

Related U.S. Application Data

[63] Continuation-in-part of Ser. No. 82,546, Aug. 7, 1987.

[51] **Int. Cl.**⁴ **H01J 40/14**

[52] **U.S. Cl.** .... **250/211 R**; 250/211 J; 357/17; 307/308; 307/239

[58] **Field of Search** .... 250/211 R, 211 J; 357/19, 17, 30 B, 30 M, 30 N; 307/239, 308

[56] **References Cited**

U.S. PATENT DOCUMENTS

3,555,282	1/1971	Vanai et al.	250/211 J
3,832,732	8/1974	Roberts	357/19
3,917,943	11/1975	Auston	250/211 J
4,001,865	1/1977	Voss	357/38
4,063,130	12/1917	Hunter, Jr.	315/150
4,240,088	12/1980	Myers	357/19
4,376,285	3/1983	Leonberger et al.	357/17
4,396,833	8/1983	Pan	250/211 J
4,438,331	3/1984	Davis	250/211 J
4,626,883	12/1986	Kash et al.	357/30
4,626,884	12/1986	Shannon	357/30

Primary Examiner—David C. Nelms
Assistant Examiner—Stephone B. Allen
Attorney, Agent, or Firm—Staas & Halsey

[57] **ABSTRACT**

An electron beam controlled semiconductor switch is capable of carrying large currents without being restricted by the space charge limited current condition. The switch includes a block of semiconductor material having ohmic contacts connectable to first and second electrical conductors. Semi-insulating GaAs may be used as the semiconductor material. A shallow donor or acceptor doped layer may be formed at the surface receiving the electron beam for increased band-edge radiation. This recombination radiation ionizes, together with X-rays produced by Bremsstrahlung, the bulk of the semiconductor block to provide relatively high current density and current gain.

6 Claims, 2 Drawing Sheets

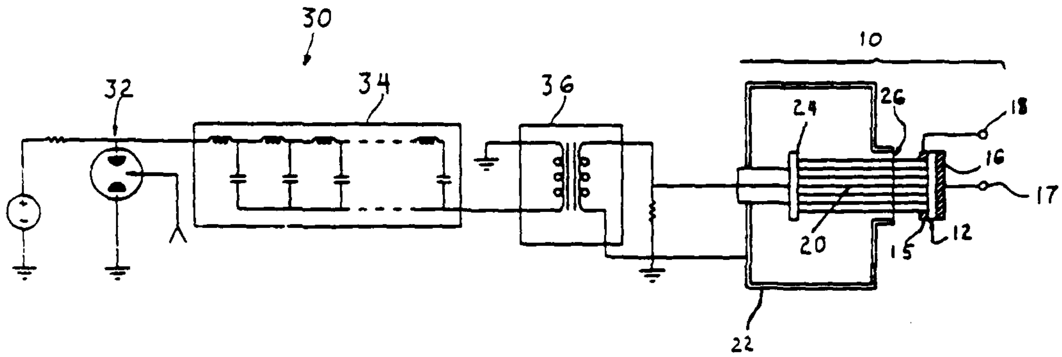

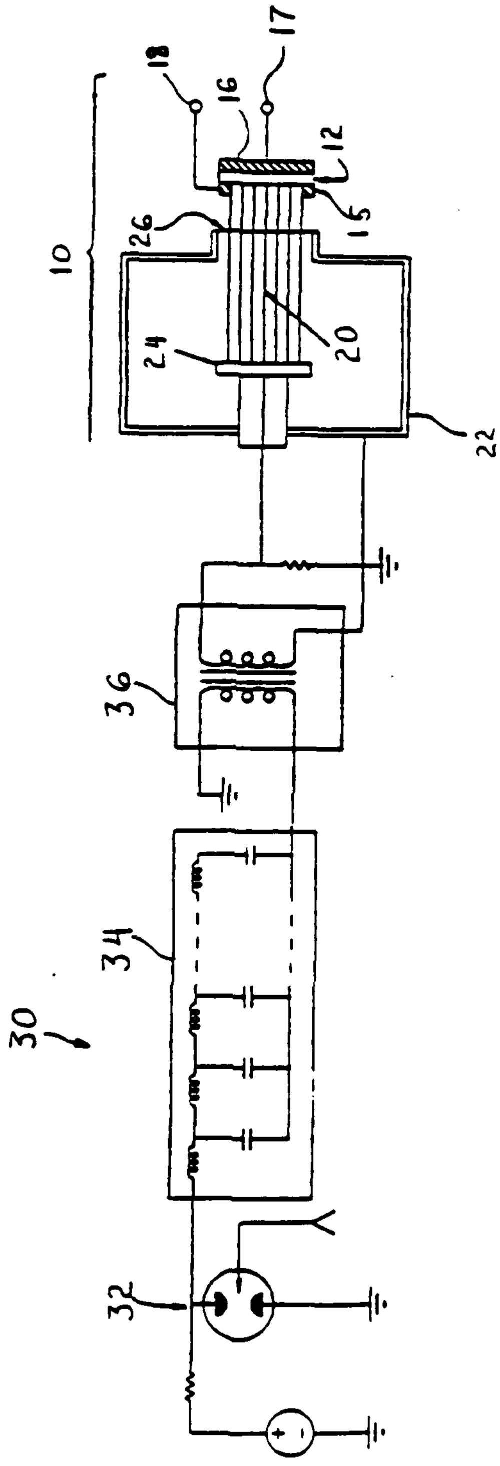

FIG. 1

FIG. 2A

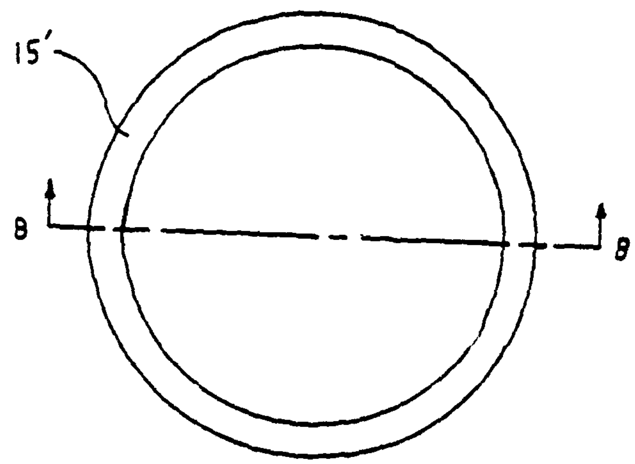

FIG. 2B

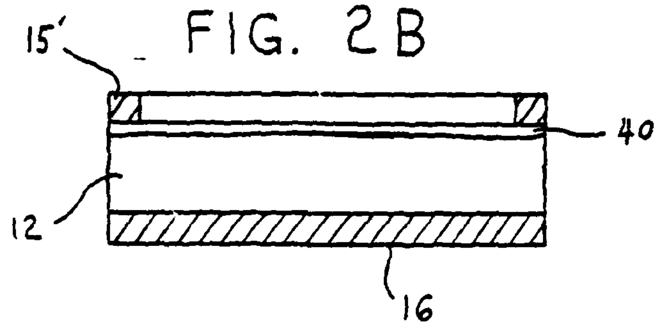

ELECTRON BEAM CONTROLLED BULK SEMICONDUCTOR SWITCH WITH CATHODOLUMINESCENT ELECTRON ACTIVATION

CROSS-REFERENCE TO RELATED APPLICATION

This is a continuation-in-part of U.S. patent application Ser. No. 082,546, filed Aug. 7, 1987, incorporated herein by reference.

BACKGROUND OF THE INVENTION

1. Field of the Invention

The present invention is related to electron beam controlled bulk semiconductor switches and, more particularly, to a switch which is not restricted by the space charge limited current condition and is capable of high current gain and high current density.

2. Description of the Related Art

Many varieties of optically controlled semiconductor switches exist, but electron beam controlled switches are less common. Photodiodes, phototransistors, photothyristors and light sensitive resistors are examples of the many types of optically controlled switches. The most commonly used light-sensitive semiconductor device is the photodiode which is used in many applications, including fiber optic communication systems, etc. The currents handled by such devices are relatively low, typically in the milliampere range. One example is the PIN diode taught by U.S. Pat. No. 4,240,088 to Myers. Other light-activated devices include the thyristors taught by U.S. Pat. Nos. 3,832,732 to Roberts and 4,001,865 to Voss, the microwave switching circuit taught by U.S. Pat. No. 4,396,833 to Pan and many other patents. Some, such as U.S. Pat. Nos. 4,626,883 to Kash et al. and 3,917,943 to Auston, describe switching elements with picosecond switching times. Other light activated switches, such as those taught by U.S. Pat. Nos. 4,438,331 to Davis and 4,376,285 to Leonberger et al., are able to carry a larger amount of current by making an entire block of semiconductor material conductive; however, like photodiodes, they require continuous light to sustain conduction.

Electron-bombarded semiconductor (EBS) devices are highspeed switching devices which use an electron beam instead of light to control switching. EBS devices typically use electron beams of 10–15 keV and are limited in output power and current density due to the space charge limited current condition. While switching time is typically below ten nanoseconds, the current density is usually a few milliamperes per square millimeter with a current gain of 2000 or less.

Higher current densities, up to 10^2 A/cm^2 are provided by diffuse discharge switches, such as the switch taught by U.S. Pat. No. 4,063,130 to Hunter. However, while diffuse discharge switches can be turned ON in less than a nanosecond, they are relatively slow to turn OFF, taking approximately 100 nanoseconds and have a moderate current gain between 10^2 and 10^3.

SUMMARY OF THE INVENTION

An object of the invention is to provide a semiconductor switch with a current density over 10^4 A/cm^2.

Another object of the present invention is to provide a high current semiconductor switch with an operating voltage drop of less than 100 volts.

A further object of the present invention is to provide an electron beam controlled semiconductor switch with a current density unrestricted by the space charge limited current condition.

The above objects are attained by providing a switch operatively connectable between first and second electrical conductors, the switch comprising a block of semiconductor material having first and second ohmic contacts operatively connectable to the first and second electrical conductors, respectively, and electron beam means for directing an electron beam onto the block through the first contact to produce an electron-hole plasma throughout the block of semiconductor material between the contacts by direct impact, recombination radiation and Bremsstrahlung.

These objects, together with other objects and advantages which will be subsequently apparent, reside in the details of construction and operation as more fully hereinafter described and claimed, reference being had to the accompanying drawings forming a part hereof, wherein like reference numerals refer to like parts throughout.

BRIEF DESCRIPTION OF THE DRAWINGS

FIG. 1 is a schematic diagram of an embodiment of the present invention; and

FIGS. 2A and 2B are a top and a cross-sectional side view of a semiconductor wafer with one ring-shaped contact, as used in a second embodiment of the present invention.

DESCRIPTION OF THE PREFERRED EMBODIMENTS

As illustrated in FIG. 1, an electron beam controlled switch 10 according to the present invention includes a block 12 of semiconductor material with ohmic contacts 15–16 operatively connectable to the electrical conductors 17 and 18. A space of a micron to a few centimeters may be used to separate contact 15 from contact 16. An electron beam 20 is used to initiate and maintain conductivity in the switch 10. The electron beam 20 may be generated in a vacuum tube diode 22 which emits electrons from a cathode 24 through an anode foil 26. The electron beam 20 passes through the vacuum chamber wall and strikes the surface of the semiconductor block 12 through contact 15. Energization of the diode 22 may be controlled in a conventional manner. A pulsing circuit 30 as illustrated in FIG. 1 as including a spark gap switch 32, pulse forming network 34 and pulse transformer 36. A pulsing circuit like that illustrated in FIG. 1 has been used to produce a one microsecond pulse.

When the block 12 of semiconductor material is formed of a highly resistive direct semiconductor material, such as semi-insulating gallium arsenide (GaAs), the electron beam 20 has a maximum energy for GaAs of approximately 200 keV since GaAs can suffer damage if the electron energy exceeds 220 keV. The lower limit of the electron energy in the embodiment illustrated in FIG. 1 is determined by the fact that the electron beam has to pass through the anode foil 26 and the contact 15. However, where the semiconductor contact 15 forms the anode of the electron beam diode 26, electrons with much lower energies, even as low as 10 keV can potentially be used. Low energy electron beams are more easily used if, as illustrated in FIGS. 2A and 2B, a ring-shaped contact 15' is used instead of the solid contact illustrated in FIG. 1. Use of a ring-shaped

contact requires that the highly conductive region formed by the electron beam at the surface of the block 12 of semiconductor material be able to serve as the inner portion of contact 15.

The range of electron energy for a device constructed according to the present invention is between the range of electron beams used in diffuse discharge switches (150–300 keV) and those used in electron-bombarded semiconductor (EBS) devices (10–15 keV). The capabilities of an electron-beam controlled bulk semiconductor switch according to the present invention is more similar to a diffuse discharge switch than an EBS device, because the space charge limited current condition is exceeded.

The space charge limitation is overcome in the present invention by converting the electron energy in the electron beam 20 into photon energy and X-rays (Bremsstrahlung). The photon energy is produced by band edge radiation due to radiative recombination of electron hole pairs produced by the electron beam. The X-rays and photon energy is then used to ionize the bulk of the semiconductor instead of only a shallow surface layer. The electron beam 20 penetrates the semiconductor material 12 to a relatively shallow depth. For example, a 10 keV electron beam will penetrate silicon to a depth of 1.5 micrometers. However, the X-rays and photon energy which is produced by higher energy electron beams can penetrate to a depth of one-half to one millimeters or more. The majority of the ionization in the semiconductor material 12 outside the electron-beam activated layer is preferably caused by photon energy. Unlike Bremsstrahlung which produces X-rays in a linear relationship to electron energy, photon energy produced by cathodoluminiscence is independent of the energy of the electron beam 20.

Preferably, the semiconductor material is a highly resistive direct semiconductor material such as semi-insulating gallium arsenide (GaAs). A shallow donor or acceptor layer 40 (FIG. 2B) may be formed at the surface of the semiconductor material 12 adjacent to the electrode 15 to increase the number of photons produced by the electron beam 20. The depth of doped layer 40 should be approximately equal to the depth the electrons penetrate the semiconductor 12. For example, a GaAs wafer 0.5 millimeter thick can be doped by diffusing zinc for 20 minutes at a temperature of 750° C. to produce a p-type layer of about 10 micrometers with an acceptor concentration of $10^{19}/cm^3$.

In experiments performed using semiconductor material 12 formed as described above, the undoped semi-insulating GaAs exhibited current densities far above the space charge limited current density for a trap free insulator which represents the optimum condition for space charge limited current flow. The characteristics exhibited by the undoped semi-insulating GaAs indicate that the bulk of the semiconductor was ionized due to X-ray Bremsstrahlung. The experimental results using zinc-doped GaAs had a slower rise time than the undoped semi-insulating GaAs, but had approximately twice the current gain of the undoped semi-insulating GaAs. The concentration, depth and composition of the doped layer can be varied to produce switches with varying characteristics using known semiconductor technology.

In comparison to a diffuse discharge switch, the present invention is capable of higher current density in the switch, e.g., 10^3 to 10^4 A/cm^2, compared to less than 100 A/cm^2 in a diffuse discharge switch. Also, the forward voltage during conduction may be less than 100 volts, while the minimum forward voltage in a diffuse

discharge switch is 1,000 volts and over 100 volts in an EBS device. Most importantly, the current gain of an electron-beam controlled bulk semiconductor switch according to the present invention is 10^4 to 10^5, depending upon the source function and recombination rate of the semiconductor material 12. The source function S_b defines the number of electron-hole pairs created per volume and time by the electron beam and is defined by equation (1).

$$S_b = (dW/dx)^*(J_b/e\,W_i) \quad (1)$$

In equation (1), dW/dx is the differential energy loss, J_b is the electron-beam current density, e is the electron charge and W_i is the effective ionization energy which is 4.3 eV for GaAs.

Many of the features and advantages of the present invention are apparent from the detailed specification, and thus, it is intended by the appended claims to cover all such features and advantages which fall within the spirit and scope of the invention. A switch constructed according to the present invention has many possible applications, a few of which include high power switching in, e.g., an inductive storage unit, and a bistable electronic device in, e.g., a high power circuit. Further, since numerous modifications and changes will readily occur to those skilled in the art, from the disclosure of the invention, it is not desired to limit the invention to the exact construction and operation illustrated and described. Accordingly, suitable modifications and equivalents may be resorted to, all falling within the scope and spirit of the invention.

What is claimed is:

1. A switch operatively connectable between first and second electrical conductors, comprising:

a block of direct semiconductor material having first and second contacts operatively connectable to the first and second electrical conductors, respectively; and

electron beam means for directing an electron beam onto said block through the first contact to produce an electron-hole plasma throughout the block of semiconductor material between the contacts by direct impact, recombination radiation and Bremsstrahlung.

2. A switch as recited in claim 1,

wherein the electron beam penetrates said block of semiconductor material to a first depth, and

wherein said block of semiconductor material includes a doped layer adjacent to the first contact and having a second depth approximately equal to the first depth.

3. A switch as recited in claim 1,

wherein the electron beam penetrates said block of semiconductor material to a first depth, and

wherein said block of semiconductor material includes a p-doped layer, adjacent to the first contact, for producing recombination radiation.

4. A switch as recited in claim 1, wherein the first contact is ring-shaped having an opening through which a substantial majority of the electron beam passes.

5. A switch as recited in claim 1, wherein said electron beam means produces the electron beam with an energy of at least 10 keV.

6. A switch as recited in claim 5, wherein said electron beam means produces the electron beam with energy below a threshold level causing damage in the direct semiconductor material.

* * * * *

ELECTRON BEAM CONTROLLED BULK SEMICONDUCTOR SWITCH WITH CATHODOLUMINESCENT ELECTRON ACTIVATION

CROSS-REFERENCE TO RELATED APPLICATION

This is a continuation-in-part of U.S. Patent Application 07/184,680, issued as U.S. Patent No. 4,831,248 on May 16, 1989 which is a continuation-in-part of U.S. Patent Application Serial No. 07/082,546, issued as U.S. Patent No. 4,825,061 on April 25, 1989.

BACKGROUND OF THE INVENTION

Field of the Invention

The present invention is related to electron beam controlled bulk semiconductor switches and, more particularly, to a switch which is not restricted by the space charge limited current condition and is capable of high current gain and high current density.

Description of the Related Art

Many varieties of optically controlled semiconductor switches exist, but electron beam controlled switches are less common. Photodiodes, phototransistors, photothyristors and light sensitive resistors are examples of the many types of optically controlled switches. The most commonly used light-sensitive semiconductor device is the photodiode which is used in many applications, including fiber optic communication systems, etc. The currents handled by such devices are relatively low, typically in the milliampere range. One example is the PIN diode taught by U.S. Patent No. 4,240,088 to Myers. Other light-activated devices include the thyristors taught by U.S. Patents 3,832,732 to Roberts and 4,001,865 to Voss, the microwave switching circuit taught by U.S. Patent 4,396,833 to Pan and many other patents. Some, such as U.S. Patent 4,626,883 to Kash et al. and 3,917,943 to Auston, describe switching elements with picosecond switching times. Other light activated switches, such as those taught by U.S. Patent No. 4,438,331 to Davis and 4,376,285 to Leonberger et al., are able to carry a larger amount of current by making an entire block of semiconductor material

conductive; however, like photodiodes, they require continuous light to sustain conduction.

Electron-bombarded semiconductor (EBS) devices are high-speed switching devices which use an electron beam instead of light to control switching. EBS devices typically use electron beams of 10-15 keV and are limited in output power and current density due to the space charge limited current condition. While switching time is typically below ten nanoseconds, the current density is usually a few milliamperes per square millimeter with a current gain of 2000 or less.

Higher current densities, up to 10^2 A/cm^2 are provided by diffuse discharge switches, such as the switch taught by U.S. Patent No. 4,0643,130 to Hunter. However, while diffuse discharge switches can be turned ON in less than a nanosecond, they are relatively slow to turn OFF, taking approximately 100 nanoseconds and have a moderate current gain between 10^2 and 10^3.

SUMMARY OF THE INVENTION

An object of the invention is to provide a semiconductor switch with a current density of over 10^4 A/cm^2.

Another object of the present invention is to provide a high current semiconductor switch with an operating voltage drop of less than 100 volts.

A further object of the present invention is to provide an electron beam controlled semiconductor switch with a current density unrestricted by the space charge limited current condition.

The above objects are attained by providing

These objects, together with other objects and advantages which will be subsequently apparent, reside in the details of construction and operation as more fully hereinafter described and claimed, reference being had to the accompanying drawings forming a part hereof, wherein like reference numerals refer to like parts throughout.

BRIEF DESCRIPTION OF THE DRAWINGS

Fig. 1 is a schematic diagram of a first embodiment of the present invention;

Figs. 2A and 2B are a top and a cross-sectional side view of a semiconductor wafer with one ring-shaped contact, as used in a second embodiment of the present invention; and

Figs. 3 and 4 are schematic diagrams of third and fourth embodiments of the present invention, respectively.

DESCRIPTION OF THE PREFERRED EMBODIMENTS

As illustrated in Fig. 1, an electron beam controlled switch 10 according to the present invention includes a block 12 of semiconductor material with ohmic contacts 15-16 operatively connectable to the electrical conductors 17 and 18. A space of a micron to a few centimeters may be used to separate contact 15 from contact 16. An electron beam 20 is used to initiate and maintain conductivity in the switch 10. The electron beam 20 may be generated in a vacuum tube diode 22 which emits electrons from a cathode 24 through an anode foil 26. The electron beam 20 passes through the vacuum chamber wall and strikes the surface of the semiconductor block 12 through contact 15. Energization of the diode 22 may be controlled in a conventional manner. A pulsing circuit 30 is illustrated in Fig. 1 as including a spark gap switch 32, pulse forming network 34 and pulse transformer 36. A pulsing circuit like that illustrated in Fig. 1 has been used to produce a one microsecond pulse.

When the block 12 of semiconductor material is formed of a highly resistive direct semiconductor material, such as semi-insulating gallium arsenide (GaAs), the electron beam 20 has a maximum energy for GaAs of approximately 200 keV since GaAs can suffer damage if the electron energy exceeds 220 keV. The lower limit of the electron energy in the embodiment illustrated in Fig. 1 is determined by the fact that the electron beam has to pass through the anode foil 26 and the contact 15. However, where the semiconductor contact 15 forms the anode of the electron beam diode 26, electrons with much lower energies, even as low as 10 keV can potentially be used. Low energy electron beams are more easily used if, as illustrated in Figs. 2A and 2B, a ring-shaped contact 15' is used instead of the solid contact illustrated in Fig 1. Use of a ring-shaped contact requires that the highly conductive region formed by the electron beam at the surface of the block

12 of semiconductor material be able to serve as the inner portion of contact 15.

The range of electron energy for a device constructed according to the present invention is between the range of electron beams used in diffuse discharge switches (150-300 keV) and those used in electron-bombarded semiconductor (EBS) devices (10-15 keV). The capabilities of an electron-beam controlled bulk semiconductor switch according to the present invention is more similar to a diffuse discharge switch than an EBS device, because the space charge limited current condition is exceeded.

The space charge limitation is overcome in the present invention by converting the electron energy in the electron beam 20 into photon energy and X-rays (Bremsstrahlung). The photon energy is produced by band edge radiation due to radiative recombination of electron hole pairs produced by the electron beam. The X-rays and photon energy is then used to ionize the bulk of the semiconductor instead of only a shallow surface layer. The electron beam 20 penetrates the semiconductor material 12 to a relatively shallow depth. For example, a 10 keV electron beam will penetrate silicon to a depth of 1.5 micrometers. However, the X-rays and photon energy which is produced by higher energy electron beams can penetrate to a depth of one-half to one millimeters or more. The majority of the ionization in the semiconductor material 12 outside the electron-beam activated layer is preferably caused by photon energy. Unlike Bremsstrahlung which produces X-rays in a linear relationship to electron energy, photon energy produced by cathodoluminiscence is independent of the energy of the electron beam 20.

Preferably, the semiconductor material is a highly resistive direct semiconductor material such as semi-insulating gallium arsenide (GaAs) or semi-insulating indium phosphide (InP). A shallow donor or acceptor layer 40 (Fig. 2B) may be formed at the surface of the semiconductor material 12 adjacent to the electrode 15. The depth of doped layer 40 should be approximately equal to the depth to which the electrons penetrate the semiconductor 12. For example, a GaAs wafer 0.5 millimeter thick can be doped by diffusing zinc for 20 minutes at a temperature of 750°C to produce a p-type layer of about 10 micrometers with an acceptor concentration of

$10^{19}/cm^3$. Donor concentrations and acceptor concentrations of 10^{17} per cubic centimeter to 10^{20} per cubic centimeter can be used. Materials such as tellurium (Te), selenium (Se), tin (Sn), sulfur (S), silicon (Si) and germanium (Ge) can be used to produce donors in gallium arsenide and material such as zinc (ZN), cadmium (Cd), carbon (C), beryllium (Be), magnesium (Mg), and lithium (Li) can be used to produce acceptors in gallium arsenide (GaAs).

There are two reasons for doping the electron-beam activated region of the semiconductor switch with a shallow donor or acceptor material. First, the probability of direct recombination and thus the number of band-edge photons per incoming electron is increased by doping gallium arsenide with, e.g., zinc. Second, the bandgap energy of a semiconductor highly doped with suitable materials, such as GaAs doped with zinc, is reduced below the bandgap energy of the same semiconductor material which has not been doped. The band-edge radiation generated in the cathodo-luminescent layer has low photon energy and therefore can penetrate deeper into the semiconductor block 12.

As a result, a high-power semiconductor switch can be constructed with a thickness between the two contacts 15, 16 of 0.5 mm to 10 mm, provided the electron-beam radiated portion 40 of the semiconductor block 12 is properly doped. If the thickness d of the semiconductor block is approximately 1 cm, the ~~voltage~~ electric field across the electrodes may be at least 150 kV/cm and may even be able to go as high as 400 kV/cm without significant current through the semiconductor block 12. For example, when the electron beam is off, an electric field of 150 kV/cm across the electrodes 15, 16 will produce a current of only 4 A/cm^2 for a thickness d of 1 cm. Thus a high hold-off voltage is obtained for such thick switches. When the electron beam irradiates the region 40, the electric field across the electrodes 15, 16 may be as high as 3 kV/cm for Ga As to produce current densities of $10kA/cm^2$.

In experiments performed using semiconductor material 12 formed as described above, the undoped semi-insulating GaAs exhibited current densities far above the space charge limited current density for a trap free insulator which represents the optimum condition for space charge limited current flow. The characteristics exhibited by the undoped semi-insulating GaAs

indicate that the bulk of the semiconductor was ionized due to X-ray Bremsstrahlung. The experimental results using zinc-doped GaAs had a slower rise time than the undoped semi-insulating GaAs, but had approximately twice the current gain of the undoped semi-insulating GaAs. The concentration, depth and composition of the doped layer can be varied to produce switches with varying characteristics using known semiconductor technology.

In comparison to a diffuse discharge switch, the present invention is capable of higher current density in the switch, e.g., 10^3 to 10^4 A/cm^2, compared to less than 100 A/cm^2 in a diffuse discharge switch. Also, the forward voltage during conduction may be less than 100 volts, while the minimum forward voltage in a diffuse discharge switch is 1000 volts and over 100 volts in an EBS device. Most importantly, the current gain of an electron-beam controlled bulk semiconductor switch according to the present invention is 10^3 to 10^4, depending upon the source function and recombination rate of the semiconductor material 12. The source function S_b defines the number of electron-hole pairs created per volume and time by the electron beam and is defined by equation (1).

$$S_b = (dW/dx) * (J_b/e\ W_i) \qquad (1)$$

In equation (1), dW/dx is the differential energy loss, J_b is the electron-beam current density, e is the electron charge and W_i is the effective ionization energy which is 4.3 eV for GaAs.

A semiconductor switch constructed according to the present invention can easily be integrated into a commercially available electron tube 42 or 43, as illustrated in Figs. 3 and 4. In the embodiment illustrated in Fig. 3, the electron tube 42 is a vacuum tube containing a heater element 44, cathode 46, control gate 48 and anode 18'. The electrode 16 is connected to a switch terminal 17', while the semiconductor block 12 is supported by an insulator 50.

Planar electron tubes with plate voltages of up to 150 kV and electron current of 15 to 20 amps are available from Varian EIMAC in San Carlos, California, such as model number YU-140. The gate voltage applied to the control gate 48 of a 150 kV tube is less than 1 kV. An electron tube constructed

as illustrated in Fig. 3 would be able to control currents between terminals 17' and 18' of 10 kA to 20 kA.

In the embodiment illustrated in Fig. 4, the vacuum tube 43 contains a photodiode in which light 52, which may be produced by a laser, passes through a window 54 to generate electrons from a photocathode 56. Multi-alkali photocathodes known in the industry by the designation S20 have a quantum efficiency of .1 or greater and thus convert 10 percent or more of received photons in visible light to electrons. The construction of the vacuum tube 43 at the anode end is essentially the same as that of the vacuum tube 42 illustrated in Fig. 3.

Photodiodes with diameters of two inches are available from International Telephone & Telegraph (ITT) in Fort Wayne, Indiana, such as Model Number F4109. An advantage of using the photodiode tube 43 is the ability to generate pulses, having a pulse width of several nanoseconds controlled by a laser drawing one-tenth to one-hundredth of the power required for existing photoconductive high power switches.

An inductive energy discharge circuit can be produced using a semiconductor switch constructed according to the present invention. For example, using the embodiment illustrated in Fig. 4 where the semiconductor block 12 is 0.5 mm thick, a hold-off voltage of 50 kV could easily be maintained. Such as switch, controlled by a laser drawing less than 1 kW could be used to produce electrical power pulses of hundreds of megawatts from inductive storage. Furthermore, the amount of current supplied can be precisely controlled because the current increases linearly for increases in the area of the switch irradiated by the electron beam.

Many of the features and advantages of the present invention are apparent from the detailed specification, and thus, it is intended by the appended claims to cover all such features and advantages which fall within the spirit and scope of the invention. A switch constructed according to the present invention has many possible applications, a few of which include high power switching in, e.g., an inductive storage unit, and a bistable electronic device in, e.g., a high power circuit. Further, since numerous modifications and changes will readily occur to those skilled in the art, from

the disclosure of the invention, it is not desired to limit the invention to the exact construction and operation illustrated and described. Accordingly, suitable modifications and equivalents may be resorted to, all falling within the scope and spirit of the invention.

CLAIMS

What is claimed is:

1. A vacuum tube switching device, comprising:

first and second terminals;

a block of direct semiconductor material with a first contact on a first surface connected to the first terminal, a second contact on a second surface, opposite the first surface, connected to the second terminal and a doped region exposed by the first surface;

electron beam means for directing an electron beam onto the first surface and into the doped region of said block to produce an electron-hole plasma between the first and second contacts by direct impact, recombination radiation and Bremsstrahlung, thereby permitting current to flow between the first and second terminals during irradiation of said block by the electron beam; and

an enclosure, surrounding said block and said electron beam means, for maintaining pressure within said enclosure below atmospheric pressure, said first and second terminals extending beyond said enclosure.

2. A vacuum tube switching device as recited in claim 1, wherein said block has a thickness, measured between the first and second contacts, of 0.5 millimeter to 10 millimeters and the doped region extends from the first surface into said block for a distance of between 1 and 100 micrometers.

3. A vacuum tube switching device as recited in claim 2, wherein the semiconductor material is one of gallium arsenide, and indium phosphide and the doped region contains one of zinc, cadmium, carbon, beryllium, magnesium, lithium, tellurium, selenium, tin, sulfur, silicon and germanium.

4. A vacuum tube switching device as recited in claim 3, wherein the doped region contains one of a donor and an acceptor with a concentration of 10^{17} to 10^{20} per cubic centimeter.

5. A vacuum tube switching device as recited in claim 1, wherein said electron beam means comprises:

a heated cathode within said enclosure for generating electrons;

a control gate, disposed between said heated cathode and said block within said enclosure, for controlling the flow of electrons; and

third and fourth terminals extending beyond said enclosure, connected to said heated cathode and said control gate, respectively.

6. A vacuum tube switching device as recited in claim 5,

wherein said heated cathode is a planar plate with a voltage of 10 to 150 kilovolts thereacross, producing electrons with 10 to 150 kiloelectron volts,

~~wherein said control gate receives from said fourth terminal a voltage of between ________ and ________ volts to permit passage of the electron beam and between ________ and ________ volts to prevent passage of the electron beam, and~~

wherein the current density conducted by said block of semiconductor material between said first and second terminals when the electron beam irradiates the first surface of said block is between 1 and 10,000 amps/cm^2.

7. A vacuum tube switching device as recited in claim 1, wherein said electron beam means comprises:

a photocathode for converting light into electrons to produce the electron beam;

a window for transmitting light from outside said enclosure to said photocathode; and

a third terminal, connected to said photocathode, extending beyond said enclosure.

8. A vacuum tube switching device as recited in claim 7, wherein said photocathode is constructed of a multi-alkali compound, wherein said third terminal receives a voltage of 10 to 150 kV; and wherein the current density conducted by said block of semiconductor material between said first and second terminals is between 1 and 10,000 amps/cm².

9. A vacuum tube switching device as recited in claim 7, further comprising a laser, outside said enclosure, generating a laser beam directed at said photocathode through said window to make said block conductive.

10. A vacuum tube switching device as recited in claim 9, wherein said laser is a visible light laser. ~~drawing between ________ and ________ watts~~.

11. An inductive storage system, comprising:

inductive storage means for storing electricity; and

a vacuum tube switching device for supplying electrical pulses to and from said inductive storage means to charge and discharge, respectively, said inductive storage means, said vacuum tube switching device comprising:

first and second terminals;

a block of direct semiconductor material with a first contact on a first surface connected to the first terminal, a second contact on a second surface, opposite the first surface, connected to the second terminal and a doped region exposed by the first surface;

electron beam means for directing an electron beam onto the first surface and into the doped region of said block to produce an electron-hole plasma between the first and second contacts by direct impact, recombination radiation and Bremsstrahlung, thereby permitting current to flow between the first and second terminals during irradiation of said block by the electron beam; and

an enclosure, surrounding said block and said electron beam means, for maintaining pressure within said enclosure below atmospheric pressure, said first and second terminals extending beyond said enclosure.

ELECTRON BEAM CONTROLLED BULK SEMICONDUCTOR SWITCH WITH CATHODOLUMINESCENT ELECTRON ACTIVATION

ABSTRACT OF THE DISCLOSURE

An electron beam controlled semiconductor switch is capable of carrying large currents without being restricted by the space charge limited current condition. The switch includes a block of semiconductor material having ohmic contacts connectable to first and second electrical conductors. Semi-insulating GaAs may be used as the semiconductor material. A shallow donor or acceptor doped layer may be formed at the surface receiving the electron beam for increased band-edge radiation. This recombination radiation ionizes, together with X-rays produced by Bremsstrahlung, the bulk of the semiconductor block to provide relatively high current density and current gain.